Palacký University in Olomouc

Dissertation Thesis

Olomouc 2024 Mgr. Eliška Zgarbová

Palacký University in Olomouc

Faculty of Science

Department of Cell Biology and Genetics

The Effects of Indole Derivatives on Aryl hydrocarbon Receptor Activity in Prostatic Cancer Cell Lines

DISSERTATION THESIS

Author:	**Mgr. Eliška Zgarbová**
Study program:	P0511D030006 Biology
Branch of study:	Molecular and Cell Biology
Form of study:	Full-time
Supervisor:	**doc. Ing. Radim Vrzal, Ph.D.**
Submitted:	2024

STATEMENT

Hereby, I honestly proclaim that the presented Ph.D. thesis is based on my research conducted at the Department of Cell Biology and Genetics, Faculty of Science, Palacký University in Olomouc. The presented study was carried out from September 2017 to May 2024. All co-authors of the publications connected with this study agree to include published results. All published literature sources cited in this thesis are listed in the "References" section.

Olomouc 10th June 2024

..……

Mgr. Eliška Zgarbová

ACKNOWLEGEMENT

I would like to express my deepest gratitude to everyone who has supported me throughout my journey.

I especially want to thank my supervisor, doc. Ing. Radim Vrzal, Ph.D., for his outstanding leadership, mentoring, and precious advice. He has been my supervisor since my undergraduate studies and has always been there to provide guidance and support whenever I needed it. I am genuinely grateful to him for many things. Professionally, his leadership style motivated me to overcome challenging experimental obstacles and continue my research. His teaching has significantly impacted career, and I feel that he has truly taught me how to be a scientist. I would also like to highlight his unceasing optimism even in the moments of failed experiments. He truly is an extraordinary mentor.

I also want to extend a heartfelt thank you to all of my colleagues in the Department of Cell Biology and Genetics for sharing their experimental skills and knowledge with me. Throughout my studies, they have been more than just coworkers – they have been like a family, always ready to listen, help, and offer guidance. Their support has meant a great deal to me. Additionally, a special acknowledgment belongs to the members of the Red Vest Club. I genuinely believe that they significantly impacted the fact that I still have some sanity.

And of course, if you dream big, you can make it to Hollywood! Therefore, I must not forget to express my sincere gratitude to my amazing team at Cedars-Sinai Medical Center in Los Angeles. Dr. Robert Barrett and his team welcomed me to their lab, shared valuable skills, and took great care of me as if I were one of their own. I definitely couldn't have had a better internship than this one.

I am also incredibly thankful to my family for their endless support throughout my studies, especially to my mum. Their support means more to me than they can ever imagine.

Last, I must express my immense gratitude to my partner, Jaromír, who stood by my side throughout my Ph.D. journey, believed in me, and provided unwavering support, especially during the dark and difficult times. Always.

BIBLIOGRAFICKÁ IDENTIFIKACE

Jméno a příjmení autora Mgr. Eliška Zgarbová

Název práce Vliv indolových derivátů na aktivitu aryl uhlovodíkového receptoru v prostatických liniích

Typ práce Disertační
Pracoviště Katedra buněčné biologie a genetiky
Vedoucí práce doc. Ing. Radim Vrzal, Ph.D.
Rok obhajoby práce 2024

Abstrakt

Karcinom prostaty se řadí mezi převládající typy onkologického onemocnění u mužů. Rozvoj tohoto typu rakoviny je velmi úzce spojen se signální dráhou androgenního receptoru (AR) a z toho důvodu se také tento receptor stal velice významným terapeutickým cílem. Nedávné studie ukázaly, že aktivace aryl uhlovodíkového receptoru (AhR) silnými ligandy může vyvolat proteasomální degradaci AR. Cílem této studie bylo analyzovat, zda vybrané indolové sloučeniny mohou vyvolat degradaci AR jako důsledek aktivace AhR a tím také narušit signální dráhu AR. Na základě předchozího výzkumu byly vybrány kandidátní sloučeniny obsahujících ve své struktuře indolový skelet, u nichž byla prokázána schopnost aktivace AhR. Z celkového počtu 22 testovaných indolů bylo zjištěno, že 8 z nich bylo schopno indukovat transkripční aktivitu AhR a současně také potlačovat DHT-indukovanou transkripční aktivitu AR, snižovat expresi AR-cílových genů, konkrétně *KLK3* a *FKBP5* na úrovni mRNA i proteinu. Pomocí chromatinové precipitace (ChIP) byla potvrzena snížená vazba AR do promotoru genu *KLK3* po inkubaci s vybranými indoly. Pro studium vztahu mezi AhR a AR byla také vytvořena AhR knock-out buněčná linie (CRISPR/Cas9 systém). Získané výsledky naznačují, že suprese AR pozorovaná na úrovni proteinu nebyla důsledkem proteasomální degradace AR, protože inhibice byla detekovaná už na úrovni transkripce (mRNA). Nicméně vybrané indolové sloučeniny vykazovaly silný potenciál potlačení signální dráhy AR. Tento mechanismus však bude odlišný, než bylo původně předpokládáno.

Klíčová slova indolové deriváty, AhR, AR
Počet stran 139
Počet příloh 2
Jazyk Anglický

BIBLIOGRAPHICAL IDENTIFICATION

Author's first name and surname	Mgr. Eliška Zgarbová
Title	The effect of indole derivatives on aryl hydrocarbon receptor activity in prostatic cell lines
Type of thesis	Dissertation
Department	Department of Cell Biology and Genetics
Supervisor	doc. Ing. Radim Vrzal, Ph.D.
Year of the thesis defense	2024

Abstract

Prostate cancer is a prevalent cancer among men, and its development is tightly linked to the signalling pathways of androgen receptor (AR). Therefore, AR has become a critical therapeutic target. Studies have shown that the activation of the aryl hydrocarbon receptor (AhR) by strong, potent ligands can induce the proteasomal degradation of AR. Based on previous research, 22 compounds with indole scaffolds reported to activate AhR were selected and analyzed to test this hypothesis in prostate cancer cell lines. Out of these 22 indoles, 8 were found to simultaneously activate AhR and suppress AR and were thus selected for further experiments. Selected indoles decreased the expression of DHT-inducible AR-target genes, specifically *KLK3* and *FKBP5*, on the mRNA and protein levels. Chromatin immunoprecipitation (ChIP) assay confirmed the reduced AR binding to *KLK3* promoter. In addition, a prostate-specific CRISPR/Cas9 AhR knockout system was developed and suggested relationship between AhR and AR was observed. However, these findings indicate that the suppression observed on AR protein levels is not likely a consequence of AhR-induced proteasomal degradation of AR since the inhibition was detected already during the transcription process. Nevertheless, selected indoles displayed a strong potential for AR-signaling suppression through a different mechanism, yet to be described.

Keywords	indole derivatives, AhR, AR
Number of pages	139
Number of appendices	2
Language	English

TABLE OF CONTENTS

ABBREVIATIONS

3MC	3-methylcholanthrene
ADT	Androgen deprivation therapy
AF1	Activation function 1
AF2	Activation function 2
AhR	Aryl hydrocarbon receptor
AhRR	AhR repressor
AIP	AhR-interacting protein
AR	Androgen receptor
ARE	Androgen response element
ARNT	AhR nuclear translocator
ATCC	American Type Culture Collection
BAFF	B-cell activating factor
BaP	Benzo[a]pyrene
BEAS-2B	Human bronchial epithelial cells
bHLH	Basic-helix-loop-helix
BRG1	Brahma-related gene 1
CCL1	C-C motif chemokine ligand 1
CE	Cryptic exon
CH223191	2-methyl-2H-pyrazole-3-carboxylic acid (2-methyl-4-o-tolylazo-phenyl)-amide
ChIP	Chromatin immunoprecipitation
CUL4B	Cullin B
$CUL4B^{AhR}$	Cullin-RING ligase 4B complex with AhR
CXCL13	Chemokine (C-X-C motif) ligand 13
CYP	Cytochrome P450
DBD	DNA binding domain
DDB1	Damaged-DNA-binding protein 1
DHEA	Dehydroepiandrosterone
DHT	Dihydrotestosterone

DMEM	Dulbecco’s modified Eagle’s medium
DMSO	Dimethylsulfoxide
DOX	Doxorubicin
DRE	Dioxin response element
DSS	Dextran sulphate sodium
E1	Ubiquitin-activating enzyme
E2	Ubiquitin-conjugating enzyme
E3	Ubiquitin-ligase
EC_{50}	Half-maximal effective concentration
EGFR	Epidermal growth factor receptor
ENZ	Enzalutamide
ER	Estrogen receptor
FBS	Fetal bovine serum
FICZ	6-formylindolo[3,2-b]carbazole
FSH	Follicle-stimulating hormone
GAPDH	Glyceraldehyde 3-phosphate dehydrogenase
GI	Gastrointestinal tract
GNF351	*N*-(2-(1*H*-indol-3-yl)ethyl)-9-isopropyl-2-(5-methyl pyridine-3-yl)-9*H*-purin-6-amine
GR	Glucocorticoid receptor
HAHs	Halogenated aromatic hydrocarbons
HATs	Histone acetyltransferase enzymes
HR	Hinge region
Hsp90	Heat shock protein 90 chaperons
IAA	Indole-3-acetate
IBD	Inflammatory bowel disease
IC_{50}	Half-maximal inhibitory concentration
iDRE	Inhibitory dioxin response element
IMP	Importin

ITE	2-(1′H-indole-3′-carbonyl)-thiazole-4-carboxylic acid methyl ester
KLF6	Krüppel-like factor 6
KO	Knock-out
LBD	Ligand binding domain
LH	Luteinizing hormone
LHCGR	Luteinizing hormone/choriogonadotropin receptor
mAhR	Mouse AhR
MNF	3-methoxy-4-nitroflavone
NAFLD	Non-alcoholic fatty liver disease
NC-XRE	Non-consensus dioxin response element
NES	Nuclear export signal
NF-κB	Nuclear factor kappa B
NLS	Nuclear localization signal
NRs	Nuclear receptors
NTD	NH_2 terminal domain
$p21^{Cip1}$	Cyclin-dependent kinase inhibitor
PAHs	Polycyclic aromatic hydrocarbons
PAI-1	Plasminogen activator inhibitor-1
PAS	Per-Arnt-Sim motif
PBS	Phosphate-buffered saline
PI3K	Phosphoinositide 3-kinase
poly-Q	Glutamine-rich segment
PPAR-γ	Peroxisome proliferation-activated receptor γ
PXR	Pregnane-X-receptor
Rbx1	RING-box protein 1
RE	Response/responsive element
RLU	Relative light unit
RPMI	Rosewell Park Memorial Institute medium
SD	Standard deviation

StAR	Steroidogenic acute regulatory protein
T	Testosterone
TAD	Transactivation domain
TBL3	Transducin-β-like protein 3
TCDD	2,3,7,8-tetrachlorodibenzo-*p*-dioxin
TIPARP	TCDD-inducible poly-ADP-ribose polymerase enzyme
TNFα	Tumor necrosis factor alpha
TR	Thyroid hormone receptor
TR4	Testicular nuclear receptor T4
Trp	L-Tryptophan
UBE2C	Ubiquitin-conjugating enzyme 2C
VDEC	Vas deferens epithelial cells
WT	Wild type
XAP2	Immunophilin-like X-associated protein 2
XRE	Xenobiotic response element
ZO-1	Tight junction protein 1

1 INTRODUCTION

Prostate cancer is a prevalent cancer in men, with over 1.4 million new cases detected every year, affecting one in six men in their lifetime. The development of this disease is a result of uncontrolled cellular growth of prostate, which is a small gland situated below the bladder and around the urethra. Male sex hormones androgens regulate the growth of prostate epithelial cells by influencing the signalling pathway of androgen receptor (AR), a member of the nuclear receptor (NRs) superfamily. The AR is a ligand-activated transcription factor that induce the expression of AR-target genes, such as *KLK3* or *FKBP5*, upon ligand binding. The AR signalling pathway is responsible for the normal development and maintenance of the male reproductive system, along with prostate epithelial cell proliferation and apoptosis. However, uncontrolled overstimulation of AR signalling is considered a significant factor in prostate cancer progression by regulating an oncogenic gene signature that promotes uncontrolled cell growth.

The treatment of prostate cancer depends on the stage of disease progression. Local approaches include surgical removal of the prostate gland (prostatectomy), targeted cryotherapy or radiation therapy. Once the disease progresses into the nearby tissues, advanced therapy methods are required, which are often referred to as androgen deprivation therapy (ADT). The suppression of circulating androgens or the blockage of AR signalling pathway are an effective approach of inhibition of the prostate cancer progression. Advanced methods include hormone therapy, chemotherapy or immunotherapy. Hormone therapy is mediated through administration of antiandrogens, such as Bicalutamide or Enzalutamide, which inhibits the binding of androgens to AR. Chemotherapy is based on usage of anticancer medication to kill or inhibit the growth of cancer cells. Docetaxel is a typical chemotherapeutic drug used in prostate cancer treatment.

Initially, ADT shows successful results as it slows down or even stops the growth of androgen-dependent prostate cancer. However, this type of cancer often develops into a castration-resistant type (CRPC) during the ADT. CRPC is characterized by the ability of the cancer cells to continue growing and progressing even in the absence of androgens. The risks of ADT include not only the development of currently untreatable CRPC but also a wide range of severe side effects associated with the administration of these drugs, such as cardiovascular diseases, osteoporosis, hepatic dysfunction, renal failure, neurotoxicity fatigue, or even death with the most severe cases. For this reason,

constant investigation of novel therapies in prostate cancer aims to overcome extreme side effects.

A novel approach for treating prostate cancer involves suppressing the AR signalling pathway through the activation of aryl hydrocarbon receptor (AhR). AhR is a ligand-activated transcription factor that plays a crucial role in maintaining homeostasis and various patho-/physiology processes such as inflammation, biotransformation of xenobiotics, and cancer progression. Although AhR is not a member of NRs, it shares similarities in structure and signalling mechanisms.

The predominant canonical genomic pathway of AhR is activated by endogenous or exogenous ligands, which translocate AhR into the nucleus. AhR then forms a heterodimer with its dimerization partner, AhR nuclear translocators (ARNT). The AhR/ARNT complex binds to specific responsive elements in the promoter, which induces the expression of AhR-target genes. AhR can also regulate various processes through non-canonical genomic pathways or in a non-genomic manner. A non-canonical genomic pathway includes the interaction of AhR with other receptors and proteins, such as Kruppel-like factor 6 (KLF6), or members of the NF-κB protein family. In a non-genomic pathway, AhR acts as a ligand-dependent E3 ubiquitin ligase, inducing proteasomal degradation of other receptors, such as estrogen receptor (ER) or AR.

Studies have demonstrated that AhR-mediated proteasomal degradation of AR occurs for various AhR ligands and activators, such as icaritin or Carbidopa. However, original research data has indicated that AR degradation only occurs for potent AhR ligands (dioxin, 3-methylcholanthrene). Consequently, several studies have shown a close association between AhR and AR in prostate cancer cells. Different AhR ligands have been reported to suppress prostate cancer development through various mechanisms, indicating that AhR/AR interactions could represent a potential target for prostate cancer treatment.

AhR ligands and activators include a variety of molecules of both endogenous and exogenous origin. Among them, many of these compounds carries an indole ring in their structure. Therefore, the aim of this study was to determine whether selected substances with an indole structure are capable of induction of the previously mentioned mechanism, meaning AR suppression through simultaneous AhR activation. To achieve this, 22 indolic compounds of endogenous and exogenous origin were selected. Our research team has previously reported that some of these indoles were capable

of AhR activation in human hepatoma carcinoma cells. However, the effect of these substances on prostate cancer cells has not yet been tested.

The theoretical section of this thesis provides an overview of the current state of the art in this field. The first few chapters thoroughly describe both receptors, covering topics such as their structure, signalling mechanisms, respective ligands, and biological functions. The subsequent chapter focuses on prostate cancer and its current therapies. Finally, the last chapter of the theoretical section summarizes the information and establishes a connection between the interaction of AhR and AR in the context of prostate cancer.

The experimental part of this study was divided into three main experimental phases. In **Phase I**, the aim was to identify indolic compounds that activate AhR and suppress AR simultaneously using Reporter gene assay (RGA). Only indoles that met both requirements were selected for further experiments. **Phase II** assessed how these particular indoles affected the expression of AhR- and AR-target genes, and respective protein levels. **Phase III** involved further in-depth functional experiments, where the effects of selected indoles were investigated by chromatin immunoprecipitation (ChIP) to analyse the recruitment of the *KLK3* promoter or by using flow cytometry for cell cycle analysis. To assess the effects of indoles in an AhR-free environment, stable AhR CRISPR/Cas9 knockout of 22Rv1 cells was constructed.

2 AIMS

The main goal of this study is to evaluate the effects of selected indole derivatives on the activity of aryl hydrocarbon receptor (AhR) in prostatic cancer cell lines and identify the predicted connection between AhR activation and suppression of the androgen receptor (AR) signalling pathway. The aims of this thesis were divided into the following subtasks:

1. To assemble a comprehensive literature review on the topic of AhR/AR crosstalk, providing a detailed description of both receptors and their connection to prostate cancer
2. Analyse the potential cytotoxic effects of selected indoles in prostate cancer cell lines
3. To screen the effects of selected indoles on AhR and AR transcription activity using the Reporter gene assay
4. To monitor the AhR- and AR-target gene's expression at both mRNA and protein levels
5. To clarify the mechanisms of action by analysing the effects of selected indolic compounds through Chromatin immunoprecipitation or flow cytometry method
6. To develop a novel AhR-knockout prostate-specific model
7. Attempt to formulate a general conclusion about the relationship between the structure of indolic compounds and AhR-mediated impact on prostate cancer cells based on the findings of this study

3 THEORETHICAL BACKGROUND

3.1 Nuclear Receptors

The nuclear receptors (NRs) superfamily is a group of ligand-activated transcription factors that participates in several physiological processes, including endogenous signalling, various metabolic pathways, or reproduction. Additionally, NRs also play a significant role in developing various pathological states, such as inflammation or cancer [10]. The discovery of the glucocorticoid receptor (GR), the first member of this family to be cloned, dates back to 1985 [11]. Subsequently, 49 distinct NRs throughout the human genome have been identified, described, and divided into six families (0-6) [12, 13]. Structurally, NRs are intracellular proteins that interact with other molecules, like hormones or vitamins, resulting in a particular biological response by regulating the expression of target genes [10]. Small lipophilic ligands such as steroids, retinoids, and phospholipids regulate most NRs. However, there are some NRs for which the specific ligand has not yet been discovered. These are called "orphan" receptors [14]. When the ligand is eventually discovered and identified, the process is referred to as "deorphanization" [15].

The structure of NRs can be divided into several domains, including a variable NH_2-terminal transactivation domain, a DNA binding domain (DBD), a hinge region (HR), and a ligand binding domain (LBD). The final sequence is the C-terminal domain, which is also highly variable among members [16, 17]. The NH_2-terminal domain, also known as the A/B or transactivation domain, is susceptible to post-translational modifications and thus represents an essential regulatory target [18-20]. The primary function of the DBD is to recognize and bind to specific sequences in target DNA throughout the genome, known as responsive or response elements (RE). These RE sequences can be arranged as direct, inverted, or everted repeats [17, 21]. HR is a flexible sequence located between DBD and LBD [22]. LBD is responsible for ligand binding, which subsequently leads to conformational changes in NRs. This region is considered a molecular switch and represents the central architectural element responsible for biological reactions based on ligand binding [17]. The final C-terminal sequence, known as the transactivation domain (TAD), varies considerably among NRs. Complete or partial deletions of this domain were reported to disturb the transcriptional activity of the affected receptor [17, 23].

Upon ligand binding, NRs form homo- or heterodimers with specific dimerization partners. This process has also been described between individual nuclear or steroid receptors [24]. Following conformational changes and nuclear translocation, this complex binds to a responsive element in the target gene's promoter [25]. Coregulator proteins (coactivators or corepressors) and the general transcriptional machinery are recruited to activate or repress target gene expression [26]. Because NRs regulate thousands of genes, their activity is strictly controlled. Abnormal NRs activity can lead to the progression of various diseases, such as cancer, diabetes, or chronic inflammation [13].

Table 1 provides a list of NRs identified in the human body along with their respective ligands, demonstrating the diverse range of biological processes they can influence. Due to their broad range of effects on multiple levels, targeting specific NRs is a significant therapeutic approach.

Table 1: List of NRs identified in human body and their corresponding ligands. Modified according to Weikum *et al.* 2018 [13].

Family	Name	Encoding gene	Ligand
0B	Dosage-sensitive sex reversal-adrenal hypoplasia congenita critical region on X ch.	*NR0B1*	Orphan
	Short heterodimeric partner	*NR0B2*	
1A	Thyroid hormone receptor-α	*THRA*	Thyroid hormones
	Thyroid hormone receptor-β	*THRB*	
1B	Retinoic acid receptor-α	*RARA*	Retinoic acids
	Retinoic acid receptor-β	*RARB*	
	Retinoic acid receptor-γ	*RARG*	
1C	Peroxisome proliferator-activated receptor-α	*PPARA*	Fatty acids
	Peroxisome proliferator-activated receptor-β	*PPARD*	
	Peroxisome proliferator-activated receptor-γ	*PPARG*	
1D	Reverse-Erb-α	*NR1D1*	Heme
	Reverse-Erb-β	*NR1D2*	
1F	Retinoic acid-related orphan-α	*RORA*	Sterols
	Retinoic acid-related orphan-β	*RORB*	
	Retinoic acid-related orphan-γ	*RORC*	

1H	Farnesoid X receptor	*NR1H4*	Bile acids
	Farnesoid X receptor-β	*NR1H5P*	Orphan
	Liver X receptor-α	*NR1H3*	Oxysterols
	Liver X receptor-β	*NR1H2*	
1I	Vitamin D receptor	*NR1I1*	Calcitriol
	Pregnane X receptor	*NR1I2*	Endo- and xenobiotics
	Constitutive androstane receptor	*NR1I3*	Xenobiotics
2A	Hepatocyte nuclear Factor-4-α	*HNF4A*	Fatty acids
	Hepatocyte nuclear Factor-4-γ	*HNF4G*	
2B	Retinoid X receptor-α	*RXRA*	9-*Cis* retinoic acid
	Retinoid X receptor-β	*RXRB*	
	Retinoid X receptor-γ	*RXRG*	
2C	Testicular Receptor 2	*NR2C1*	Orphan
	Testicular Receptor 4	*NR2C2*	
2E	Tailless homolog orphan receptor	*NR2E1*	Orphan
	Photoreceptor-cell-specific nuclear receptor	*NR2E3*	
2F	Chicken ovalbumin upstream promoter-TF α	*NR2F1*	Orphan
	Chicken ovalbumin upstream promoter-TF β	*NR2F2*	
	Chicken ovalbumin upstream promoter-TF γ	*NR2G6*	
3A	Estrogen receptor-α	*NR3A1*	Estrogens
	Estrogen receptor-β	*NR3A2*	
3B	Estrogen-related receptor-α	*ESRRA*	Orphan
	Estrogen-related receptor-β	*ESRRB*	
	Estrogen-related receptor-γ	*ESRRG*	
3C	Glucocorticoid receptor	*NR3C1*	Glucocorticoids
	Mineralocorticoid receptor	*NR3C2*	Mineralocarticoids
	Progesterone receptor	*NR3C3*	Progesterone
	Androgen receptor	*NR3C4*	Androgens
4A	Nerve growth Factor 1B	*NR4A1*	Orphan
	Nurr-related Factor 1	*NR4A2*	Unsaturated fatty acids
	Neuron-derived orphan Receptor	*NR4A3*	Orphan
5A	Steroidogenic Factor 1	*NR5A1*	Phospholipids
	Liver receptor Homolog-1	*NR5A2*	
6A	Germ cell nuclear factor	*NR6A1*	Orphan

3.1.1 Ligands

A ligand is an endogenous or exogenous compound that binds to a receptor protein and triggers a biological response [27]. According to receptor theory, two key events can define ligand-receptor interactions. The first is recognition, which occurs when the ligand binds to the receptor. The second is an early biological response, which involves the activation of the receptor [28, 29].

During the binding process, the ligand physically interacts with the receptor at the orthosteric or allosteric site. Orthosteric ligands bind to the active site, known as conventional LBD. On the other hand, allosteric ligands can bind elsewhere on the protein structure, out of the ordinary LBD, which is why this position is called an allosteric binding site [30]. The strength of this bond is determined by affinity, which is defined by the dissociation constant (K_D) and half-maximal inhibitory concentration (IC_{50}). According to receptor theory, these values refer to the respective ligand concentration required to bind to 50 % of the receptors. Therefore, the affinity indicates how tightly the ligand is bonded with the receptor [29, 31]. Ligand-induced receptor activation is assessed based on its potency and efficacy. Efficacy represents the extent of the response and is expressed in %. It is derived as a ratio of maximal efficacy (E_{MAX}) of a particular ligand compared to the E_{MAX} of a reference full agonist ligand. Potency (EC_{50}) refers to the effective concentration of a ligand that elicits a half-maximal response. Ligands can be classified based on their binding affinity and response as full agonists (eliciting a maximal response equal to the reference ligand), partial agonists (occupying 100% of the receptor but eliciting only submaximal response), antagonists (binding to the receptor but not eliciting any response), or inverse agonists (binding of the ligand inhibits the activity of the receptor) [32]. Among others, the biological response upon ligand binding is highly tissue-specific [33].

Figure 1 illustrates the conformational changes of NR in its inactive state and upon ligand binding.

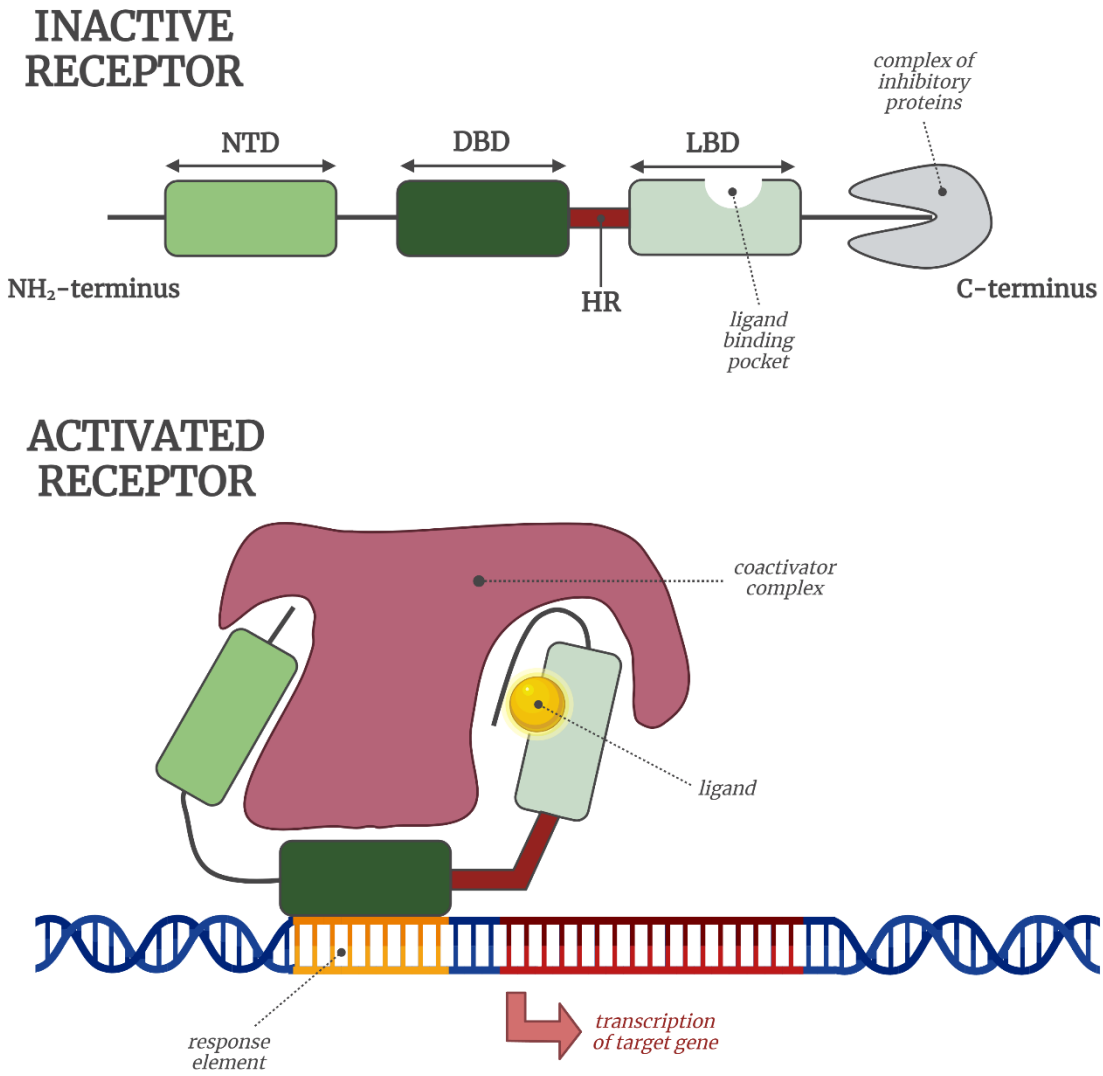

Figure 1: Nuclear receptor structure and conformation. Nuclear receptors (NRs) have a specific structure consisting of different domains, each with a specific role: the NH_2-terminal domain (NTD) is also known as the transactivation domain, the DNA-binding domain (DBD), and the ligand-binding domain (LBD). The DBD and LBD are usually connected by a small hinge region (HR). The correct functioning of the individual domains is essential for maintaining proper NR activity. In their inactive state (upper part of the figure), NRs are located in the cytoplasm, bound to chaperones and other inhibitory proteins. Upon binding to a ligand, i.e. receptor activation (lower part of the figure), NRs undergo conformational changes, translocate into the nucleus, and bind to the response element in the promoter sequence. Following the recruitment of coactivators, this process results in the transcription of the respective target gene (modified according to Alberts *et al*. 2008, *Chapter 15: Mechanisms of Cell Communication* [8]).

3.2 Aryl Hydrocarbon Receptor

Although not classified as a member of the NR superfamily, the aryl hydrocarbon receptor (AhR) shares several similarities with NRs, including structure or signalling mechanisms, and is considered more of a xenoreceptor. AhR is also a ligand-activated transcription factor essential for regulating host physiology. Developing and regulating a broad range of pathophysiological conditions, including cancer, inflammation, or immune disorders, are also closely affiliated with this receptor. The existence of AhR was confirmed in 1976 by Poland and Glover using specific radiolabelled potent inducer 2,3,7,8-tetrachlorodibenzo-*p*-dioxin (TCDD) [34]. However, based on *in vivo* experiments, the existence of AhR was already predicted in the 1960s [35]. A study conducted in 1993 by Dolwick *et al*. compared human AhR with its murine homologue using cDNA analysis. Additionally, this study showed that the expression of human AhR on mRNA level occurs highly in the placenta, lungs, pancreas, and liver. This experimental evidence proved the expression of human AhR for the first time [36, 37].

Over the years, it was demonstrated that AhR is widely distributed in various vertebrate tissues. Additionally, the occurrence of homologous AhR genes has also been demonstrated in invertebrates. The *Spineless* gene in *Drosophila melanogaster* is an example of such AhR homolog. It encodes a specific transcription factor that plays a role in specifying the identity of distal antennal segments. AhR-like genes and their encoded proteins act through different pathways in invertebrates' systems than vertebrates [35, 38].

In the human genome, AhR is encoded by the *AhR* gene, which consists of 11 exons [16]. This gene is localized on the short p arm of chromosome 7 (p21-15) [39, 40]. Due to its wide distribution in organism and the capability of influencing many metabolic pathways, AhR recently became a promising therapeutic target for various diseases, e.g., atopic dermatitis, inflammatory bowel disease, or multiple sclerosis [41]. Several synthetic and environmental substances, including elements found in food, components originating from the microbiota, and endogenous tryptophan (Trp) metabolites, can trigger or influence AhR signalling pathways [42]. The following chapters will describe the structure of AhR, activation, and role in human patho-/physiology.

3.2.1 AhR Structure

AhR belongs to the basic-helix-loop-helix/Per-Arnt-Sim (bHLH/PAS) family [43]. Members of this family are divided into two main classes based on their function. Class I includes proteins directly involved in regulating the response to changes in the surrounding environment [35, 44]. Proteins classified as class II members are heterodimerization partners for class I proteins. The proper function of regulating target gene expression can only be accomplished if the dimer of two bHLH-PAS proteins is formed [45]. AhR is classified as a class I protein, while its dimerization partner, AhR nuclear translocator (ARNT), is classified as a class II protein. AhR shares a similar structure with ARNT but also with AhR repressor (AhRR) [1, 46]. Besides DBD, AhR, ARNT, and AhRR contain the PAS-A domain responsible for dimerization. Despite having a PAS-B domain, ARNT is incapable of binding ligands. AhRR lacks the PAS-B region completely (**Figure 2**) [1]. The function of individual domains is well understood today. However, the isolation and crystallization of pure human AhR have not yet been achieved [47, 48].

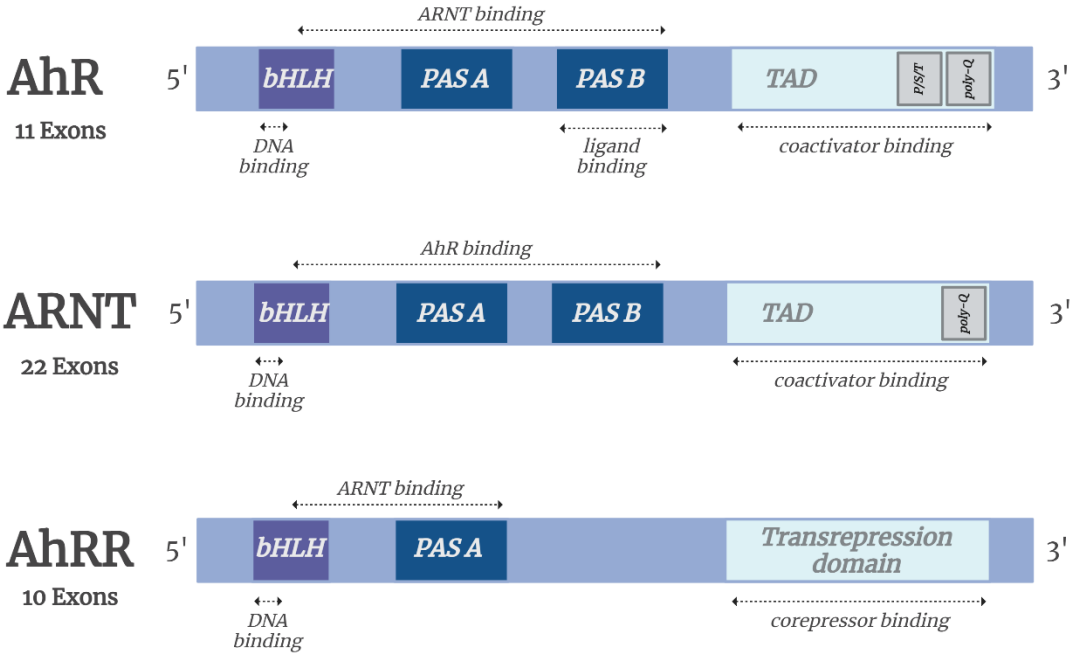

Figure 2: Human AhR, ARNT, and AhRR: bHLH/PAS proteins. The **AhR protein** is encoded by the *AhR* gene, which consists of 11 exons. It contains three functional domains: the DBD, the PAS domain (A and B), and the TAD domain. The PAS domains are responsible for dimerization and ligand binding, while the TAD domain allows specific coactivators to bind. The **ARNT protein**, encoded by the *ARNT* gene consisting of 12 exons, shares similar functional domains with AhR. However, ARNT is not capable of binding ligands. On the other hand, the **AhRR protein** contains the DBD and the PAS-A, but it completely lacks the PAS-B domain. Therefore, AhRR can form a heterodimer, but it is not able to bind ligands. Additionally, AhRR contains the TAD domain on the C-terminal region, which is susceptible to corepressor binding (modified according to Larigot *et al*. 2018 [1]).

3.2.1.1 bHLH Domain

In the NH_2-terminal region of AhR lies specific DBD, basic helix-loop-helix (bHLH). This motif's existence was first described in 1989 and further characterized by Murre *et al*. [49, 50]. bHLH is formed by two α-helices, which are paired together through a short loop. The first region includes mainly basic residues and is responsible for interaction with target DNA. The second section consists substantially of hydrophobic residues and is involved in the dimerization process [2, 50]. According to Ikuta *et al*., AhR possesses a nuclear localization signal (NLS) in this NH_2-terminal region between 13 and 61 amino acid residues [51]. This NLS was reported to be consisted of two segments (bipartite NLS) separated by approximately 10 amino acids [52]. Phosphorylation on two positions of NLS (Ser12 and Ser36) inhibited the ligand-dependent nuclear translocation of AhR [53]. NLS displays the contrary role compared to nuclear export signal (NES), which is localized within the helix 2 of the bHLH domain [51]. It appears to be a leucin-rich region consisting of 11 amino acids. AhRR was reported to contain a similar NES as AhR [54]. The dimerization region, including sequences from the bHLH domain and PAS-A domain, is crucial for ARNT binding and formation of a functional AhR/ARNT heterodimer [1].

3.2.1.2 PAS Domain

bHLH is followed by two tandemly incorporated PAS motifs (PAS-A and PAS-B) responsible for ligand binding (LBD) [55]. "PAS" is a shortage for Per-Arnt-Sim. This term is based on specific proteins that contain this region: *Droshophila* Period, AhR nuclear translocator, and *Droshophila* Single-minded [56, 57]. Using the nuclear magnetic resonance, the structure of the PAS domain was determined as a fold of five-stranded β-sheets in antiparallel order surrounded by α-helices [58, 59]. This motif creates a pocket that enables ligand attachment [60]. Each of the two PAS regions was defined to be approx. 50 amino acid residues long and are linked through an additional 150 amino acids [57, 61]. PAS-A region is also involved in the dimerization process. The PAS-B domain is directly responsible for ligand binding [55, 62]. However, an AhR mutant without a specific PAS-B region was also described to be constitutively active. This mutant shows transcriptional activity even without sufficient ligand binding [63, 64].

3.2.1.3 C-terminal Domain

Within the C-terminal region lies TAD, which is responsible for influencing the transcriptional activity of AhR. Typically, it is divided into three segments: acidic, glutamine-rich, and proline-serine-threonine-rich regions [65]. This terminal part binds specific co-activators and co-repressors of AhR, like AhRR [1, 66].

In summary, all the above-mentioned domains are crucial for maintaining proper AhR signalling. AhR functional domains and their respective functions are illustrated in **Figure 3**.

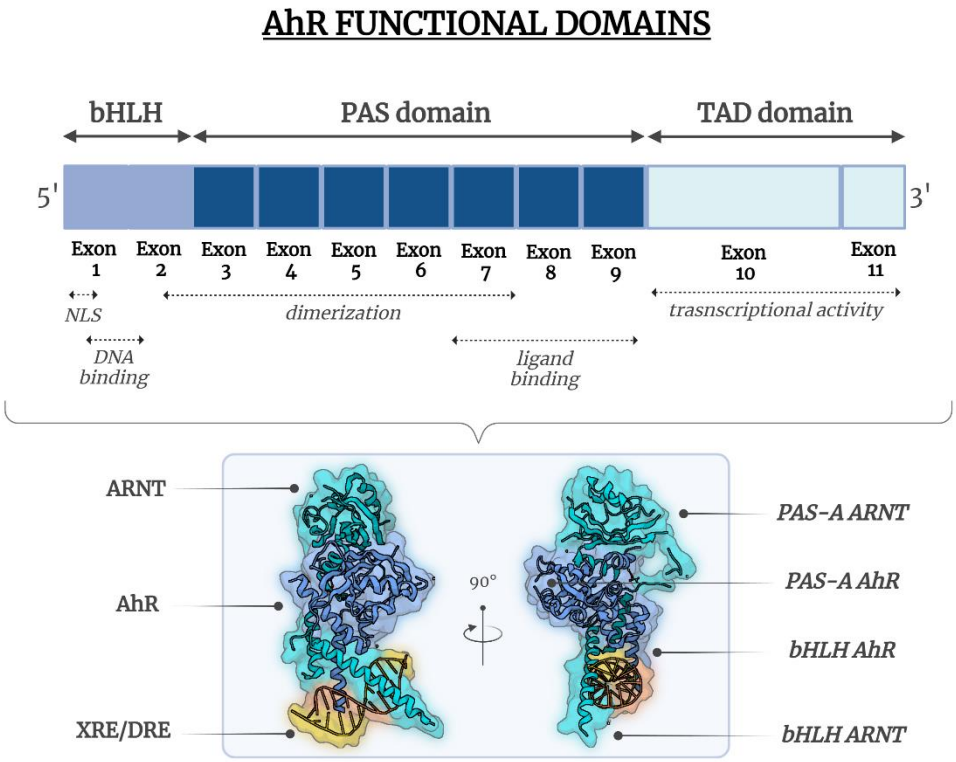

Figure 3: Human AhR domains and their respective functions. The bHLH domain is encoded by exons 1 and 2. Additionally, this domain contains sequences responsible for proper nuclear import (NLS) and export (NES) of AhR. The following PAS domain is divided into two regions, A and B, and is encoded by seven exons (3-9). The C-terminal TAD domain is encoded by exons 10 and 11. Once AhR forms a heterodimer with ARNT, the AhR/ARNT complex binds to specific XRE/DRE in DNA, influencing the expression of AhR target genes. The crystal structure of the AhR/ARNT complex binding to XRE/DRE is shown at the bottom of this figure (modified according to Larigot *et al*. 2018 and Seok *et al*. 2017 [1, 2]).

3.2.2 AhR Signalling

A plethora of exogenous and endogenous ligands can activate AhR. This activation triggers downstream signalling pathways that result in various physiological responses. Therefore, the regulation of AhR signalling is critical for maintaining proper cellular function and homeostasis.

In its inactive form, AhR is localized in the cytoplasm as a complex with two heat shock protein 90 chaperons (Hsp90), co-chaperone p23, and the immunophilin-like X-associated protein 2 (XAP2; also known as AhR-interacting protein, AIP) [67]. It was previously demonstrated that Hsp90 can bind to both domains, bHLH and PAS, to maintain the conformation susceptible to ligand binding [55, 68]. Studies indicate that the protein tyrosine kinase c-Src is also a member of this protein aggregate [68, 69]. The entire complex is responsible for maintaining the appropriate folding and stability of unliganded AhR. This conformation helps to recognize ligands correctly. Additionally, it prevents unwanted nuclear translocation in the absence of ligands [67, 70]. Once the ligand is bound to the LBD, Hsp90, and XAP2 are released from the multiprotein complex, leading to the conformational changes of AhR. Triggered changes expose NLS, which can be recognized by members of the importin superfamily (IMPα, IMPβ1), enabling a nuclear import. [53, 71]. Subsequently, the whole complex is transported into the nucleus through the nuclear pore complexes. On the nuclear interface, IMPβ1 binds to the RanGTP, and subsequently, NLS dissociates [72]. Thus, AhR nuclear translocation is completed.

For a long time, AhR common canonical genomic signalling pathway was believed to be the primary mechanism through which AhR agonists elicit their biological and toxicological impacts. However, additional AhR signalling pathways have been identified over time, proving that AhR can exert its influence through various non-canonical and non-genomic mechanisms.

3.2.2.1 AhR Canonical Genomic Signalling

The canonical genomic pathway is presumably the most thoroughly studied signalling pathway of AhR, which was also the first to be described [1]. The conventional AhR canonical genomic mechanism of signal transduction can be summarized as the formation of a complex involving ligand, AhR, and ARNT binding to XRE/DRE, followed by the transcription of target genes in a ligand-dependent manner.

Upon ligand binding, AhR translocates into the nucleus and forms a stable heterodimer with its dimerization partner ARNT, which is predominantly localized in the nucleus, regardless of the presence or absence of ligand [73]. This AhR/ARNT heterodimer recruits several co-factors and binds covalently to regulatory sequences in the DNA of target genes. These regions are known as xenobiotic, or also dioxin, response elements (XRE/DRE) and contain specific 5′-GCGTC-3′sequence. XRE/DRE are typically situated close to the promoter of target genes [1, 35]. Recruitment of coactivators and co-factors includes CBP/p300 histone-acetyltransferase, RIP140, or SRC-1 [42]. This mechanism requires the attendance of ATP-dependent chromatin remodelling factors, such as Brahma-related gene 1 (BRG1) [74]. The result of this process is the regulation of the expression of AhR-target genes. Ultimately, once the expression of target genes is triggered, AhR is exported out of the nucleus to the cytosol through NES, where it undergoes rapid ubiquitin-proteasome-mediated degradation [1, 75, 76]. The nuclear export process is ATP-dependent and is established through exportin CRM1, which binds to the NES [77, 78].

AhR canonical genomic pathway is shown in **Figure 4**, along with its regulation by AhRR (*Chapter 3.2.2.4*).

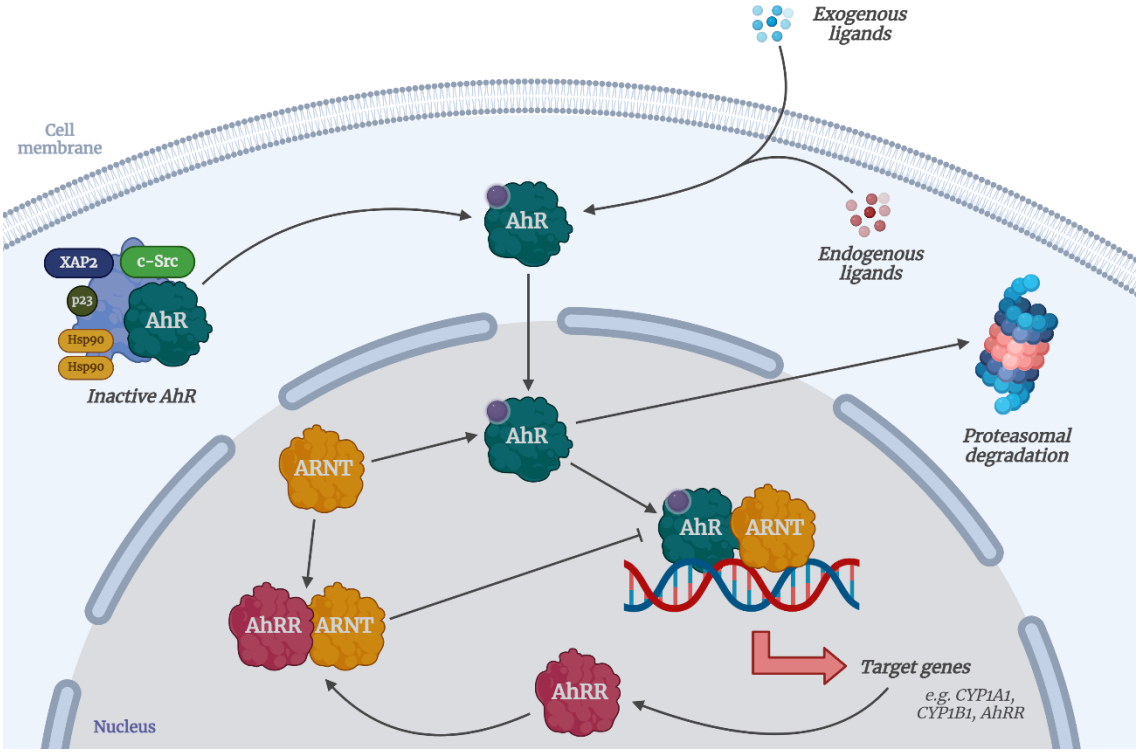

Figure 4: Overview of AhR canonical genomic pathway and regulation. In its inactive form, AhR is present in the cytoplasm in a complex with chaperones and inhibitor proteins. Upon binding of endogenous or exogenous ligands, AhR undergoes conformational changes and translocates to the nucleus. Inside the nucleus, AhR forms a heterodimer with ARNT and binds to XRE/DREs, which initiates the expression of AhR target genes. AhRR mediates negative regulatory feedback of AhR signalling. It forms a complex with ARNT and acts as a competitive inhibitor for AhR/ARNT, which prevents the expression of AhR target genes. Subsequently, AhR is transported outside the nucleus and undergoes proteasomal degradation (modified according to Larigot *et al*. 2018 [1]).

3.2.2.2 AhR Non-canonical Genomic Signalling

Predominantly, non-canonical genomic pathways include AhR forming a heterodimer with a different dimerization partner than ARNT [79]. The existence of this type of signalling was first suggested by Dere *et al*. This study involved a chromatin immunoprecipitation (ChIP) in mouse liver, identifying that half of the TCDD-AhR complexes were bound to DNA sequences that lacked a consensus XRE/DRE motif [80]. In following genomic studies, the presence of a unique non-consensus XRE (NC-XRE) with a 5'-GGGA-3'nucleotide motif was confirmed [81-83].

Crosstalk between AhR and members of the nuclear factor kappa B (NF-κB) family, which are involved in immunity, cell proliferation, and inflammation, was one of the first non-canonical interactions described [84]. In the pilot studies, mouse hepatoma cells were exposed to TNFα to activate NF-κB, and expression of *CYP1A1*, the AhR-target gene, was evaluated. Obtained results showed a suppression of TCDD-induced *CYP1A1* mRNA after TNFα treatment [85, 86]. In mammals, the NF-κB complex consists of five protein subunits: RelA (p65), RelB, *c*-Rel, NF-κB1 (p105/p50), and NF-κB2 (p100/p52) [84]. AhR can interact with RelA and RelB subunits and bind into NC-XRE regulated by both AhR or NF-κB. Studies suggest that when both AhR and NF-κB pathways are activated simultaneously, it can lead to either synergistic or antagonistic effects on respective target genes [87-89]. The formation of the AhR/ARNT/NF-κB complex decreased the expression of *CYP1A1* [9]. While AhR/RelB interaction results mainly in target-gene expression induction (e.g., *IL-8*), AhR interaction with RelA appears to have the opposite effect [90-92]. The formation of AhR/NF-κB heterodimer leads to the expression of target genes, which subsequently encode cytokines or chemokines, such as B-cell activating factor (BAFF), chemokine (C-X-C motif) ligand 13 (CXCL13), or C-C motif chemokine ligand 1 (CCL1) [93, 94].

Krüppel-like factor 6 (KLF6) was identified as a novel AhR binding partner by Wilson *et al.* [95]. The formation of AhR/KLF6 heterodimer was confirmed by ChIP and DNA binding studies. Mutational analyses also demonstrated that the protein-protein interaction of this complex occurs between the C-terminal domain of AhR and the N-terminal domain of KLF6 [79, 95]. It was recently demonstrated that cyclin-dependent kinase inhibitor $p21^{Cip1}$ induction depends on the AhR/KLF6 pathway [79, 82]. Moreover, the AhR/KLF6 complex promotes the expression of plasminogen activator inhibitor-1 (PAI-1), also known as serpine 1 [96].

Numerous studies described the interactions between AhR and other receptors, such as pregnane X receptor (PXR) [97], glucocorticoid receptor (GR) [98, 99], estrogen receptor (ER) [100], or thyroid hormone receptor (TR) [101]. To this day, the most studied crosstalk is between AhR and ER [102, 103]. It involves a combination of both, genomic and non-genomic mechanisms. However, both AhR/ER pathways lead to the inhibition of ER signalling [102, 104]. Through the genomic pathway, AhR triggers the expression of *CYP1A1* and *CYP1B1* target genes, ultimately enhancing estrogen catabolism [104]. Another AhR/ER interaction mechanism includes binding of the ligand:AhR:ARNT complex to specific inhibitory DRE (iDRE) [105]. Ligand:AhR:ARNT:iDRE complex cannot activate AhR target gene expression but it can prevent ER signalling from activating target genes [33, 106]. Direct AhR/ER interaction belongs to the non-genomic category. This protein-protein interaction leads to ubiquitination of ER, resulting in its proteasomal degradation [107].

Additionally, the crosstalk between AhR and AR was also reported (detailed in *Chapter 3.5*). **Figure 5** shows an overview of various types of AhR non-canonical genomic pathways.

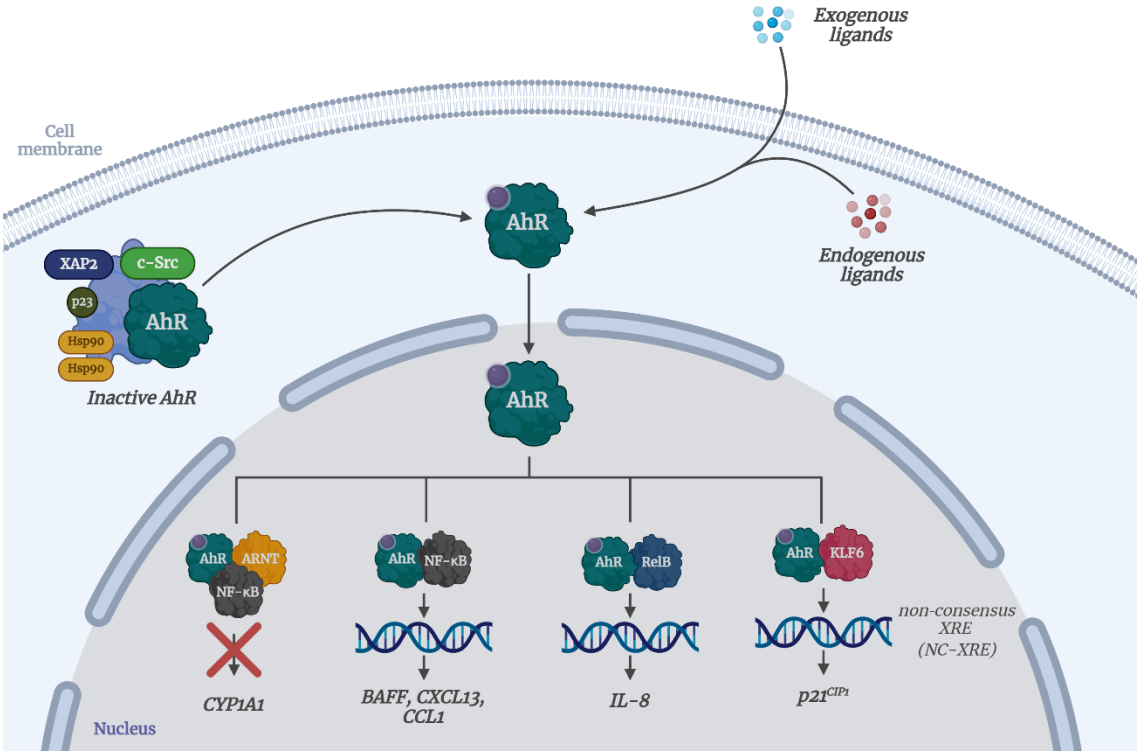

Figure 5: AhR non-canonical genomic signalling pathways. In its inactive form, AhR is present in the cytoplasm in a complex with chaperones and inhibitor proteins. Upon binding endogenous or exogenous ligands, AhR undergoes conformational changes and translocates to the nucleus. AhR forms a heterodimer inside the nucleus with different dimerization partners than ARNT, such as NF-κB (or its subunits RelA, RelB) and KLF6. Subsequently, this complex binds to NC-XRE, which initiates the expression of respective target genes. The formation of the AhR/ARNT/NF-κB complex suppresses the expression of *CYP1A1*. AhR/NF-κB complex binds to NC-XRE and initiates the expression of *BAFF*, *CXCL13*, or *CCL1*. The expression of *IL-8* is induced by the AhR/RelB heterodimer. The AhR/KLF6 complex induces expression of $p21^{Cip1}$ (modified according to Grishanova and Perepechaeva 2022 [9]).

3.2.2.3 AhR Non-genomic Signalling Pathway

AhR also can modulate molecular interactions through non-genomic mechanisms. The central system influencing various cellular processes of proteins includes posttranslational modifications, such as ubiquitination, phosphorylation, or adjusting of Ca^{2+} levels [108-110]. A novel AhR ability to act as a ligand-dependent E3 ubiquitin ligase was demonstrated in 2007 [111]. The ubiquitin-proteasome system is a crucial regulator of cellular homeostasis that targets specific proteins for degradation. To begin the process, an activating enzyme (E1) transfers a ubiquitin protein to a ubiquitin-conjugating enzyme (E2). The E2 enzyme, with the assistance of the ubiquitin ligase (E3), catalyses the transfer of small ubiquitin units to a target protein. This process is commonly called polyubiquitinylation and is followed by proteasomal degradation of ubiquitinated protein [112, 113]. It has been reported that AhR is a component of an atypical cullin-RING ligase 4B complex ($CUL4B^{AhR}$). This complex comprises five different proteins, including the scaffold protein Cullin 4B (CUL4B), RING-box protein 1 (Rbx1), damaged-DNA-binding protein 1 (DDB1), transducin-β-like protein 3 (TBL3), and the proteasome 19S cap [111, 114, 115]. Upon ligand binding, AhR acts as an adapter within this complex, enabling proteins to be targeted and processed through the ubiquitin-proteasome pathway [111]. Leucke-Johansson *et al*. have shown AhR to be capable of switching between its roles as E3 ubiquitin ligase and transcription factor based on the availability of ARNT [116]. If ARNT is available, AhR acts as a ligand-activated transcription factor through canonical genomic signalling. On the other hand, if ARNT interacts with other proteins, like AhRR, AhR switches its function and acts as an E3 ligase, triggering the formation of the $CUL4B^{AHR}$ complex [116, 117]. As previously stated, AhR-dependent protein degradation was reported for ER, but also for other receptors, e.g. AR or peroxisome proliferation-activated receptor γ (PPAR γ) [118, 119]. These non-genomic effects of AhR are an area of active research and may have implications for developing new therapeutics.

The existence of Src-mediated crosstalk between AhR and the epidermal growth factor receptor (EGFR) has also been reported. The Xie *et al*. study examined the ability of TCDD to induce phosphorylation of EGFR and ERK1/2 in human colon cancer cells (H508 and SNUC-C4) in a dose- and time-dependent manner. The phosphorylation of EGFR occurred at Tyr845, and the maximum effect was observed with 30 nM TCDD after 5 to 10 minutes upon TCDD addition. This TCDD-induced phosphorylation was

prevented by adding a ligand-selective AhR antagonist (CH223191) or a Src kinase selective inhibitor (PP2) in combination with TCDD. The experiments showed that AhR forms a complex with Src, which regulates Src kinase activity through phosphorylation at Tyr416 and dephosphorylation at Tyr527. The obtained data supported novel observations of Src-mediated AhR/EGFR crosstalk in colon cancer cells, resulting in ERK1/2 activation, thus stimulating cell proliferation [120]. Moreover, Src-mediated crosstalk between AhR and ERK1/2 was also reported after BaP treatment in human bronchial epithelial cells (BEAS-2B) [121]. The study conducted in hepatoma cells (HepG2) and breast epithelial cells (MCF-10A) by Dong *et al*. reported another link between AhR and Src kinase. The results showed that the activation of Src kinase induced by TCDD was everted by adding an AhR antagonist [122].

To conclude, several factors determine which path AhR will follow upon its activation. This interdisciplinary area covers a broad range of molecular components.

3.2.2.4 Regulation of AhR Signalling

AhR signalling has been reported to be regulated by several mechanisms, which represent a critical control point. One of the feedback loops is created as the ligand is metabolically eliminated. This process relates to accumulating active AhR in the nucleus and degrading the total AhR protein. Therefore, as a result of ligand activation of AhR and triggering the expression of target genes, the levels of AhR protein are decreased [77].

A negative feedback loop belongs among the well-studied AhR regulations. One of the crucial components of the negative regulatory feedback mechanism is *AhRR*, one of the AhR-target genes [46, 123]. The mechanism has been described in several *in vitro* studies using human cell lines. Additionally, *in vitro* and *in vivo* studies have been conducted in animal models to demonstrate this pathway [124]. AhRR negative feedback loop blocks the transcriptional activation of other AhR-target genes, like *CYP1A1*. AhRR, initially identified as a competitive repressor of AhR activity, can form a heterodimer with ARNT. This complex leads to direct competition between AhR/ARNT and AhRR/ARNT complexes to bind to XRE/DREs [125]. As previously described, the AhRR protein shares a similar structure with AhR; however, it lacks LBD and TAD domains [46]. The promoter sequence of the *AhRR* gene contains XRE/DREs that regulate the expression of AhRR [123]. Research indicates that AhR is in control of its own repressor protein expression [125-127]. Like AhR and ARNT, AhRR is also widely distributed in tissues of humans and other mammals, like the intestine, lungs, ovary, or testis [128].

AhR protein degradation mediated by the TIPARP mechanism is another example of AhR regulation. The name is based on the TCDD-inducible poly-ADP-ribose polymerase enzyme (TIPARP) encoded by the human *TIPARP* gene [129, 130]. This enzyme induces ribosylation, leading to its degradation in proteasome [77]. ADP-ribosylation occurs on various amino acid residues of AhR, including arginine, lysine, or cysteine [131]. Silencing of TIPARP using the siRNA method increased the expression of *CYP1A1* and *CYP1B1* AhR-target genes while also preventing the proteasomal degradation of AhR following the treatment with TCDD [132]. On the other hand, overexpressing TIPARP significantly decreased CYP1A1 protein levels. These findings indicate that TIPARP appears to act as a selective repressor of AhR [133, 134].

3.2.3 Ligands and activators of AhR

The spectrum of AhR ligands is composed of various components with different structures. These components include endogenous compounds, like Trp microbial metabolites or eicosanoids, and exogenous compounds, such as PAHs, synthetic compounds, or drugs [135]. Generally, endogenous ligands of AhR are reported to have a range of low to moderate affinity [136]. Because of its ability to bind many structurally diverse chemicals, AhR is commonly referred to as a "*promiscuous receptor*" [137]. However, it is essential to differentiate between AhR ligands (agonists or antagonists) and activators [138].

3.2.3.1 Environmental Pollutants

Originally, AhR was defined as a xenosensor for substances without natural origin (xenobiotics). AhR agonists were initially identified as constituents of environmental pollutants, including non-halogenated PAHs, like benzo[a]pyrene (BaP) [139] and 3-methylcholantherene (3MC) [140], or halogenated aromatic hydrocarbons (HAHs), such as TCDD [141] and biphenyls [142]. Three herbicides, namely linuron, diuron, and propanil, exhibited stronger AhR agonist activity than other pesticides during the *in vitro* screening study of 200 different pesticides [143]. **Figure 6** provides a summary of various environmental pollutants with the ability to activate AhR.

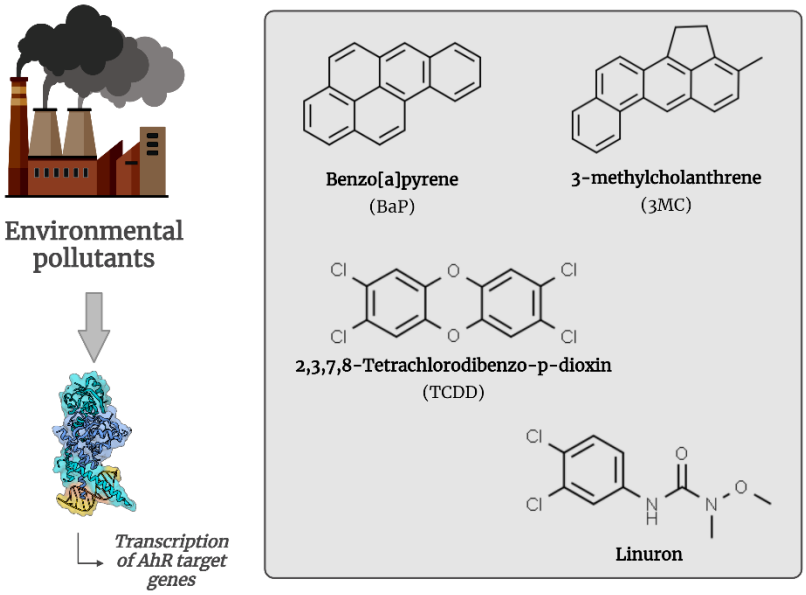

Figure 6: Environmental pollutants activating AhR. Many xenobiotics were identified as potent AhR agonists. This group includes PAHs (BaP, 3MC), HAHs (TCDD), or pesticides (linuron).

3.2.3.2 Drugs

AhR has been extensively studied as a potential therapeutic target. Tapinarof is a naturally occurring compound with anti-inflammatory properties that has been found to be effective in treating patients with plaque psoriasis and atopic dermatitis [144]. Recently, this drug was approved by the FDA [145]. Moreover, it was reported that Tapinarof is capable of activating AhR. Multiple *in vitro* and *in vivo* studies have shown that it induces expression of AhR-target genes in various cell types, e.g. skin cell line HaCaT, or in murine model. Findings suggest that the anti-inflammatory properties of Tapinarof may be related to AhR activation [144].

Omeprazole works as a proton pump inhibitor and was reported to have the ability to induce nuclear translocation of AhR followed by expression of *CYP1A1* [146, 147]. Omeprazole-sulfide, a metabolic product of omeprazole, has been discovered to act as an AhR antagonist in both mouse and human liver cancer cells [97]. Multiple studies have demonstrated that Omeprazole can switch between states from an AhR ligand-independent activator to an AhR pro-antagonist [138].

Weak AhR agonist activity was also reported with antimigraine triptan drugs, namely Donitriptan, and Avitriptan [148]. Carbidopa, a medication used during Parkinson's disease treatment, was reported to have the ability to activate AhR and trigger the expression of *CYP1A1* and *CYP1B1*. Ogura *et al*. showed that the activation of AhR induced by Carbidopa was blocked by the presence of AhR antagonists [149].

Several distinct research groups have identified Ketoconazole, an antifungal medicine, as an AhR activator [150, 151]. Commercially, ketoconazole is available as a mixture of two *cis* enantiomers, but the drug also contains various impurities. It was found afterward that this medication’s strong AhR-activating abilities depend on its purity. The strong AhR activation observed was due to the presence of impurities, not the effect of the drug itself [152].

Chemical structures of various drugs which were reported to activate AhR are displayed in the **Figure 7**.

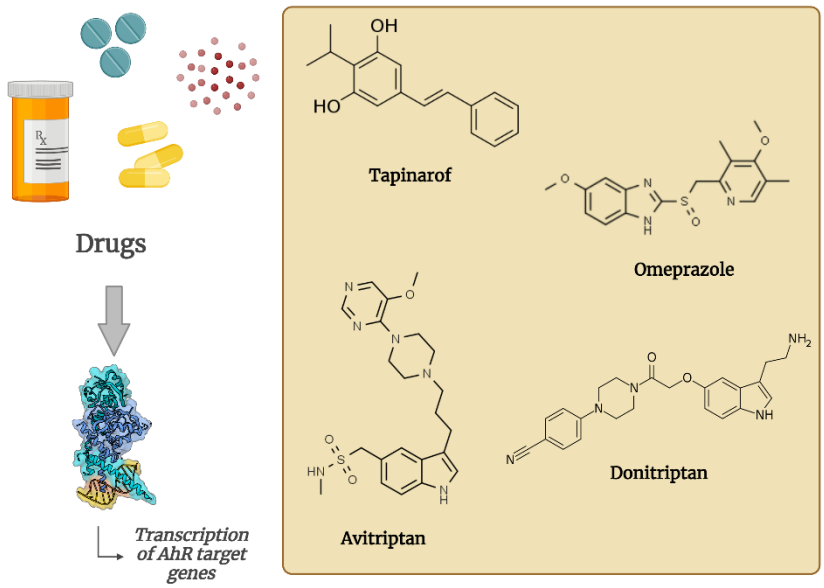

Figure 7: Drugs activating AhR. Various drugs showed the ability to activate AhR. Due to its role in human patho-/physiology, AhR has become an important therapeutic target. The AhR-targeting medication comes in the form of pills, capsules, or creams. Tapinarof (cream) is a steroid-free treatment for plaque psoriasis or dermatitis. Omeprazole (capsules) was reported to switch states from AhR ligand-independent activator to AhR pro-antagonist (omeprazole-sulfide). Antimigraine triptan drugs (Avitriptan, Donitriptan) were reported to be weak AhR agonists.

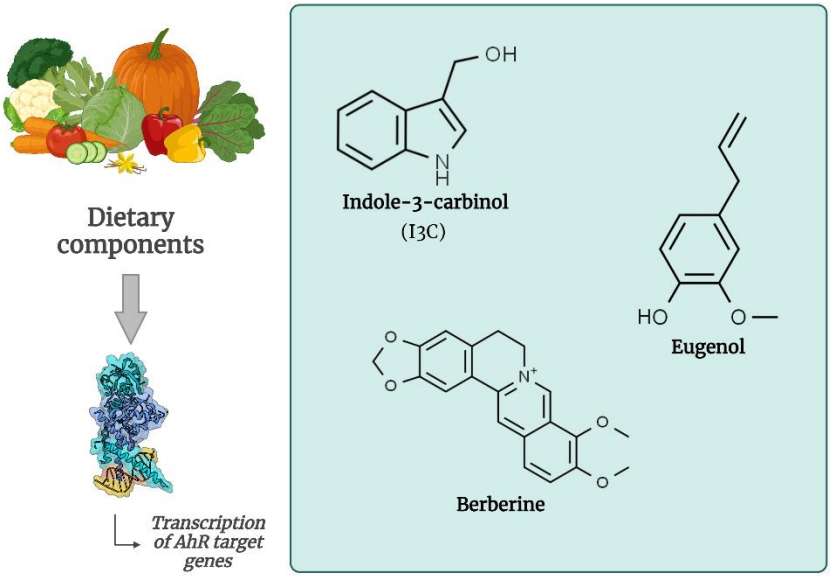

Figure 8: Dietary components activating AhR. This group represents a rich source of AhR ligands and activators. AhR-activating abilities were demonstrated with carotenoids, flavonoids, berberine, essential oils (eugenol), or indolic compounds naturally occurring in vegetables (I3C).

3.2.3.3 Dietary Components

The most significant exposure to AhR ligands and activators is believed to come from diet (**Figure 8**), as the food is a natural source of various AhR-activating compounds [153]. This group includes carotenoids [154], flavonoids [155], or alkaloid berberine [156].

Essential oils are a rich source of dietary components. Many of them were identified as AhR ligands with the ability to induce nourishment/drug interactions [157]. A study conducted on 31 essential oils naturally occurring in diet identified 14 of them as AhR-inactive. However, others displayed full agonistic (e.g., vanilla, jasmine, or cumin), partial agonistic (e.g., dill, nutmeg, or oregano), or even antagonistic effects (e.g., turmeric, spearmint, or anise) [158]. One of the examples is eugenol, an essential oil component occurring in clove, which acts as an AhR activator by inducing AhR nuclear translocation and expression of target genes in human keratinocytes [159, 160].

Indolic compounds, e.g., indole-3-carbinol (I3C), belong to the main class of AhR dietary ligands. I3C naturally occurs in vegetables such as broccoli, Brussels sprouts, or cabbage, and acts as a low-affinity AhR ligand [161]. Various products are formed when I3C undergoes chemical transformation, one of which is indolo[3,2-b]carbazole. Studies have identified this compound as a potent AhR agonist. Interestingly, in murine model experiments, indolo[3,2-b]carbazole exhibited a higher binding affinity towards mouse AhR (mAhR) than I3C itself [161, 162]. Moreover, indolic compounds also belong to the following groups of AhR ligands.

3.2.3.4 Gut Microbiota Metabolites

Microbial metabolism produces valuable endogenous AhR ligands. The gastrointestinal tract (GI) has a diverse community of microorganisms that play a crucial role in digesting food, especially proteins containing Tryptophan (Trp) [163]. Trp is metabolized in the GI by three main pathways: kynurenine, serotonin, and direct (microbiota-mediated) transformation, resulting in the formation of several AhR activators and ligands as products [164]. Indole, a major Trp metabolite, displays strong AhR agonist activity [165]. Other Trp metabolites like tryptamine, indole-3-acetic acid (IAA), or 3-methylindole (3MI; skatole) can also activate AhR [166]. 3MI was reported to activate AhR in various cell lines, such as primary human hepatocytes [167], intestinal Caco-2 cells [168], or human bronchial epithelial cells [169]. However, mRNA levels of *CYP1A1*, an AhR-activation marker, were not elevated in LS180 cancer cells after treatment with 3MI [170].

Several studies refer to kynurenine as an AhR ligand. In 2010, a novel study discovered kynurenine-induced AhR activation [171], followed by a finding that kynurenine is a low-affinity ligand mAhR [172]. However, recent investigation suggests that kynurenine itself is not an AhR ligand but rather a precursor to a super-potent AhR agonist [138]. Regardless, kynurenine is known to regulate levels of reactive oxygen species by interacting with AhR signalling [173].

Among microbiota-derived AhR ligands was considered butyrate, a major short-chain fatty acid produced by gut bacteria during the fermentation of dietary fibres. However, a recent study has questioned the previous findings [174, 175]. The Marinelli *et al*. study initially demonstrated that AhR antagonists could inhibit butyrate-induced AhR activation, implying butyrate as an AhR ligand and activator [174]. However, the study by Modoux *et al*. used a radioligand binding assay to show that butyrate is not a true ligand of mAhR. In addition, *in vitro* experiments found that butyrate treatment did not induce the formation of AhR/ARNT heterodimer [175]. Thus, the latest findings suggest that butyrate is not an AhR ligand but rather an enhancer of ligand-activated AhR [138].

Nevertheless, many metabolites of gut microbiota possess a crucial AhR-activating ability (**Figure 9**).

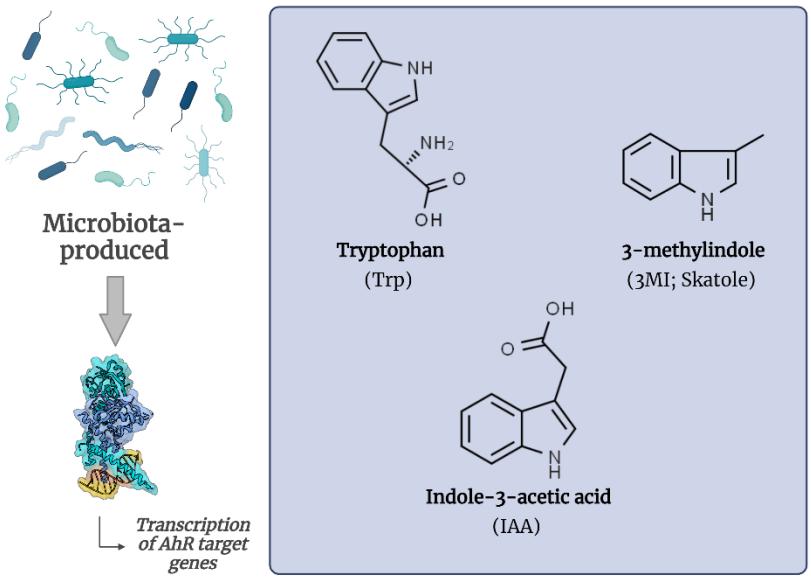

Figure 9: Gut microbiota metabolites as AhR ligands and activators. Tryptophan metabolites, produced by gut microbiota, are an essential group of AhR activators. This group also includes compounds containing an indole ring in the chemical structure, like 3MI (skatole), IAA, or indole itself.

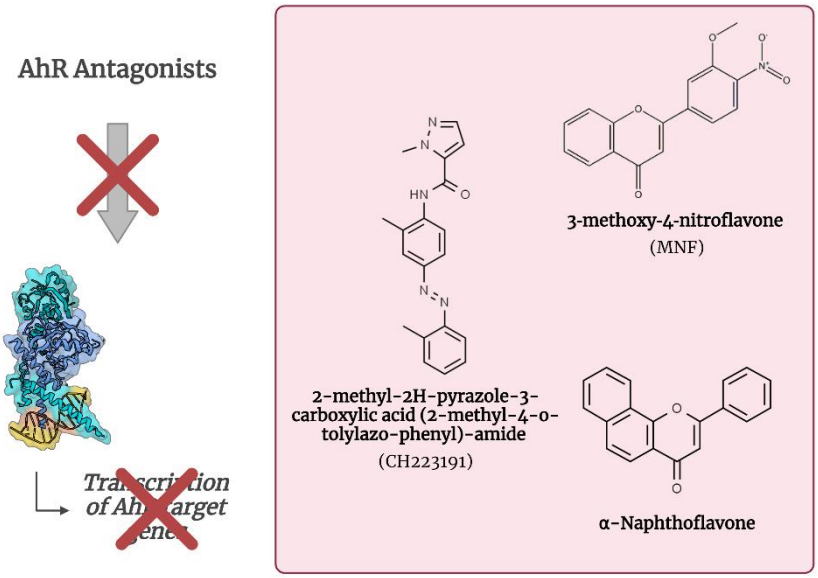

Figure 10: AhR Antagonists. These compounds bind to AhR to prevent its activations and subsequent transcription of AhR-target genes. One of the first compounds that demonstrated AhR-antagonistic properties was α-naphthoflavone. Additionally, MNF was also reported to be a competitive AhR antagonist. CH223191 is a ligand-selective AhR antagonist, as it averted AhR activation by potent exogenous ligands, like TCDD, but not by endogenous FICZ.

3.2.3.5 AhR Antagonists

Unlike agonists, AhR antagonists compete for binding to AhR to prevent its activation (**Figure 10**). One of the first AhR antagonists, α-naphthoflavone, was described in 1992. This study was conducted in mouse, rat, and human hepatoma cell lines and revealed the ability of α-naphthoflavone to antagonize *CYP1A1* expression induced by TCDD [176]. Additionally, antagonist effects of α-naphthoflavone were reported in various cell types, such as human breast cancer cells [177], ovarian follicles [178], or hepatoma cells [179].

In 1995, another synthetic compound, 3-methoxy-4-nitroflavone (MNF), was identified as a competitive antagonist of AhR [180].

Zhao *et al.* study discovered 2-methyl-2H-pyrazole-3-carboxylic acid (2-methyl-4-o-tolylazo-phenyl)-amide (CH223191) as an AhR antagonist. This compound inhibited AhR activation by highly potent ligands, like TCDD or related HAHs, but not by others, such as FICZ, flavonoids, or indirubin. Thus, CH223191 was disclosed as a ligand-selective AhR antagonist [181]. Subsequently, a series of CH223191-derived antagonists were synthesized [182].

Another high-affinity AhR antagonist, *N*-(2-(1*H*-indol-3-yl)ethyl)-9-isopropyl-2-(5-methyl pyridine-3-yl)-9*H*-purin-6-amine (GNF351), was reported to inhibit both genomic and non-genomic pathway [183].

A recent study by Ondrová *et al*. reported that carvones, naturally occurring compounds and major components of essential oils, act as noncompetitive AhR antagonists. The mechanism of action of carvones does not prevent the ligand-induced nuclear translocation of AhR but inhibits AhR/ARNT heterodimerization and subsequent binding to the *CYP1A1* promoter. This effect was confirmed in both *in vitro* (HepG2, LS180, HaCaT cell lines, and primary human hepatocytes) and *in vivo* experiments (female mice) [184].

3.2.3.6 Other AhR Ligands and Activators

Contrary to AhR antagonist α-naphthoflavone, β-naphthoflavone was reported to be a potent AhR agonist [185, 186]. Seidel *et al.* identified several prostaglandins as weak agonists of AhR [187], while indigo and indirubin, endogenous compounds containing an indole ring, were reported to be potent AhR activators [188].

One of the highly potent AhR ligands of Trp origin, 6-formylindolo[3,2-b]carbazole (FICZ), is produced endogenously by UV irradiation [189]. Therefore, FICZ is frequently used as a model endogenous agonist in many *in vitro* studies.

In 2002, 2-(1′ H-indole-3′ -carbonyl)- thiazole-4-carboxylic acid methyl ester (ITE) was reported to activate AhR with high affinity and was marked as "*a human endogenous AhR ligand*" [190]. However, in 2014, the presence of ITE in myxobacterial strains was reported [191]. Subsequently, ITE was isolated from *Thermosporothrix hazakensis*, a thermophilic bacterium naturally occurring in compost and not in the human body [192]. Additionally, Grycová *et al*. investigated the presence of ITE in blood serum samples of 20 healthy patients. Nevertheless, ITE or its metabolites were not detected in either sample [193]. These findings demonstrate that ITE should not be classified as "a human endogenous ligand," as described in 2002. The ability of ITE to activate AhR was demonstrated in several studies. However, the question arises whether ITE should be classified as a ligand of ITE-producing bacteria [138].

In addition to endogenous compounds, various synthetic indole derivatives have been found to have the ability to influence AhR activity. Stepankova *et al*. studied 22 methylindoles and methoxyindoles, mostly of synthetic origin, to investigate their effects on AhR in LS180 and HepG2 cells. The study revealed that multiple indolic compounds could activate AhR, but some also displayed antagonistic effects.

The leading indoles of this study, 4-methylindole (4MI) and 7-methoxyindole (7MeO), exhibited the ability to enrich the recruitment to *CYP1A1* promoter in HepG2 cells at concentrations of 200 μM. This enrichment was comparable to the effect of TCDD. However, the combination of 4MI and 7MeO slightly decreased *CYP1A1* enrichment. Furthermore, 4MI and 7MeO strongly induced AhR nuclear translocation, confirmed using fluorescent microscopy [170].

Figure 11 shows chemical structures and sources of other AhR ligands and activators.

In conclusion, endogenous and exogenous indolic compounds represent a broad group with a significant impact on the AhR signalling pathway.

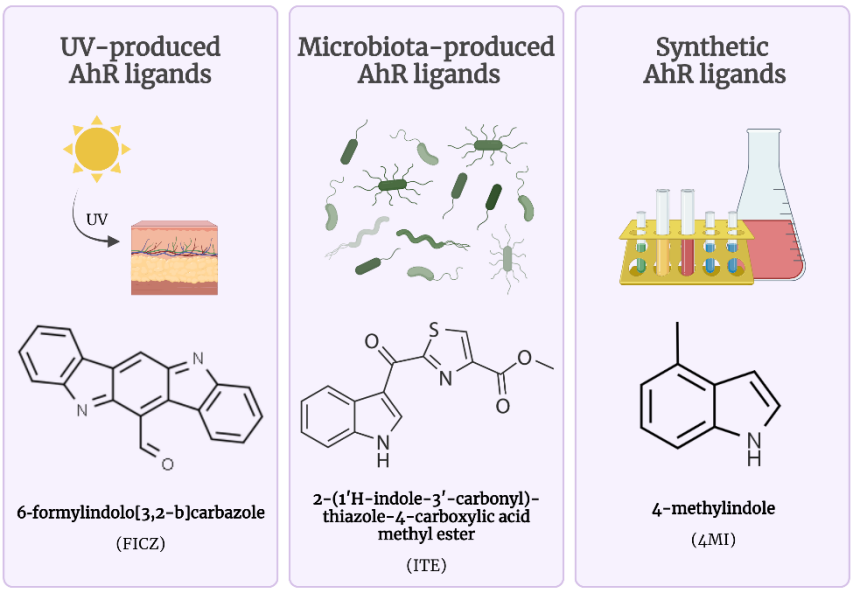

Figure 11: Other AhR ligands and activators. In the human skin, UV irradiation produces FICZ, a model endogenous AhR ligand. ITE is another AhR agonist produced by bacterial strains. Other synthetic AhR activators, such as 4MI or 7MeO, also represent a broad and vital group.

3.2.4 The Role of AhR in Human Patho-/Physiology

Upon its discovery, AhR was believed to be a xenoreceptor that responded to toxic chemicals, posing a risk to human health. At that time, it was not considered a potential therapeutic target [138]. TCDD is a very potent ligand with high affinity. Once it enters the human body, it is poorly metabolized and causes persistent activation of AhR, leading to the dysregulation of various physiological functions [37, 194]. However, several studies revealed that AhR plays a crucial role in various physiological functions, such as chemical and microbial defence, cell differentiation, angiogenesis, or immune response [37, 195].

One of the first areas investigated regarding AhR's involvement in human metabolism was the biotransformation of xenobiotics. AhR signalling mediates the activation of respective biotransformation proteins, such as cytochrome P450 enzymes, UDP-glucuronosyltransferases, and ATP-binding cassette transporters [1, 196].

The involvement of AhR was investigated in the cardiology field, leading to multiple suggestions that AhR is vital for maintaining normal cardiac functions. AhR signalling was reported to control the expression of genes connected to cardiac development and homeostasis. Moreover, AhR is essential for differentiating cardiomyocyte progenitors or preventing cardiac hypertrophy [197, 198].

Intestinal inflammation was connected to low AhR activity. Studies on the intestinal epithelium layer and its barrier function have shown that AhR ligands, which enter the GI, play a vital role in reducing local inflammation in the gut and preserving the integrity of the intestinal barrier in an AhR-dependent manner. Research indicates that AhR can regulate tight-junction proteins and myosin kinase, control cell permeability and muscle contraction, and thus influence the gut barrier function [199]. AhR pathway activation by FICZ was found to improve colonic inflammation, reduce the expression of IL-6 and Claudin-2, and preserve intestinal barrier function in a murine model of colitis induced by dextran sulphate sodium (DSS). The study found that FICZ also prevented the increase of intestinal epithelial permeability (leaky gut barrier) in Caco-2 and T84 epithelial cell lines. The cells lacking AhR exhibited higher levels of Claudin-2 after the treatment compared to cells with regular AhR expression. According to the study, AhR activation by FICZ prevented intestinal barrier dysfunction by downregulation of the Claudin-2 (*CLDN2*) gene expression [200]. The absence of tight junction protein 1 (ZO-1) in the intestinal epithelium has been connected with low AhR activity, leading

to epithelial barrier dysfunction. After AhR activation by FICZ in Caco-2 cells, ZO-1 expression was restored [201]. Results suggest that the AhR signalling pathway mediates the tight junctions between the intestinal epithelial cells. Studies have also shown that it is associated with regulating goblet cell differentiation. The absence of AhR has been observed to cause a loss of goblet cells in the AhR-knockout model. In HT29 cells, the treatment with an AhR inhibitor has been shown to prevent the differentiation of goblet cells [202]. Additionally, protective effects were observed in DSS-induced colitis in a murine model upon AhR activation by microbial metabolites ITE and ITE-$CONHCH_3$ [193].

In addition to the gut, AhR activation was also connected to skin inflammation, skin barrier function, and wound healing [203]. Nowadays, some skin diseases, like plaque psoriasis [204] or atopic dermatitis [205], are already treated through targeted AhR therapy, e.g., with the prescription of Tapinarof [144].

Thus, it is evident that the list of AhR involvement in patho-/physiological processes is extensive. In addition to the diseases already mentioned, AhR was reported to play a role in cancer progression [206], hyperglycemia [207], non-alcoholic fatty liver disease (NAFLD) [208], intestinal fibrosis [209], cystic fibrosis [210], asthma [211], multiple sclerosis [212], depressive disorder [213], rheumatoid arthritis [214], or viral diseases (e.g. Zika or coronaviruses) [215, 216].

In conclusion, AhR was previously associated only with toxicity, but recent research has revealed its potential as an important therapeutic target. While some treatment methods are still in the proposal stage, others have already entered clinical studies. Regardless, the significance of AhR in human patho-/physiology cannot be denied.

3.3 Androgen Receptor

Androgen receptor (AR) activity is closely related to the group of steroid hormones, androgens. Together, AR and androgens play an irreplaceable role in the development of male phenotype during prenatal development and later in the maintenance of the proper function of male reproductive organs [4]. Additionally, it has a vital role in affecting the nervous system [217]. AR is widely distributed in tissues of the male's urogenital tract, like the testis or prostate. On the other hand, numerous other tissues, such as the kidney, liver, brain, mammary gland, or salivary glands, showed low AR expression [218]. AR, a 110 kDa protein consisting of approximately 919 amino acids, is encoded by the *AR* gene localized on the human X chromosome between q13 and centromere [219, 220]. This gene is about 90 kb in size, consisting of 8 exons divided by 0.7-2.6 kb introns [220, 221]. Moreover, the existence of several AR splicing variants was reported due to the presence of cryptic exons (further in *Chapter 3.3.4*) [222]. The outcomes of several studies, including transcriptome analysis or next-generation sequencing, have validated the importance of AR activity in the progression of prostate cancer [223].

3.3.1 AR Structure

AR is a member of NRs and can also be found under the abbreviation NR3C4 (nuclear receptor subfamily 3, group C, member 4) [224]. Therefore, it is also a ligand-activated transcription factor and shares the same structural division described in *Chapter 3.1*. Briefly, AR is composed of four domains. NH_2 terminal transactivation domain (NTD) is encoded by exon 1, DBD by exons 2–3, HR by exon 4, and exons 5–6 encode LBD [221].

3.3.1.1 NH_2-terminal Domain

With the range from 1 to 555 residues, NTD occupies almost half of the AR size and was reported to contain a glutamine-rich segment (poly-Q) and glycine-rich region [4, 225]. Both segments are highly variable among the population [226]. AR also contains CAG segments that vary in number, typically ranging from 19 to 25 [227]. Shorter CAG repeats have been connected to increased AR transcriptional activity but also a higher risk of developing prostate cancer [228, 229]. On the other hand, long CAG repeats (more than 40) were connected to low AR transcriptional activity in patients suffering from Kennedy's disease [227, 230]. Complete deletion of poly-Q region resulted in rapidly increased AR activation, approximately 4x fold compared to control AR

protein without deletion [231]. NTD contains a modular activation function 1 (AF1), located between residues from 142 to 485, which is constitutively active [232]. AF1 plays a vital role in regulating gene expression and facilitating protein-protein interactions [233]. In 1991, deletion mutagenesis discovered that AF1 is a significant effector region that consists of two separable transcription activation units, Tau1 and Tau5 [234]. The ^{23}FQNLF^{27} motif was identified within Tau-1, while Tau-5 contains the ^{433}WHTLF^{437} motif. Both promote androgen-dependent NTD-LBD interaction, also known as N/C interaction [235, 236]. This interplay plays a vital role in AR/AR dimer stabilization. Additionally, it contributes to the reduction of ligand dissociation rate [237]. This interaction occurs between NH_2-terminal AF1 motif ^{23}FQNLF^{27} and activation function 2 domain (AF2) in the LBD of the C-terminal region [238].

3.3.1.2 DNA-binding Domain

The DBD of AR, located between the NTD and the C-terminal domain (residues 555-623), is a cysteine-rich region highly conserved among all steroid receptors [4]. After dimerization, DBD recognized a specific pattern in the promoter of the target gene, known as the AR response element (ARE). Generally, steroid receptors share similar response elements, which consist of two identical hexameric half-sites, 5'-AGAACA-3', separated by a 3 bp spacer region [239]. DBD also possesses NLS responsible for proper nuclear translocation after recognition by IMPα [240]. DBD is connected to the C-terminal domain through a flexible HR in position between 623-665 amino acids [4]. Within HR is localized the ^{629}RKLKKL^{634} motif, which is a target for various post-translational modifications, such as methylation, acetylation, or ubiquitination [241].

3.3.1.3 C-terminal Domain

The C-terminal domain, or the LBD, is in position between 666-919 amino acid residues and is responsible for crucial functions, such as ligand binding or interaction with the NTD [242]. Structurally, the LBD of AR has a sandwich-like formation of two anti-parallel β-sheets and twelve α-helixes (H1-H12) [243, 244]. Approximately 18 amino acid residues of the middle region (H3, H4, H5, H7, H11, H12, and one β-sheet) create a ligand binding pocket [242, 245]. Unlike other NRs, AR lacks H2. This region is instead replaced by a long, flexible linker [4]. LBD contains AF2, which comprises H3, H4, and H12, and is ligand-dependent [246-248]. H12 is a flexible region that can change its conformation in the presence or absence of ligands. Upon ligand binding, H12 is stabilized, resulting in the formation of the AF2 core and sealing off the ligand-binding

pocket, preventing it from dissociation [4, 244]. AF2 is also a target for binding various coregulators [248]. Mutations in H12, particularly in proline 892, led to the inability to stabilize and seal a ligand-binding pocket, which was connected with complete androgen insensitivity [244]. Additionally, disrupted N/C connection upon ligand binding was also linked to androgen insensitivity [248]. Thus, maintaining precise N/C interaction is, among other things, crucial for precise AR function and transactivation. The C-terminal domain also contains NES located in the position between 742 and 817 amino acids [249].

Figure 12 illustrates the structure of the human *AR* gene, which encodes AR protein.

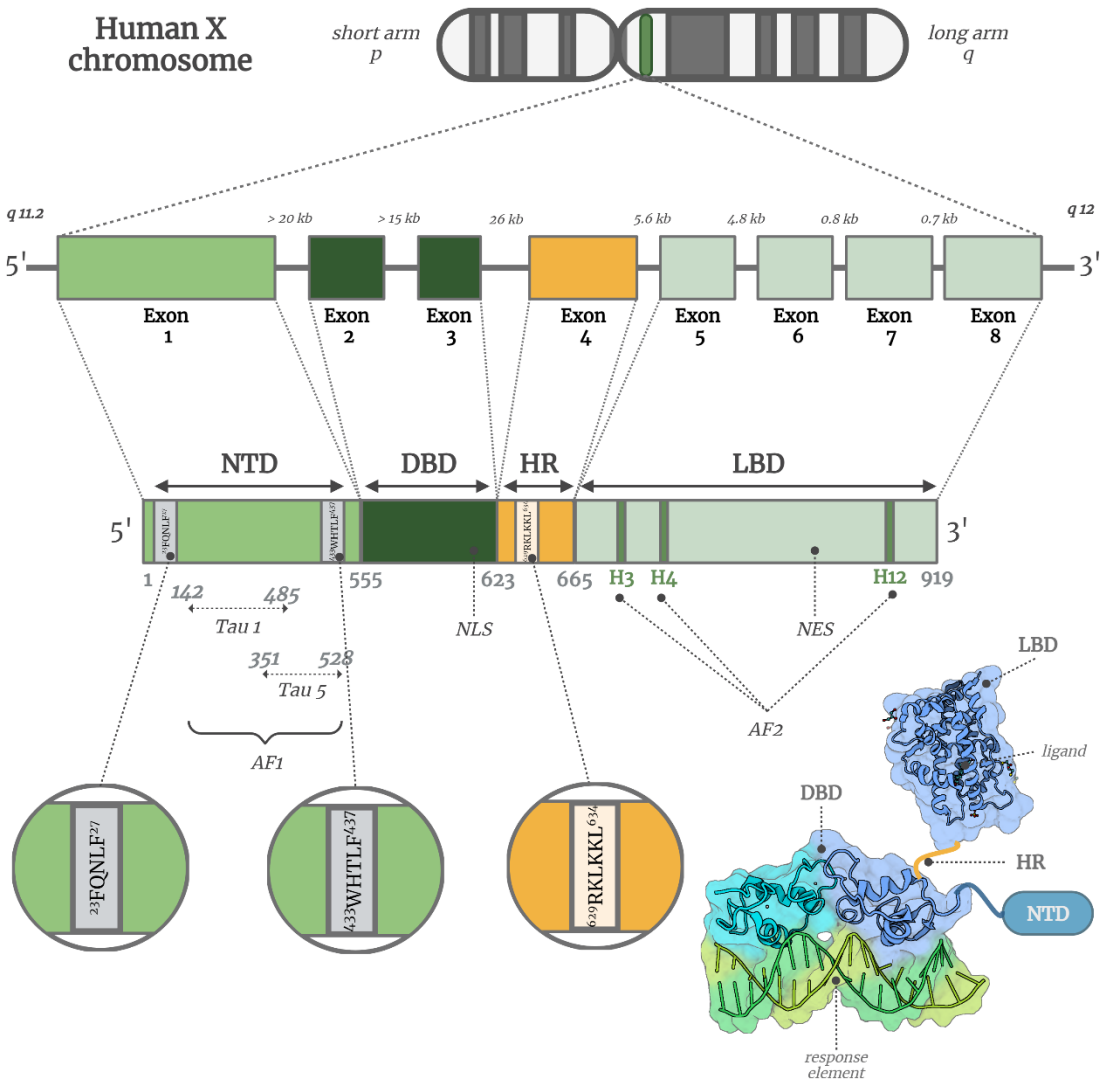

Figure 12: Androgen receptor. AR is encoded by the *AR* gene localized on the long arm (q) of the X chromosome in position between q11.2 and q12. Predominantly, this gene is encoded by eight exons. However, the existence of distinct cryptic exons has been reported. Approximate sizes of introns between individual exons are shown above. NTD, encoded by exon 1, contains activation function 1 (AF1), together with Tau1 and Tau5, and two specific amino acid motifs: ^{23}FQNLF^{27} and ^{433}WHTLF^{437}. DBD, encoded by exons 2 and 3, is responsible for binding to response elements in the DNA. Moreover, DBD contains NLS. DBD is connected with LBD through short HR (exon 4), which contains a ^{629}RKLKKL^{634} amino acid motif. LBD, encoded by exons 5-8, also contains activation function 2 (AF2) and NES. In the lower right corner of this figure, the 3D crystal structure of activated AR is shown schematically. Nevertheless, the separate crystal structure of HR and NTD has yet to be achieved (modified according to Tan *et al.* 2015 and Socorro *et al*. 2014, *Chapter 3: Structural and functional analysis of the androgen receptor in disease* [3, 4]).

3.3.2 AR Signalling

AR, like other NRs (detailed in *Chapter 3.1*), is initially located in the cytoplasm in the absence of ligands, forming a complex with heat shock proteins (Hsp90, Hsp70, Hsp56, Hsp27), cytoskeletal proteins (e.g., filamin-A), and other chaperones [250-252].

3.3.2.1 AR Genomic Signalling Pathway

Upon ligand binding, AR undergoes conformational changes, enabling it to interact with co-regulators [253]. Hsp27 plays a crucial role in the activation of receptors. When a ligand binds to AR, the receptor undergoes phosphorylation at the Ser78 and Ser82 positions. This phosphorylation is mediated by p38 kinase. As a result, Hsp90 dissociates from the receptor, and the receptor is translocated to the nucleus [250, 254]. Unlike the AhR/ARNT heterodimer complex, AR dimerize with itself, resulting in the formation of AR/AR homodimer [243]. The homodimerization of AR is a predominant process. However, the existence of a unique heterodimer complex with other partners, such as testicular nuclear receptor T4 (TR4), has also been reported [255]. The tissue-specific binding of AR/AR to ARE in the promoter of target genes is followed by the recruitment of co-regulators and histone acetyltransferase enzymes (HATs), which subsequently trigger transcription [249, 256]. Approximately, the existence of 170 different AR coregulators was reported [249]. One of the well-known AR-target gene is *KLK3,* which encodes the prostate specific antigen (PSA) protein [257]. Another known AR-regulated gene is *FKBP5,* which encodes a small protein immunophilin. This protein regulates the distribution of steroid hormones between the cytosol and nucleus [258].

After the ligand dissociates, NES coordinates the export of AR from the nucleus to the cytoplasm. There, AR returns to the initial inactive conformation and awaits the rebinding of a ligand [252, 259]. Alternatively, AR degradation can be achieved by targeting it for the ubiquitin-proteasome system, which leads to a decrease in AR protein level. The recognition of AR by E3 ubiquitin ligase requires phosphorylation of specific residues [260, 261]. It was previously demonstrated that phosphorylation of Ser515 by TFIIH, a cdk7 kinase, or Ser210 and Ser790 mediated by protein kinase B, led to subsequent proteasomal degradation of AR [262, 263].

Additionally, it was demonstrated that AR activation by a ligand prolongs the half-life of AR protein and reduces its degradation. This phenomenon is commonly referred to as protein stabilization by ligand binding [264, 265].

3.3.2.2 AR Non-genomic Signalling Pathway

Studies have demonstrated that AR can interact with other signalling pathways beyond its well-known genomic pathways. This type of interaction is known as a non-genomic pathway, where the cellular response time is rapid, within minutes. Unlike genomic signalling, these pathways do not appear to involve transcription or translation from AR-target genes, suggesting a direct interaction and stimulation of other signalling cascades [266, 267]. A previous study has shown that AR can activate the phosphoinositide 3-kinase (PI3K) and trigger the PI3K/Akt signalling pathway by interacting with p85 in androgen-sensitive epithelial cells. The study used mouse vas deferens epithelial cells (VDEC). Usually, activation of the PI3K/Akt pathway reduces the levels of caspase 3 and caspase 9, which are key initiators of apoptosis. Baron *et al*. have demonstrated the activation of the PI3K/Akt pathway in VDEC due to AR non-genomic signalling [266]. In a separate study, it was reported that AR has the ability to interact with caveolae and trigger the Src or ERK signalling pathways [252].

Recent findings indicate that co-activation of AR and Src kinase is essential for prostate tumor progression [268, 269]. It was observed that the crosstalk between AR and Src kinase can occur even in the absence or presence of androgens. In the absence of androgens, AR transcriptional activity can be mediated by growth factors, such as EGF, or cytokines, such as IL-8 [270, 271]. These factors can induce the phosphorylation of AR, leading to the induction of AR transcriptional activity even in the absence of androgens. Src kinase is a crucial mediator of the various signalling pathways of growth factors and cytokines [270, 272]. AR transcriptional activity was downregulated in the Src mutant model with inactive kinase in C4-2 cells. Additionally, a decrease in recruitment to the *KLK3* gene promoter was reported in this model. Furthermore, inhibiting Src led to a significant decrease in cellular growth. The findings suggest that targeting Src kinase could be a promising approach to disrupt the growth and metastasis of prostate cancer [273].

Several studies have reported that Src-mediated phosphorylation of AR at Tyr534 induced AR nuclear translocation and binding to ARE, even in the absence of androgens. These findings suggest that Src kinase may play a role in the development of castration-resistant prostate cancer (CRPC) [274, 275].

3.3.3 Androgens and Antiandrogens

Androgens, main agonists of the AR, play a crucial role in male phenotype development and modulate various biological responses in the human body, such as fertility. Testosterone (T), dihydrotestosterone (DHT), and dehydroepiandrosterone (DHEA) are the most essential androgens. These male sex steroid hormones are synthesised within Leydig cells in the testicles, or the adrenal gland [180]. The process of androgen synthesis and secretion is initially regulated through the hypothalamic-pituitary-gonadal axis (HPG) [276]. Androgens, like other steroid hormones such as estrogens, glucocorticoids, or mineralocorticoids, are also derived from cholesterol [277]. The primary precursor is free cholesterol, which can be formed in one of three pathways: *de novo* synthesis, by hydrolysis of stored cholesterol esters, or from lipoproteins circulating in the serum [6, 278]. The process is initiated when the luteinizing hormone (LH) binds to the luteinizing hormone/choriogonadotropin receptor (LHCGR) and induces phosphorylation of the steroidogenic acute regulatory protein (StAR). This phosphorylation regulates the transfer of cholesterol into the inner mitochondrial membrane of Leydig cells [6, 279]. Inside Leydig cells, free cholesterol is converted into pregnenolone using the CYP11A1 enzyme. Pregnenolone is subsequently transported out of the mitochondria into the smooth endoplasmic reticulum by passive diffusion [280]. Pregnenolone can be also converted to progesterone by HSD3B1/2 enzymes [281]. An enzyme catalysing the following reactions, CYP17A1, displays 17α-hydroxylase and lyase activity. CYP17A1, through its 17α-hydroxylase activity, converts pregnenolone or progesterone to 17α-hydroxypregnenolone or 17α-hydroxyprogesterone [282]. Lyase activity of CYP17A1 mediates the transformation of 17α-hydroxypregnenolone and 17α-hydroxyprogesterone into DHEA or androstenedione, respectively [6, 283]. Another enzyme, HSD17B3, converts DHEA into androstenediol and androstenedione into testosterone (T). Testosterone can also be formed from androstenediol by the HSDB1/2 enzyme [283]. Thus, synthesized T is released and can subsequently participate in regulating respective cell processes through interaction with AR in both genomic and non-genomic manner [284]. Serum proteins, like sex hormone-binding globulin (SHBG) or albumin, are responsible for the distribution of T throughout the bloodstream [285, 286]. Under physiological conditions, only approximately 1-3 % of T in the bloodstream is free [287]. Free T is a biologically active hormone that circulates in the body. However, its concentration

levels can rapidly vary throughout the lifetime of a healthy man. According to Cleveland HeartLab, the concentration of T in men under 18 years of age ranges from 4.5 to 25.0 ng/dl. In men aged between 18 to 49 years old, the normal level of free T is between 249 to 836 ng/dl. The highest levels of T in healthy adult men are typically observed between the ages of 30 and 40. For men aged 50 years or older, a normal free T concentration ranges from 193-740 ng/dl [288].

An additional 20-30 % of T is bound to albumin, and approximately 70 % is bound to SHBG [287]. These carrier proteins transport T to androgen-specific organs, where T can be converted to DHT by 5α-reductase enzyme. In a bloodstream of a healthy adult men, a normal DHT concentration in serum was reported to range from 11 to 95 ng/dl [289]. Depending on tissue localization, 5α-reductase enzyme can exist in two primary forms: A1, predominantly localized in tissues of non-reproductive organs (e.g., liver), or A2, isoform occurring in tissues of reproductive organs (e.g., seminal vesicles) [6, 290]. It was reported that the prostate can express both of these isoforms [291]. Additionally, the existence of the A3 isoform was also reported. However, this isoform converts polyprenol into dolichol [292]. Testosterone and DHT are considered the main AR ligands, but DHT is more potent than T [221, 293]. An alternate pathway of DHT synthesis bypassing its formation T has also been described [6]. **Figure 13** displays the process of biosynthesis of androgens.

Imbalanced secretion of androgens is associated with several diseases or syndromes, such as congenital lipoid adrenal hyperplasia, pseudohermaphroditism, or even the development of prostate cancer [221, 294, 295].

Antiandrogens inhibit the activity of androgens by competing with them for AR binding sites [4]. They are often used in clinical applications, particularly for prostate cancer treatment. Antiandrogens can be divided into four groups: steroidal (Cyproterone acetate), first-generation nonsteroidal (Flutamide, Bicalutamide), second-generation nonsteroidal antiandrogens (Enzalutamide, Apalutamide), and N-terminal domain antagonists (Ralaniten) [296]. However, treatment with synthetic antiandrogens may cause undesirable side effects (further in *Chapter 3.4.3*) [297]. Additionally, the existence of naturally occurring antiandrogens has been described. The mechanism of action of these compounds lies in the decrease of testosterone synthesis (liquorice [298], spearmint [299]) or reduction of DHT by 5α-reductase inhibition (red reishi [300], Camellia sinensis [300]). Nevertheless, these substances are not used as a medicine in prostate cancer therapy [298, 301].

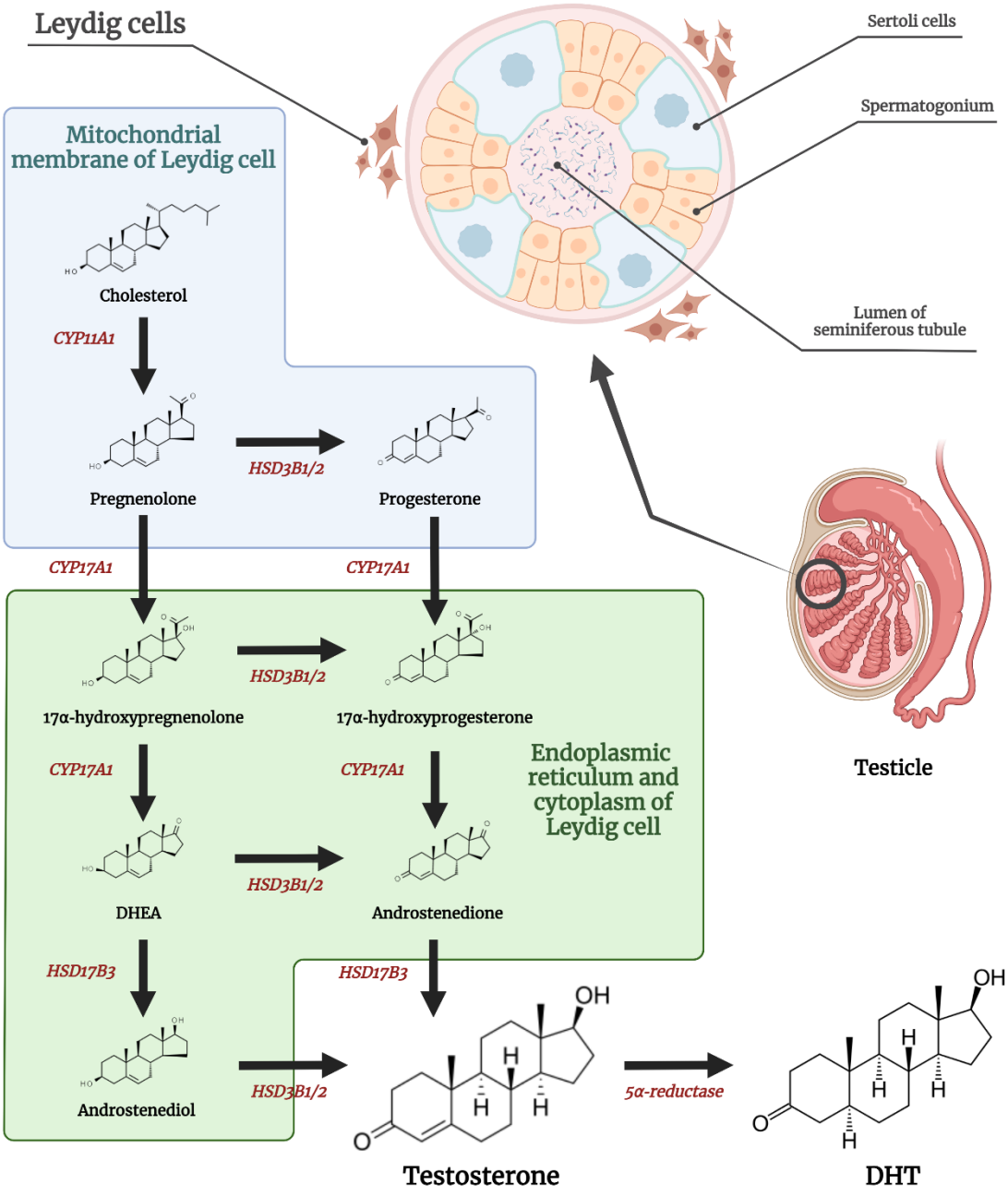

Figure 13: Androgens biosynthesis. The process of androgen biosynthesis begins when cholesterol is transported into the inner mitochondrial membrane of the Leydig cell. In this membrane, it is converted to pregnenolone by the CYP11A1 enzyme. Pregnenolone can also be converted to progesterone by the HSD3B1/2 enzyme. Then, these proteins are transported outside the mitochondrial membrane, where they are further converted to 17α-hydroxypregnenolone or 17α-hydroxyprogesterone, respectively, by the 17α-hydroxylase activity of the CYP17A1 enzyme. Afterward, 17α-hydroxypregnenolone is converted to DHEA by the lyase activity of the CYP17A1 enzyme, and androstenediol by the HSD17B3 enzyme. Finally, androstenediol is converted to testosterone by the HSD3B1/2 enzyme. Additionally, 17α-hydroxyprogesterone is converted to androstenedione by the lyase activity of the CYP17A1 enzyme and, subsequently, to testosterone by the HSD17B3 enzyme. The synthetized testosterone is transported out of the Leydig cell and through the bloodstream by binding with albumin or SHBG to target organs. In androgen-specific organs, testosterone can be converted to DHT by the 5α-reductase enzyme. Although both testosterone and DHT are considered to be the main AR ligands, DHT is more potent. Thus, the AR signalling pathway is modified through interactions of androgens with AR (modified according to Hu *et al.* 2021 and Lawrence *et al*. 2022 [5, 6]).

3.3.4 Mutations and Splicing Variants of AR

Most mutations in AR occur as a substitution of a single amino acid, which typically develops within the LBD [302]. These mutations have functional consequences that enable antiandrogens to act as agonists for AR, thereby promoting cancer progression. One of the most common examples is mutation T877A, which is present in around 30% of cases of metastatic CRPC [303, 304]. Additionally, this mutation allows the activation of AR by other adrenal androgens, such as DHEA, progesterone, and androstenediol [305, 306]. This finding may explain why castration therapy fails in some patients with tumors that have AR mutations [304].

In the early 2000s, Gregory *et al*. published the first evidence of endogenous expression of various AR variants [307]. By using specific antibodies against different protein regions of AR, they discovered a complete lack of LBD within these variants. At that time, it was hypothesized that these variants resulted from proteolytic cleavage of AR. However, further research has shown that AR variants arise from alternative mRNA splicing [307-309]. Later, AR splice variants with intact LBD have also been discovered. In 2008, the existence of cryptic exons (CE), specifically CE4, was demonstrated experimentally in 22Rv1 cell line. CE4 is localized within the intronic region between exon 2 and exon 3 [310]. Additionally, CE4 was also reported to exist in LNCaP and other prostate cell lines, indicating that the existence of CEs is not a sporadic phenomenon [308, 310]. Many AR variants lack exon 4. Despite this, many of them, including AR-v7, can enter the nucleus and trigger the transcription through the AR canonical pathway, even in the absence of the AR full-length variant (AR-fl) [222, 311]. AR splicing variants can be divided into four categories: similar to the canonical pathway (ligand-dependent, e.g., AR-23), constitutively active (e.g., AR-v4, AR-v7), conditionally active (e.g., AR-v1, AR-v9), and inactive (e.g., AR-v8, AR-v13) [312-314]. Additionally, more new variants are still being identified. Clinical treatments targeting LBD for diseases connected with AR signalling may be ineffective as many AR splicing variants lack this domain [314]. Extensive research has been conducted on the genomic localizations of AR-fl homodimers binding sites in the chromatin. However, the exact chromatin binding sites for AR-v7 dimers are not yet fully understood [315]. The lack of LBD in AR splicing variants results in encoding a shorter protein: AR-fl (~110 kDa) vs. AR-v7 (~89 kDa) [316]. **Figure 14** illustrates the differences in the length and structure of selected AR variants.

Generally, AR-v7 (also known as AR3) is considered to be the most crucial constitutively active AR splicing variant. This splicing variant is encoded by cryptic exon CE3, which is localized within intron 3 [317]. AR-v7 contains NTD and DBD, but its LBD is replaced by a short sequence of 16 amino acids (EKFRVGNCKHLKMTRP). This unique sequence is often used to design specific antibodies against this splicing variant for its detection [318]. Some studies suggest that this variant can be a predictive and prognostic biomarker [314, 319]. It was previously demonstrated that *AR-v7* mRNA levels were significantly increased in patients suffering from prostate cancer, especially with the castration-resistant type (detailed in *Chapter 3.4.4*) [222, 319].

According to clinical evidence, patients with prostate cancer expressing these shortened AR variants have a more difficult diagnosis and prognosis, whereas those with tumors expressing only AR-fl are less likely to have an aggressive form of the disease [7, 320].

Figure 14: AR splicing variants. More than 20 AR splicing variants have been identified so far. In most of these variants, the LBD is completely absent due to the presence of cryptic exons and alternative splicing. This figure illustrates the structures of some of the most well-known AR splicing variants with their respective cryptic exons (modified according to Miller *et al*. 2023 [7]).

3.4 Prostate Cancer

Prostate cancer affects men of all races and ethnic groups and is one of the most common types of cancer. Several factors, including genetic predisposition, age, obesity, and environmental impacts, influence the probability of developing prostate cancer. Patients with relatives diagnosed with prostate cancer are at higher risk (approximately 50 %) of developing the disease compared to those with no family record of prostate cancer occurrence [321]. However, the exact genetic factors that contribute to the development of this type of tumor are not yet fully understood. The most affected group is middle-aged men, but the risk of developing the disease increases with age, with more than 75% of patients being 65 years or older [322]. Due to the rapidly growing population and increasing number of men reaching 65 years of age, studies predicted that there will be approximately 1.7 million new cases of prostate cancer by the year 2030 [323].

Generally, gene mutations are considered to contribute significantly to cancer development. Aberrations in certain genes, like *BRCA1* or *BRCA2*, are potential candidates for prostate cancer predisposition [324]. Additionally, a rare G84E mutation of the *HOXB13* gene has also been connected with prostate cancer heredity [325]. The proper function of AR signalling and interaction with androgens is crucial for the normal growth of prostate epithelium. In prostate cancer cells, this signalling pathway is disrupted [326]. As previously mentioned, various mutations in AR have been connected with prostate cancer development.

This disease is typically diagnosed by a combination of several screening methods such as rectal examination, detection of elevated prostate-specific antigen (PSA) level, or prostate biopsy procedure [321]. Determination of PSA levels in blood samples continues to be one of the most used diagnostic indicators. Normal PSA levels vary slightly with age. According to Johns Hopkins Medicine, a concentration from 0.6 to 0.7 ng/ml is considered a normal range for men between 40 and 50 years. The normal range for men above 60 years is between 1.0 to 1.5 ng/ml. Generally, PSA levels above 4.0 ng/ml is considered abnormal [327]. Statistically, patients with PSA levels above 10 ng/ml were reported to have a 50% possibility of having prostate cancer [321, 328]. However, PSA is not a definitive marker for prostate cancer. Increased PSA levels can also be an indication of different pathologies like prostatitis and not necessarily cancer [329]. Other proteins also used as prostate cancer markers are homeobox protein

Nkx-3.1 (encoded by *Nkx-3.1* gene) or transmembrane serine protease 2 (encoded by *TMPRSS2* gene) [330, 331].

In order to confirm whether the patient has prostate cancer or not, a tissue biopsy needs to be performed, as it is the most reliable method of diagnosis but also the most invasive one [332]. Early detection of prostate cancer can reduce mortality rates. However, developing universal screening techniques is challenging due to the heterogeneity of prostate cancer tissue. Currently, there are no generally approved conventional screening techniques for early cancer detection [333].

Prostate cancer progression can be divided into four clinical stages (I – IV). During Stage I, the tumor is not detectable during rectal examination, and it is usually identified randomly during surgery for other medical conditions or through a biopsy performed due to an increased PSA level. In Stage II, the tumor can be detected during rectal examination and/or visualized with certain types of imaging, such as transrectal ultrasound. During Stage III, the tumor has already grown outside the prostate gland and may have spread to the seminal vesicles. Finally, in Stage IV, the tumor has already spread to other tissues adjacent to the prostate gland, such as the bladder or rectum [334].

3.4.3 Therapy

Prostate cancer treatment involves various clinical approaches depending on the severity of the disease. Each approach is associated with a number of mild to serious side effects, such as erectile dysfunction, urinary incontinence, fatigue, diarrhoea, osteoporosis, anaemia, cardiovascular disease, or myelosuppression [321]. **Table 2** lists the standard procedures for prostate cancer treatment. However, only hormonal therapy, chemotherapy and immunotherapy will be discussed in detail in the following paragraphs.

Table 2: Common approaches in prostate cancer treatment. Therapeutic procedures and their brief description, modified according to Sekhoacha *et al*. 2022 [321].

Treatment	Progression	Procedure
Prostatectomy	Locale	Surgical removal of the prostate gland
External beam radiation	Locale	Local radiation beam towards the cancer cells
Internal radiation (brachytherapy)	Locale	Placing radioactive material (seed, capsule, or ribbon) inside body near the tumor
Cryotherapy	Locale	Usage of extreme cold to freeze abnormal prostate tissue and its removal
Hormone therapy	Advanced	Blockage of androgen production
Chemotherapy	Advanced	Usage of anticancer drugs to kill of inhibit growth of cancer cells
Immunotherapy	Advanced	Utilization of immune response mechanisms to target malignant cells

Hormone therapy, also known as androgen deprivation therapy (ADT), is a treatment for advanced prostate cancer that involves the reduction of circulating androgen levels in the body through surgical or chemical means. This can be achieved through surgical castration or through the use of medications that either inhibit the production of androgens or prevent them from interacting with AR. Studies have shown that surgical castration, which is achieved by orchiectomy, can reduce androgen levels by approximately 90 % within 24 h [296, 335]. Chemical castration involves the use of LHRH analogues

(agonists) or antagonists. LHRH analogues stimulate receptors in the hypophysis, adjusting LH and follicle-stimulating hormone (FSH) levels, which ultimately suppressing testosterone production. The FDA has approved several common LHRH agonists, including Leuprolide (*Lupron*®), Goserelin (*Zoladex*®), or Triptorelin (*Trelstar*®) [336]. In contrast, LHRH antagonists, such as Degarelix (*Firmagon*®), block hypophysis receptors, inhibiting testosterone synthesis [321, 337, 338]. As mentioned above, prostate cancer treatment is associated with multiple side effects. Severe and long-lasting complications connected with ADT treatment include insulin resistance, osteoporosis, or cardiovascular disease [339].

Antiandrogen Flutamide (*Eulexin*®) is a known hormonal drug for prostate cancer treatment. It works by inhibiting the AR signalling pathway through displacement of the ligand in the LBD [340]. However, clinical studies conducted on Flutamide have not provided the most effective outcomes [341]. Additionally, the following research connected Flutamide medication with subsequent hepatic dysfunction [342].

Bicalutamide (*Casodex*®), is an antiandrogen drug that is derived from Flutamide. However, it differs from Flutamide in its mechanism of action. Bicalutamide binds to the allosteric binding site of the receptor, which induces conformational changes of AR. These changes ultimately lead to the inhibition of AR signalling [343]. Additionally, clinical trials have shown that Bicalutamide is more effective than Flutamide in prostate cancer treatment [344, 345].

Another medication, Abiraterone, is also commonly used in prostate cancer treatment since 2011 [346]. Oral Abiraterone acetate for CRPC treatment (*Zytiga*®) acts as a selective inhibitor of the CYP17A1 enzyme, leading to the inhibition of androgen synthesis [347].

Enzalutamide (ENZ; *Xtandi*®) is a hormonal therapy drug commonly used for prostate cancer treatment since 2012. Generally, ENZ prevents androgens from reaching cancer cells. It works by inhibiting AR signalling in multiple ways. Specifically, ENZ can act as a competitive inhibitor of AR binding, an inhibitor of nuclear translocation, or an inhibitor of binding of activated AR into ARE [321, 348].

Docetaxel (*Taxotere*®), the first drug to be used as a chemotherapeutic in prostate cancer therapy, inhibits depolymerization of microtubules, resulting in suppressing mitotic cell division and initiating apoptosis [349]. However, cases of Docetaxel resistance have been reported, usually associated with cancer relapse [350].

A novel antineoplastic drug Cabazitaxel (*Jevtana*®) was designed to suppress the Docetaxel resistance [351]. However, severe side effect were connected with use of Cabazitaxel, like renal failure, alopecia, neurotoxicity fatigue, or even death [350].

Immunotherapy has demonstrated promising outcomes in treating patients with aggressive stages of cancer, such as CRPC [352]. Sipuleucel-T (*Provenge*®) was the first vaccine-based type of immunotherapy approved by FDA [353]. The mechanism of action utilizes patient's immune system to identify and target prostate cancer cells [352].

Figure 15 displays common approaches in prostate cancer therapy and the chemical structures of different types of therapeutic drugs.

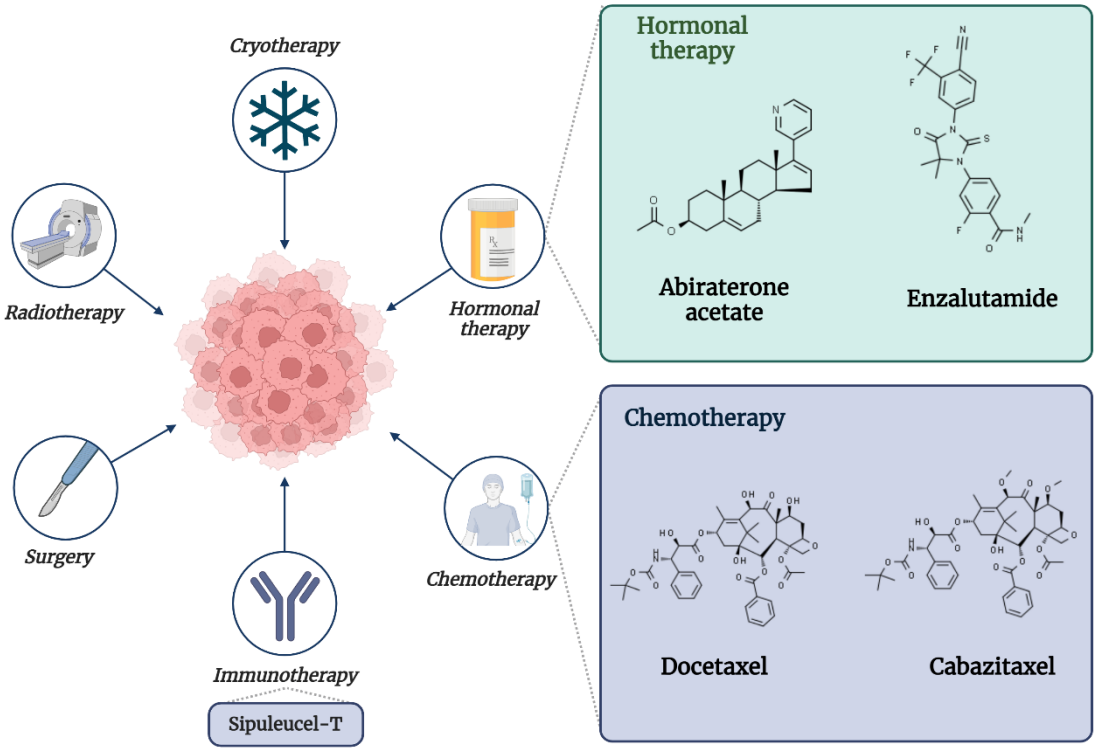

Figure 15: Common approaches in prostate cancer therapy. Surgery, radiotherapy, or cryotherapy are commonly used to treat localized prostate cancer. For advanced stages, hormonal therapy, chemotherapy, or immunotherapy drugs are administrated. Abiraterone acetate, available in the form of pills for oral administration, is a selective inhibitor of the CYP17A1 enzyme. Pills containing enzalutamide block androgens from reaching prostate cancer cells by suppressing AR signalling. Docetaxel is a prevalent chemotherapeutic drug, while Cabazitaxel was designed to counteract Docetaxel resistance. Sipuleucel-T is currently the only vaccine-based immunotherapy approved by FDA.

3.4.4 Castration-resistant Prostate Cancer

At the early stages of the disease, prostate cancer cells usually respond well to the hormonal medication known as ADT [354]. Over time, prostate cancer cells develop a resistance to commonly used hormonal therapy, eventually leading to a progression of castration-resistant prostate cancer (CRPC) [354]. The currently preferred term is "castrate-resistant, but historically, CRPC has been referred to as "androgen-independent" or "hormone-refractory prostate cancer" [355, 356]. CRPC progression occurs due to failing ADT, which targets AR signalling pathway. However, the exact mechanisms responsible for the transition from androgen-dependent prostate cancer to CRPC are not yet fully clarified [356]. During the CRPC, the AR signalling is restored despite the AR suppression and depletion of naturally circulating androgens in the bloodstream [357]. The reactivation of AR transcription activity was suggested to be restored by multiple mechanisms.

One mechanism that enables prostate cancer cells to survive and proliferate even in an environment with a limited source of androgens is AR overexpression [356]. This mechanism enables bypassing the inhibition of AR by antiandrogenic drugs [358]. Detection of increased AR on mRNA and protein levels is one of the defining indications of CRPC [359]. It has been observed that AR gene overexpression can occur even in the absence of AR gene amplification, indicating the presence of independent regulators of AR gene expression, such as miRNA or epigenetic factors. These epigenetic modifications include DNA methylation or histone acetylation [354, 360]. Prostate cancer cells overexpressing AR display increased binding ability to chromatin, leading to the formation of an altered AR transcriptome [361].

Another suggested mechanism of AR reactivation is through mutations of the *AR* gene, which usually occurs within the LBD. These mutations can alter its ligand selectivity and allow other hormones to bind and activate the receptor, such as estrogen or progesterone [354, 362].

As previously discussed, AR splicing variants are commonly found in samples of patients with CRPC (*Chapter 3.3.4*). These splicing variants allow constitutive activation of AR even in the absence of androgens [7]. AR-v7 is the most prevalent splicing variant associated with CRPC. In primary stages of prostate cancer, AR-v7 occurs rarely (< 1 %), but in CRPC cases, its occurrence increases up to 94 % [363]. Additionally, AR-v7 induces transcription of various genes involved in regulating the cell

cycle, such as *CDK1* or *UBE2C,* and thus can positively modulate prostate cancer growth even in the absence of androgens [7]. Ubiquitin-conjugating enzyme 2C is encoded by the *UBE2C* gene, which was reported to be regulated by AR-v7 exclusively [364]. Novel therapies are being developed to target AR splicing variants as they play a significant role in the progression of CRPC. For instance, some drugs target AR variants either directly, such as niclosamide, which inhibits AR-v7 by inducing its protein degradation, or indirectly, such as PLK inhibitors, which block cell cycle progression [365, 366].

Metastatic castration-resistant prostate cancer (mCRPC) is the final stage of the disease. It is characterized by the inability of hormone therapy to control the cancer's growth and the cancer spreading to lymph nodes or other parts of the body [296]. To this day, this type of cancer is classified as incurable and fatal [367].

To conclude, prostate cancer is a severe disease that requires extensive treatment. However, existing therapies for prostate cancer display multiple extreme side effects. As a result, new research is focused on alternative treatment options, such as using genetic biomarkers for targeted gene therapy, utilizing nanotechnology for precise and controlled treatment, and exploring novel therapeutic approaches [321]. Thus, novel approaches in prostate cancer therapy are constantly investigated.

3.5 AhR/AR crosstalk

The crosstalk between AhR and AR is a topic that has been discussed extensively, but its mechanisms are yet to be fully comprehended. Both of these receptors have been found to interact with other NRs, which suggests that a potential mechanism for AhR and AR interaction is through direct contact with these receptors [295, 368]. Additionally, a protein-protein interaction between AhR and ER, another hormone receptor, has also been demonstrated (as described in *Chapter 3.2.2.2*). The direct interaction of AhR and ER triggers the ubiquitination of ER, resulting in its proteasomal degradation [107]. Given that AR shares many similarities with ER, the question of whether AhR could also interact with AR through a similar mechanism arose.

Ohtake *et al*. investigated the connection between AhR and sex hormone signalling. Findings suggest that upon AhR activation by strong and potent ligands or through the expression of a constitutively active AhR, the AR protein levels were significantly reduced. In contrast, mRNA levels remained unchanged [369].

AhR and AR may also interact through shared coactivator proteins such as SRC1 and p300 [295, 370]. Another possible AhR/AR crosstalk mechanism involves the phosphorylation of AR by Src kinase. As described previously in *Chapters 3.2.2.3* and *3.3.2.2*, the crosstalk between AhR and AR with Src kinase has been reported multiple times. AhR may play a crucial role in controlling AR signalling in CRPC through Src as an intermediary signal. The simultaneous inhibition of AhR and Src kinase decreased AR signalling in CRPC cells [371]. Thus, research suggest that AhR/Src kinase crosstalk could result in maintaining the AR signalling in CRPC [295].

3.5.1 AhR/AR Crosstalk in the Context of Prostate Cancer

As mentioned earlier, recent research indicates the involvement of AhR in various types of cancer, including prostate cancer. However, the precise mechanisms underlying this association are not yet entirely established.

A study by Thomas *et al*. combined the use of antiandrogen bicalutamide and Carbidopa to observe their antitumoral activity and impact on AR suppression. The results showed that the combination treatment was highly effective in reducing cell viability and inducing apoptosis in LNCaP and C4-2 cell lines. During *in vivo* experiments, the combined treatment was more effective in reducing serum PSA levels compared to bicalutamide alone. However, this investigation did not elucidate the exact mechanism of action [372].

As previously mentioned, Carbidopa was also reported to activate AhR [149]. A recent study investigated the connection between AhR activation and AR suppression, reducing prostate cancer progression in DU145 and LNCaP cell lines. This study revealed that AhR activation by Carbidopa induced proteasomal degradation of AR. Furthermore, treatment with Carbidopa in a murine cancer model increased AhR protein level, decreased AR protein level, and suppressed prostate cancer progression [373]. This may be due to the E3 ubiquitin ligase activity of AhR, which also has been reported multiple times [116, 374, 375]. Ohtake *et al*. conducted a study that demonstrated that AhR may be able to modulate steroid receptor functions through its E3 ubiquitin ligase activity [374]. Taken together, the antitumoral activity of combined treatment with Carbidopa and bicalutamide observed previously by Thomas *et al*. may have occurred due to activation of AhR and its subsequent E3 ligase activity.

Several PAHs and dioxins were connected to antiandrogenic properties. In LNCaP cells, these AhR ligands decreased cell proliferation, reduced PSA levels, and inhibited the 5α-reductase enzyme [376, 377]. AR degradation in LNCaP cells induced by 3MC, another AhR ligand, is suggested to occur due to direct interaction between AhR and AR proteins [111]. Furthermore, the androgen-independent mechanism of 3MC was recently reported to induce a formation of AhR/ARNT/AR complex, capable of binding to androgen-specific chromatin binding sites and subsequently inducing the expression of AR-target genes [378].

Non-steroidal antiandrogen drug flutamide was recently identified as a novel AhR activator in an *in vivo* murine model [379]. Chen *et al*. identified another common prostate

cancer therapy drug, cyproterone acetate, as a potent AhR agonist in mouse Hepa-1c1c7 cells. However, the same drug displayed AhR antagonist effects in human HepG2 and MCF7 cell lines [380].

As previously mentioned, Bicalutamide or Enzalutamide are commonly used antiandrogens in prostate cancer therapy. However, they fail to suppress the expression of AR splicing variants, as they lack LBD, the target for antiandrogenic treatment. Surprisingly, naturally occurring prenylflavonoid icaritin has shown the ability to co-target both AR-fl and its splicing variants. It was observed that icaritin also induces proteasomal degradation of AR-fl through the activation of AhR. Additionally, icaritin also induced AhR-mediated proteasomal degradation of AR splicing variants. Knockdown of the AhR gene restored AR stability and partially evoked the suppression of cancer cell growth. In a murine model of CRPC, icaritin was found to target both AR-fl and AR splicing variants and inhibit AR signalling without any toxic effect [381].

In summary, recent research indicates that AhR ligands can precisely regulate the degradation of proteins and gene expression through the E3 ubiquitin ligase activity of AhR. This mechanism of action may make AhR a promising target for prostate cancer therapy, as it could potentially avoid the harsh side effects associated with commonly used antiandrogenic drugs and chemotherapeutics.

3.5.2 Suggested Hypothesis

Based on the available literature and published research, it is evident that substances containing an indole aromatic ring are significant AhR ligands and activators. Therefore, this study aimed to investigate whether selected indole compounds can induce the same effect, i.e., AR proteasomal degradation through the activation of AhR. The tested substances were selected based on the previous experiments of our research group when it was found that some of the 22 tested indoles demonstrated the ability to activate AhR in the human hepatoma carcinoma cell line [170]. Four different prostate cancer cell lines were used as a model of different conditions: 22Rv1, human prostate carcinoma epithelial cell line derived from a xenograft with AhR, AR-fl, and AR-v7 [382]; LNCaP androgen-sensitive prostate cancer cell line from the biopsy of the left supraclavicular lymph node with AhR and AR-fl [383]; its clone C4-2 [384], and PC-3 cell line from bone metastasis containing only AhR and no AR variant [385]. A novel approach of prostate cancer therapy and this hypothesis are displayed in **Figure 16**.

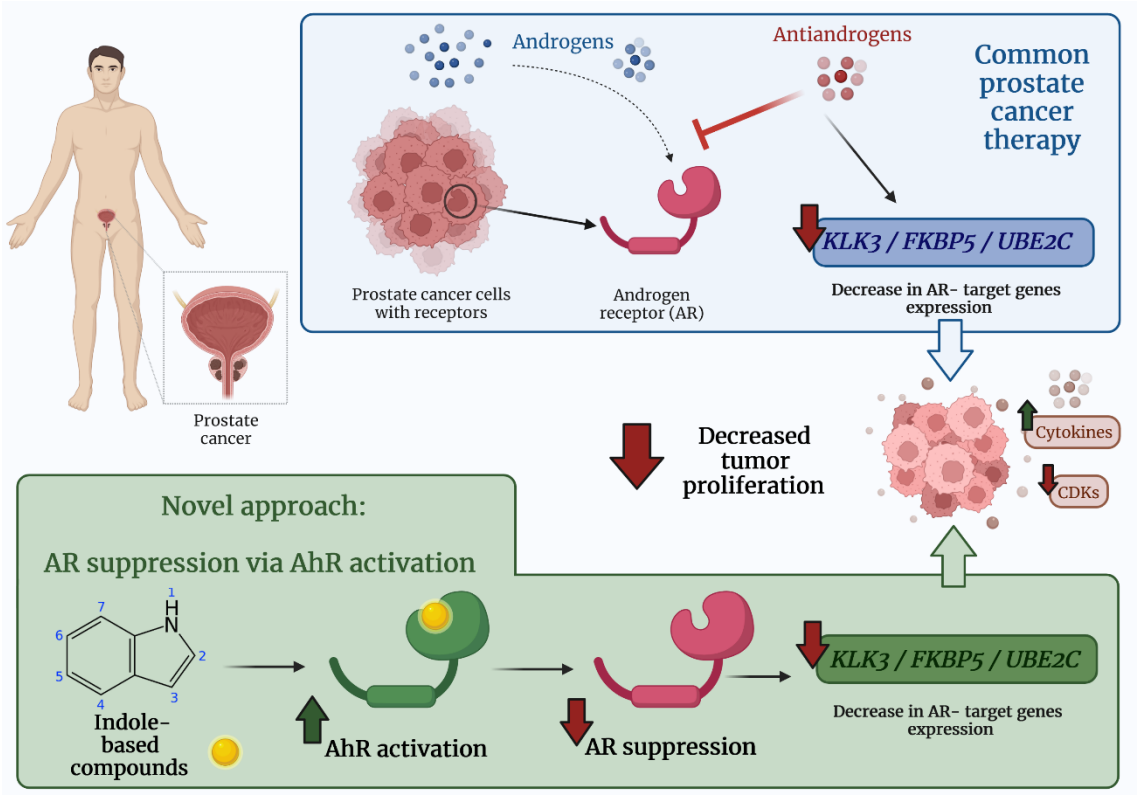

Figure 16: Suggested hypothesis. A typical treatment approach for prostate therapy involves blocking the AR signalling pathway using specific antiandrogens. Unfortunately, this hormone therapy can come with serious side effects, as well as the development of CRPC. However, recent studies have shown that AhR can act as an E3 ubiquitin ligase, leading to the proteasomal degradation of AR and, thus, inhibition of AR signalling. This novel approach may help avoid the unwanted side effects of ADT. In this study, the ability of selected indoles to activate AhR and simultaneously suppress the AR signalling pathway was evaluated in series of *in vitro* experiments.

4 MATERIALS

4.1 Biological materials

Humane prostate carcinoma epithelial cell lines PC-3 (ATCC No. CRL-1435), 22Rv1 (ATCC No. CRL-2505), and AIZ-AR [386] were cultured in Rosewell Park Memorial Institute (RPMI) 1640 medium. RPMI medium was supplemented with 10% fetal bovine serum (FBS), 1% non-essential amino acids (NEAA), and 2 mM L-glutamine (L-Gln). Human prostate carcinoma cell line LNCaP (ATCC No. CRL-1740) and C4-2 (ATCC No. CRL-3314) were cultured in Dulbecco's modified Eagle's Medium (DMEM) supplemented with 10% FBS, 1% NEAA, and 2 mM L-Gln. Cells were maintained in a humidified incubator at 37°C and 5% CO_2. All cell lines were regularly tested for the presence of mycoplasma using MycoAlert^{TM} Mycoplasma Detection Kit (Lonza).

Before the beginning of this project, 22Rv1, PC-3, and LNCaP cell lines were subjected to authentication by genotyping. This was performed by GENERI BIOTECH s. r. o.

4.2 Tested compounds

Compounds of interest were selected based on the previous study by our research group. In this preceding research, the effect of the same indoles on AhR activity was monitored in the intestinal LS180 cell line [170]. Tested indoles, along with their chemical structures, are given in **Figure 17**.

Compound	Abbreviation	Structure	Compound	Abbreviation	Structure
1-methylindole	1MI		2,3,3-trimethylindolenine	2,3,3TMI	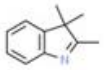
2-methylindole	2MI	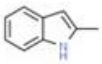	2,3,7-trimethylindole	2,3,7TMI	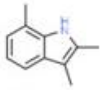
3-methylindole	3MI		4-methoxyindole	4MeO	
4-methylindole	4MI		5-methoxyindole	5MeO	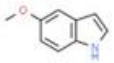
5-methylindole	5MI		6-methoxyindole	6MeO	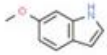
6-methylindole	6MI		7-methoxyindole	7MeO	
7-methylindole	7MI		4,6-dimethoxyindole	4,6DMI	
1,2-dimethylindole	1,2DMI	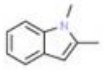	5,6-dimethoxyindole	5,6DMI	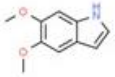
1,3-dimethylindole	1,3DMI		4-methoxy-1-methylindole	4MeO1MI	
2,3-dimethylindole	2,3DMI	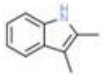	5-methoxy-2-methylindole	5MeO2MI	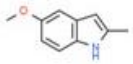
2,5-dimethylindole	2,5DMI	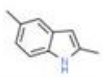	7-methoxy-4-methylindole	7MeO4MI	

Figure 17: Tested indoles. A total of 22 indolic compounds were tested and divided into four groups: monomethylindole, di- and tri-methylindoles, monomethoxyindoles, and methoxyindole. The name, abbreviation, and chemical structure of each compound are displayed in this figure.

4.3 Chemicals

- **CELL MAINTENANCE**
  - DMEM medium – high glucose — Merck, D6546
  - DMSO — Merck, D4540
  - Dulbecco's PBS — Serana, BDL-001
  - Ethyl alcohol, 99.8% — Lach-Ner, 20025-A99
  - Fetal Bovine Serum — Merck, F7524
  - H_2O, nuclease free — Merck, W4502
  - Hygromycin B — Santa Cruz Biotech., sc-29067
  - L-glutamine — Serana, RGL-001
  - MEM Nonessential amino acid solution — Merck, M7145
  - Methyl alcohol — Penta Chemicals, 21210-20005
  - MyAlert Mycoplasma Detection kit — Lonza, LT07-118
  - RPMI-1640 medium — Merck, R0883
  - Trypan blue, cell culture tested — Merck, T9650
  - Trypsin 0.25% - EDTA in HBSS — Biosera, MS00CY100B

- **TREATMENT**
  - BaP — Merck, B1760
  - DHT — Merck, D073
  - ENZ — Santa Cruz Biotech., MDV3100
  - FICZ — Merck, SML1489
  - MNF — a gift (Dr. Haarmmann-Stemman)
  - TCDD — Ultra Scientific, RPE-029

- **CYTOTOXICITY AND PROLIFERATION ASSAY**
  - Crystal Violet 1% — Merck, B0253S
  - Doxorubicin — PromoCellGmbH, PK-CA577-K329
  - Thiazolyl Blue Tetrazolium Bromide — Merck, MT2128
  - Triton X-100 — Merck, T9284

- **REPORTER GENE ASSAY**
  - ATP — Merck, A2383
  - Coenzyme A sodium salt hydrate — Merck, C4780
  - D-Luciferin — Merck, L9504
  - DTT — Merck, 43819
  - EDTA — Merck, E9884
  - $MgSO_4$ x $7H_2O$ — Lachema
  - Reporter Lysis 5x Buffer — Promega, E3971
  - Tris-Acetate-EDTA Buffer — Merck, T9650

- **RT-qPCR**
  - 10x M-MuLV Reaction Buffer — BioLabs®, B0253S
  - Chloroform — Merck, C2432
  - dATP — TaKaRa, 4026
  - dCTP — TaKaRa, 4028

- dGTP — TaKaRa, 4027
- dTTP — TaKaRa, 4029
- Isopropyl alcohol — Lach-Ner, 20037-AT0
- KiCqStart Probe qPCR ReadyMix — Merck, KCQS04
- LightCycler® 480 SYBR® Green I — Roche, 4707516001
- M-MuLV (reverse transcriptase) — BioLabs®, M0253L
- Random Primers 6 — BioLabs®, S1230S
- RNase inhibitor — BioLabs®, M0307L
- Tri Reagent® — Molecular Research Center, TR118

- **WESTERN BLOT**
  - 10x Tris/Glycine Buffer — BioRad, 1610771
  - 10x Tris/Glycine/SDS Buffer — BioRad, 1610732
  - 20x TBS Buffer — ThermoFisher Scientific, 28358
  - Acetic acid, 99.8% — Penta Chemicals, 607-002-00-6
  - Acrylamide/Bis-acrylamide — Merck, A2792
  - Ammonium persulfate — Merck, A3678
  - Anti-β-actin antibody — Cell Signaling, 4967
  - Anti-AhR antibody (D5S6H) — Cell Signaling, 83200
  - Anti-AR antibody (D6F11) — Cell Signaling, 5153
  - Anti-mouse IgG, HRP-linked antibody — Cell Signaling, 7076
  - Anti-PSA antibody (D6B1) — Cell Signaling, 5365
  - Anti-rabbit IgG, HRP-linked antibody — Cell Signaling, 7074
  - Bovine serum albumin — Merck, A2153
  - Bradford Reagent — Merck, B6916
  - Bromophenol blue — Merck, B0126
  - Glycerol — Lach-Ner, 40058-A50
  - Halt Protease Inhibitor Cocktail — ThermoFisher Scientific, 78430
  - HEPES — Merck, H3375
  - Immobilon® Transfer membrane — Merck, IPVH00010
  - Non-fat dried milk Lactino — ARTIFEX Instant s.r.o.
  - PhosSTOP EASYpack — Roche, 4906837001
  - Ponceau S. solution — Santa Cruz Biotech., sc-301558
  - Re-Blot Plus Strong Solution (10x) — Merck, 2504
  - Running buffer — BioRad, 1610798
  - Sodium chloride — LachNer, 30093-AP0
  - Sodium dodecyl sulphate — Merck, L3771
  - Stacking buffer — BioRad, 1610799
  - TEMED — Merck, 110732
  - Tween 20 — Merck, P1379
  - WesternSure® PREMIUM Chemiluminescent Substrate — Li-Cor, 926-95000
  - WesternSure® Pre-Stained Chemiluminescent Protein Ladder — Li-Cor, 926-98000

- **CHROMATIN IMMUNOPRECIPITATION**
  - 100bp DNA Ladder — Promega, G210A
  - Agarose — Serva, 11380.02
  - Agarose, LMP — Promega, V3841
  - Blue/Orange 6x Loading Dye — Promega, G190A
  - ChIP-Grade Protein G Magnetic Beads — Cell Signaling, 9006
  - Formaldehyde solution — Merck, 47608
  - GelRed® Nucleic Acid Stain — Biotium, 41003
  - Micrococcal Nuclease — Cell Signaling, 10011S
  - Proteinase K — ThermoFisher Scientific, 4333793
  - SimpleChIP® KLK3 Promoter Primers — Cell Signaling, 32784S
  - SimpleChIP® Plus Enzymatic Chromatin IP Kit — Cell Signaling, 9005
  - Ultra Low Range DNA Ladder — Invitrogen, 10597012

- **TRANSFECTION AND CRISPR/Cas9 REAGENTS**
  - Ah Receptor CRISPR/Cas9 KO Plasmid — Santa Cruz Biotech., sc-400297
  - Ah Receptor HDR Plasmid — Santa Cruz Biotech., sc-400297
  - Control CRISPR/Cas9 Plasmid — Santa Cruz Biotech., sc-418922
  - FuGENE® HD transfection reagent — Promega, E231A
  - Plasmid Transfection Medium — Santa Cruz Biotech., sc-108062
  - Puromycin — Merck, P9620
  - UltraCruz® Transfection Reagent — Santa Cruz Biotech., sc-395739

4.4 Solutions

Table 3: Firefly luciferase substrate for Reporter Gene Assay.

Reagent	Quantity
D-Luciferin	50 mg
ATP	100 mg
Coenzyme A	50 mg
DTT	1.68 g
1 M Tris-Acetate (pH 7.8)	13.2 ml
100 mM $MgSO_4 \cdot 7H_2O$	12.3 ml
0.5 M EDTA	66 µl
dH_2O	up to 300 ml

Table 4: Protein lysis buffer.

Solution/compound	Reagent	Quantity
Base Solution for Protein Lysis Buffer pH 7.5	50 mM HEPES 5 mM EDTA 150 mM NaCl 1% Triton X-100 (v/v)	Total volume 10 ml
Phosphatase inhibitor		1 capsule
Protease inhibitor		100 µl

Table 5: 2x Loading buffer (LB) for Western blot.

Reagent	Quantity	Total volume
4x Stacking Buffer	2.5 ml	10 ml
10% SDS (w/w)	4.0 ml	
Glycerol	2.0 ml	
Bromophenol blue	2.0 mg	
DTT	310 mg	
dH_2O	up to 10 ml	

Table 6: Buffers for SDS-PAGE and Western blot.

Buffer	Reagent	Volume
1x Migration Buffer	10x Tris/Glycine/SDS Buffer	100 ml
	dH_2O	900 ml
1x Transfer Buffer	10x Tris/Glycine Buffer	100 ml
	MeOH	200 ml
	dH_2O	700 ml
1x TBS/Tween	20x TBS	50 ml
	Tween 20	500 µl
	dH_2O	950 ml

Table 7: Buffers for ChIP. The volumes indicated are calculated for a single sample.

Buffer	Reagent	Volume
1x PBS + PIC	1x PBS	1000 µl
	200x PIC	5 µl
1x Buffer A	4x Buffer A Solution	250 µl
	dH_2O	750 µl
	1 M DTT	0.5 µl
	200x PIC	5 µl
1x Buffer B	4x Buffer B Solution	275 µl
	dH_2O	825 µl
	1 M DTT	0.5 µl
1x ChIP Buffer	10x ChIP Buffer	10 µl
	dH_2O	90 µl
	200x PIC	0.5 µl
Low-salt Buffer	10x ChIP Buffer	40 µl
	dH_2O	3 600 µl
High-salt Buffer	10x ChIP Buffer	50 µl
	dH_2O	4 500 µl
	5 M NaCl	35 µl
1x ChIP Elution Buffer	2x ChIP Elution Buffer	75 µl
	dH_2O	50 µl

4.5 Equipment

- Analytical scales — Kern, ABS 80-4N
- Aspirator — Biosan, FTA-1
- Centrifuge 5415 R — Eppendorf
- Centrifuge Z 100M — Hermle
- Eppendorf Xplorer® electronic pipettor — Eppendorf
- FACS Verse — BD Biosciences
- Fluorescence microscope — Olympus
- Genius Dry Bath Incubator — Major Science, md-02n
- Immersion Bath Incubator — Daihan LabTech, LCB22D
- Incubator — Conterm Mitre 4000 series
- Laminar box Labculture® — ESCO
- Li-Cor C-DiGiT™ blot scanner — Li-Cor Biosciences
- LightCycler 480 II — Roche
- Microscope — Olympus
- Mini-PROTEAN Tetra Cell — BioRad, 1658004EDU
- Mini-Rocker shaker — Biosan, MR-1
- Nanodrop Lite — ThermoFisher Scientific
- Rocker shaker — Biosan, MR-12
- Sonorex Digitec Ultrasonic bath — Bandelin electronics, DT-31
- TECAN Infinite M200 — Tecan Trading
- Trans-Blot® SD Semi-Dry Transfer Cell — BioRad. 1703940
- Voltage source MP-500V — Cleaver Scientific Ltd.
- Vortex Reax Top — Heidolph

4.6 Software

- BioRender: Scientific Image and Illustration Software, Canada
- EndNote™ 20, Clarivate™
- GraphPad Prism Version 9.4.1, GraphPad Software, San Diego, California, USA
- Image Studio 5.0 for C-DiGit Scanner Software, Li-Cor
- Infinite® M200 Software, TECAN
- LightCycler 480® Software, Roche Diagnostics
- Scope Image 9.0, Bioimager

5 METHODS

5.1 Cytotoxicity and Proliferation Assays

Cells, either 22Rv1, PC-3, or C4-2, were seeded in 96-well plates at a density of 2.5 x 10^4 cells per well in a total volume of 200 µl. The cells were then left to stabilize overnight. The medium was then replaced with a fresh one containing compounds of interest with increasing concentrations (0.1-100 µM) or control compounds such as DMSO (untreated/UT; 0.1%; v/v), doxorubicin (20 µM), or Triton X-100 (2%) for 24 h.

5.1.1 MTT Assay

After the treatment with tested compounds, MTT cytotoxicity assay was performed to determine cell viability. This colorimetric test relies on the activity of mitochondrial dehydrogenases, which convert a yellow soluble compound called 3-(4,5-dimethyl-2-thiazolyl)-2,5-diphenyl-2H-tetrazolium bromide (MTT) into purple formazan crystals. These crystals are then dissolved, and the intensity of the colour directly correlates with the number of living cells [387].

To perform this assay, the medium was replaced with 100 µl MTT solution (MTT diluted in RPMI medium, final concentration 0.3 mg/ml), and cells were incubated for 30 min at 37°C. After incubation, the MTT solution was aspirated, and cells were rinsed twice with 100 µl 1x PBS. Formed formazan crystals were dissolved in 70 µl of DMSO, and the absorbance was measured at a wavelength of 595 nm using TECAN Infinite M200.

5.1.2 Crystal Violet Assay

Crystal violet proliferation assay was then conducted, which relies on the ability of a triarylmethane dye to bind to nuclear DNA. This method measures cellular proliferation by staining living cells that remain attached to the culture plates, while dead cells lose their adherence ability and are removed during washing procedures [388].

Following the incubation with tested compounds, the medium was replaced with 60 µl of Crystal violet solution (1x diluted in dH_2O, final concentration 0.5% v/v), and incubated on a rocking shaker for 1 h. The staining solution was then removed, and adherent cells washed five times with 100 µl of 1x PBS. To dissolve the bound dye, 200 µl of methanol (MeOH) was added to the stained cells, and the absorbance at a wavelength of 595 nm was detected using TECAN Infinite M200.

5.2 Stable Transfection of 22Rv1 and PC-3 Cells

Initially, a new model was needed to conduct further experiments on AhR transcription activity in a prostate-specific environment. To achieve this, two stably transfected cell lines containing luciferase reporter gene were constructed. For this purpose, pGL4.27 [luc2P/minP/Hygro] plasmid originally designed by Novotna *et al.* in 2011 was utilized [389].

The cells were seeded in RPMI medium at a density of 5 x 10^4 cells per well of a 12-well plate, and then immediately transfected with pGL4.27-DRE reporter plasmid (concentration of 200 ng per well) using FuGENE® Transfection Kit, following the manufacturer's protocol. The cells were then incubated with the transfection medium for 48 h. After this, the medium was replaced with selection medium containing Hygromycin B (HygB).

Firstly, the inhibitory concentrations (IC_{25} and IC_{50}) of HygB were determined for each cell line. The transfected cells were then exposed to IC_{25} selection medium for 4 days, followed by incubation with IC_{50} selection medium for 4 weeks. The IC_{50} selection medium was renewed every 3-4 days. Finally, after the selection process, polyclonal populations were isolated.

Polyclonal populations of each cell line were seeded into 10 mm culture dishes at a concentration of 1 x 10^3 cells per dish and cultured for an additional three weeks in IC_{50} selection medium. By this time, colonies of monoclonal populations had formed in each individual dish. In total, 10 monoclonal populations were isolated for the 22Rv1 cell line and 7 for the PC-3 cell line. The respective monoclonal populations were collected, labelled, and analysed using the Reporter gene assay (RGA) detailed in *Chapter 5.3*. Initially, the responsiveness of each monoclone to the AhR model ligand TCDD (10 nM) was evaluated. The monoclonal population with the most eligible response was selected for functional characterization for each cell line. For 22Rv1, the selected monoclonal population was titled as 22AhRv1, and for PC-3 as PAhRC3. HygB in the respective IC_{50} concentration was added to each cell line once a week to maintain the selection pressure.

5.2.1 Dose-dependent Analysis with Model AhR Ligands

These series of experiments were conducted to determine whether the 22AhRv1 and PAhRC3 cell lines can react to typical AhR ligands, namely TCDD, BaP, and FICZ. The cells were seeded into 96-well plates at a density of 2.5 x 10^4 cells per well with a total volume of 200 µl and left to stabilize overnight. The following day, the cells

were treated with the model AhR ligands at following concentrations: TCDD (0.01, 0.1, 1, 5, 10, 50, 100 nM), BaP and FICZ (0.01, 0.1, 1, 5, 10, 50 µM). RPMI medium with DMSO (untreated; 0.1%; v/v) was used as a negative control. After 24 h of incubation with the tested compounds, the cells were analysed using RGA (detailed in *Chapter 5.3*).

5.2.2 Maintenance of Luciferase Inducibility after TCDD Treatment

In this section of the functional experiments, we evaluated the ability of the inducibility of luciferase over an extended period. To investigate this, 22AhRv1 and PAhRC3 cells were cultured in standard RPMI medium without HygB for 10 weeks. Each week, an experiment was conducted to determine whether luciferase activity remained stable even without the selection antibiotic. The cells were seeded into 96-well plates at a density of 2.5 x 10^4 cells per well in a total volume of 200 µl and stabilized overnight. The following day, the cells were treated with TCDD (10 nM) for 24 h. RPMI medium with DMSO (untreated; 0.1%; v/v) was used as a negative control. Results were analysed using RGA (detailed in *Chapter 5.3*).

5.2.3 Time-dependent Cryopreservation Analysis

The third group of functional experiments was conducted to investigate the response of 22AhRv1 and PAhRC3 cells to TCDD after undergoing freeze-thaw cycles. Cells from each cell line were collected and frozen using standard procedures with FBS and DMSO as cryoprotectants (3 x 10^6 cells/cryovial). The cell lines were stored in liquid nitrogen and thawed after 2 and 6 months. The cells were then seeded into 96-well plates at a density of 2.5 x 10^4 cells per well in a total volume of 200 µl and stabilized overnight. The next day, the cells were treated with TCDD (10 nM) for 24 h. RPMI medium with DMSO (untreated; 0.1% v/v) was used as a negative control. The outcomes were analysed using RGA (detailed in *Chapter 5.3*).

5.2.4 Analysis of AhR Antagonist Treatment

Cells were exposed to the AhR antagonist MNF to verify the functionality of the AhR signalling pathway. 22AhRv1 or PAhRC3 cells were seeded into 96-well plates at a density of 2.5 x 10^4 cells per well in a total volume of 200 µl and stabilized overnight. The following day, the cells were treated with TCDD (10 nM) in combination with MNF (0.1, 1, 5, 10 µM) for 24 h. RPMI medium with DMSO (untreated; 0.1%; v/v) was used as a negative control, and TCDD (10 nM) was used as a positive control. Results were analysed using RGA (detailed in *Chapter 5.3*).

5.3 Reporter Gene Assay

For monitoring AhR transcription activity in prostate-specific environment, newly developed cell lines 22AhRv1 and PAhRC3 were used (detailed in *Chapter 5.2*). Stably transfected cell line AIZ-AR [386] derived from the parental 22Rv1 cell line was used as a cellular model for monitoring AR activity.

Cells from each cell line were seeded at a density of 2 x 10^4 cells per well in a 96-well plate, with 200 µl of RPMI medium per well, and stabilized overnight. The following day, cells were treated with tested indole compounds for 4 and 24 h at concentrations of 1, 10, and 100 µM. In all experiments, DMSO (0.1% v/v) was used as a negative control/vehicle. For the 22AhRv1 and PAhRC3 cell lines, TCDD (10 nM) was used as a positive control of AhR transcription activity. For the AIZ-AR cell line, DHT (10 nM) was used as a positive control of AR transcription activity, and antiandrogen ENZ (10 µM) was used as a control of AR suppression. The effects of indoles were evaluated in the absence and presence of DHT (10 nM). Thus, AIZ-AR experiments were executed in two modes: agonist (without DHT) and antagonist (indoles in combination with DHT). The effects of AhR ligands, TCDD (10 nM), and FICZ (10 µM) were also determined.

Treatment was terminated by aspiration of the medium. Adherent cells were lysed with 25 µl of 1x Reporter Lysis Buffer and kept at -80°C for at least 1 h. The samples were then thawed at room temperature (RT). A total sample volume of 6 µl was mixed with 30 µl of luciferase substrate (*Chapter 4.4 Solutions*, **Table 3**). The emitted light was measured with the TECAN Infinite M200. The intensity of the luminescence is directly proportional to the activity of the monitored receptor.

5.4 Quantitative Reverse Transcriptase PCR (RT-qPCR)

Only indoles that met both primary criteria at the RGA level, meaning AhR activation and simultaneous AR suppression, were chosen to proceed to the second experimental phase. The impact of 8 selected indoles on the mRNA expression of AhR- and AR-target genes was evaluated using RT-qPCR.

22Rv1 or PC-3 cells were seeded in a 6-well plate at a density of 1.5 x 10^6 cells per well in of 1.5 ml RPMI medium. After overnight stabilization, the cells were treated with the 8 selected indoles in 4 different concentrations (1, 10, 50, and 100 µM) in the presence of DHT (10 nM). DMSO (untreated; 0.1% v/v) was used as a negative control/vehicle, TCDD (10 nM) as a positive control for AhR-target genes, and DHT (10 nM) as a positive control for AR-target genes. The cells were treated with the tested compounds for 24 h.

5.4.1 RNA Isolation and Reverse Transcription

After the incubation, total RNA was isolated using TRI Reagent®, according to the manufacturer's protocol. Using a NanoDrop™ Spectrophotometer, the concentration of the isolated samples was determined, and the A260/A280 ratio was used to monitor the quality. Based on the concentrations obtained, samples for reverse transcription were prepared, with each sample containing 1000 ng of RNA. Random Primers 6 (1 µl; 100 pmol/l) were added to each sample and incubated at 65°C for 5 min. The reaction solution was prepared according to **Table 8**. 6 µl of this solution was added to each sample, incubated at 42°C for 1 h, at 65°C for 10 min, and then cooled down on ice. The resulting cDNA samples were diluted 5 times with nuclease-free H_2O.

Table 8: Composition of Reverse transcription reaction solution. The volumes indicated are calculated for a single sample.

Reagent	Volume [µl]
M-MuLV Reverse Transcriptase (200 U/µl)	0.6
10x Reverse Transcriptase Reaction Buffer	1.2
RNase inhibitor (40 U/µl)	0.3
dNTPs (10 mM stock)	0.6
Nuclease-free H_2O	3.3
Total	**6.0**

5.4.2 RT-qPCR

AhR- and AR-target genes expressions were determined using either TaqMan® or SYBR® Green reagent systems. TaqMan® system was used to analyse the expression of *AhR*, *AhRR*, *AR-fl*, *CYP1A1*, *FKBP5*, *KLK3*, and *UBE2C* genes. The reaction solution was prepared according to **Table 9**. The expression of *AR-v7* was analysed with SYBR® Green system. The reaction solution was prepared according to **Table 10**. The expression of the housekeeping gene *GAPDH* was measured with both systems. Nuclease-free H_2O was used as a non-template control (NTC). Sample measurements were performed in technical triplicates in the 96-well LightCycler® plate.

The plate containing samples with PCR mixture was centrifuged at 450 rcf for 3 min and analysed using LightCycler® 480 II equipment. The reaction setting for TaqMan® system is listed in **Table 11**, and for SYBR® Green in the **Table 12**. The expression of the monitored genes was normalized to *GAPDH*. Relative gene expression values were then determined using the ΔΔ Ct method. **Table 13** contains a list of all primers and probes that have been used.

Table 9: RT-qPCR KiCqStart® Probe reaction solution. The volumes indicated are calculated for a single sample.

Reagent	Volume [µl]
KiCqStart® Probe qPCR ReadyMix	5.0
F+R primer (100 µM)	0.3
TaqMan® Probe (10 µM)	0.2
Nuclease-free H_2O	2.5
cDNA sample	2.0
Total	**10.0**

Table 10: RT-qPCR SYBR® Green reaction solution. The volumes indicated are calculated for a single sample.

Reagent	Volume [µl]
SYBR® Green	5.0
F+R primer (100 µM)	1.0
Nuclease-free H_2O	2.0
cDNA sample	2.0
Total	**10.0**

Table 11: LightCycler® 480 II reaction setting. RT-qPCR setting used for TaqMan® system analysis.

Detection Format:	**Mono Color Hydrolysis Probe/UPL Probe**		
Program	**Temperature**	**Time**	**Number of Cycles**
Pre-incubation	95 °C	20 s	1
Amplification	95 °C	5 s	45
	58 °C	30 s	
Cooling	40 °C	30 s	1

Table 12: LightCycler® 480 II reaction setting. RT-qPCR setting used for SYBR® Green system analysis.

Detection Format:	**SYBR® Green I/HRM Dye**		
Program	**Temperature**	**Time**	**Number of Cycles**
Pre-incubation	95 °C	10 min	1
Amplification	95 °C	15 s	40
	60 °C	1 min	
Melting Curve	95 °C	5 s	1
	65 °C	1 min	
	97 °C	-	
Cooling	40 °C	30 s	1

Table 13: List of primes and probes. Sequences of used forward primers (f), reverse primers (r), and probes (p).

Target gene	Sequence
AhR	f: 5' ATTGGTTGTGATGCCAAAGG 3' r: 5' CATTCGGATATGGGACTCGG 3' p: [6FAM]AGCAGAGCTGTGCACGAGAGGCTCA[OQA] 3'
AhR exon 5	f: 5' TGAATTTCAGCGTCAGCTACA 3' r: 5' AACAGACTACTGTCTGGGGGA 3'
AhRR	f: 5' GAGATGAAAATGAGGAGCGC 3' r: 5' TTTTACTTTTGCATCCGCGG 3' p: [6FAM]AAACCCAGAGCAGACACCGCAGCCA[OQA] 3'
AR-fl	f: 5' TGTGTCAAAAGCGAAATGGG 3' r: 5' TTCATCTCCACAGATCAGGC 3' p: [6FAM]TGCGTTTGGAGACTGCCAGGGACCA[OQA] 3'
AR-v7	f: 5' GAAATGTTAGAAGCAGGGATGACT 3' r: 5' GGTCATTTTGAGATGCTTGCAA 3'
CYP1A1	f: 5' GGAAGTGTATCGGTGAGACC 3' r: 5' CATAGATGGGGGTCATGTCC 3' p: 5' [6FAM]GCAACGGGTGGAATTCAGCGTGCCA[OQA] 3'
FKBP5	f: 5' TCCAAGACTCAGATGATGCC 3' r: 5' GGCACCCTGTAGTTATTTGC 3' p: 5' [6FAM]AAGTGTGTGTGGGGAGGGGAAGGGT[OQA] 3'
GAPDH	f: 5' GAAGGAAATGAATGGGCAGC 3' r: 5' TCTAGGAAAAGCATCACCCG 3' p: 5' [6FAM]ACTAACCCTGCGCTCCTGCCTCGAT[OQA] 3'
KLK3	f: 5' ACTGCATCAGGAACAAAAGC 3' r: 5' GGAGGCTCATATCGTAGAGC 3' p: 5' [6FAM]TGGGTCGGCACAGCCTGTTTCATCC[OQA] 3'
UBE2C	f: 5' CCACAGTGAAGTTCCTCACG 3' r: 5' GTTGGGTTCTCCTAGAAGGC 3' p: 5' [6FAM]ACCCCAACGTGGACACCCAGGGTAA[OQA] 3'

5.5 Western blot

In the **Phase II** experiments, Western blot analysis was the second technique used to investigate the possibility of 8 previously selected indoles affecting the levels of proteins of interest.

To carry out the experiment, prostate cancer cells were seeded into a 6-well plate at a density of 1.5×10^6 cells per well in 1.5 ml of RPMI or DMEM medium and stabilized overnight. 22Rv1 cells were treated with 8 selected indoles in 4 concentrations (1, 10, 50, and 100 µM) in the presence of DHT (10 nM). PC-3 cells were treated with only one selected compound, 3MI (skatole), at the same concentrations. C4-2 cells were treated with 8 selected indoles (100 µM) in the presence of DHT (10 nM). DMSO (untreated; 0.1% v/v) was used as a negative control/vehicle. As a positive control for the AhR pathway, TCDD (10 nM), BaP (10 µM), and FICZ (10 µM) were used. DHT (10 nM) was used as a positive control for the AR pathway in 22Rv1 cells.

5.5.1 Protein Isolation

Following a 24 h treatment period, total protein extracts were isolated from each sample. The medium was aspirated, and adherent cells were rinsed with 1x PBS and scraped out of the well into 1 ml of 1x PBS (ice cold). The samples were centrifuged (1500 rcf, 3 min, 4°C). The resulting pellet was resuspended in 80 µl of protein lysis buffer (*Chapter 4.4 Solutions*, **Table 4**), vortexed, sonicated, and centrifuged again (14 500 rcf, 15 min, 4°C). Subsequently, the supernatant was collected for each sample, and the protein concentration was determined using a Bradford reagent. The individual samples were measured in duplicates in a 96-well plate. 1x Bradford reagent (200 µl) was added into 10 µl of each sample. The calibration curve was created using nuclease-free H_2O and BSA (0.2, 0.4, 0.6 mg/ml). TECAN Infinite M200 was used to detect the absorbance at a wavelength of 595 nm. Eventually, the absolute protein concentration was calculated for each sample.

5.5.2 SDS-PAGE

Initially, samples were diluted with nuclease-free H_2O based on the concentration obtained, resulting in a total volume of 20 µl with 30 µg of protein per sample. 20 µl of 2x LB buffer (*Chapter 4.4 Solutions*, **Table 5**) was added to 20 µl of each prepared sample. The samples were denatured at 95°C for 5 min and cooled down on ice. Using the BioRad Miniprotean system, sodium dodecyl sulfate-polyacrylamide gel

electrophoresis (SDS-PAGE) was used for the separation of protein samples in 10% resolving gel (**Table 14**) and 4% stacking gel (**Table 15**). Prepared gels were placed into the BioRad Miniprotean chamber filled with 1x Migration buffer (*Chapter 4.4 Solutions*, **Table 6**). Samples were pipetted into a gel (38 µl per well), and WesternSure® Pre-stained chemiluminescent protein ladder (5 µl) was added to one well as a marker. SDS-PAGE was performed with four gels in a single chamber with the following settings: the current was set to 60 mA for 20 minutes, and then it was increased to 120 mA for an additional 1 h.

Table 14: Resolving gel for Western blot. TEMED and APS were added as the last components to begin the polymerization process. Listed volumes correspond to the preparation of 1 gel in 1.5 mm spacer plates.

Reagent	Volume	
	10% gel	12.5% gel
dH_2O	4.9 ml	4.28 ml
Resolving gel buffer (1.5M Tris-HCl buffer, pH 8.8)	2.5 ml	2.5 ml
Acrylamide/Bis-acrylamide (29:1 ratio)	2.5 ml	3.13 ml
10% SDS (w/v)	100 µl	100 µl
TEMED	10 µl	10 µl
10% APS (w/v)	100 µl	100 µl

Table 15: 4% Stacking gel for Western blot. TEMED and APS were added as the last components to begin the polymerization process. Listed volumes correspond to the preparation of 1 gel in 1.5 mm spacer plates.

Reagent	Volume
dH_2O	2.56 ml
Stacking gel buffer (0.5M Tris-HCl buffer, pH 6.8)	1.0 ml
Acrylamide/Bis-acrylamide (29:1 ratio)	400 µl
10% SDS (w/v)	40 µl
TEMED	8 µl
10% APS (w/v)	20 µl

5.5.3 Semi-dry Transfer to PVDF Membrane

Polyvinylidene difluoride (PVDF) membrane was rehydrated in MeOH (3 min), in dH_2O (2x 5 min), and submerged into 1x Transfer buffer (*Chapter 4.4 Solutions*, **Table 6**). Transfer of proteins after SDS-PAGE separation from a gel into PVDF membrane took

place in a Transblot Semi-dry transfer cell for 2 h at 380 mA. Subsequently, membranes were rinsed with 1x TBS/Tween (5x 2 min; *Chapter 4.4 Solutions*, **Table 6**) and stained with Ponceau S Rouge solution (0.1% w/v in 5% acetic acid) to detect protein bands. Membrane strip containing protein of interest was rinsed with 1x TBS/Tween and then incubated with blocking buffer (5% not-fat dried milk in 1x TBS/Tween; w/v) for 1 h at RT on a rocking shaker.

5.5.4 Chemiluminescent Protein Detection

After the blocking process, membrane strips were incubated overnight with the appropriate primary antibody in a solution containing 5% BSA in 1x TBS/Tween (w/v) at 4°C on a rocking shaker. Afterward, the membranes were washed with 1x TBS/Tween (3x 5 min), incubated with the respective secondary antibody in blocking buffer for 1 h at RT on a rocking shaker, and washed again. The list of used antibodies is given in **Table 16**. Proteins of interest were then visualized with WesternSure® Chemiluminescent Substrate and the C-DiGit Chemiluminescent Western Blot Scanner, according to the manufacturer's recommendations. The Image Studio 5.0 software was used to process the results obtained. After the target proteins were detected, the membrane strips were exposed to 1x Re-Blot Plus Strong solution for 15 minutes, rinsed with 1x TBS/Tween, and incubated in blocking buffer for 2x 5 minutes. Finally, β-actin was visualized on each individual membrane. The relative levels of proteins of interest were normalized to β-actin.

Table 16: List of used primary and secondary antibodies. Secondary antibody dilution ratio 1:4000 was utilized for polyclonal primary antibodies (*).

Antibody	Type	Ratio	Diluting Solution
Primary antibody			
β-actin	mouse monoclonal	1:2000	5% BSA in 1x TBS/Tween (w/v)
AhR	rabbit monoclonal	1:1000	
AR	mouse monoclonal	1:500	
CYP1A1	rabbit polyclonal*	1:500	
PSA	rabbit monoclonal	1:1000	
Secondary antibody			
Anti-mouse	IgG, HRP-linked	1:2000	Blocking buffer
Anti-rabbit	IgG, HRP-linked	1:2000	

5.6 Chromatin Immunoprecipitation

Phase III experiments began with an investigation of recruitment to the *KLK3* promoter after treatment with 8 previously selected indoles. 22Rv1 cells were seeded in a 60-mm Petri dish at a density of 4 x 10^6 cells per well in 4 ml of RPMI medium and stabilized overnight. Afterward, cells were treated with 8 selected indoles (10 µM) or control compounds. DMSO (untreated; 0.1% v/v) was used as a negative control/vehicle. TCDD (10 nM) and FICZ (10 µM) were used as a positive control for the AhR signalling pathway. DHT (10 nM) and ENZ (10 µM) were used as a positive control for the AR pathway. The results of all tested conditions were evaluated in the presence of DHT (10 nM). Cells were incubated with tested compounds for 90 min at 37°C. Subsequently, Chromatin immunoprecipitation (ChIP) was performed with SimpleChIP® Plus Enzymatic Chromatin IP Kit according to the manufacturer's recommendations with minor modifications. All used buffers are listed in *Chapter 4.4 Solutions*, **Table 7**.

5.6.1 Chromatin Crosslinking

Initially, 37% formaldehyde (108 µl) was added to treated cells for 9 min at RT to crosslink proteins to DNA. The crosslinking process was terminated by adding 400 µl of glycine solution for 5 min at RT. A crosslinking solution was aspirated, and cells were rinsed 2x with 1x PBS, and 1 ml of 1x PBS with a protease inhibitor cocktail (PIC) was added to each Petri dish. Adherent cells were scrapped off the Petri dishes into safe-lock tubes and centrifuged at 2000 rcf for 3 min at 4°C.

5.6.2 Nuclei Preparation and Chromatin Digestion

The supernatant was aspirated, the pellet was resuspended in 1 ml of ice cold 1x Buffer A and incubated for 10 min on ice with swirling every 3 min. Samples were centrifuged at 3000 rcf for 3 min at 4°C. The supernatant was aspirated, the pellet was resuspended in ice cold 1x Buffer B, and the samples were centrifuged again. Pelleted nuclei samples were resuspended in a Micrococcal nuclease solution and incubated at a thermo shaker for 15 min at 37°C with shaking (1000 rpm) to digest DNA. Digestion was terminated by adding 0.5 EDTA, and samples were centrifuged at 13 000 rcf for 1 min at 4°C. Thepellet was resuspended in 100 µl of 1x ChIP Buffer, incubated for 9 min on ice, sonicated (5 sets of 30 s pulses), and centrifuged at 10 000 rcf for 9 min at 4°C. The supernatant was collected, and dsDNA concentration was determined

with NanoDrop™ for each sample. The A260/A280 ratio was used to monitor the quality of collected samples.

5.6.3 Chromatin Immunoprecipitation

Samples were diluted in 1x ChIP Buffer to contain 15 µg of cross-linked chromatin in a total volume of 500 µl. Chromatin samples were incubated with anti-AR primary antibody (1µg per IP sample in ChIP Buffer) overnight at 4°C on a 360° rotation shaker. Moreover, control samples containing 2% Input and IgG were prepared. The IgG sample was incubated with normal rabbit IgG antibody under the same conditions. The 2% Input control sample was not incubated with any antibody. Following the overnight incubation, 25 µl of ChIP-Grade protein G Magnetic Beads were added to each reaction and incubated for 2 h (4°C, with rotation). Magnetic beads containing bounded chromatin of interest were separated from the solution using a magnetic separation rack, following the washing steps with low-salt buffer (3x 4 min, 4°C with rotation) and high-salt buffer (1x 4 min, 4°C with rotation).

5.6.4 Elution of Bounded Chromatin

After aspirating the supernatant, the chromatin was eluted from the magnetic beads by adding 150 µl of 1x ChIP Elution Buffer. The IP samples were then placed in a thermos-shaker and incubated for 30 min at 65°C with 1200 rpm. The eluted supernatant was then transferred into new tubes. Similarly, the 2% Input samples were incubated with 1x ChIP Elution Buffer at RT for 30 min. To reverse crosslinks, eluted samples (including 2% Input samples) were incubated with 5 M NaCl (6 µl) and Proteinase K (2 µl) for 15 min at 65°C with 1200 rpm. DNA Binding Buffer (750 µl) was added to each IP sample and purified in DNA spin columns (14,000 rpm, 30 s), according to the manufacturer's recommendations. The final DNA was eluted by adding 45 µl of DNA Elution Buffer.

5.6.5 Recruitment to *KLK3* promoter

The changes in recruitment to *KLK3* promoter of eluted IP samples were determined by RT-qPCR using SYBR Green® protocol (*Chapter 5.4*). The samples were analysed in technical tetraplicates and normalized to 2% Input samples. Subsequently, agarose gel electrophoresis was used to examine the obtained PCR fragments. An additional PCR run was conducted with elongation for only 30 cycles, and products were collected. The samples for agarose gel electrophoresis were prepared by mixing PCR product with dye in a 5:1 ratio. The obtained PCR fragments were separated in a 4% agarose gel containing GelRed nucleic acid stain for 1.5 hours at 65 V. Finally, the PCR products were visualized with the Syngene G:BOX gel documentation system.

5.7 CRISPR/Cas9 AhR Knock-out System

In the next step of **Phase III** experiments, the relationship between AhR and AR was investigated. To achieve this, a transient and stable CRISPR/Cas9 AhR knock-out systems were developed using the 22Rv1 cell line. The AhR CRISPR/Cas9 KO plasmid system (Santa Cruz Biotechnology) was used according to manufacturer's protocol, with minor modifications. Prior to transfection, the appropriate ratios of plasmid DNA and UltraCruz® Transfection Reagent were determined. Specific *AhR exon 5* primers were designed for RT-qPCR analysis of AhR KO samples, as this sequence corresponds with one of the target DNA sequences for the used CRISPR/Cas9 AhR KO plasmid (**Table 13**).

5.7.1 Transient CRISPR/Cas9 AhR Knock-out System

22Rv1 cells were seeded in a 6-well plate with a density of 2 x 10^5 cells per well in 3 ml of RPMI medium and stabilized overnight. The following day, the cells were transfected with either the CRISPR/Cas9 AhR KO plasmid for developing a transient AhR knock-out system or the Control CRISPR/Cas9 plasmid for the negative control sample. The transfection solution was prepared by combining Solution A (1 µg of plasmid DNA in 150 µl of plasmid transfection medium per well) with Solution B (5 µl of UltraCruz® Transfection Reagent in 150 µl of plasmid transfection medium per well) and incubated for 20 min at RT.

The growth medium was aspirated from the wells containing stabilized 22Rv1 cells and replaced with transfection medium (3 ml RPMI + 300 µl of the prepared transfection solution per well), then incubated for 48 h. The transiently transfected 22Rv1 cells were treated with tested compounds for 24 h. Based on previous experiments, only 4MI (100 µM) was tested in the presence or absence of DHT (10 nM), along with the negative control DMSO (untreated; 0.1% v/v), and the respective positive controls, TCDD (10 nM) and DHT (10 nM).

Total mRNA was isolated, and samples were analysed using RT-qPCR, as described in *Chapter 5.4*.

5.7.2 Stable CRISPR/Cas9 AhR Knock-out 22Rv1 Cell Line

22Rv1 cells were seeded in a 6-well plate with a density of 2 x 10^5 cells per well in 3 ml of RPMI medium and stabilized overnight. The next day, 22Rv1 cells were co-transfected with the CRISPR/Cas9 AhR KO plasmid and HDR plasmid, which contains the gene

for puromycin selection. Solution A was prepared with both plasmids in equivalent ratios, 1 µg of plasmid DNA of each in 150 µl of plasmid transfection medium. Solution B was then combined with Solution A. The mixture was incubated for 20 min at RT. The growth medium was replaced by the transfection medium (3 ml RPMI + 300 µl prepared transfection solution per well) and incubated for 72 h. The success of transfection was visually verified using fluorescent microscopy, detecting the presence of GFP (CRISPR/Cas9 AhR KO plasmid) and RFP (HDR plasmid). After 72 h, the transfection medium was replaced by the selection medium with antibiotic puromycin (0.7 µg/ml). Selection pressure was increased after additional 72 h up to 1.5 µg/ml of puromycin. Transfected cells were incubated in this increased selection medium for an additional 18 days with regular media change. Subsequently, single-cell colonies were passaged for the first time and transferred from the 6-well plate into a tissue culture flask. From this point, the newly developed 22Rv1 AhR KO cells were cultured as a regular adherent cell line with the addition of puromycin 10 µg/ml once a week. The expression of AhR target genes and proteins was evaluated by RT-qPCR and Western blot in 22Rv1 wildtype (WT) cells and newly developed 22Rv1 AhR KO cells and compared.

For experiments, stably transfected 22Rv1 AhR KO cells were seeded in a 6-well plate at a density of 1.5 x 10^6 cells per well in 1.5 ml of RPMI medium and stabilized overnight. The next day, stabilized cells were treated with 4MI (10 and 100 µM) in the presence or absence of DHT (10 nM), along with negative control DMSO (untreated; 0.1% v/v), and respective positive controls, TCDD (10 nM), FICZ (10 µM), and DHT (10 nM).

Total mRNA was isolated, and samples were analysed using RT-qPCR, as described in *Chapter 5.4*.

5.8 Cell Cycle Analysis

Fluorescent-activated Cell Sorting (FACS) was used to analyse the impact of one selected indole, 3MI, on the cell cycle in different prostatic cell lines.

22Rv1, PC-3, LNCaP, and C4-2 cells were seeded in a 60-mm Petri dish at a density of 4 x 10^6 cells per well in 4 ml of appropriate media. Following overnight stabilization, cells were treated with 3MI (100 μM) and control compounds – DMSO (untreated; 0.1%; v/v) or doxorubicin 20 μM for 24 h.

Treated cells were rinsed with EDTA (0.01% in 1x PBS; w/v), harvested after trypsinization, and centrifuged (1000 rcf, 10 min, 4°C). The supernatant was aspirated, the pellet was washed with 2 ml of 1x PBS and centrifuged again. The supernatant was aspirated, and the pellet was resuspended in 100 μl of 1x PBS (ice cold). Ice cold 70% EtOH was added dropwise to each sample (1 ml per 1x10^6 cells). Samples were stored at -20°C overnight. Upon thawing, samples were centrifuged (1000 rcf, 10 min, 4°C), pellet was washed two times with 2 ml of 1x PBS and centrifuged again. Supernatant was aspirated and pellet resuspended in 1x PBS (filtrated). Samples in a total volume of 600 μl were incubated with propidium iodide (1 mg/ml; 6 μl) for 30 min. Subsequently, samples were analysed by FACS Verse Machine.

5.9 Statistical Analysis

The data obtained from the experiments were analysed using GraphPad Prism Version 9.4.1. The figure legends specify the number of independent repeats and technical replicates for each experiment. If applicable, the obtained values were subjected to two-way analysis of variance (ANOVA) followed by Dunnett's test or Student's t-test. Results with $p < 0.05$ were considered significant. The IC_{25} and IC_{50} values were calculated using the nonlinear regression with the least-squares fitting method.

6 RESULTS

6.1 Cytotoxicity and Proliferation Assays after Treatment with Indoles

Before beginning the experiments, the viability and cell proliferation effects of 22 tested indoles were evaluated. To determine whether the selected indolic compounds have any cytotoxic effects against 22Rv1, PC-3, and C4-2 cells, the MTT assay was performed. The proliferation analysis was carried out using the crystal violet assay. Doxorubicin (DOX, 20 uM; common chemotherapeutic drug for cancer treatment [390]) was used as a positive control along with Triton X-100 (2 %).

After 24 h of incubation, a total of 22 indolic compounds were analysed using the MTT assay with concentration ranges between 0.1-100 μM. According to the obtained results, all tested indoles were determined as nontoxic in 22Rv1, PC-3, and C4-2 cell lines, as the decrease in cell viability did not exceed 20 %. Only 3MI (100 μM) displayed a decrease of approximately 23 % in the C4-2 cell line. This decrease was considered non-significant by statistical analysis. Positive control DOX decreased cell viability by approximately 70 % in 22Rv1 cells and 30 % in PC-3 and C4-2 cells. Triton X-100 decreased cell viability in all cell lines by approximately 80-90 %.

However, the Crystal violet assay showed that cell proliferation significantly decreased in the 22Rv1 cell line for 3MI and partially for 4MI. Compared to the untreated (UT) cells, cell proliferation decreased by approximately 60 % for 3MI (100 μM) and 40 % for 4MI (100 μM). An estimated IC_{50} of ~60 μM was calculated for 3MI in the 22Rv1 cell line. In C4-2 cells, 3MI (100 μM) also decreased cell proliferation by approximately 20 %. On the other hand, the decrease in cell proliferation was not observed in the PC-3 cell line for any of the tested indolic compounds. Positive control DOX decreased cell viability by approximately 70 % in 22Rv1 cells, 40 % in PC-3 cells, and 30 % in C4-2. Triton X-100 decreased cell viability in all cell lines by approximately 80-90 %.

Results of cytotoxicity and proliferation assays for 22Rv1 cell line are displayed in **Figure 18**, for PC-3 cell line in **Figure 19**, and for C4-2 cell line in **Figure 20**. Based on their respective chemical structures, all tested indoles were divided into groups titled as Monomethylindoles (parts **A** and **B** in all figures), Di- and Tri-Methylindoles (parts **C** and **D**), Monomethoxyindoles (parts **E** and **F**), and Methoxyindoles (parts **G** and **H**).

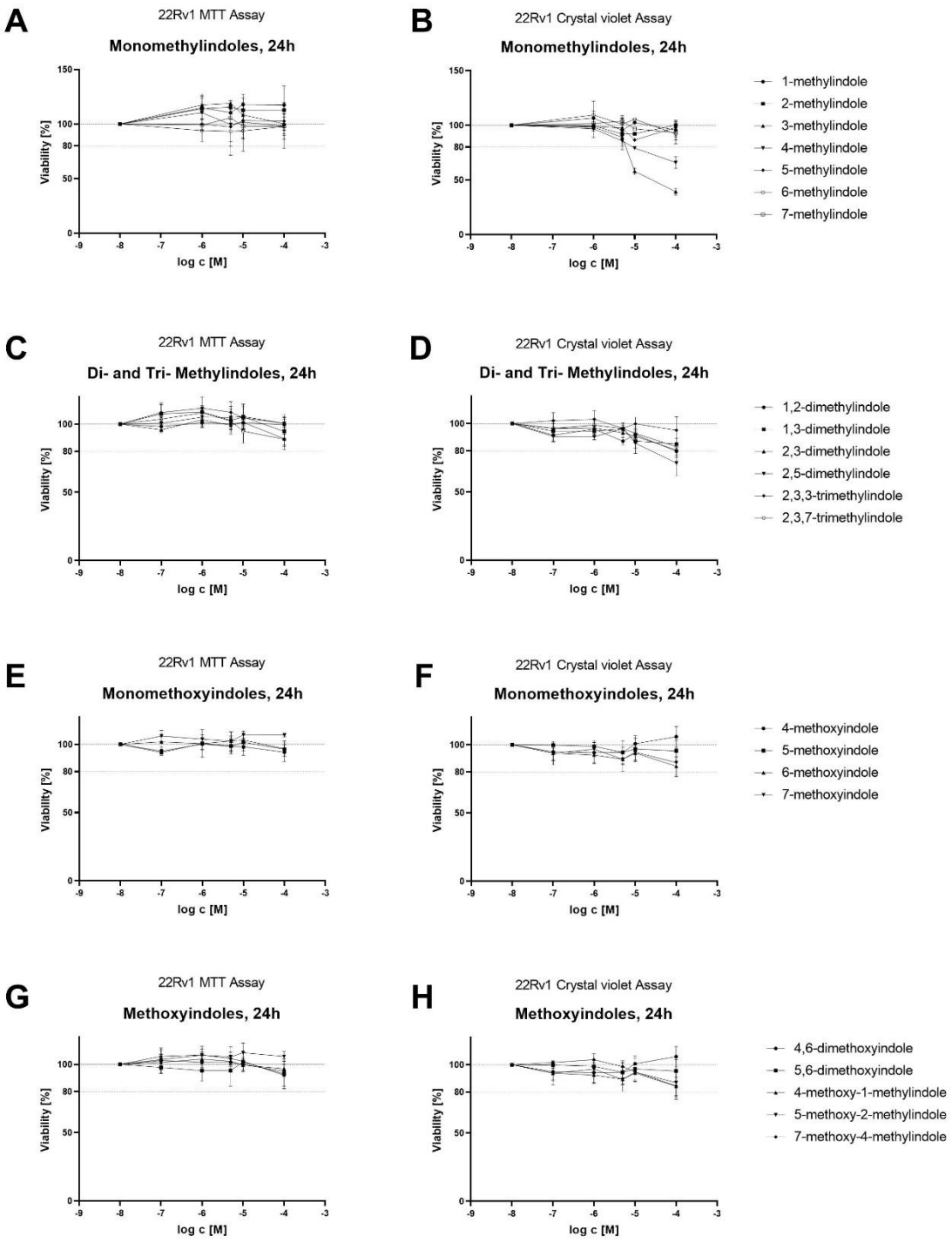

Figure 18: The effects of tested indoles on 22Rv1 cells. Cells were exposed to concentrations of indoles ranging from 0.1 to 100 μM or with the control compounds for 24 h. DMSO (UT; 0.1 %; v/v) was used as a negative control, and DOX (20 μM) and Triton X-100 (2 %) were used as positive controls. The cytotoxic effects of indoles were subsequently analysed using MTT assay. The results of the cytotoxicity assay are presented in the left column. Crystal violet assay was conducted for cell proliferation analysis, and the results are presented in the right column. Presented data are a mean value of 4-6 independent experiments, ± standard deviation (SD), and are expressed in percentages of UT. Incubation and measurements were performed in 4 technical replicates. Cell viability and proliferation percentages at the lowest concentration of tested indoles were comparable with UT.

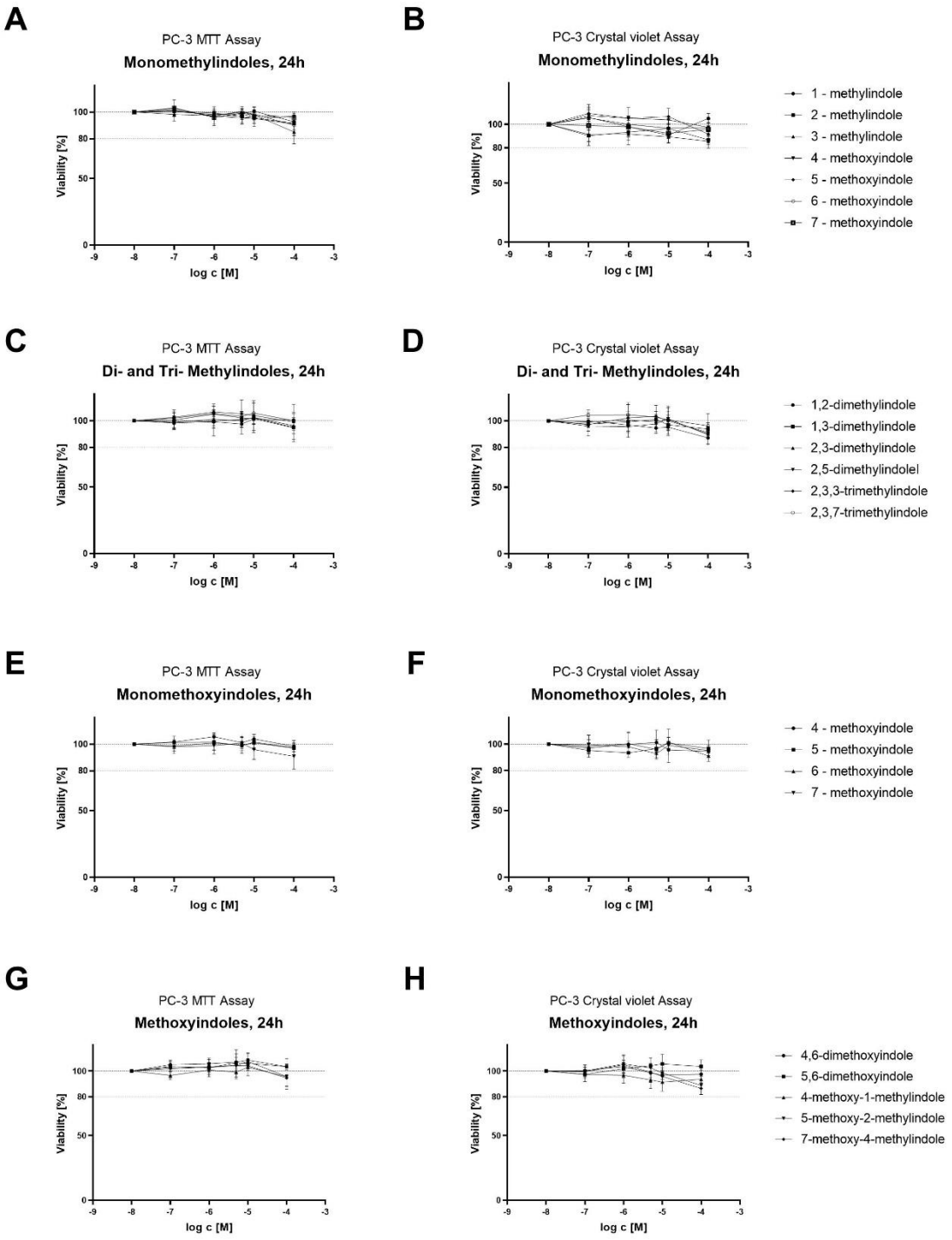

Figure 19: The effects of tested indoles on PC-3 cells. Cells were exposed to concentrations of indoles ranging from 0.1 to 100 μM or with the control compounds for 24 h. DMSO (UT; 0.1 %; v/v) was used as a negative control, and DOX (20 μM) and Triton X-100 (2 %) were used as positive controls. The cytotoxic effects of indoles were subsequently analysed using MTT assay. The results of the cytotoxicity assay are presented in the left column. Crystal violet assay was conducted for cell proliferation analysis, and the results are presented in the right column. Presented data are a mean value of 3-5 independent experiments, ± SD, and are expressed in percentages of UT. Incubation and measurements were performed in 4 technical replicates. Cell viability and proliferation percentages at the lowest concentration of tested indoles were comparable with UT.

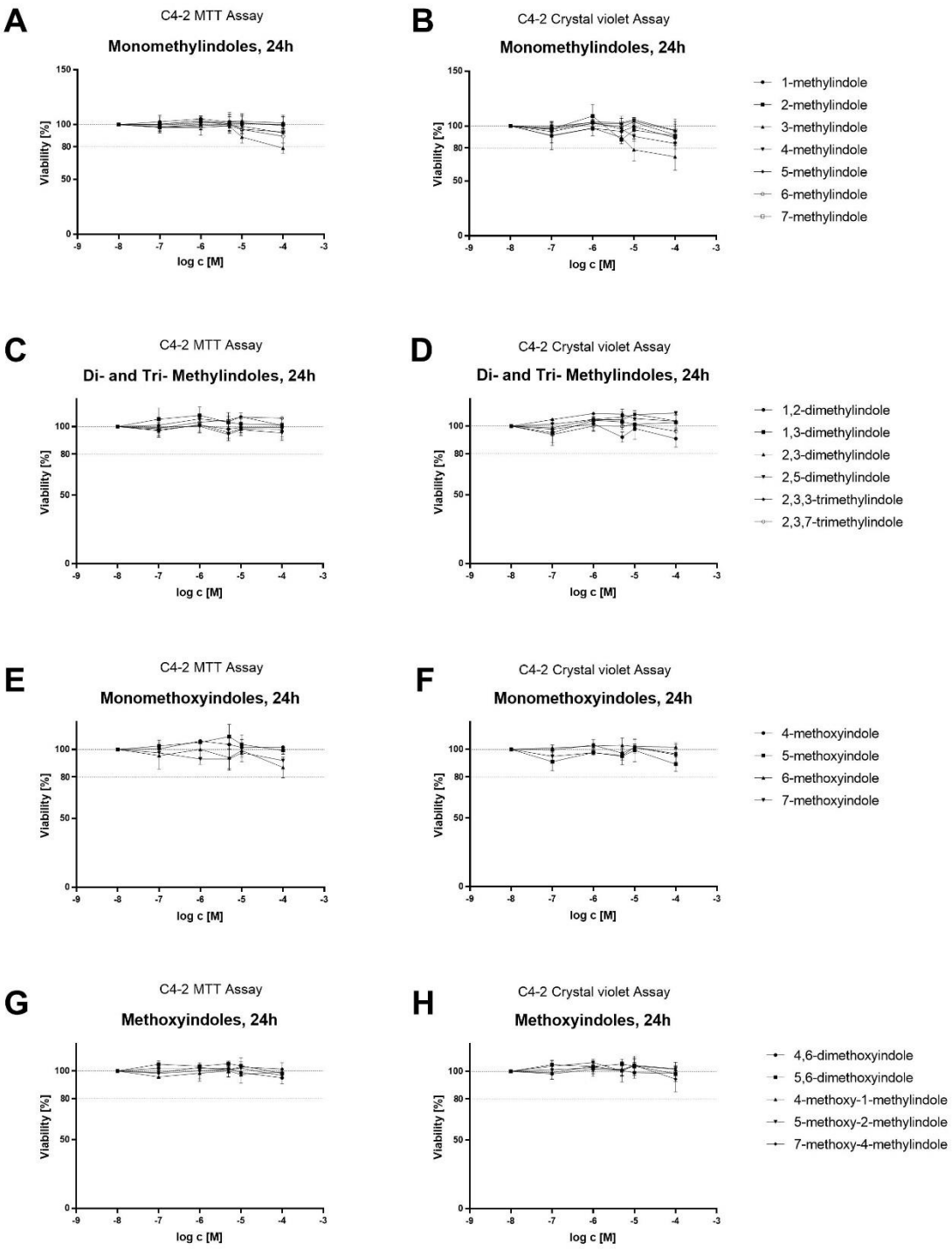

Figure 20: The effects of tested indoles on C4-2 cells. Cells were exposed to concentrations of indoles ranging from 0.1 to 100 μM or with the control compounds for 24 h. DMSO (UT; 0.1 %; v/v) was used as a negative control, and DOX (20 μM) and Triton X-100 (2 %) were used as positive controls. The cytotoxic effects of indoles were subsequently analysed using MTT assay. The results of the cytotoxicity assay are presented in the left column. Crystal violet assay was conducted for cell proliferation analysis, and the results are presented in the right column. Presented data are a mean value of 4-6 independent experiments, ± SD, and are expressed in percentages of UT. Incubation and measurements were performed in 6 technical replicates. Cell viability and proliferation percentages at the lowest concentration of tested indoles were comparable with UT.

6.2 Development of Novel Prostate-specific AhR Reporter Cell Lines

Initially, a cellular system was established to monitor AhR transcriptional activity in the 22Rv1 and PC-3 cell lines. To achieve this, stably transfected 22AhRv1 and PAhRC3 cell lines with the luciferase reporter gene were constructed. The parental 22Rv1 and PC-3 cells were transfected with the plasmid pGL4.27 [luc2P/minP/Hygro] designed by Novotna *et al*. 2011 [389]. Monoclones were isolated for each cell line and incubated with the model AhR ligand TCCD (10 nM) for 24 h. Results were analysed using RGA. Determined inhibitory concentrations (IC_{25} and IC_{50}) of selection antibiotic HygB for individual cell lines are shown in **Table 17**.

Table 17: Determined inhibitory concentration of HygB for 22Rv1 and PC-3 cell lines.

Cell line	IC_{25} [µg/ml]	IC_{50} [µg/ml]
22Rv1	60	110
PC-3	3	15

In total, 10 monoclonal populations were isolated for the 22Rv1 cell line and 7 for the PC-3 cell line. For 22Rv1 monoclones, clone 10 displayed the highest responsiveness to TCDD (10 nM) at approximately $2x10^6$ RLU (relative light unit; **Figure 21 A**). For PC-3 monoclones, clone 5 displayed the highest responsiveness to TCDD (10 nM) at approximately $4.2x10^5$ RLU (**Figure 21 B**). 22Rv1 clone 10 was labelled as 22AhRv1 cell line and PC-3 clone 5 was labelled as PAhRC3 cell line. These new stably transfected prostate-specific AhR reporter cell lines were subjected for further characterization.

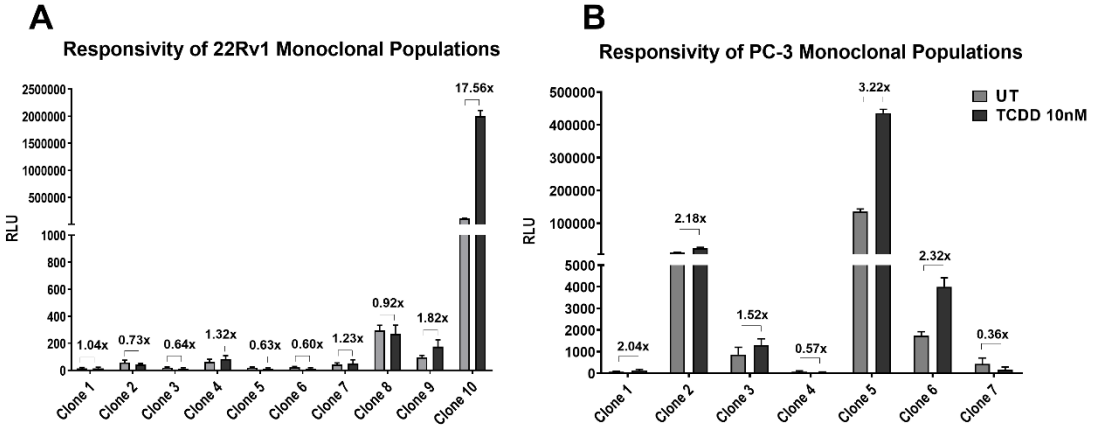

Figure 21: Response of selected 22Rv1 and PC-3 monoclones to TCDD. Isolated monoclones for 22Rv1 **(A)** and PC-3 **(B)** cell lines were incubated with TCDD (10 nM). After 24 h, the response of each monoclone to this model AhR ligand was determined by RGA. The data presented are a mean value of 3 independent experiments, expressed as RLU, with fold induction to UT, ± SD above each column. Incubation and measurements were performed in 3 technical replicates. The highest response to TCDD (10 nM) determined the selected monoclone from each cell line for further experiments.

Subsequent dose-dependent analyses confirmed the transcriptional activation of AhR by model exogenous and endogenous ligands (TCDD, BaP, and FICZ) in both cell lines (**Figure 22 A, 23 A**). Both cell lines displayed dose-dependent decrease in AhR transcription activity after 24 h upon incubation with AhR antagonist MNF (**Figure 22 B, 23 B**). For 22AhRv1 cells, the luciferase activity remained stable upon cryopreservation and after long-term cultivation without the presence of the selection antibiotic HygB (**Figure 22 C, D**). In PAhRC3 cells, the luciferase activity slightly decreased after cryopreservation and luciferase activity decreased in a time-dependent manner when cultured without the addition of HygB (**Figure 23 C, D**). Obtained results show that in the case of the 22AhRv1 cell line, the inducibility of luciferase was more stable over time than in the case of the PAhRC3 cell line.

Finally, the two newly constructed cell lines were exposed to the effects of tested indoles.

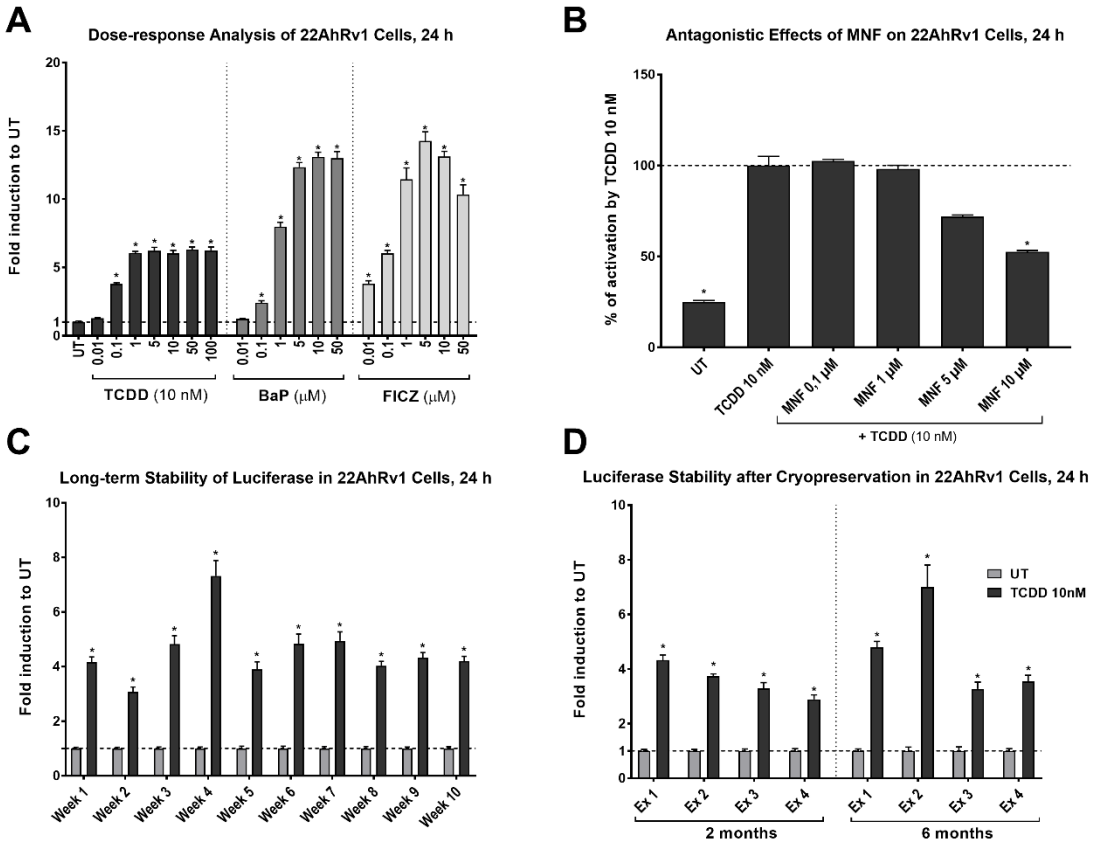

Figure 22: Characterization of newly developed 22AhRv1 cell line. (A) 22AhRv1 cells were incubated with AhR exogenous ligands, TCDD (0.01-100nM) and BaP (0.01-50 μM), and endogenous ligand FICZ (0.1-50 μM) for 24 h. Results are expressed as fold to UT.**(B)** To determine the antagonistic effect, cells were incubated with AhR antagonist MNF (0.1-10 μM) in combination with TCDD (10 nM). Results are expressed as a percentage of maximal activation by TCDD (10 nM), equal to 100 %. **(C)** The long-term inducibility of luciferase was monitored for 10 weeks when 22AhRv1 cells were incubated without HygB. **(D)** The luciferase stability was also evaluated upon cryopreservation after 2 and 6 months. All experiments used DMSO (UT; 0.1 %; v/v) as a negative control. All data were obtained using RGA. The (A) data are a mean value of 4 independent experiments and are expressed as fold induction to UT, ± SD. The (B) data are a mean value of 3 independent experiments and are expressed as a percentage of maximal activation of AhR by TCDD (10 nM), equal to 100 %. Incubation and measurements were performed in 3 technical replicates.

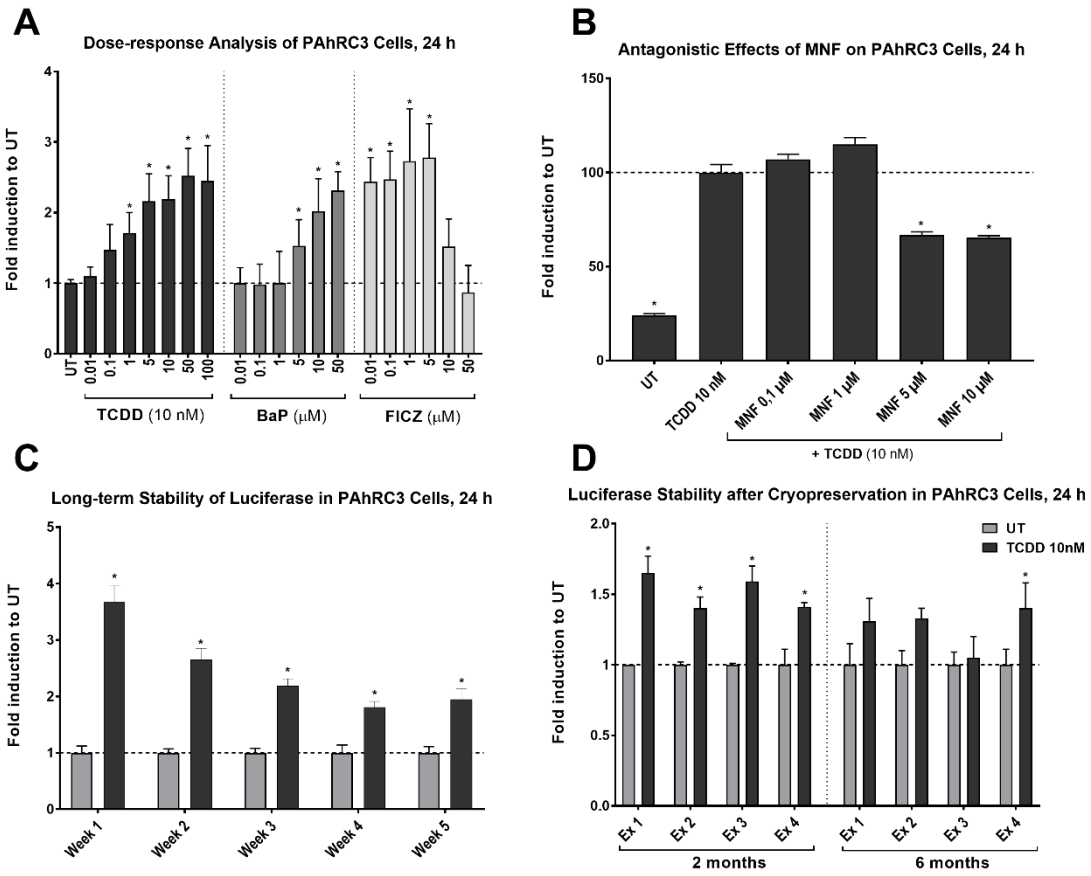

Figure 23: Characterization of newly developed PAhRC3 cell line. (A) PAhRC3 cells were incubated with AhR exogenous ligands, TCDD (0.01-100nM) and BaP (0.01-50 μM), and endogenous ligand FICZ (0.1-50 μM) for 24 h. Results are expressed as fold to UT.**(B)** To determine the antagonistic effect, cells were incubated with AhR antagonist MNF (0.1-10 μM) in combination with TCDD (10 nM). Results are expressed as a percentage of maximal activation by TCDD (10 nM), equal to 100 %. **(C)** The long-term inducibility of luciferase was monitored for 10 weeks when 22AhRv1 cells were incubated without HygB. **(D)** The luciferase stability was also evaluated upon cryopreservation after 2 and 6 months. All experiments used DMSO (UT; 0.1 %; v/v) as a negative control. All data were obtained using RGA. The (A) data are a mean value of 4 independent experiments and are expressed as fold induction to UT, ± SD. The (B) data are a mean value of 3 independent experiments and are expressed as a percentage of maximal activation of AhR by TCDD (10 nM), equal to 100 %. Incubation and measurements were performed in 3 technical replicates.

6.3 The Effects of Indoles on AhR and AR Transcription Activity

Prostate-specific monitoring of AhR transcription activity was performed using novel 22AhRv1 and PAhRC3 cell lines. The AIZ-AR reporter cell line [386] was used to monitor AR transcription activity in the presence or absence of DHT.

In the 22AhRv1 reporter cell line, the ability of tested indoles to induce AhR transcription activity was determined after 4 (**Figure 24 A**) and 24 h (**Figure 24 B**). After 4 h, significant AhR activation was observed for 1MI, 2MI, 4MI, 5MI, 6MI, 7MI, 2,5DMI, 6MeO, 4MeO1MI, and 7MeO4MI at the highest used concentration (100 μM). Surprisingly, TCDD (10nM), which was used as a positive control, did not activate AhR significantly above the level of UT after 4 h, although it did show significant activation after 24 h. After 24 h, all indoles, except for 3MI, activated AhR significantly and dose-dependently, with efficacy comparable to TCDD (10 nM). Nevertheless, the highest effect of 3MI on AhR activation was observed at the concentration 10 μM, but the concentration 100 μM displayed no effect at AhR activation at all.

In the PAhRC3 reporter cell line, the ability of tested indoles to induce AhR transcription activity was determined after 24 h (**Figure 25**). Interestingly, 3MI exhibited the highest dose-dependent increase in AhR transcription activity with efficacy highest than TCDD (10 nM). Additionally, 4MI, 5MI, 6MI, 7MI, 1,2DMI, 1,3DMI, 2,3DMI, 2,3,7TMI, 7MeO, 4MeO1MI, and 7MeO4MI also significantly activated AhR, generally in a dose-dependent manner.

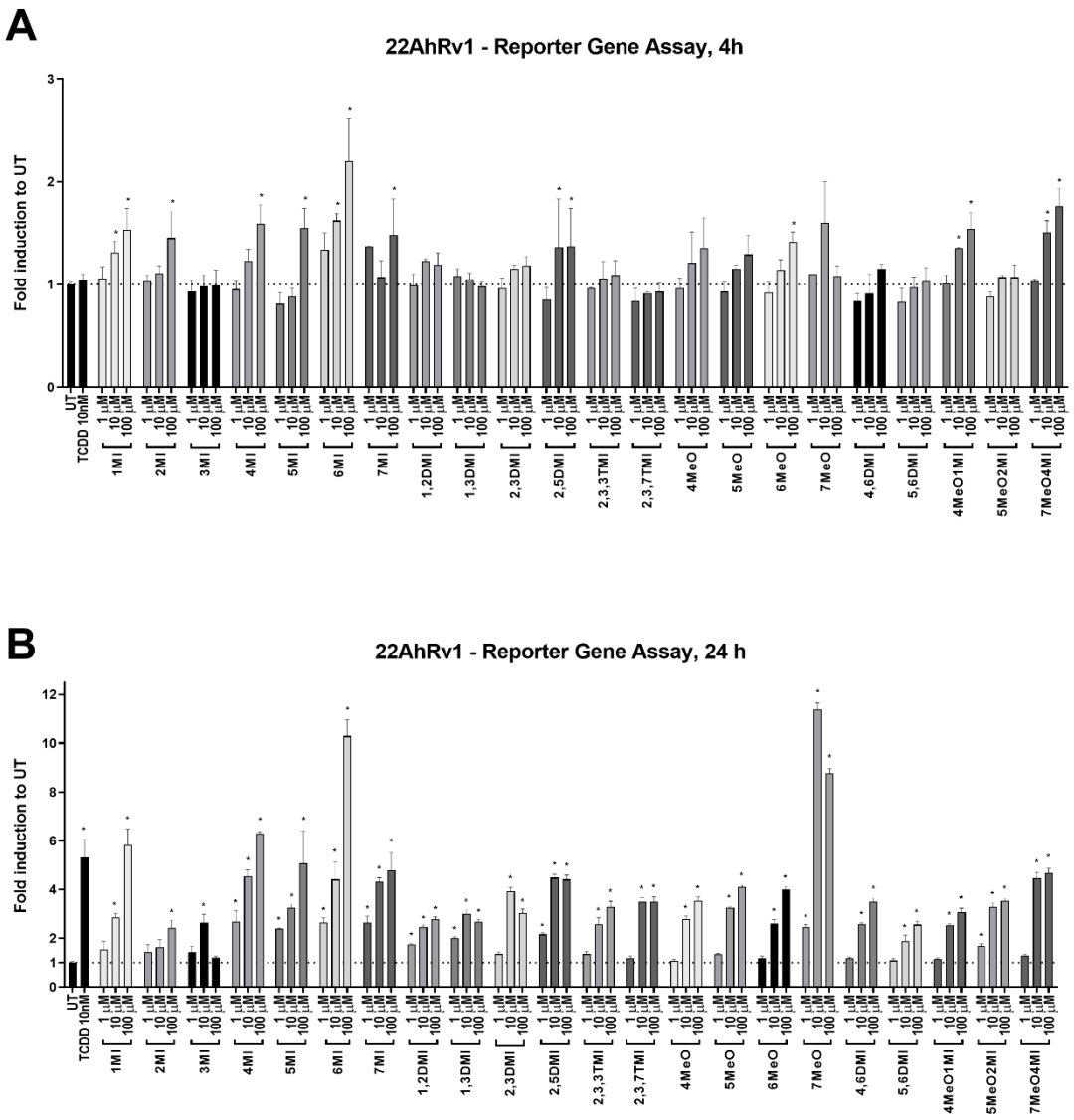

Figure 24: Effects of tested indoles on AhR transcription activity in 22AhRv1 reporter cell line. Cells were incubated with indoles in concentrations ranging from 1 to 100 μM for 4 h (A) and 24 h (B). DMSO (0.1 %; v/v) was used as a negative control, and TCDD (10 nM) as a positive control. Transcription activity of AhR was determined using RGA. The data presented are a mean value of 4 independent experiments and are expressed as fold induction to UT, ± SD. Incubation and measurements were performed in 4 technical replicates. The symbol * represents values identified as significant by statistical analysis.

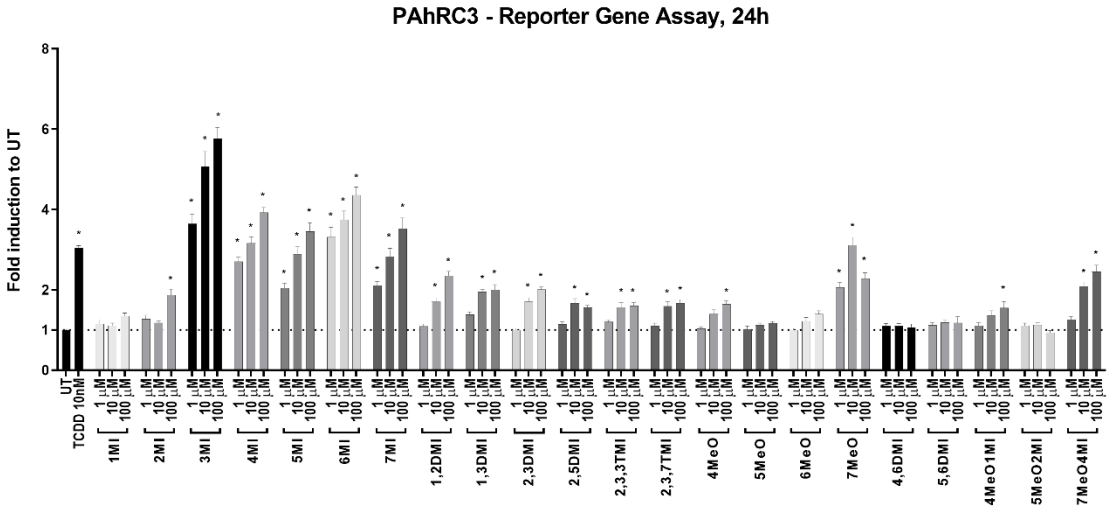

Figure 75: Effects of tested indoles on AhR transcription activity in PAhRC3 reporter cell line. Cells were incubated with indoles in concentrations ranging from 1 to 100 µM for 24 h. DMSO (0.1 %; v/v) was used as a negative control, and TCDD (10 nM) as a positive control. Transcription activity of AhR was determined using RGA. The data presented are a mean value of 3 independent experiments and are expressed as fold induction to UT, ± SD. Incubation and measurements were performed in 4 technical replicates. The symbol * represents values identified as significant by statistical analysis.

In the AIZ-AR reporter cell line, the ability of tested indoles to influence AR transcription activity was determined after 24 h. These experiments were carried out in agonist (in the absence of DHT; **Figure 26 A**) and antagonist mode (with the presence of DHT; **Figure 26 B**).

In agonist mode, AR transcription activity induced by ligand DHT (10 nM) increased approximately 7x to UT. The only indoles which displayed the ability to induce AR transcription activity were 2,3,3TMI, 7MeO, and 5MeO2MI. Interestingly, a dose-dependent decrease in luciferase activity was observed for 3MI with IC_{50} at approximately 10 μM. The effects of AhR ligands TCDD (10 nM) and FICZ (10 μM) on AR transcription activity were also evaluated. While TCDD (10 nM) displayed no effect comparable to the UT, FICZ (10 μM) slightly increased AR-mediated luciferase activity.

In the antagonist mode, the ability of tested indoles to suppress the AR transcription activity induced by DHT was evaluated. These results are expressed in percentage, where the induction of AR transcription activity by ligand DHT (10 nM) represents 100 %. The positive control, antiandrogen ENZ (10 μM), decreased DHT-inducible AR-dependent luciferase activity to the level of UT. A significant dose-dependent suppression of AR activity was observed with 3MI, 4MI, 1,3DMI, 2,3DMI, 2,3,7TMI, 4,6DMI, 5,6DMI, and 7MeO4MI. The most significant decrease in DHT-induced AR activity was observed with 3MI (IC_{50} approximately at 5 μM) and 4MI (IC_{50} approximately at 50 μM). Some indoles, such as 2,5DMI, 2,3,3TMI, 7MeO, or 5MeO2MI, displayed synergistic effects on AR activation in combination with DHT (10 nM). However, this observation was consistent with their activity detected in the agonist mode. Interestingly, a combination of TCDD (10 nM) with DHT (10 nM) suppressed AR-mediated luciferase activity by around 30 %. On the other hand, FICZ (10 μM) combined with DHT (10 nM) increased this luciferase activity by around 20 %. These findings suggest that the impact of AhR activation on AR activity may be heavily dependent on the nature of the AhR ligand.

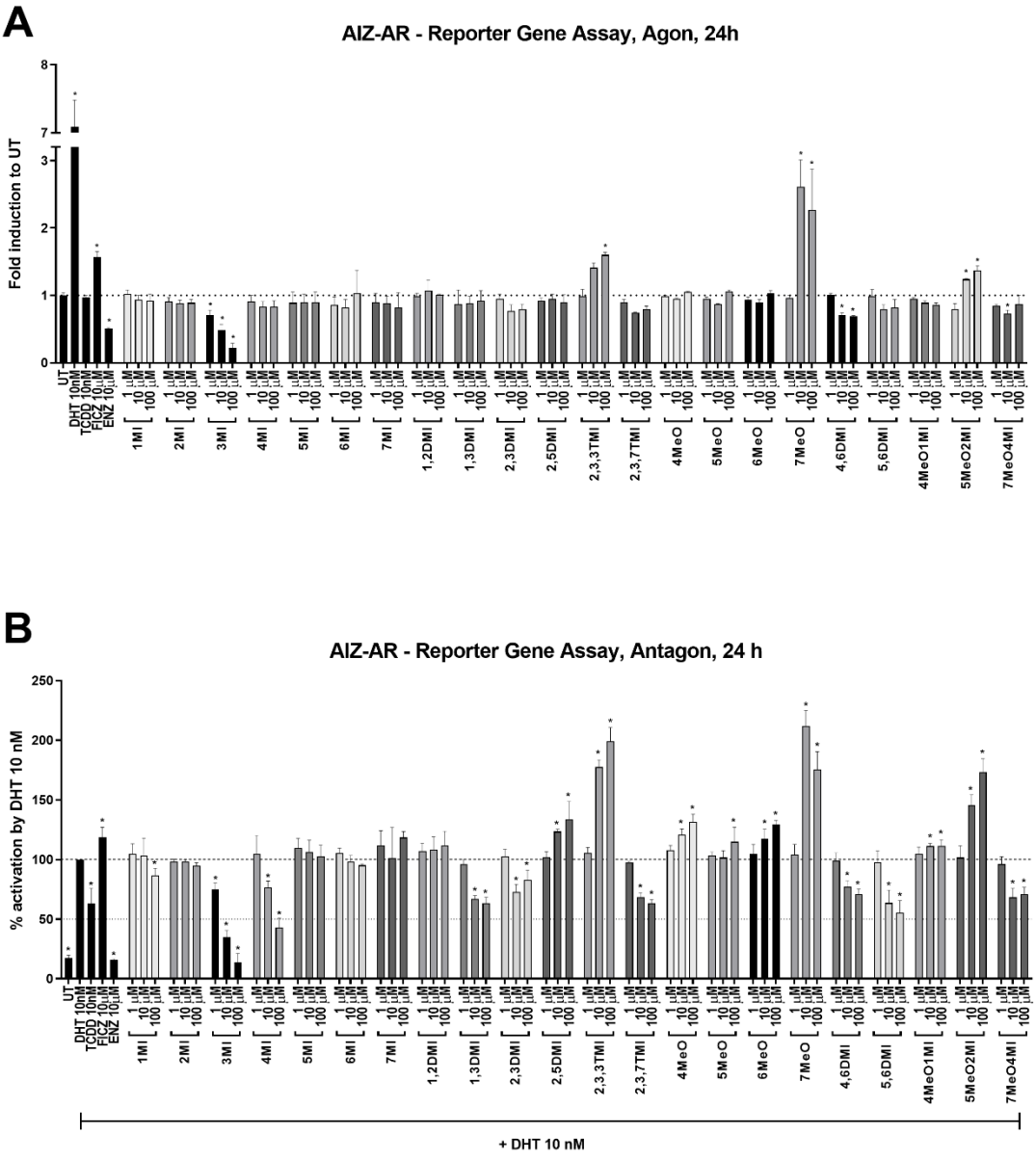

Figure 26: Effects of tested indoles on AR transcription activity in AIZ-AR reporter cell line. Cells were incubated with indoles in concentrations ranging from 1 to 100 μM for 24 h in the absence **(A)** or presence **(B)** of DHT (10 nM). DMSO (0.1 %; v/v) was used as a negative control, and DHT (10 nM) as a positive control. Additionally, AIZ-AR cells were also activated with AhR agonists, TCDD (10 nM), and FICZ (10 μM) in combination with DHT (10 nM). Antiandrogen ENZ (10 μM) combined with DHT (10 nM) was used as a control of AR activity decrease. Transcription activity of AR was determined using RGA. Incubation and measurements were performed in 4 technical replicates. The data presented are a mean value of 3 independent experiments. In agonist mode **(A)**, results are expressed as fold induction to UT, ± SD. In antagonist mode **(B)**, results are expressed as a percentage of maximal activation by DHT (10 nM), equal to 100 %, ± SD. The symbol * represents values identified as significant by statistical analysis.

Only the compounds that met both criteria, significant induction of AhR transcription activity and simultaneous suppression of DHT-activated AR, were selected for further experiments in **Phase II**. Out of 22 tested indoles, only 8 satisfied both criteria. **Table 18** presents selected indoles and their effects on AhR activation in the 22AhRv1 cell line and AR suppression in the AIZ-AR cell line. These cell lines were derived from the parental 22Rv1 prostate cancer cell line.

Table 18: Selected indoles for Phase II experiments. Based on RGA results in 22AhRv1 and AIZ-AR cell lines, 8 indoles were selected for further experiments.

Compound	AhR activation (24 h)		AR suppression (24 h)
	10 μM	100 μM	100 μM
3MI	2.6 fold	1.2 fold	decrease to 13.5 %
4MI	4.5 fold	6.3 fold	decrease to 43.1 %
1,3 DMI	3.0 fold	2.7 fold	decrease to 63.5 %
2,3 DMI	3.9 fold	3.1 fold	decrease to 82.8 %
2,3,7 TMI	3.5 fold	3.5 fold	decrease to 63.5 %
4,6 DMI	2.6 fold	3.5 fold	decrease to 70.9 %
5,6 DMI	1.9 fold	2.6 fold	decrease to 55.5 %
7MeO4MI	4.5 fold	4.7 fold	decrease to 70.8 %

6.4 The Effects of Selected Indoles on the Expression of Target Genes

The first series of experiments in experimental **Phase II** were to determine the effect of indoles in the presence of absence of DHT (10 nM) on the expression of AhR- and AR-target genes in 22Rv1 and PC-3 cell lines. Based on previous experiments, 8 indoles out of 22 were selected, namely 3MI, 4MI, 1,3DMI, 2,3DMI, 2,3,7TMI, 4,6DMI, 5,6DMI, and 7MeO4MI.

In 22Rv1 cell line, all 8 tested indoles showed a dose-dependent increase in the expression of *CYP1A1* mRNA (**Figure 27 A**), which is a marker of AhR activation [76]. TCDD (10 nM) as a positive control displayed the most significant increase in *CYP1A1* mRNA levels (106x fold to UT). The weakest induction of *CYP1A1* was observed with 4,6DMI and 5,6 MI, while the strongest was 4MI (100 μM). The expression of *AhRR* was also induced by positive control TCDD (10 nM), but only weakly by 4MI, 1,3DMI, and 7MeO4MI. Surprisingly, *AhRR* mRNA levels were decreased after the treatment with 3MI (**Figure 27 B**).

All selected indoles significantly reduced the DHT-induced expression of AR-target genes in 22Rv1 cell line. This dose-dependent decrease was observed for *KLK3* (**Figure 27 C**) and *FKBP5* genes (**Figure 27 D**), and is expressed in percentage, when DHT (10 nM) represents 100 %. The most significant decrease in DHT-inducible *KLK3* and *FKBP5* gene's expression were observed for 3MI, 4MI, and 7MeO4MI.

The expression of *UBE2C*, a gene which is regulated by AR-v7 [391], showed slight dose-dependent decrease (approximately to 75 % of DHT) after the treatment with all selected indoles (**Figure 27 E**).

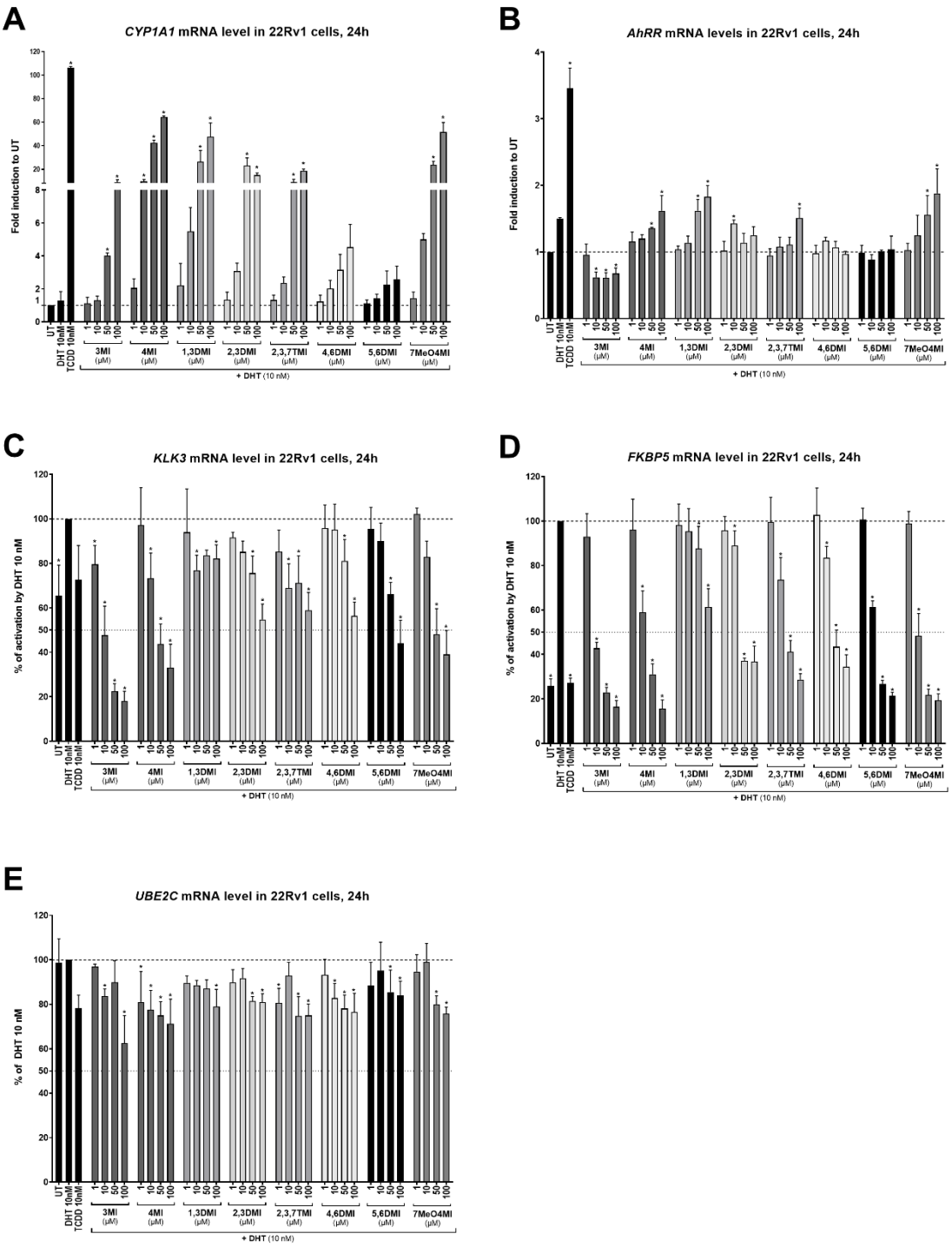

Figure 27: Effects of indoles on the expression of AhR- and AR-target genes in the 22Rv1 cell line. Cells were incubated with selected indoles (concentrations ranging from 1 µM to 100 µM) in combination with DHT (10 nM) for 24 h. DMSO (0.1 %; v/v) was used as a negative control, and TCDD (10 nM) and DHT (10 nM) as respective positive controls. Upon incubation with tested compounds, RNA was isolated, reverse transcription was performed, and samples were analysed using RT-qPCR. Measurements were performed in 3 technical replicates. The data presented are a mean value of 5 independent experiments. Induction of AhR-target genes *CYP1A1* **(A)** and *AhRR* **(B)** was determined, as well as induction of AR-target genes *KLK3* **(C)**, *FKBP5* **(D)**, and *UBE2C* **(E)**. The relative expression of the monitored genes was normalized to the housekeeping gene *GAPDH*. For AhR-target genes, results are expressed as fold induction to UT, ± SD. For AR-target genes, results are expressed as a percentage of maximal activation by DHT (10 nM), equal to 100 %, ± SD. The symbol * represents values identified as significant by statistical

In the PC-3 cell line, all 8 tested indoles also showed a dose-dependent increase in the expression of *CYP1A1* mRNA, except 4,6DMI and 5,6DMI (**Figure 28 A**). Interestingly, tested indoles showed higher *CYP1A1* mRNA levels than TCDD (10 nM). *AhRR* mRNA levels significantly increased only after the treatment with 3MI in a dose-dependent manner (**Figure 28 B**). The expression of *FKBP5* slightly decreased for most compounds, but this decrease was not significant. However, 3MI dose-dependently increased *FKBP5* mRNA levels (**Figure 28 C**). The expression levels of *UBE2C* slightly decreased after the treatment with indoles, but none of these declines were determined as significant by statistical analysis (**Figure 28 D**). Naturally, the expression of *KLK3* was not detected, as the PC-3 cell line completely lacks AR.

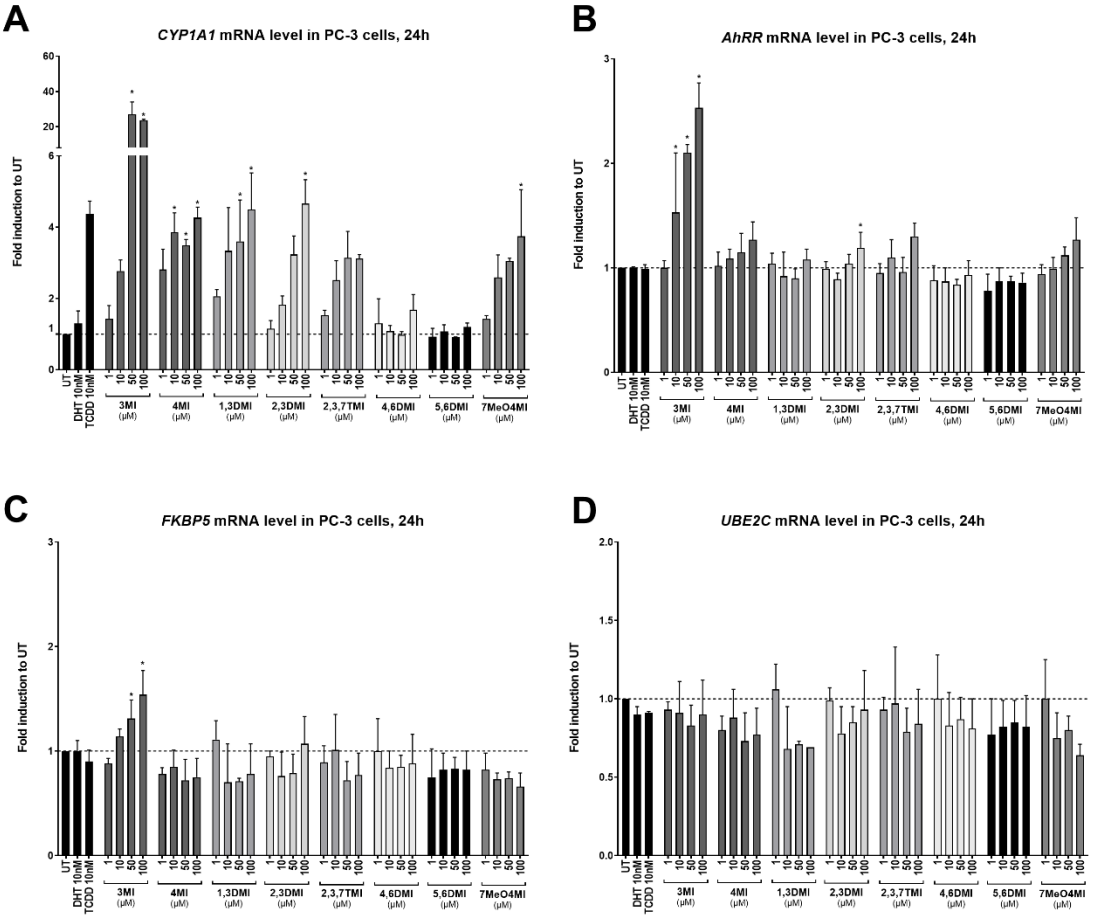

Figure 28: Effects of indoles on the expression of AhR- and AR-target genes in the PC-3 cell line. Cells were incubated with selected indoles (concentrations ranging from 1 μM to 100 μM) for 24 h. DMSO (0.1 %; v/v) was used as a negative control, and TCDD (10 nM) as a positive control. Upon incubation with tested compounds, RNA was isolated, reverse transcription was performed, and samples were analysed using RT-qPCR. Measurements were performed in 3 technical replicates. The data presented are a mean value of 3 independent experiments. Induction of AhR-target genes *CYP1A1* **(A)** and *AhRR* **(B)** was determined, as well as induction of AR-target genes *FKBP5* **(C)**, and *UBE2C* **(D)**. The relative expression of the monitored genes was normalized to the housekeeping gene *GAPDH*. Obtained results are expressed as fold induction to UT, ± SD. The symbol * represents values identified as significant by statistical analysis.

6.5 The Effects of Selected Indoles on Protein Levels

The second series of experiments in the **Phase II** were to determine the effect of indoles in the presence of absence DHT (10 nM) on the levels of target proteins. To begin with, the basal levels of AhR protein (~ 100 kDa) were evaluated in untreated prostate cancer cell lines other cell types using Western blot analysis. For this, untreated samples of intestinal cells (LS180) and hepatoma cells (HepG2) that naturally express high levels of AhR protein, obtained from previous projects, were used as positive controls of AhR presence. Among all tested cell lines, the highest AhR protein level was detected in LS180 cells (**Figure 29**). Interestingly, the second-highest basal levels of AhR protein were observed in the PC-3 prostate cancer cell line. In comparison to other cell types, 22Rv1 cells displayed low levels of AhR protein. The LNCaP cell line and its clone, C4-2 cell line, showed only minor basal levels of AhR protein that were hard to detect.

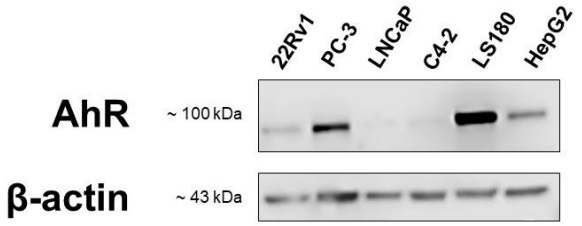

Figure 29: Basal levels of AhR protein in various cell types. Total proteins were isolated from untreated prostate cancer cell lines (22Rv1, PC-3, LNCaP, and C4-2), colon adenocarcinoma cell line (LS180), and hepatoma cells (HepG2). Samples were analysed using Western blot, incubated anti-AhR antibody, and AhR protein (~ 100 kDa) visualised on a chemiluminescence scanner. β-actin (~ 43 kDa) was used as a control.

Evaluation of AR protein levels was performed in the context of the proposed hypothesis. Both variants, AR-fl (~ 110 kDa, **Figure 30 A, C**) and AR-v7 (~ 89 kDa, **Figure 30 B, C**) exhibited a significant dose-dependent decrease when exposed to 3MI, 4MI, 2,3,7TMI, and 7MeO4MI. Interestingly, 4MI (1 μM) increased the level of DHT-inducible AR-v7 protein by up to 200 %. To determine whether the change in degradation or transcription is responsible, mRNA levels were measured. Surprisingly, the mRNA level of both AR variants decreased in a similar pattern, with the strongest effect shown by 3MI (IC_{50} approx. 10 μM) followed by 4MI, 2,3DMI, 2,3,7TMI, and 7MeO4MI (**Figure 30 D, E**). Therefore, the tested indoles are likely to induce downregulation in *AR* mRNA, which is further reflected in a decrease of AR proteins.

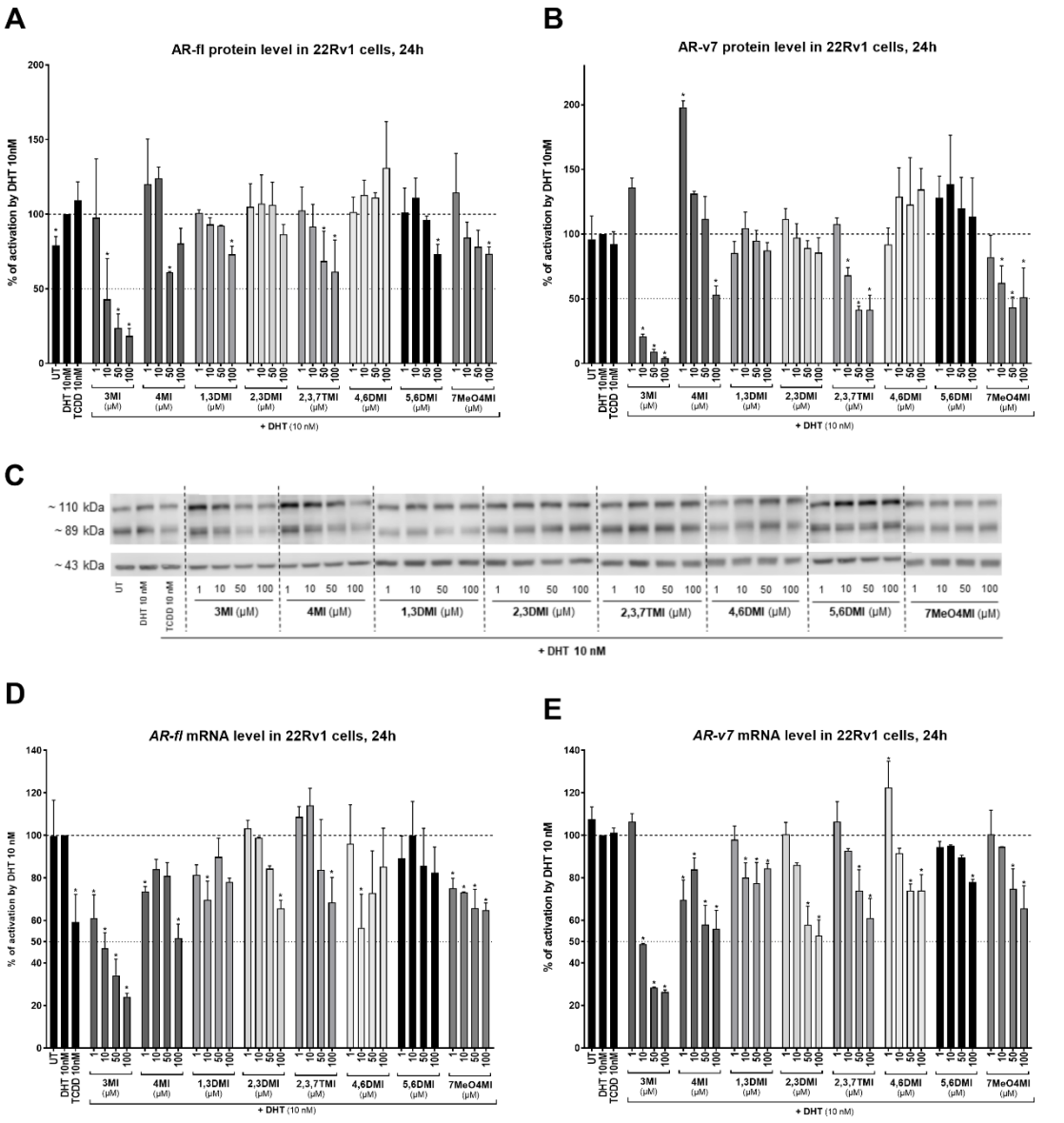

Figure 30: AR protein and mRNA levels after incubation with selected indoles, 22Rv1 cell line. Cells were incubated with selected indoles (concentrations ranging from 1 μM to 100 μM) in combination with DHT (10 nM) for 24 h. DMSO (0.1 %; v/v) was used as a negative control, and TCDD (10 nM) and DHT (10 nM) as respective positive controls. **(A, B)** Total proteins were isolated upon incubation with tested compounds, and the Bradford method determined respective concentrations. Samples were prepared in order to contain 30 μg of protein. Prepared samples were analysed using Western blot, incubated anti-AR antibody, and visualised on a chemiluminescence scanner. Relative levels of AR-fl protein (~ 110 kDa; **A**) or AR-v7 protein (~ 89 kDa; **B**) were normalized to β-actin (~ 43 kDa). Section **(C)** displays a representative blot. **(D, E)** For comparison, respective mRNA levels of AR-fl **(D)** and AR-v7 **(E)** were also determined. Upon incubation with tested compounds, RNA was isolated, reverse transcription was performed, and samples were analysed using RT-qPCR. Measurements were performed in 3 technical replicates. All data presented are a mean value of 3 independent experiments. Obtained results are expressed as a percentage of maximal activation by DHT (10 nM), equal to 100 %, ± SD. The symbol * represents values identified as significant by statistical analysis.

Based on previous experiments, AhR protein levels in the PC-3 cell line were determined only upon incubation with 3MI (1-100 μM) and AhR ligands TCDD (10 nM), FICZ (10 μM), and BaP (10 μM) for 24 h. The results indicated a significant decrease in AhR protein levels after the incubation with AhR ligands. While 3MI exhibited a dose-dependent decrease in AhR protein levels, statistical analysis did not confirm its significance (**Figure 31**).

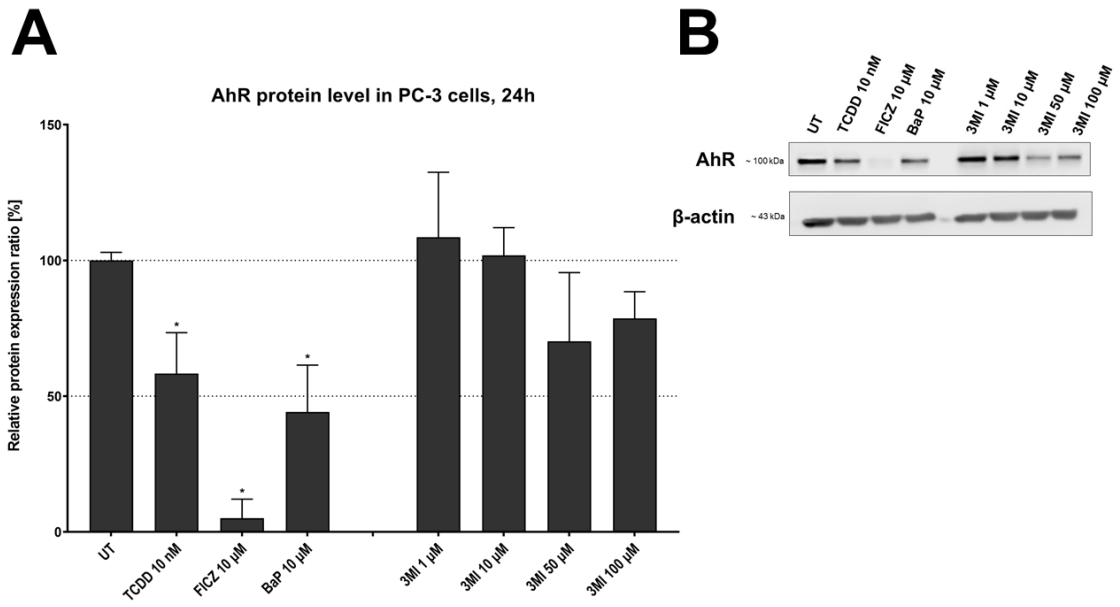

Figure 31: AhR protein levels after incubation with 3MI, PC-3 cell line. Cells were incubated with 3MI (concentrations ranging from 1 μM to 100 μM) for 24 h. DMSO (0.1 %; v/v) was used as a negative control, and TCDD (10 nM), FICZ (10 μM), and BaP (10 μM) as positive controls. Total proteins were isolated upon incubation with tested compounds, and the Bradford method determined respective concentrations. Samples were prepared in order to contain 30 μg of protein. Prepared samples were analysed using Western blot, incubated with anti-AhR antibody, and visualised on a chemiluminescence scanner. Relative levels of AhR protein (~ 100 kDa; **A**) were normalized to β-actin (~ 43 kDa). A representative blot is shown in the section **B**. The data presented are a mean value of 3 independent experiments. Obtained results are expressed in percentages of relative protein expression to UT, ± SD. The symbol * represents values identified as significant by statistical analysis.

Additionally, AR protein levels were determined in C4-2 cells upon incubation with selected indoles (100 μM) in the presence of DHT (10 nM; **Figure 32**). The effects of these indoles were evaluated after 24 h. However, it was not possible to isolate sufficient protein amount for 3MI (100 μM). The results showed that none of the tested indoles decreased AR-fl protein levels after 24 h of treatment (**Figure 32 A, C**). On the contrary, AR-fl protein levels significantly increased when treated with 4,6DMI, 5,6DMI, and 4MI in combination with DHT (10 nM). Furthermore, no significant decrease in PSA levels, a protein product of AR-target gene *KLK3*, was observed after 24 h (**Figure 32 B, D**).

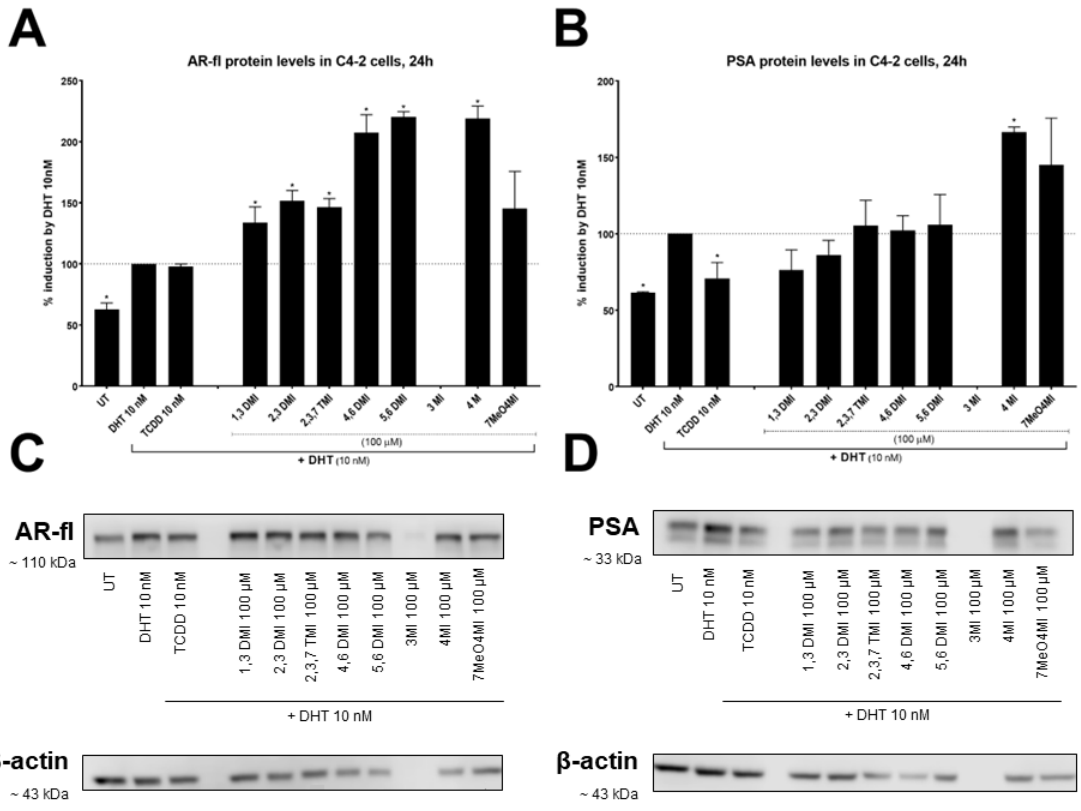

Figure 32: AR-fl and PSA protein levels after incubation with selected indoles in the C4-2 cell line. Cells were incubated with selected indoles (100 μM) in the presence of DHT (10 nM) for 24 h. DMSO (0.1 %; v/v) was used as a negative control, and DHT (10 nM) was used as positive control Effects of TCDD (10 nM) in combination with DHT (10 nM) were also evaluated. Total proteins were isolated upon incubation with tested compounds, and the Bradford method determined respective concentrations. Samples were prepared in order to contain 30 μg of protein. Prepared samples were analysed using Western blot, incubated anti-AR or anti-PSA antibody, and visualised on a chemiluminescence scanner. Relative levels of AR-fl protein (~ 110 kDa; **A, C**) or PSA protein (~ 33 kDa; **B, D**) were normalized to β-actin (~ 43 kDa). Representative blots are shown in sections **C** and **D**. The data presented are a mean value of 3 independent experiments. Obtained results are expressed in percentages of relative protein expression to DHT (10 nM), ± SD. The symbol * represents values identified as significant by statistical analysis.

6.6 The Effects of Indoles on the Enrichment of the *KLK3* Promoter

Phase III experiments began by investigating changes in the recruitment to the *KLK3* promoter, one of the AR-target genes, after the treatment with 8 previously selected indoles. A ChIP assay was conducted to assess the impact of the tested indoles on the transcription of the *KLK3* gene (**Figure 33**). 22Rv1 cells were treated with selected indoles (10 μM) and controls in antagonist mode (with DHT 10 nM) for 90 min. The positive control DHT (10 nM) increased the enrichment to the *KLK3* promoter by 2.8-4.9x fold. On the other hand, the presence of antiandrogen ENZ (10 nM) led to a significant decrease compared to DHT (10 nM). This rapid decrease was almost similar to the UT level. Common AhR ligands, TCDD (10 nM) and FICZ (10 μM), decreased a DHT-induced AR enrichment to the *KLK3* promoter by approximately 35 %. All tested indoles showed a decrease in the enrichment of the *KLK3* promoter by approximately 30-50 %, which was determined as significant by statistical analysis. These data suggest that the previously observed decrease in *KLK3* and *FKBP5* mRNA levels began already during AR binding to the response element in DNA, thereby affecting AR functionality.

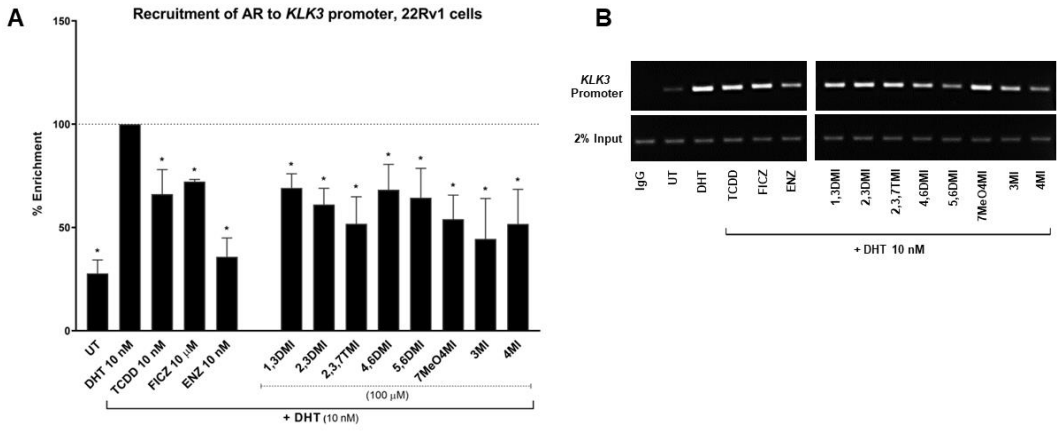

Figure 33: Enrichment of the *KLK3* promoter in 22Rv1 cells upon treatment with indoles. Cells were incubated with selected indoles (10 μM) in the presence of DHT (10 nM) for 90 min. DMSO (0.1 %; v/v) was used as a negative control, and DHT (10 nM) was used as a positive control. Effects of TCDD (10 nM) and FICZ (10 μM) in combination with DHT (10 nM) were also evaluated. Antiandrogen ENZ (10 nM) was used as a control of suppression of AR recruitment to the *KLK3* promoter. Subsequently, enrichment of the *KLK3* promoter by AR binding was evaluated using ChIP assay. Results were analysed using PCR and normalized to respective 2% inputs **(A)**. DNA products of such a reaction were separated using agarose electrophoresis and visualized **(B)**. The data presented are a mean value of 3 independent experiments. Obtained results are expressed in enrichment percentages by the positive control DHT (10 nM; 100 %), ± SD. The symbol * represents values identified as significant by statistical analysis.

6.7 CRISPR/Cas9 AhR Knock-out Model

At the second part of the **Phase III** experiments, a novel CRISPR/Cas9 AhR Knock-out model was developed by transient and stable transfection to further investigate the suggested interaction between AhR and AR signalling pathways. Additionally, specific AhR exon 5 primers were designed for RT-qPCR analysis of AhR KO samples, as this sequence corresponds with one of the target DNA sequences for the used CRISPR/Cas9 AhR KO plasmid.

A transiently transfected 22Rv1 AhR KO model was successfully developed, as a decrease in *AhR* (exon 5) mRNA levels was observed between WT and AhR KO samples in all conducted experiments (**Figure 34 A**). Therefore, 22Rv1 cells with transient AhR KO were incubated with only 1 indole (4MI 100 μM), which displayed the most potent effects in previous experiments with the 22Rv1 cell line. After the treatment with TCDD (10 nM) or 4 MI (100 μM) in the presence or absence of DHT (10 nM), *CYP1A1* mRNA levels in transient AhR KO cells decreased slightly (**Figure 34 B**).

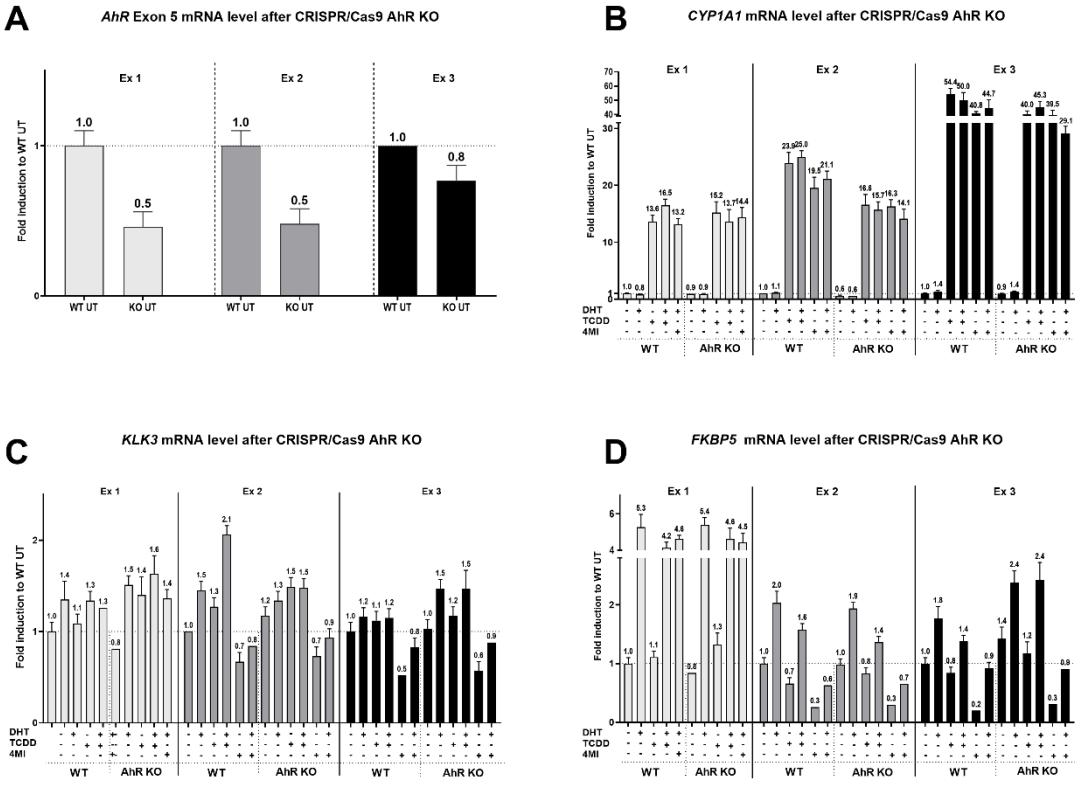

Figure 34: 22Rv1 transient AhR KO model. 22Rv1 cells were transiently transfected with the CRISPR/Cas9 AhR KO plasmid or with the Control CRISPR/Cas9 plasmid for 48 h. Transiently transfected 22Rv1 AhR KO cells were treated with controls (UT, TCDD 10 nM, DHT 10 nM) and tested indole, 4MI (100 μM) for 24 h. Following this, the expression of *AhR* exon 5 **(A)**, *CYP1A1* **(B)**, *KLK3* **(C)**, and *FKBP5* **(D)** on mRNA levels was evaluated using RT-qPCR. Measurements were performed in 3 technical replicates and the relative expression of the monitored genes was normalized to the housekeeping gene *GAPDH*. The data presented represents 3 independent experiments and the results are expressed as fold induction to 22Rv1 WT UT. The symbol * represents values identified as significant by statistical analysis.

However, the combined treatment of 4 MI (100 μM) and DHT (10 nM) did not show any consistent trend in *KLK3* mRNA levels (**Figure 34 C**) and had a minimal impact on *FKBP5* mRNA levels (**Figure 34 D**) when comparing 22Rv1 WT and transient 22Rv1 AhR KO cells, where the reversal of 4MI-elicited decrease in *KLK3* of *FKBP5* mRNAs was expected.

The results could have been partially due to the less than 100% effectiveness of the AhR knockout process. Therefore, a novel cell line with a stable AhR knockout was derived from 22Rv1 parental cells.

The construction of a stably transfected AhR-KO model was visually confirmed by Western blot analysis. 22Rv1 AhR KO cells were incubated with AhR exogenous ligand, TCDD (10 nM), and with AhR endogenous ligand, FICZ (10 μM), for 24 h. After the incubation, AhR and CYP1A1 protein levels were evaluated and compared with 22Rv1 WT levels. As expected, TCDD (10 nM) and FICZ (10 μM) decreased AhR protein levels and simultaneously increased CYP1A1 protein levels in 22Rv1 WT cells. On the contrary, no decrease in the AhR protein levels was observed in 22Rv1 AhR KO cells upon treatment with AhR ligands. CYP1A1 protein was not induced in 22Rv1 AhR KO cells at all (**Figure 35**).

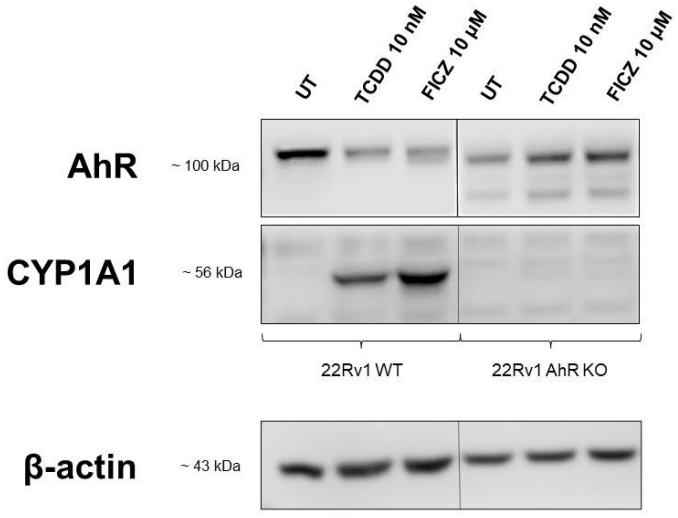

Figure 35: Stably transfected 22Rv1 AhR KO cell line. 22Rv1 cells were stably transfected with CRISPR/Cas9 AhR KO plasmid. Subsequently, 22Rv1 AhR KO cells were incubated with TCDD (10 nM) and FICZ (10 μM) for 24 h. DMSO (0.1 %; v/v) was used as a negative control. Total proteins were isolated upon incubation with tested compounds, and the Bradford method determined respective concentrations. Samples were prepared in order to contain 30 μg of protein. Prepared samples were analysed using Western blot, incubated with respective antibodies. Using chemiluminescent detection, AhR protein (~ 100 kDa), CYP1A1 protein (~ 56 kDa), and β-actin (~ 43 kDa) were visualized. This figure illustrates a representative blot and shows a comparison of detected protein levels in 22Rv1 WT and 22Rv1 AhR KO cells.

Subsequently, newly developed stable AhR KO cells were used to evaluate changes in the expression of AhR- and AR-target genes. AhR ligand TCDD (10 nM) induced expression of the *CYP1A1* gene in the 22Rv1 AhR KO cells up to approximately 4x fold, but up to 106x fold in the 22Rv1 WT cells (**Figure 36 A**). After the treatment with 4MI (100 μM), *CYP1A1* mRNA levels significantly decreased in the 22Rv1 AhR KO cells (~ 4x fold) in comparison to the 22Rv1 WT cells (~ 60x fold; **Figure 36 A**). TCDD (10 nM) did not induce *AhRR* mRNA levels in 22Rv1 AhR KO cells, while in 22Rv1 WT cells, the induction of *AhRR* was about 3.5x fold to UT (**Figure 36 B**).

TCDD-elicited DHT inducible *KLK3* mRNA decrease was observed in 22Rv1 WT, but not in 22Rv1 AhR KO cells (**Figure 36 C**). The very same effect was observed for 10 μM, but not for 100 μM 4MI at *KLK3* and *FKBP5* mRNA (**Figure 36 C, D**). These results indicate the reversal of the process and the existence of the connection between AhR and AR signalling. However, since 100 μM 4MI elicited the suppression of DHT-induced *KLK3* and *FKBP5* mRNAs in AhR KO cells (**Figure 36 C, D**). This might suggest either non-genomic action of AhR or 4MI off-target, which affects AR signalling.

In the presence of DHT (10 nM), the expression of the *UBE2C* gene did not change upon incubation with 4MI (10 or 100 μM) in 22Rv1 AhR KO cells (**Figure 36 E**), while *UBE2C* levels decreased to less than 80 % upon the incubation with 4MI in 22Rv1 WT cells.

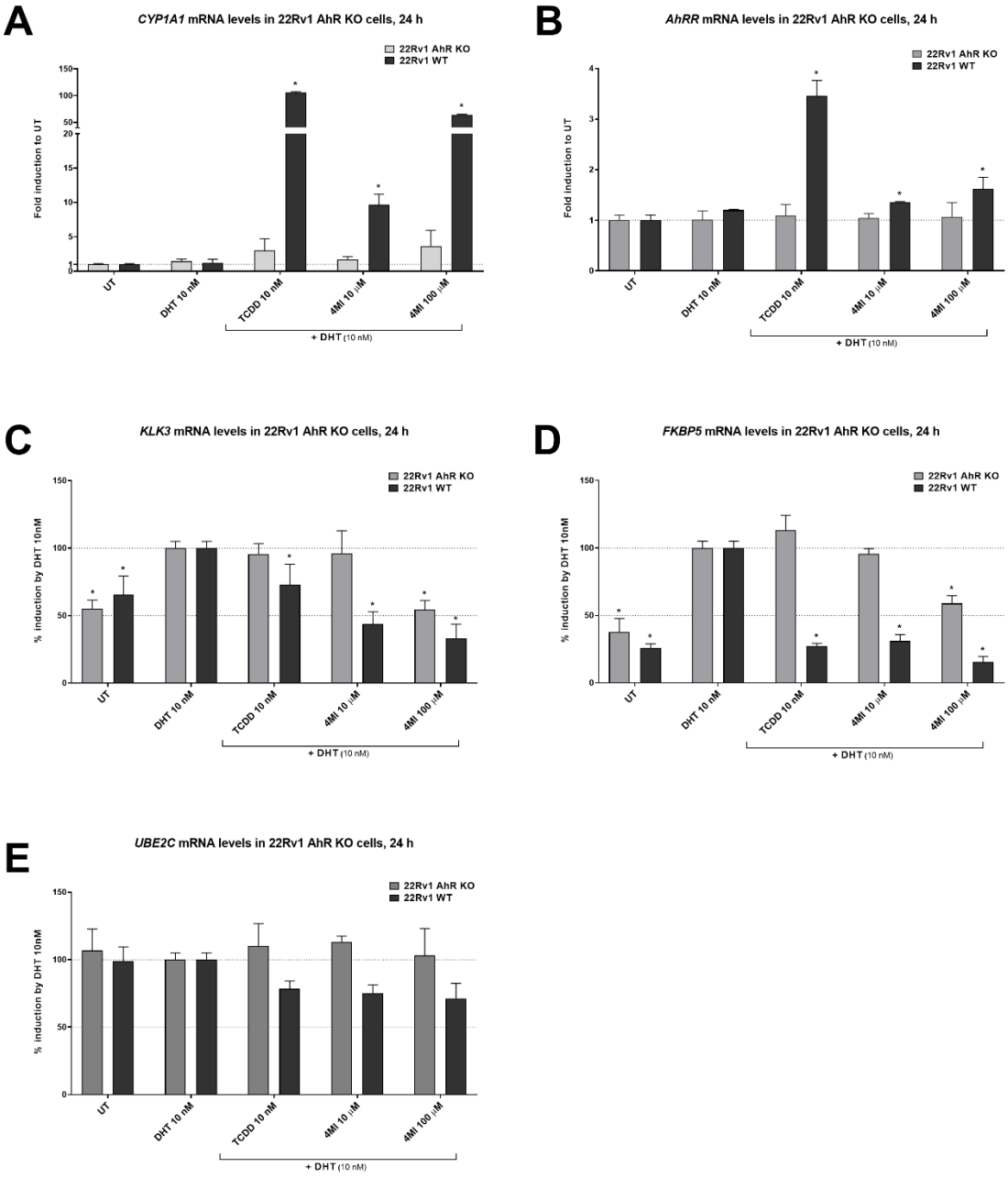

Figure 36: Levels of AhR- and AR-target genes in 22Rv1 AhR KO cell line. Stably transfected 22Rv1 AhR KO cells were treated with controls (UT, TCDD 10 nM, DHT 10 nM) and tested indole, 4MI (10 and 100 µM) in the presence of DHT (10 nM) for 24 h. Upon incubation with tested compounds, RNA was isolated, reverse transcription was performed, and samples were analysed using RT-qPCR. Measurements were performed in 3 technical replicates. The data presented are a mean value of 3 independent experiments. Induction of AhR-target genes *CYP1A1* **(A)** and *AhRR* **(B)** was determined as well as the induction of AR-target genes *KLK3* **(C)**, *FKBP5* **(D)**, and *UBE2C* **(E)**. Results were compared with data obtained from the 22Rv1 WT cell line. The left panel displays results from 22Rv1 WT cells, and the right panel from 22Rv1 AhR KO cells. The relative expression of the monitored genes was normalized to the housekeeping gene *GAPDH*. The results are expressed as fold induction to UT, ± SD. The symbol * represents values identified as significant by statistical analysis.

6.8 The Effect of 3MI on Cell Cycle Analysis

During the final phase of the **Phase III** experiments, the FACS Verse Machine was used to analyse the cell cycle. This analysis was conducted due to the observation that different prostatic cell lines exhibited varying effects on cell viability and proliferation after incubation with selected indoles during experiments.

Out of all the examined indoles, 3MI (skatole) displayed the most interesting results, which varied notably between individual cell lines. Therefore, only this compound (3MI 100 μM) was used to determine its effect on changes in the cell cycle of 22Rv1, PC-3, LNCaP, and C4-2 cell lines. Individual phases of the cell cycle were analysed (G1, G2, S), as well as the induction of apoptosis.

The results obtained from the study indicate that incubation with 3MI caused apoptosis in 93 % of the 22Rv1 cells. However, in the PC-3 cell line, only about 10 % of the cells underwent apoptosis. In the case of LNCaP cells, apoptosis was observed in 62 % of the cells, and in C4-2 cells, the percentage was 70 % (**Figure 37**).

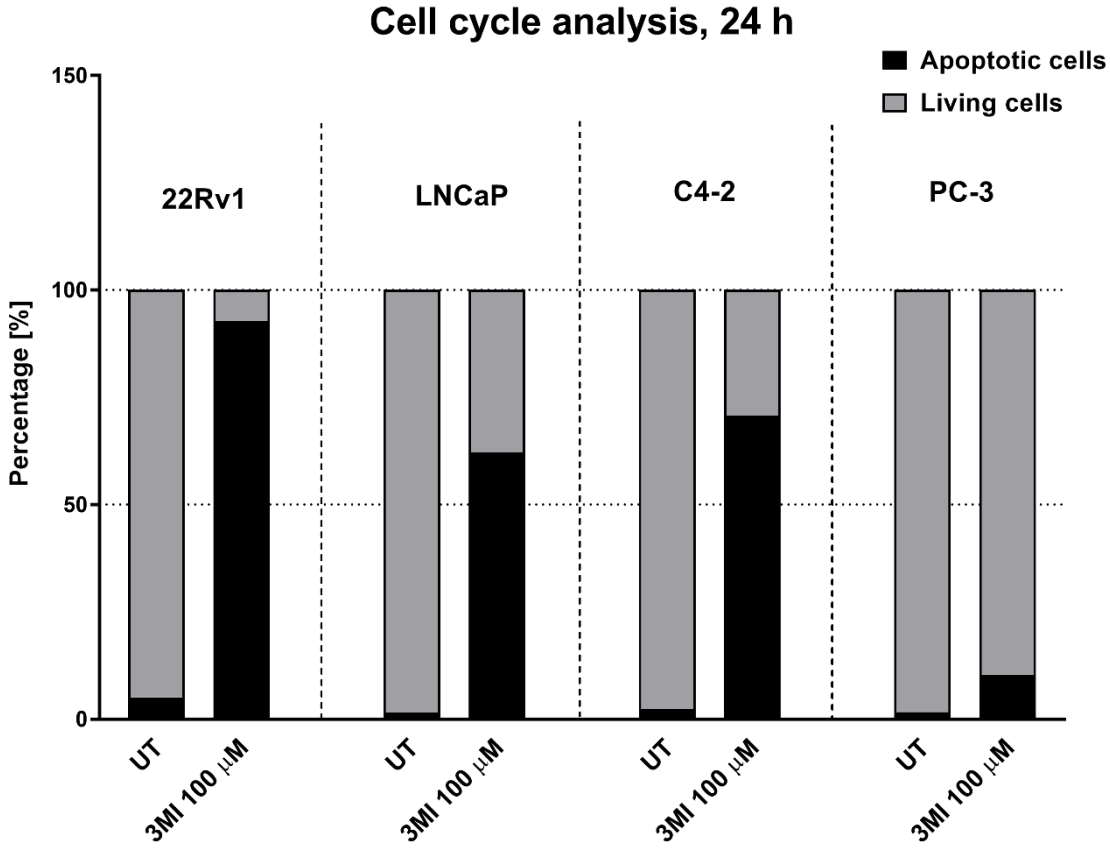

Figure 37: The impact of 3MI on the induction of apoptosis. Cells were incubated with 3MI (100 μM) or DMSO at a concentration of 0.1 % (v/v; UT) as a negative control for 24 h. The analysis of cell cycle phases showed that 3MI induced apoptosis in the observed cell lines to varying degrees. Specifically, 93 % of 22Rv1 cells underwent apoptosis, while only 10 % of PC-3 cells underwent apoptosis. In the case of LNCaP, the percentage of cells undergoing apoptosis was 62 %, and for C4-2, it was 70 %. The results are represented as a percentage, with 100 % representing the total number of cells analysed.

In **Figure 38**, the percentages of cells in different phases of the cell cycle after treatment with 3MI (100 μM) are compared to untreated (UT) cells. Across all tested cell lines, the most significant change in the composition of cell cycle phases after treatment with 3MI was observed in 22Rv1 cells, showing an approximately 10% increase in G1 and G2 phases and a nearly 20% decrease in the number of cells in the S phase (**Figure 38 A, B**). For LNCaP cells, there was an approximately 10% increase in cells in the G1 phase, and a decrease of about 6% in the S phase (**Figure 38 C, D**). In C4-2 cells, the number of cells in the G1 and G2 phases did not change significantly (about 3-4%), but the number of cells in the S phase increased by 12% (**Figure 38 E, F**). For PC-3 cells, the change in the number of cells in the G1 and G2 phases was about 4%, and the number of cells in the S phase increased by 7% (**Figure 38 G, H**).

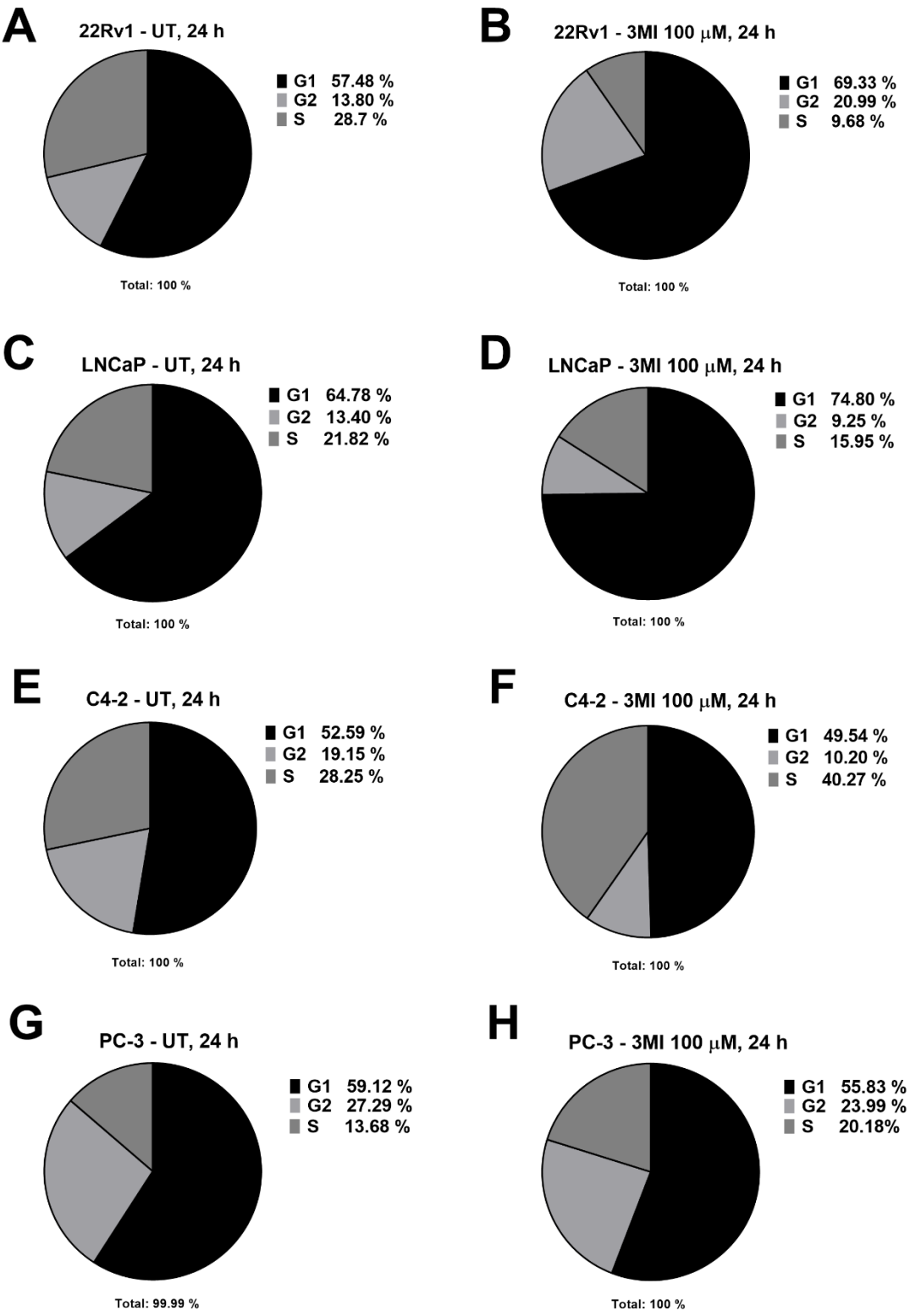

Figure 38: Cell cycle analysis upon incubation with 3MI compared to UT. Cells were incubated with 3MI (100 μM) or DMSO at a concentration of 0.1 % (v/v) as a negative control for 24 h. The graphs display the percentage of cells in each phase of the cell cycle (G1, G2, or S) for 22Rv1 (**A, B**), LNCaP (**C, D**), or C4-2 (**E, F**), and PC-3 (**G, H**) cell lines. The results are expressed as a percentage, with 100 % representing the total number of living cells analysed.

7 DISCUSSION

Prostate cancer is one of the most common types of cancer in men. Unfortunately, its incidence has rapidly increased in the past few years and is still on the rise. The therapeutics commonly used during chemotherapy (such as Docetaxel) or hormonal therapy (such as Enzalutamide or Flutamide) may lead to severe side effects or even to the development of CRPC [304]. Therefore, researchers are still investigating novel approaches in prostate cancer therapy to increase its efficiency and to overcome these unwanted side effects.

A novel mechanism suggests that the activation of AhR can suppress the AR signalling through a non-genomic pathway via E3 ubiquitin ligase activity of AhR [374].

Previous studies have observed the mechanism of AhR-induced AR proteasomal degradation with potent AhR ligands [369, 374], Carbidopa [373], or icaritin [381]. It is evident from the available literature that compounds containing an indole moiety are a significant group of AhR ligands and activators [164, 167, 188].

Therefore, the aim of this study was to determine whether selected indoles can induce proteasomal degradation of AR as a result of AhR activation. The effects of selected indoles were analysed in four prostate cancer cell lines, each containing a different set of monitored receptors: 22Rv1 (AhR, AR-fl, AR-v7), LNCaP and its clone C4-2 (AhR, AR-fl), and PC-3 (AhR, completely lacks AR). Based on previous experiments by our research group [170], 22 selected indolic compounds were tested in prostate carcinoma environment. Among them, some were identified as AhR activators in intestinal cells (LS180) and hepatoma cells (AZ-AhR; stably transfected HepG2 reporter cell line) [170, 389].

The experimental part of this study was divided into three phases. In **Phase I**, the goal was to identify indolic compounds that activate AhR and suppress AR simultaneously by monitoring respective transcription activity of each receptor using RGA. Only indoles that met both requirements, AhR activation and DHT-induced AR suppression, were selected for further experiments. In **Phase II**, the effects of selected indoles on the expression of AhR- and AR-target genes and respective protein levels were evaluated. **Phase III** involved further in-depth functional experiments, where the effects of selected indoles were investigated by chromatin immunoprecipitation (ChIP) to analyse the recruitment of AR to the *KLK3* promoter, by using flow cytometry for cell

cycle analysis, and to evaluate the effects of indoles in an AhR-restricted environment, by constructing a stable AhR CRISPR/Cas9 knockout of 22Rv1 cell line.

Prior to conducting the experiments, all indoles underwent testing for potential cytotoxicity using MTT and Crystal violet assays. The obtained results indicate that tested indoles did not exhibit any significant toxic effects on prostate cancer cell lines, regardless of the concentration used (0.1-100 μM). Interestingly, it was observed that higher concentrations of 3MI and 4MI resulted in a significant decrease in cell proliferation for 22Rv1 and C4-2 cell lines. Specifically, 3MI resulted in a decrease of approximately 60 % for 22Rv1 and approximately 20 % for C4-2, while 4MI resulted in a decrease of approximately 40 % for 22Rv1. However, there was no significant decrease in cell viability observed by MTT assay for the same compounds. Conversely, exposure of PC-3 cells to 3MI or 4MI did not display any effect.

In **Phase I** experiments, the effects of selected indoles on AhR or AR transcription activity were evaluated. For this purpose, two novel prostate-specific AhR reporter cell lines were successfully constructed (22AhRv1 and PAhRC3) and characterized. In the terms of AhR activation, all 22 indoles displayed this ability in AZ-AhR cells (derived from parental HepG2 cells [389]) in the previous study by Stepankova *et al*. [170]. After 24 h of treatment, the most potent ones were 4MI, 5MI, 6MI, 2,5DMI, and 7MeO [170]. After 24 hours, the same set of indoles were found to activate AhR in the 22AhRv1 prostate cancer cell line with similar efficacy to TCDD (10 nM). Among these indolic compounds, 1MI, 4MI, 5MI, 6MI, 7MI, and 7MeO were identified as the most potent ones in 22AhRv1 cells. However, this has not been confirmed in PAhRC3 prostate cancer cell line, where 3MI was the most potent one with a higher activation rate than TCDD (10 nM). This difference only highlights the unpredictable outcomes in AhR signalling among prostate cancer cells that drastically differ in AhR protein amount (Figure 35).

Although all indoles activated AhR as effectively as TCDD (10 nM) in 22AhRv1 cells, only some of them were able to significantly suppress DHT-induced AR transcription activity in AIZ-AR cells, which were also derived from parental 22Rv1 cell line [386]. Surprisingly, 3MI displayed dose-dependent suppression of AR transcription activity event in the absence of DHT. This, however, can be partially contribution to suppression of proliferation, as measured by the Crystal violet assay. Nevertheless, it is important to notice that IC_{50} for inhibition of proliferation was 60 μM, while IC_{50} of 3MI alone or in combination with DHT (10 nM) in AIZ-AR cells was roughly 5 μM. This suggests

that the suppression of AR transcription activity by 3MI is not solely due to the inhibition of the proliferation process. Additionally, it is interesting to note that TCDD (10 nM) and FICZ (10 μM), model high-affinity AhR ligands, had opposite effects on DHT-induced AR transcription activity in AIZ-AR cells, despite inducing AhR-mediated luciferase activity in 22AhRv1 cells. This may be given by the nature of a ligand itself as well as activation or inhibition of other signalling pathways, e.g. MAP kinases (MAPK/ERK pathway or MAPK/JNK pathway) [392].

Indole is a molecule made up of two rings - pyrrole and benzene. The two rings are fused together at the 2,3-positions, creating a bicyclic compound. Indole derivatives can have a variety of residues attached at different positions, leading to different compounds with unique biological effects. Different positions of various residues have been associated with different biological effects [393]. A previous study by Stepankova *et al.* found that 4MI and 7MeO were the most potent activators of AhR. In an attempt to create a compound with even more potent effects, researchers synthesized a new compound, 7MeO4MI. However, the results were surprising - the compound had a lower activating effect on AhR activation than the individual substances 4MI and 7MeO [170].

Based on results from **Phase I**, 8 indoles were selected for **Phase II** experiments, namely 3MI, 4MI, 1,3DMI, 2,5DMI, 2,3,7TMI, 4,6DMI, 5,6DMI, and 7MeO4MI. On mRNA levels, selected indoles induced the expression of *CYP1A1*, a marker of AhR activation in 22Rv1 and PC-3 cell lines. The dimethoxyindoles, specifically 4,6DMI and 5,6DMI, showed the lowest *CYP1A1* mRNA induction in both cell lines. The suppression of AR-target genes followed the same pattern as in **Phase I** AIZ-AR experiments. Based on the results from above mentioned experiments, certain conclusion about the effect of structure and AR activity-related decrease can be estimated. These results suggest that the presence of a methyl group (CH3-) at position 3 of the indole causes a decrease in DHT-induced AR activity, which is mildly counteracted by methyls at positions 1 (1,3DMI) and 2 (2,3DMI). Additionally, a methyl group at position 7 of 2,3DMI retains the AR suppressing activity (2,3,7TMI), while a second methyl group at position 3 has co-activating effect (2,3,7TMI). While single methoxy group (at positions 4, 5, or 6) slightly co-activated AR, the simultaneous presence of two methoxy groups positions 4, 5, or 6 (4,6DMI, 5,6DMI) displayed suppressive activity. Interestingly, the methoxy group at position 7 resulted in a strong co-activating effect on AR activity, but this effect was overridden by a methyl group at position 4 (as seen in the comparison of 4MI vs 7MeO and 7MeO4MI).

During all three experimental phases of this study, it was discovered that certain indoles have the ability to suppress AR activity to some extent and also inhibit DHT-inducible AR binding to the *KLK3* promoter. Furthermore, these indoles were found to suppress *AR* mRNA levels, which resulted in a decrease in AR protein levels. This indicates a different type of mechanism from what was initially expected, i.e. proteasomal degradation with no effect on mRNA level.

In the original study conducted on LNCaP cells by Ohtake *et al*., the AR protein levels were significantly reduced while *AR* mRNA levels remained unchanged [369]. A study conducted by Chen *et al*. identified that Carbidopa, a strong AhR activator of natural origin, inhibited cell proliferation and induced apoptosis in LNCaP cell line. However, this mechanism was not observed in the AR-independent DU145 prostate cancer cell line [373]. These observations supported the original hypothesis of AR proteasomal degradation induced by AhR activation. However, the results obtained in this study suggest that the mechanism of AR suppression by selected indoles in 22Rv1 cells is induced already at the transcription level and upon binding of the AR to the response elements in the promoters of target genes. Moreover, indoles-induced decrease in the level of AR transcript and AR protein likely contributed to observed suppression of AR signalling.

Previous studies have demonstrated that the mechanism of AhR-mediated AR proteasomal degradation is associated with full AhR agonists, such as TCDD, B[a]P, or 3MC [111, 376, 377]. However, this mechanism was not observed with partial AhR agonists or weak activators, such as indirubin or β-napthoflavone [111]. Although tested indoles have been shown to be strong AhR activators, sometimes with higher efficacy than TCDD (10 nM), they were not identified as true AhR ligands so far.

One of the most intriguing discoveries in this study is the behaviour of 3MI (skatole) in different types of prostate cancer cells, as it is the only natural indole tested in this research [170, 394]. The presence of 3MI not only showed a distinct impact on AhR transcription activity evaluated by RGA, but also on the induction of AhR target genes in 22Rv1 and PC-3 cell lines. Although 3MI exhibited only minor induction of AhR transcription activity in 22Rv1 cells, it showed high AhR-activating ability in the PC-3 cell line, even higher than TCDD (10 nM). Skatole, which is a naturally occurring product of intestinal microbiota, can be found in varying concentrations in the serum of patients with hepatic encephalopathy [395]. However, the average concentration of 3MI in the serum of healthy individuals is still unknown.

In summary, the toxic effects of 3MI (skatole) were found to be species- and tissue-specific. 3MI was found to induce lung damage in cattle or rodents but not in boars or pigs [394, 396]. Additionally, 3MI was found to create 3-methyleneindolenine (3MEIN), a reactive intermediate metabolic product detected in rabbit Clara cells or normal human bronchial epithelial cells (BEAS-2B) [397-399]. However, most of the studies on 3MI toxicity are outdated, and there is limited recent research on the effects of 3MI on the human body. Therefore, further investigation into this area of research is needed, especially since 3MI is the only naturally occurring indolic compound tested in this study, and the precise boundary between physiological and pathophysiological levels of this substance is still not determined. The fact that 3MI is used as a malodorant substance in non-lethal weapon systems (patent number: US 6386113 B1) [400] is also concerning due to its proven pulmonotoxicity.

Additionally, visible changes in the morphology of 22Rv1 an C4-2, but not PC-3, were observed after 24 h treatment with 3MI (*personal observation*). This observation suggests that 3MI may induce some form of apoptotic event and could have multiple molecular targets within cells. This hypothesis is supported by the fact that effects of 3MI differed from those of other indoles. 3MI decreased *AhRR* mRNA levels in 22Rv1 cells, but significantly increased the *AhRR* mRNA levels in PC-3 cells, which was quite the opposite to other tested indoles. The regulation of *AhRR* and *AhR* expression is controlled by p53 signalling and the unique action of 3MI compared to other indoles may be explained by its genotoxic action (as demonstrated in bronchial cells [399]) which involves p53 activation, along with NF-kB activation [1, 394]. While PC-3 do not contain functional p53 protein, 22Rv1 cells do.

Due to the huge differences between 3MI behaviour in 22Rv1 and PC-3 cells, it was suggested that the sensitivity of cells for 3MI is just a reflection of AR presence. Therefore, all four prostate cancer cell lines were incubated with 3MI (100 μM) for 24 h before performing cell cycle analysis using FACS. Obtained results revealed that incubation with 3MI rapidly induced apoptosis in 22Rv1 cells (~93 %) but not in PC-3 cell line (~10 %). This is in correlation with the presence of two isoforms of AR in 22Rv1 cells and the absence of AR in PC-3 cells [382, 385]. Moreover, LNCaP and C4-2 cells were somewhere between. Another factor that controls the cell cycle and the response to DNA damage is the transcription factor p53, which is absent in PC-3 cells as mentioned earlier [401].

If the result of this study should have been translated into the *in vivo* model, it may be speculated that males who possess noticeable levels of 3MI in their serum could be less susceptible to developing AR-dependent prostate cancer. This hypothesis is based on the observed decline in all AR-mediated parameters we studied and the most significant decline in the Crystal violet assay, which reflects the cells' proliferative capacity. However, this relationship must be explored in future research to determine whether there is any link between skatole blood levels and the incidence of prostate cancer in men.

Many important compounds that have a biological role in our body contain an indole moiety in their structure [402]. This observation led to the concept of bacterial mimicry, which simply states that these substances are better tolerated by the body than the synthetic compounds, which are commonly used in prostate cancer treatment, due to the evolutionary coexistence of human cells and bacteria. The use of hormonal therapy and chemotherapy drugs has been linked to severe side effects, which could be overcome with the use of drugs that have a more natural structure. Most of the tested indoles were found to be well tolerated by prostate cancer cells, even at high concentrations.

To conclude, some indoles showed the ability to suppress significantly DHT-induced AR activation and, this phenomenon may be associated with AhR activation, despite only minor confirming proofs. However, the hypothesis of AR degradation via AhR activation for selected indoles has not been confirmed, since AR mRNA was affected to the same extent as AR protein. Thus, the suppression of AR signalling pathway by selected indolic compounds is likely mediated thought a different mechanism. Nevertheless, certain compounds containing the indole scaffold remain promising candidates for studying their role in the process of prostate cancer suppression.

8 CONCLUSION

The presented dissertation thesis tested the hypothesis of AR-signalling pathway suppression through the AhR activation with selected indolic compounds. This study evaluated the hypothesis of AhR-mediated proteasomal degradation of AR upon the activation of AhR by selected indolic compounds. The newly developed 22AhRv1 and PAhRC3 reporter cell line were used to test all 22 indoles, and all of them showed promising AhR-activating potential. However, only 8 of 22 tested compounds were able to simultaneously suppress DHT-induced AR activation. These 8 indoles (3MI, 4MI, 1,3DMI, 2,3DMI, 2,3,7TMI, 4,6DMI, 5,6DMI, and 7MeO4MI) were selected for further experiments. At the mRNA level, the 8 selected indoles increased *CYP1A1* expression and significantly reduced DHT-inducible *KLK3* and *FKBP5* expression (AR-target genes). The ChIP analysis also revealed that selected indoles reduced DHT-inducible binding of AR to the *KLK3* promoter. The study further monitored the effect of the strongest AhR activator in 22Rv1, 4MI, using transient and stable transfection with the CRISPR/Cas9 AhR KO plasmid. However, only significant change in the expression of AR-target genes was observed with *FKBP5*, which is also regulated by other signalling pathways (such as GR) and not only by AR-signalling [403].

The main findings of this study are:

1. All tested indoles displayed the ability to activate AhR in prostate-specific environment
2. Eight selected indoles were capable of simultaneous suppression of DHT-induced AR signalling
3. The decrease was observed already on the *AR* mRNA level, thus it not likely mediated by AhR-induced proteasomal degradation of AR
4. Selected indolic compounds inhibit AR signalling pathway already at the point of AR-target genes expression initiation
5. Results suggest a potential relationship between the structure of tested indoles and suppression of AR activity; however, further experiments are required to confirm this claim

9 REFERENCES

1. Larigot, L., et al., *AhR signaling pathways and regulatory functions.* Biochim Open, 2018. **7**: p. 1-9.
2. Seok, S.H., et al., *Structural hierarchy controlling dimerization and target DNA recognition in the AHR transcriptional complex.* Proc Natl Acad Sci U S A, 2017. **114**(21): p. 5431-5436.
3. Socorro, S., *Androgen receptors : structural biology, genetics and molecular defects*, in *Protein biochemistry, synthesis, structure and cellular functions*. 2014, Nova Biomedical,: New York. p. 1 online resource.
4. Tan, M.H., et al., *Androgen receptor: structure, role in prostate cancer and drug discovery.* Acta Pharmacol Sin, 2015. **36**(1): p. 3-23.
5. Hu, L., et al., *MicroRNA regulation of the proliferation and apoptosis of Leydig cells in diabetes.* Mol Med, 2021. **27**(1): p. 104.
6. Lawrence, B.M., et al., *New Insights into Testosterone Biosynthesis: Novel Observations from HSD17B3 Deficient Mice.* Int J Mol Sci, 2022. **23**(24).
7. Miller, K.J., et al., *A compendium of Androgen Receptor Variant 7 target genes and their role in Castration Resistant Prostate Cancer.* Front Oncol, 2023. **13**: p. 1129140.
8. Alberts, B., *Molecular biology of the cell*. 5th ed. 2008, New York: Garland Science.
9. Grishanova, A.Y. and M.L. Perepechaeva, *Aryl Hydrocarbon Receptor in Oxidative Stress as a Double Agent and Its Biological and Therapeutic Significance.* Int J Mol Sci, 2022. **23**(12).
10. Kininis, M. and W.L. Kraus, *A global view of transcriptional regulation by nuclear receptors: gene expression, factor localization, and DNA sequence analysis.* Nucl Recept Signal, 2008. **6**: p. e005.
11. Govindan, M.V., et al., *Cloning of the human glucocorticoid receptor cDNA.* Nucleic Acids Res, 1985. **13**(23): p. 8293-304.
12. Frigo, D.E., M. Bondesson, and C. Williams, *Nuclear receptors: from molecular mechanisms to therapeutics.* Essays Biochem, 2021. **65**(6): p. 847-856.
13. Weikum, E.R., X. Liu, and E.A. Ortlund, *The nuclear receptor superfamily: A structural perspective.* Protein Sci, 2018. **27**(11): p. 1876-1892.
14. Isigkeit, L. and D. Merk, *Opportunities and challenges in targeting orphan nuclear receptors.* Chem Commun (Camb), 2023. **59**(31): p. 4551-4561.
15. Dvorak, Z., H. Sokol, and S. Mani, *Drug Mimicry: Promiscuous Receptors PXR and AhR, and Microbial Metabolite Interactions in the Intestine.* Trends Pharmacol Sci, 2020. **41**(12): p. 900-908.
16. Bennett, P., D.B. Ramsden, and A.C. Williams, *Complete structural characterisation of the human aryl hydrocarbon receptor gene.* Clin Mol Pathol, 1996. **49**(1): p. M12-6.
17. Pawlak, M., P. Lefebvre, and B. Staels, *General molecular biology and architecture of nuclear receptors.* Curr Top Med Chem, 2012. **12**(6): p. 486-504.
18. Picard, N., et al., *Phosphorylation of activation function-1 regulates proteasome-dependent nuclear mobility and E6-associated protein ubiquitin ligase recruitment to the estrogen receptor beta.* Mol Endocrinol, 2008. **22**(2): p. 317-30.
19. Garza, A.M., S.H. Khan, and R. Kumar, *Site-specific phosphorylation induces functionally active conformation in the intrinsically disordered N-terminal*

activation function (AF1) domain of the glucocorticoid receptor. Mol Cell Biol, 2010. **30**(1): p. 220-30.
20. Poukka, H., et al., *Covalent modification of the androgen receptor by small ubiquitin-like modifier 1 (SUMO-1).* Proc Natl Acad Sci U S A, 2000. **97**(26): p. 14145-50.
21. Rastinejad, F., et al., *Structural determinants of nuclear receptor assembly on DNA direct repeats.* Nature, 1995. **375**(6528): p. 203-11.
22. Rochel, N., et al., *Common architecture of nuclear receptor heterodimers on DNA direct repeat elements with different spacings.* Nat Struct Mol Biol, 2011. **18**(5): p. 564-70.
23. Schwartz, J.A., et al., *Mutations targeted to a predicted helix in the extreme carboxyl-terminal region of the human estrogen receptor-alpha alter its response to estradiol and 4-hydroxytamoxifen.* J Biol Chem, 2002. **277**(15): p. 13202-9.
24. Nuclear Receptors Nomenclature, C., *A unified nomenclature system for the nuclear receptor superfamily.* Cell, 1999. **97**(2): p. 161-3.
25. Nagy, L. and J.W. Schwabe, *Mechanism of the nuclear receptor molecular switch.* Trends Biochem Sci, 2004. **29**(6): p. 317-24.
26. Lonard, D.M. and B.W. O'Malley, *Nuclear receptor coregulators: modulators of pathology and therapeutic targets.* Nat Rev Endocrinol, 2012. **8**(10): p. 598-604.
27. Finlay, D.B., S.B. Duffull, and M. Glass, *100 years of modelling ligand-receptor binding and response: A focus on GPCRs.* Br J Pharmacol, 2020. **177**(7): p. 1472-1484.
28. Stephenson, R.P., *A modification of receptor theory.* Br J Pharmacol Chemother, 1956. **11**(4): p. 379-93.
29. Kenakin, T., *Principles: receptor theory in pharmacology.* Trends Pharmacol Sci, 2004. **25**(4): p. 186-92.
30. Nussinov, R. and C.J. Tsai, *The different ways through which specificity works in orthosteric and allosteric drugs.* Curr Pharm Des, 2012. **18**(9): p. 1311-6.
31. Cheng, Y. and W.H. Prusoff, *Relationship between the inhibition constant (K1) and the concentration of inhibitor which causes 50 per cent inhibition (I50) of an enzymatic reaction.* Biochem Pharmacol, 1973. **22**(23): p. 3099-108.
32. Berg, K.A. and W.P. Clarke, *Making Sense of Pharmacology: Inverse Agonism and Functional Selectivity.* Int J Neuropsychopharmacol, 2018. **21**(10): p. 962-977.
33. Denison, M.S., et al., *Exactly the same but different: promiscuity and diversity in the molecular mechanisms of action of the aryl hydrocarbon (dioxin) receptor.* Toxicol Sci, 2011. **124**(1): p. 1-22.
34. Poland, A., E. Glover, and A.S. Kende, *Stereospecific, high affinity binding of 2,3,7,8-tetrachlorodibenzo-p-dioxin by hepatic cytosol. Evidence that the binding species is receptor for induction of aryl hydrocarbon hydroxylase.* J Biol Chem, 1976. **251**(16): p. 4936-46.
35. Skálová, L., *Ah Receptor*, in *Metabolismus léčiv a jiných xenobiotik*. 2018, Charles University, Karolinum. p. 170.
36. Dolwick, K.M., et al., *Cloning and expression of a human Ah receptor cDNA.* Mol Pharmacol, 1993. **44**(5): p. 911-7.
37. Bock, K.W., *From TCDD-mediated toxicity to searches of physiologic AHR functions.* Biochem Pharmacol, 2018. **155**: p. 419-424.
38. Hahn, M.E., *Aryl hydrocarbon receptors: diversity and evolution.* Chem Biol Interact, 2002. **141**(1-2): p. 131-60.

39. Le Beau, M.M., et al., *Chromosomal localization of the human AHR locus encoding the structural gene for the Ah receptor to 7p21-->p15.* Cytogenet Cell Genet, 1994. **66**(3): p. 172-6.
40. Micka, J., et al., *Human Ah receptor (AHR) gene: localization to 7p15 and suggestive correlation of polymorphism with CYP1A1 inducibility.* Pharmacogenetics, 1997. **7**(2): p. 95-101.
41. Cannon, A.S., P.S. Nagarkatti, and M. Nagarkatti, *Targeting AhR as a Novel Therapeutic Modality against Inflammatory Diseases.* Int J Mol Sci, 2021. **23**(1).
42. Gargaro, M., et al., *The Landscape of AhR Regulators and Coregulators to Fine-Tune AhR Functions.* Int J Mol Sci, 2021. **22**(2).
43. Gu, Y.Z., J.B. Hogenesch, and C.A. Bradfield, *The PAS superfamily: sensors of environmental and developmental signals.* Annu Rev Pharmacol Toxicol, 2000. **40**: p. 519-61.
44. Fribourgh, J.L. and C.L. Partch, *Assembly and function of bHLH-PAS complexes.* Proc Natl Acad Sci U S A, 2017. **114**(21): p. 5330-5332.
45. Wu, D. and F. Rastinejad, *Structural characterization of mammalian bHLH-PAS transcription factors.* Curr Opin Struct Biol, 2017. **43**: p. 1-9.
46. Mimura, J., et al., *Identification of a novel mechanism of regulation of Ah (dioxin) receptor function.* Genes Dev, 1999. **13**(1): p. 20-5.
47. Schulte, K.W., et al., *Structural Basis for Aryl Hydrocarbon Receptor-Mediated Gene Activation.* Structure, 2017. **25**(7): p. 1025-1033 e3.
48. Sakurai, S., T. Shimizu, and U. Ohto, *The crystal structure of the AhRR-ARNT heterodimer reveals the structural basis of the repression of AhR-mediated transcription.* J Biol Chem, 2017. **292**(43): p. 17609-17616.
49. Murre, C., P.S. McCaw, and D. Baltimore, *A new DNA binding and dimerization motif in immunoglobulin enhancer binding, daughterless, MyoD, and myc proteins.* Cell, 1989. **56**(5): p. 777-83.
50. Murre, C., et al., *Structure and function of helix-loop-helix proteins.* Biochim Biophys Acta, 1994. **1218**(2): p. 129-35.
51. Ikuta, T., et al., *Nuclear localization and export signals of the human aryl hydrocarbon receptor.* J Biol Chem, 1998. **273**(5): p. 2895-904.
52. Gorlich, D. and I.W. Mattaj, *Nucleocytoplasmic transport.* Science, 1996. **271**(5255): p. 1513-8.
53. Ikuta, T., Y. Kobayashi, and K. Kawajiri, *Phosphorylation of nuclear localization signal inhibits the ligand-dependent nuclear import of aryl hydrocarbon receptor.* Biochem Biophys Res Commun, 2004. **317**(2): p. 545-50.
54. Pollenz, R.S. and E.R. Barbour, *Analysis of the complex relationship between nuclear export and aryl hydrocarbon receptor-mediated gene regulation.* Mol Cell Biol, 2000. **20**(16): p. 6095-104.
55. Fukunaga, B.N., et al., *Identification of functional domains of the aryl hydrocarbon receptor.* J Biol Chem, 1995. **270**(49): p. 29270-8.
56. Zelzer, E., P. Wappner, and B.Z. Shilo, *The PAS domain confers target gene specificity of Drosophila bHLH/PAS proteins.* Genes Dev, 1997. **11**(16): p. 2079-89.
57. Jones, S., *An overview of the basic helix-loop-helix proteins.* Genome Biol, 2004. **5**(6): p. 226.
58. Card, P.B., P.J. Erbel, and K.H. Gardner, *Structural basis of ARNT PAS-B dimerization: use of a common beta-sheet interface for hetero- and homodimerization.* J Mol Biol, 2005. **353**(3): p. 664-77.

59. Kolonko, M. and B. Greb-Markiewicz, *bHLH-PAS Proteins: Their Structure and Intrinsic Disorder.* Int J Mol Sci, 2019. **20**(15).
60. Henry, J.T. and S. Crosson, *Ligand-binding PAS domains in a genomic, cellular, and structural context.* Annu Rev Microbiol, 2011. **65**: p. 261-86.
61. Crews, S.T., *Control of cell lineage-specific development and transcription by bHLH-PAS proteins.* Genes Dev, 1998. **12**(5): p. 607-20.
62. Lindebro, M.C., L. Poellinger, and M.L. Whitelaw, *Protein-protein interaction via PAS domains: role of the PAS domain in positive and negative regulation of the bHLH/PAS dioxin receptor-Arnt transcription factor complex.* EMBO J, 1995. **14**(14): p. 3528-39.
63. McGuire, J., et al., *Definition of a dioxin receptor mutant that is a constitutive activator of transcription: delineation of overlapping repression and ligand binding functions within the PAS domain.* J Biol Chem, 2001. **276**(45): p. 41841-9.
64. Andersson, P., et al., *A constitutively active dioxin/aryl hydrocarbon receptor induces stomach tumors.* Proc Natl Acad Sci U S A, 2002. **99**(15): p. 9990-5.
65. Ma, Q., L. Dong, and J.P. Whitlock, Jr., *Transcriptional activation by the mouse Ah receptor. Interplay between multiple stimulatory and inhibitory functions.* J Biol Chem, 1995. **270**(21): p. 12697-703.
66. Jain, S., et al., *Potent transactivation domains of the Ah receptor and the Ah receptor nuclear translocator map to their carboxyl termini.* J Biol Chem, 1994. **269**(50): p. 31518-24.
67. Petrulis, J.R. and G.H. Perdew, *The role of chaperone proteins in the aryl hydrocarbon receptor core complex.* Chem Biol Interact, 2002. **141**(1-2): p. 25-40.
68. Antonsson, C., et al., *Distinct roles of the molecular chaperone hsp90 in modulating dioxin receptor function via the basic helix-loop-helix and PAS domains.* Mol Cell Biol, 1995. **15**(2): p. 756-65.
69. Enan, E. and F. Matsumura, *Identification of c-Src as the integral component of the cytosolic Ah receptor complex, transducing the signal of 2,3,7,8-tetrachlorodibenzo-p-dioxin (TCDD) through the protein phosphorylation pathway.* Biochem Pharmacol, 1996. **52**(10): p. 1599-612.
70. Pongratz, I., G.G. Mason, and L. Poellinger, *Dual roles of the 90-kDa heat shock protein hsp90 in modulating functional activities of the dioxin receptor. Evidence that the dioxin receptor functionally belongs to a subclass of nuclear receptors which require hsp90 both for ligand binding activity and repression of intrinsic DNA binding activity.* J Biol Chem, 1992. **267**(19): p. 13728-34.
71. Petrulis, J.R., et al., *The hsp90 Co-chaperone XAP2 alters importin beta recognition of the bipartite nuclear localization signal of the Ah receptor and represses transcriptional activity.* J Biol Chem, 2003. **278**(4): p. 2677-85.
72. Kosyna, F.K. and R. Depping, *Controlling the Gatekeeper: Therapeutic Targeting of Nuclear Transport.* Cells, 2018. **7**(11).
73. Hord, N.G. and G.H. Perdew, *Physicochemical and immunocytochemical analysis of the aryl hydrocarbon receptor nuclear translocator: characterization of two monoclonal antibodies to the aryl hydrocarbon receptor nuclear translocator.* Mol Pharmacol, 1994. **46**(4): p. 618-26.
74. Wang, S. and O. Hankinson, *Functional involvement of the Brahma/SWI2-related gene 1 protein in cytochrome P4501A1 transcription mediated by the aryl hydrocarbon receptor complex.* J Biol Chem, 2002. **277**(14): p. 11821-7.

75. Poellinger, L., *Mechanistic aspects--the dioxin (aryl hydrocarbon) receptor*. Food Addit Contam, 2000. **17**(4): p. 261-6.
76. Mimura, J. and Y. Fujii-Kuriyama, *Functional role of AhR in the expression of toxic effects by TCDD.* Biochim Biophys Acta, 2003. **1619**(3): p. 263-8.
77. Davarinos, N.A. and R.S. Pollenz, *Aryl hydrocarbon receptor imported into the nucleus following ligand binding is rapidly degraded via the cytosplasmic proteasome following nuclear export.* J Biol Chem, 1999. **274**(40): p. 28708-15.
78. Haidar, R., et al., *The nuclear entry of the aryl hydrocarbon receptor (AHR) relies on the first nuclear localization signal and can be negatively regulated through IMPalpha/beta specific inhibitors.* Sci Rep, 2023. **13**(1): p. 19668.
79. Wright, E.J., et al., *Canonical and non-canonical aryl hydrocarbon receptor signaling pathways.* Curr Opin Toxicol, 2017. **2**: p. 87-92.
80. Dere, E., et al., *Integration of genome-wide computation DRE search, AhR ChIP-chip and gene expression analyses of TCDD-elicited responses in the mouse liver.* BMC Genomics, 2011. **12**: p. 365.
81. Huang, G. and C.J. Elferink, *A novel nonconsensus xenobiotic response element capable of mediating aryl hydrocarbon receptor-dependent gene expression.* Mol Pharmacol, 2012. **81**(3): p. 338-47.
82. Jackson, D.P., et al., *Ah receptor-mediated suppression of liver regeneration through NC-XRE-driven p21Cip1 expression.* Mol Pharmacol, 2014. **85**(4): p. 533-41.
83. Joshi, A.D., et al., *Homocitrullination Is a Novel Histone H1 Epigenetic Mark Dependent on Aryl Hydrocarbon Receptor Recruitment of Carbamoyl Phosphate Synthase 1.* J Biol Chem, 2015. **290**(46): p. 27767-78.
84. Oeckinghaus, A. and S. Ghosh, *The NF-kappaB family of transcription factors and its regulation.* Cold Spring Harb Perspect Biol, 2009. **1**(4): p. a000034.
85. Tian, Y., et al., *Ah receptor and NF-kappaB interactions, a potential mechanism for dioxin toxicity.* J Biol Chem, 1999. **274**(1): p. 510-5.
86. Ke, S., et al., *Mechanism of suppression of cytochrome P-450 1A1 expression by tumor necrosis factor-alpha and lipopolysaccharide.* J Biol Chem, 2001. **276**(43): p. 39638-44.
87. Matsumura, F. and C.F. Vogel, *Evidence supporting the hypothesis that one of the main functions of the aryl hydrocarbon receptor is mediation of cell stress responses.* Biol Chem, 2006. **387**(9): p. 1189-94.
88. Muku, G.E., et al., *Ligand-mediated cytoplasmic retention of the Ah receptor inhibits macrophage-mediated acute inflammatory responses.* Lab Invest, 2017. **97**(12): p. 1471-1487.
89. Kado, S., et al., *Aryl hydrocarbon receptor signaling modifies Toll-like receptor-regulated responses in human dendritic cells.* Arch Toxicol, 2017. **91**(5): p. 2209-2221.
90. Vogel, C.F., et al., *RelB, a new partner of aryl hydrocarbon receptor-mediated transcription.* Mol Endocrinol, 2007. **21**(12): p. 2941-55.
91. Vogel, C.F. and F. Matsumura, *A new cross-talk between the aryl hydrocarbon receptor and RelB, a member of the NF-kappaB family.* Biochem Pharmacol, 2009. **77**(4): p. 734-45.
92. Vogel, C.F., et al., *Interaction of aryl hydrocarbon receptor and NF-kappaB subunit RelB in breast cancer is associated with interleukin-8 overexpression.* Arch Biochem Biophys, 2011. **512**(1): p. 78-86.

93. Grishanova, A.Y., L.S. Klyushova, and M.L. Perepechaeva, *AhR and Wnt/beta-Catenin Signaling Pathways and Their Interplay.* Curr Issues Mol Biol, 2023. **45**(5): p. 3848-3876.
94. Vogel, C.F., E. Sciullo, and F. Matsumura, *Involvement of RelB in aryl hydrocarbon receptor-mediated induction of chemokines.* Biochem Biophys Res Commun, 2007. **363**(3): p. 722-6.
95. Wilson, S.R., A.D. Joshi, and C.J. Elferink, *The tumor suppressor Kruppel-like factor 6 is a novel aryl hydrocarbon receptor DNA binding partner.* J Pharmacol Exp Ther, 2013. **345**(3): p. 419-29.
96. Jackson, D.P., A.D. Joshi, and C.J. Elferink, *Ah Receptor Pathway Intricacies; Signaling Through Diverse Protein Partners and DNA-Motifs.* Toxicol Res (Camb), 2015. **4**(5): p. 1143-1158.
97. Gerbal-Chaloin, S., et al., *Role of CYP3A4 in the regulation of the aryl hydrocarbon receptor by omeprazole sulphide.* Cell Signal, 2006. **18**(5): p. 740-50.
98. Dvorak, Z., et al., *An evidence for regulatory cross-talk between aryl hydrocarbon receptor and glucocorticoid receptor in HepG2 cells.* Physiol Res, 2008. **57**(3): p. 427-435.
99. Sato, S., et al., *The aryl hydrocarbon receptor and glucocorticoid receptor interact to activate human metallothionein 2A.* Toxicol Appl Pharmacol, 2013. **273**(1): p. 90-9.
100. Gottel, M., et al., *Estrogen receptor alpha and aryl hydrocarbon receptor cross-talk in a transfected hepatoma cell line (HepG2) exposed to 2,3,7,8-tetrachlorodibenzo-p-dioxin.* Toxicol Rep, 2014. **1**: p. 1029-1036.
101. Vrzal, R., et al., *Activated thyroid hormone receptor modulates dioxin-inducible aryl hydrocarbon receptor-mediated CYP1A1 induction in human hepatocytes but not in human hepatocarcinoma HepG2 cells.* Toxicol Lett, 2017. **275**: p. 77-82.
102. Beischlag, T.V., et al., *The aryl hydrocarbon receptor complex and the control of gene expression.* Crit Rev Eukaryot Gene Expr, 2008. **18**(3): p. 207-50.
103. Safe, S. and L. Zhang, *The Role of the Aryl Hydrocarbon Receptor (AhR) and Its Ligands in Breast Cancer.* Cancers (Basel), 2022. **14**(22).
104. Swedenborg, E. and I. Pongratz, *AhR and ARNT modulate ER signaling.* Toxicology, 2010. **268**(3): p. 132-8.
105. Safe, S., et al., *Ah receptor agonists as endocrine disruptors: antiestrogenic activity and mechanisms.* Toxicol Lett, 1998. **102-103**: p. 343-7.
106. Wang, F., I. Samudio, and S. Safe, *Transcriptional activation of cathepsin D gene expression by 17beta-estradiol: mechanism of aryl hydrocarbon receptor-mediated inhibition.* Mol Cell Endocrinol, 2001. **172**(1-2): p. 91-103.
107. Ohtake, F., et al., *Modulation of oestrogen receptor signalling by association with the activated dioxin receptor.* Nature, 2003. **423**(6939): p. 545-50.
108. Grosskopf, H., et al., *Non-Genomic AhR-Signaling Modulates the Immune Response in Endotoxin-Activated Macrophages After Activation by the Environmental Stressor BaP.* Front Immunol, 2021. **12**: p. 620270.
109. Mejia-Garcia, A., et al., *Activation of AHR mediates the ubiquitination and proteasome degradation of c-Fos through the induction of Ubcm4 gene expression.* Toxicology, 2015. **337**: p. 47-57.
110. Holme, J.A., et al., *Combustion Particle-Induced Changes in Calcium Homeostasis: A Contributing Factor to Vascular Disease?* Cardiovasc Toxicol, 2019. **19**(3): p. 198-209.

111. Ohtake, F., et al., *Dioxin receptor is a ligand-dependent E3 ubiquitin ligase.* Nature, 2007. **446**(7135): p. 562-6.
112. El Hokayem, J., et al., *Ubiquitination of nuclear receptors.* Clin Sci (Lond), 2017. **131**(10): p. 917-934.
113. Nandi, D., et al., *The ubiquitin-proteasome system.* J Biosci, 2006. **31**(1): p. 137-55.
114. Higa, L.A., et al., *CUL4-DDB1 ubiquitin ligase interacts with multiple WD40-repeat proteins and regulates histone methylation.* Nat Cell Biol, 2006. **8**(11): p. 1277-83.
115. Angers, S., et al., *Molecular architecture and assembly of the DDB1-CUL4A ubiquitin ligase machinery.* Nature, 2006. **443**(7111): p. 590-3.
116. Luecke-Johansson, S., et al., *A Molecular Mechanism To Switch the Aryl Hydrocarbon Receptor from a Transcription Factor to an E3 Ubiquitin Ligase.* Mol Cell Biol, 2017. **37**(13).
117. Sondermann, N.C., et al., *Functions of the aryl hydrocarbon receptor (AHR) beyond the canonical AHR/ARNT signaling pathway.* Biochem Pharmacol, 2023. **208**: p. 115371.
118. Dou, H., et al., *Aryl hydrocarbon receptor (AhR) regulates adipocyte differentiation by assembling CRL4B ubiquitin ligase to target PPARgamma for proteasomal degradation.* J Biol Chem, 2019. **294**(48): p. 18504-18515.
119. Ghotbaddini, M. and J.B. Powell, *The AhR Ligand, TCDD, Regulates Androgen Receptor Activity Differently in Androgen-Sensitive versus Castration-Resistant Human Prostate Cancer Cells.* Int J Environ Res Public Health, 2015. **12**(7): p. 7506-18.
120. Xie, G., Z. Peng, and J.P. Raufman, *Src-mediated aryl hydrocarbon and epidermal growth factor receptor cross talk stimulates colon cancer cell proliferation.* Am J Physiol Gastrointest Liver Physiol, 2012. **302**(9): p. G1006-15.
121. Vazquez-Gomez, G., et al., *Benzo[a]pyrene activates an AhR/Src/ERK axis that contributes to CYP1A1 induction and stable DNA adducts formation in lung cells.* Toxicol Lett, 2018. **289**: p. 54-62.
122. Dong, B., et al., *FRET analysis of protein tyrosine kinase c-Src activation mediated via aryl hydrocarbon receptor.* Biochim Biophys Acta, 2011. **1810**(4): p. 427-31.
123. Baba, T., et al., *Structure and expression of the Ah receptor repressor gene.* J Biol Chem, 2001. **276**(35): p. 33101-10.
124. Evans, B.R., et al., *Repression of aryl hydrocarbon receptor (AHR) signaling by AHR repressor: role of DNA binding and competition for AHR nuclear translocator.* Mol Pharmacol, 2008. **73**(2): p. 387-98.
125. Vogel, C.F.A. and T. Haarmann-Stemmann, *The aryl hydrocarbon receptor repressor - More than a simple feedback inhibitor of AhR signaling: Clues for its role in inflammation and cancer.* Curr Opin Toxicol, 2017. **2**: p. 109-119.
126. Haarmann-Stemmann, T., et al., *Analysis of the transcriptional regulation and molecular function of the aryl hydrocarbon receptor repressor in human cell lines.* Drug Metab Dispos, 2007. **35**(12): p. 2262-9.
127. Cauchi, S., et al., *Structure and polymorphisms of human aryl hydrocarbon receptor repressor (AhRR) gene in a French population: relationship with CYP1A1 inducibility and lung cancer.* Pharmacogenetics, 2003. **13**(6): p. 339-47.

128. Yamamoto, J., et al., *Characteristic expression of aryl hydrocarbon receptor repressor gene in human tissues: organ-specific distribution and variable induction patterns in mononuclear cells.* Life Sci, 2004. **74**(8): p. 1039-49.
129. Bindesboll, C., et al., *TCDD-inducible poly-ADP-ribose polymerase (TIPARP/PARP7) mono-ADP-ribosylates and co-activates liver X receptors.* Biochem J, 2016. **473**(7): p. 899-910.
130. Katoh, M. and M. Katoh, *Identification and characterization of human TIPARP gene within the CCNL amplicon at human chromosome 3q25.31.* Int J Oncol, 2003. **23**(2): p. 541-7.
131. Vyas, S., et al., *Family-wide analysis of poly(ADP-ribose) polymerase activity.* Nat Commun, 2014. **5**: p. 4426.
132. Rijo, M.P., et al., *Roles of the ubiquitin ligase CUL4B and ADP-ribosyltransferase TiPARP in TCDD-induced nuclear export and proteasomal degradation of the transcription factor AHR.* J Biol Chem, 2021. **297**(2): p. 100886.
133. MacPherson, L., et al., *Aryl hydrocarbon receptor repressor and TiPARP (ARTD14) use similar, but also distinct mechanisms to repress aryl hydrocarbon receptor signaling.* Int J Mol Sci, 2014. **15**(5): p. 7939-57.
134. MacPherson, L., et al., *2,3,7,8-Tetrachlorodibenzo-p-dioxin poly(ADP-ribose) polymerase (TiPARP, ARTD14) is a mono-ADP-ribosyltransferase and repressor of aryl hydrocarbon receptor transactivation.* Nucleic Acids Res, 2013. **41**(3): p. 1604-21.
135. Lin, L., Y. Dai, and Y. Xia, *An overview of aryl hydrocarbon receptor ligands in the Last two decades (2002-2022): A medicinal chemistry perspective.* Eur J Med Chem, 2022. **244**: p. 114845.
136. Henry, E.C., S.L. Welle, and T.A. Gasiewicz, *TCDD and a putative endogenous AhR ligand, ITE, elicit the same immediate changes in gene expression in mouse lung fibroblasts.* Toxicol Sci, 2010. **114**(1): p. 90-100.
137. Soshilov, A.A. and M.S. Denison, *Ligand promiscuity of aryl hydrocarbon receptor agonists and antagonists revealed by site-directed mutagenesis.* Mol Cell Biol, 2014. **34**(9): p. 1707-19.
138. Sladekova, L., S. Mani, and Z. Dvorak, *Ligands and agonists of the aryl hydrocarbon receptor AhR: Facts and myths.* Biochem Pharmacol, 2023. **213**: p. 115626.
139. Minkina, T., et al., *Accumulation and transformation of benzo[a]pyrene in Haplic Chernozem under artificial contamination.* Environ Geochem Health, 2020. **42**(8): p. 2485-2494.
140. Dasari, S., et al., *Role of glutathione S-transferases in detoxification of a polycyclic aromatic hydrocarbon, methylcholanthrene.* Chem Biol Interact, 2018. **294**: p. 81-90.
141. Travis, C.C. and H.A. Hattemer-Frey, *Human exposure to dioxin.* Sci Total Environ, 1991. **104**(1-2): p. 97-127.
142. Li, S., et al., *Comparison of the contributions of polychlorinated dibenzo-p-dioxins and dibenzofurans and other unintentionally produced persistent organic pollutants to the total toxic equivalents in air of steel plant areas.* Chemosphere, 2015. **126**: p. 73-7.
143. Takeuchi, S., et al., *In vitro screening for aryl hydrocarbon receptor agonistic activity in 200 pesticides using a highly sensitive reporter cell line, DR-EcoScreen cells, and in vivo mouse liver cytochrome P450-1A induction by propanil, diuron and linuron.* Chemosphere, 2008. **74**(1): p. 155-65.

144. Smith, S.H., et al., *Tapinarof Is a Natural AhR Agonist that Resolves Skin Inflammation in Mice and Humans.* J Invest Dermatol, 2017. **137**(10): p. 2110-2119.
145. Keam, S.J., *Tapinarof Cream 1%: First Approval.* Drugs, 2022. **82**(11): p. 1221-1228.
146. Jin, U.H., et al., *The aryl hydrocarbon receptor ligand omeprazole inhibits breast cancer cell invasion and metastasis.* BMC Cancer, 2014. **14**: p. 498.
147. Daujat, M., et al., *Omeprazole, an inducer of human CYP1A1 and 1A2, is not a ligand for the Ah receptor.* Biochem Biophys Res Commun, 1992. **188**(2): p. 820-5.
148. Vyhlidalova, B., et al., *Antimigraine Drug Avitriptan Is a Ligand and Agonist of Human Aryl Hydrocarbon Receptor That Induces CYP1A1 in Hepatic and Intestinal Cells.* Int J Mol Sci, 2020. **21**(8).
149. Ogura, J., et al., *Carbidopa is an activator of aryl hydrocarbon receptor with potential for cancer therapy.* Biochem J, 2017. **474**(20): p. 3391-3402.
150. Korashy, H.M., et al., *Induction of cytochrome P450 1A1 by ketoconazole and itraconazole but not fluconazole in murine and human hepatoma cell lines.* Toxicol Sci, 2007. **97**(1): p. 32-43.
151. Tsuji, G., et al., *Identification of ketoconazole as an AhR-Nrf2 activator in cultured human keratinocytes: the basis of its anti-inflammatory effect.* J Invest Dermatol, 2012. **132**(1): p. 59-68.
152. Grycova, A., A. Doricakova, and Z. Dvorak, *Impurities contained in antifungal drug ketoconazole are potent activators of human aryl hydrocarbon receptor.* Toxicol Lett, 2015. **239**(2): p. 67-72.
153. Stejskalova, L., Z. Dvorak, and P. Pavek, *Endogenous and exogenous ligands of aryl hydrocarbon receptor: current state of art.* Curr Drug Metab, 2011. **12**(2): p. 198-212.
154. Gradelet, S., et al., *Ah receptor-dependent CYP1A induction by two carotenoids, canthaxanthin and beta-apo-8'-carotenal, with no affinity for the TCDD binding site.* Biochem Pharmacol, 1997. **54**(2): p. 307-15.
155. Ashida, H., et al., *Flavones and flavonols at dietary levels inhibit a transformation of aryl hydrocarbon receptor induced by dioxin.* FEBS Lett, 2000. **476**(3): p. 213-7.
156. Vrzal, R., et al., *Activation of the aryl hydrocarbon receptor by berberine in HepG2 and H4IIE cells: Biphasic effect on CYP1A1.* Biochem Pharmacol, 2005. **70**(6): p. 925-36.
157. Naderi-Kalali, B., et al., *Suppressive effects of caraway (Carum carvi) extracts on 2, 3, 7, 8-tetrachloro-dibenzo-p-dioxin-dependent gene expression of cytochrome P450 1A1 in the rat H4IIE cells.* Toxicol In Vitro, 2005. **19**(3): p. 373-7.
158. Bartonkova, I. and Z. Dvorak, *Essential oils of culinary herbs and spices display agonist and antagonist activities at human aryl hydrocarbon receptor AhR.* Food Chem Toxicol, 2018. **111**: p. 374-384.
159. Kalmes, M. and B. Blomeke, *Impact of eugenol and isoeugenol on AhR translocation, target gene expression, and proliferation in human HaCaT keratinocytes.* J Toxicol Environ Health A, 2012. **75**(8-10): p. 478-91.
160. Kalmes, M., et al., *Impact of the arylhydrocarbon receptor on eugenol- and isoeugenol-induced cell cycle arrest in human immortalized keratinocytes (HaCaT).* Biol Chem, 2006. **387**(9): p. 1201-7.

161. Bjeldanes, L.F., et al., *Aromatic hydrocarbon responsiveness-receptor agonists generated from indole-3-carbinol in vitro and in vivo: comparisons with 2,3,7,8-tetrachlorodibenzo-p-dioxin.* Proc Natl Acad Sci U S A, 1991. **88**(21): p. 9543-7.
162. Wei, Y.D., et al., *Rapid and transient induction of CYP1A1 gene expression in human cells by the tryptophan photoproduct 6-formylindolo[3,2-b]carbazole.* Chem Biol Interact, 1998. **110**(1-2): p. 39-55.
163. Hubbard, T.D., I.A. Murray, and G.H. Perdew, *Indole and Tryptophan Metabolism: Endogenous and Dietary Routes to Ah Receptor Activation.* Drug Metab Dispos, 2015. **43**(10): p. 1522-35.
164. Gao, J., et al., *Impact of the Gut Microbiota on Intestinal Immunity Mediated by Tryptophan Metabolism.* Front Cell Infect Microbiol, 2018. **8**: p. 13.
165. Heath-Pagliuso, S., et al., *Activation of the Ah receptor by tryptophan and tryptophan metabolites.* Biochemistry, 1998. **37**(33): p. 11508-15.
166. Jin, U.H., et al., *Microbiome-derived tryptophan metabolites and their aryl hydrocarbon receptor-dependent agonist and antagonist activities.* Mol Pharmacol, 2014. **85**(5): p. 777-88.
167. Rasmussen, M.K., et al., *Skatole (3-Methylindole) Is a Partial Aryl Hydrocarbon Receptor Agonist and Induces CYP1A1/2 and CYP1B1 Expression in Primary Human Hepatocytes.* PLoS One, 2016. **11**(5): p. e0154629.
168. Kurata, K., et al., *Skatole regulates intestinal epithelial cellular functions through activating aryl hydrocarbon receptors and p38.* Biochem Biophys Res Commun, 2019. **510**(4): p. 649-655.
169. Weems, J.M. and G.S. Yost, *3-Methylindole metabolites induce lung CYP1A1 and CYP2F1 enzymes by AhR and non-AhR mechanisms, respectively.* Chem Res Toxicol, 2010. **23**(3): p. 696-704.
170. Stepankova, M., et al., *Methylindoles and Methoxyindoles are Agonists and Antagonists of Human Aryl Hydrocarbon Receptor.* Mol Pharmacol, 2018. **93**(6): p. 631-644.
171. Mezrich, J.D., et al., *An interaction between kynurenine and the aryl hydrocarbon receptor can generate regulatory T cells.* J Immunol, 2010. **185**(6): p. 3190-8.
172. Opitz, C.A., et al., *An endogenous tumour-promoting ligand of the human aryl hydrocarbon receptor.* Nature, 2011. **478**(7368): p. 197-203.
173. Kaiser, H., E. Parker, and M.W. Hamrick, *Kynurenine signaling through the aryl hydrocarbon receptor: Implications for aging and healthspan.* Exp Gerontol, 2020. **130**: p. 110797.
174. Marinelli, L., et al., *Identification of the novel role of butyrate as AhR ligand in human intestinal epithelial cells.* Sci Rep, 2019. **9**(1): p. 643.
175. Modoux, M., et al., *Butyrate acts through HDAC inhibition to enhance aryl hydrocarbon receptor activation by gut microbiota-derived ligands.* Gut Microbes, 2022. **14**(1): p. 2105637.
176. Merchant, M., et al., *Mechanism of action of aryl hydrocarbon receptor antagonists: inhibition of 2,3,7,8-tetrachlorodibenzo-p-dioxin-induced CYP1A1 gene expression.* Arch Biochem Biophys, 1992. **298**(2): p. 389-94.
177. Merchant, M., V. Krishnan, and S. Safe, *Mechanism of action of alpha-naphthoflavone as an Ah receptor antagonist in MCF-7 human breast cancer cells.* Toxicol Appl Pharmacol, 1993. **120**(2): p. 179-85.
178. Hao, J., et al., *Resveratrol supports and alpha-naphthoflavone disrupts growth of human ovarian follicles in an in vitro tissue culture model.* Toxicol Appl Pharmacol, 2018. **338**: p. 73-82.

179. Xia, H., et al., *Alpha-naphthoflavone attenuates non-alcoholic fatty liver disease in oleic acid-treated HepG2 hepatocytes and in high fat diet-fed mice.* Biomed Pharmacother, 2019. **118**: p. 109287.
180. Andersson, S., R.W. Bishop, and D.W. Russell, *Expression cloning and regulation of steroid 5 alpha-reductase, an enzyme essential for male sexual differentiation.* J Biol Chem, 1989. **264**(27): p. 16249-55.
181. Zhao, B., et al., *CH223191 is a ligand-selective antagonist of the Ah (Dioxin) receptor.* Toxicol Sci, 2010. **117**(2): p. 393-403.
182. Choi, E.Y., et al., *Development of novel CH223191-based antagonists of the aryl hydrocarbon receptor.* Mol Pharmacol, 2012. **81**(1): p. 3-11.
183. Smith, K.J., et al., *Identification of a high-affinity ligand that exhibits complete aryl hydrocarbon receptor antagonism.* J Pharmacol Exp Ther, 2011. **338**(1): p. 318-27.
184. Ondrova, K., et al., *Monoterpenoid aryl hydrocarbon receptor allosteric antagonists protect against ultraviolet skin damage in female mice.* Nat Commun, 2023. **14**(1): p. 2728.
185. Zhou, X., et al., *beta-Naphthoflavone Activation of the Ah Receptor Alleviates Irradiation-Induced Intestinal Injury in Mice.* Antioxidants (Basel), 2020. **9**(12).
186. El-Dairi, R., et al., *Aryl hydrocarbon receptor (AhR) agonist beta-naphthoflavone regulated gene networks in human primary trophoblasts.* Reprod Toxicol, 2020. **96**: p. 370-379.
187. Seidel, S.D., et al., *Activation of the Ah receptor signaling pathway by prostaglandins.* J Biochem Mol Toxicol, 2001. **15**(4): p. 187-96.
188. Adachi, J., et al., *Indirubin and indigo are potent aryl hydrocarbon receptor ligands present in human urine.* J Biol Chem, 2001. **276**(34): p. 31475-8.
189. Rannug, A. and U. Rannug, *The tryptophan derivative 6-formylindolo[3,2-b]carbazole, FICZ, a dynamic mediator of endogenous aryl hydrocarbon receptor signaling, balances cell growth and differentiation.* Crit Rev Toxicol, 2018. **48**(7): p. 555-574.
190. Song, J., et al., *A ligand for the aryl hydrocarbon receptor isolated from lung.* Proc Natl Acad Sci U S A, 2002. **99**(23): p. 14694-9.
191. Jansen, R., et al., *Indothiazinone, an indolyl thiazolyl ketone from a novel myxobacterium belonging to the Sorangiineae.* J Nat Prod, 2014. **77**(4): p. 1054-60.
192. Park, J.S., et al., *New 2-(1'H-indole-3'-carbonyl)-thiazoles derived from the thermophilic bacterium Thermosporothrix hazakensis SK20-1(T).* J Antibiot (Tokyo), 2015. **68**(1): p. 60-2.
193. Grycova, A., et al., *Targeting the Aryl Hydrocarbon Receptor with Microbial Metabolite Mimics Alleviates Experimental Colitis in Mice.* J Med Chem, 2022. **65**(9): p. 6859-6868.
194. Kawajiri, K. and Y. Fujii-Kuriyama, *The aryl hydrocarbon receptor: a multifunctional chemical sensor for host defense and homeostatic maintenance.* Exp Anim, 2017. **66**(2): p. 75-89.
195. Ichihara, S., et al., *A role for the aryl hydrocarbon receptor in regulation of ischemia-induced angiogenesis.* Arterioscler Thromb Vasc Biol, 2007. **27**(6): p. 1297-304.
196. Wang, X., B.T. Hawkins, and D.S. Miller, *Aryl hydrocarbon receptor-mediated up-regulation of ATP-driven xenobiotic efflux transporters at the blood-brain barrier.* FASEB J, 2011. **25**(2): p. 644-52.

197. Kou, Z. and W. Dai, *Aryl hydrocarbon receptor: Its roles in physiology.* Biochem Pharmacol, 2021. **185**: p. 114428.
198. Carreira, V.S., et al., *Ah Receptor Signaling Controls the Expression of Cardiac Development and Homeostasis Genes.* Toxicol Sci, 2015. **147**(2): p. 425-35.
199. Postal, B.G., et al., *AhR activation defends gut barrier integrity against damage occurring in obesity.* Mol Metab, 2020. **39**: p. 101007.
200. Ma, Y., et al., *6-Formylindolo(3,2-b)carbazole induced aryl hydrocarbon receptor activation prevents intestinal barrier dysfunction through regulation of claudin-2 expression.* Chem Biol Interact, 2018. **288**: p. 83-90.
201. Han, B., et al., *Aryl Hydrocarbon Receptor Activation in Intestinal Obstruction Ameliorates Intestinal Barrier Dysfunction Via Suppression of MLCK-MLC Phosphorylation Pathway.* Shock, 2016. **46**(3): p. 319-28.
202. Yin, J., et al., *Aryl hydrocarbon receptor activation alleviates dextran sodium sulfate-induced colitis through enhancing the differentiation of goblet cells.* Biochem Biophys Res Commun, 2019. **514**(1): p. 180-186.
203. Fernandez-Gallego, N., F. Sanchez-Madrid, and D. Cibrian, *Role of AHR Ligands in Skin Homeostasis and Cutaneous Inflammation.* Cells, 2021. **10**(11).
204. Stein Gold, L., et al., *A phase 2b, randomized clinical trial of tapinarof cream for the treatment of plaque psoriasis: Secondary efficacy and patient-reported outcomes.* J Am Acad Dermatol, 2021. **84**(3): p. 624-631.
205. Paller, A.S., et al., *Efficacy and patient-reported outcomes from a phase 2b, randomized clinical trial of tapinarof cream for the treatment of adolescents and adults with atopic dermatitis.* J Am Acad Dermatol, 2021. **84**(3): p. 632-638.
206. Safe, S., Y. Cheng, and U.H. Jin, *The Aryl Hydrocarbon Receptor (AhR) as a Drug Target for Cancer Chemotherapy.* Curr Opin Toxicol, 2017. **2**: p. 24-29.
207. Rojas, I.Y., et al., *Kynurenine-Induced Aryl Hydrocarbon Receptor Signaling in Mice Causes Body Mass Gain, Liver Steatosis, and Hyperglycemia.* Obesity (Silver Spring), 2021. **29**(2): p. 337-349.
208. Bock, K.W., *Modulation of aryl hydrocarbon receptor (AHR) and the NAD(+)-consuming enzyme CD38: Searches of therapeutic options for nonalcoholic fatty liver disease (NAFLD).* Biochem Pharmacol, 2020. **175**: p. 113905.
209. Amamou, A., et al., *Dietary AhR Ligands Have No Anti-Fibrotic Properties in TGF-beta1-Stimulated Human Colonic Fibroblasts.* Nutrients, 2022. **14**(16).
210. Pariano, M., et al., *Aryl Hydrocarbon Receptor Agonism Antagonizes the Hypoxia-driven Inflammation in Cystic Fibrosis.* Am J Respir Cell Mol Biol, 2023. **68**(3): p. 288-301.
211. Poulain-Godefroy, O., et al., *The Aryl Hydrocarbon Receptor in Asthma: Friend or Foe?* Int J Mol Sci, 2020. **21**(22).
212. Neavin, D.R., et al., *The Role of the Aryl Hydrocarbon Receptor (AHR) in Immune and Inflammatory Diseases.* Int J Mol Sci, 2018. **19**(12).
213. Liu, D., et al., *Beta-defensin 1, aryl hydrocarbon receptor and plasma kynurenine in major depressive disorder: metabolomics-informed genomics.* Transl Psychiatry, 2018. **8**(1): p. 10.
214. Wei, Z.F., et al., *Norisoboldine, an Anti-Arthritis Alkaloid Isolated from Radix Linderae, Attenuates Osteoclast Differentiation and Inflammatory Bone Erosion in an Aryl Hydrocarbon Receptor-Dependent Manner.* Int J Biol Sci, 2015. **11**(9): p. 1113-26.
215. Giovannoni, F., et al., *AHR is a Zika virus host factor and a candidate target for antiviral therapy.* Nat Neurosci, 2020. **23**(8): p. 939-951.

216. Giovannoni, F., et al., *AHR signaling is induced by infection with coronaviruses.* Nat Commun, 2021. **12**(1): p. 5148.
217. Sheridan, P.J., *Androgen receptors in the brain: what are we measuring?* Endocr Rev, 1983. **4**(2): p. 171-8.
218. Ruizeveld de Winter, J.A., et al., *Androgen receptor expression in human tissues: an immunohistochemical study.* J Histochem Cytochem, 1991. **39**(7): p. 927-36.
219. Lubahn, D.B., et al., *Cloning of human androgen receptor complementary DNA and localization to the X chromosome.* Science, 1988. **240**(4850): p. 327-30.
220. Gelmann, E.P., *Molecular biology of the androgen receptor.* J Clin Oncol, 2002. **20**(13): p. 3001-15.
221. Kenji, A. and a.t.o. authors, *Androgens and androgen receptor: Mechanisms, functions and clinical applications*. 1st ed. 2002: Springer, Boston, MA.
222. Hu, R., et al., *Ligand-independent androgen receptor variants derived from splicing of cryptic exons signify hormone-refractory prostate cancer.* Cancer Res, 2009. **69**(1): p. 16-22.
223. Baca, S.C., et al., *Punctuated evolution of prostate cancer genomes.* Cell, 2013. **153**(3): p. 666-77.
224. Lu, N.Z., et al., *International Union of Pharmacology. LXV. The pharmacology and classification of the nuclear receptor superfamily: glucocorticoid, mineralocorticoid, progesterone, and androgen receptors.* Pharmacol Rev, 2006. **58**(4): p. 782-97.
225. Sasaki, M., et al., *The polyglycine and polyglutamine repeats in the androgen receptor gene in Japanese and Caucasian populations.* Biochem Biophys Res Commun, 2003. **312**(4): p. 1244-7.
226. Chang, C.S., J. Kokontis, and S.T. Liao, *Structural analysis of complementary DNA and amino acid sequences of human and rat androgen receptors.* Proc Natl Acad Sci U S A, 1988. **85**(19): p. 7211-5.
227. Fujita, K. and N. Nonomura, *Role of Androgen Receptor in Prostate Cancer: A Review.* World J Mens Health, 2019. **37**(3): p. 288-295.
228. Beilin, J., et al., *Effect of the androgen receptor CAG repeat polymorphism on transcriptional activity: specificity in prostate and non-prostate cell lines.* J Mol Endocrinol, 2000. **25**(1): p. 85-96.
229. Yoo, S., et al., *Androgen receptor CAG repeat polymorphism and risk of TMPRSS2:ERG-positive prostate cancer.* Cancer Epidemiol Biomarkers Prev, 2014. **23**(10): p. 2027-31.
230. Finsterer, J., *Bulbar and spinal muscular atrophy (Kennedy's disease): a review.* Eur J Neurol, 2009. **16**(5): p. 556-61.
231. Callewaert, L., et al., *Implications of a polyglutamine tract in the function of the human androgen receptor.* Biochem Biophys Res Commun, 2003. **306**(1): p. 46-52.
232. McEwan, I.J., *Molecular mechanisms of androgen receptor-mediated gene regulation: structure-function analysis of the AF-1 domain.* Endocr Relat Cancer, 2004. **11**(2): p. 281-93.
233. Simental, J.A., et al., *Transcriptional activation and nuclear targeting signals of the human androgen receptor.* J Biol Chem, 1991. **266**(1): p. 510-8.
234. Callewaert, L., N. Van Tilborgh, and F. Claessens, *Interplay between two hormone-independent activation domains in the androgen receptor.* Cancer Res, 2006. **66**(1): p. 543-53.

235. Schaufele, F., et al., *The structural basis of androgen receptor activation: intramolecular and intermolecular amino-carboxy interactions.* Proc Natl Acad Sci U S A, 2005. **102**(28): p. 9802-7.
236. Doesburg, P., et al., *Functional in vivo interaction between the amino-terminal, transactivation domain and the ligand binding domain of the androgen receptor.* Biochemistry, 1997. **36**(5): p. 1052-64.
237. Langley, E., J.A. Kemppainen, and E.M. Wilson, *Intermolecular NH2-/carboxyl-terminal interactions in androgen receptor dimerization revealed by mutations that cause androgen insensitivity.* J Biol Chem, 1998. **273**(1): p. 92-101.
238. Wilson, E.M., *Analysis of interdomain interactions of the androgen receptor.* Methods Mol Biol, 2011. **776**: p. 113-29.
239. Shaffer, P.L., et al., *Structural basis of androgen receptor binding to selective androgen response elements.* Proc Natl Acad Sci U S A, 2004. **101**(14): p. 4758-63.
240. Jenster, G., J. Trapman, and A.O. Brinkmann, *Nuclear import of the human androgen receptor.* Biochem J, 1993. **293 (Pt 3)**(Pt 3): p. 761-8.
241. Clinckemalie, L., et al., *The hinge region in androgen receptor control.* Mol Cell Endocrinol, 2012. **358**(1): p. 1-8.
242. Matias, P.M., et al., *Structural evidence for ligand specificity in the binding domain of the human androgen receptor. Implications for pathogenic gene mutations.* J Biol Chem, 2000. **275**(34): p. 26164-71.
243. Nadal, M., et al., *Structure of the homodimeric androgen receptor ligand-binding domain.* Nat Commun, 2017. **8**: p. 14388.
244. Elhaji, Y.A., et al., *Impaired helix 12 dynamics due to proline 892 substitutions in the androgen receptor are associated with complete androgen insensitivity.* Hum Mol Genet, 2006. **15**(6): p. 921-31.
245. Sack, J.S., et al., *Crystallographic structures of the ligand-binding domains of the androgen receptor and its T877A mutant complexed with the natural agonist dihydrotestosterone.* Proc Natl Acad Sci U S A, 2001. **98**(9): p. 4904-9.
246. He, B., et al., *Activation function 2 in the human androgen receptor ligand binding domain mediates interdomain communication with the NH(2)-terminal domain.* J Biol Chem, 1999. **274**(52): p. 37219-25.
247. Chai, X., et al., *Discovery of N-(4-(Benzyloxy)-phenyl)-sulfonamide Derivatives as Novel Antagonists of the Human Androgen Receptor Targeting the Activation Function 2.* J Med Chem, 2022. **65**(3): p. 2507-2521.
248. Thompson, J., et al., *Disrupted amino- and carboxyl-terminal interactions of the androgen receptor are linked to androgen insensitivity.* Mol Endocrinol, 2001. **15**(6): p. 923-35.
249. Heinlein, C.A. and C. Chang, *Androgen receptor (AR) coregulators: an overview.* Endocr Rev, 2002. **23**(2): p. 175-200.
250. Veldscholte, J., et al., *Hormone-induced dissociation of the androgen receptor-heat-shock protein complex: use of a new monoclonal antibody to distinguish transformed from nontransformed receptors.* Biochemistry, 1992. **31**(32): p. 7422-30.
251. Loy, C.J., K.S. Sim, and E.L. Yong, *Filamin-A fragment localizes to the nucleus to regulate androgen receptor and coactivator functions.* Proc Natl Acad Sci U S A, 2003. **100**(8): p. 4562-7.
252. Bennett, N.C., et al., *Molecular cell biology of androgen receptor signalling.* Int J Biochem Cell Biol, 2010. **42**(6): p. 813-27.

253. Cutress, M.L., et al., *Structural basis for the nuclear import of the human androgen receptor.* J Cell Sci, 2008. **121**(Pt 7): p. 957-68.
254. Zoubeidi, A., et al., *Cooperative interactions between androgen receptor (AR) and heat-shock protein 27 facilitate AR transcriptional activity.* Cancer Res, 2007. **67**(21): p. 10455-65.
255. Lee, Y.F., et al., *Convergence of two repressors through heterodimer formation of androgen receptor and testicular orphan receptor-4: a unique signaling pathway in the steroid receptor superfamily.* Proc Natl Acad Sci U S A, 1999. **96**(26): p. 14724-9.
256. Powell, S.M., et al., *Mechanisms of androgen receptor signalling via steroid receptor coactivator-1 in prostate.* Endocr Relat Cancer, 2004. **11**(1): p. 117-30.
257. Penney, K.L., et al., *Association of KLK3 (PSA) genetic variants with prostate cancer risk and PSA levels.* Carcinogenesis, 2011. **32**(6): p. 853-9.
258. Davies, T.H., Y.M. Ning, and E.R. Sanchez, *A new first step in activation of steroid receptors: hormone-induced switching of FKBP51 and FKBP52 immunophilins.* J Biol Chem, 2002. **277**(7): p. 4597-600.
259. He, B., et al., *Dependence of selective gene activation on the androgen receptor NH2- and COOH-terminal interaction.* J Biol Chem, 2002. **277**(28): p. 25631-9.
260. Gaughan, L., et al., *Regulation of androgen receptor and histone deacetylase 1 by Mdm2-mediated ubiquitylation.* Nucleic Acids Res, 2005. **33**(1): p. 13-26.
261. Lee, D.K. and C. Chang, *Endocrine mechanisms of disease: Expression and degradation of androgen receptor: mechanism and clinical implication.* J Clin Endocrinol Metab, 2003. **88**(9): p. 4043-54.
262. Chymkowitch, P., et al., *The phosphorylation of the androgen receptor by TFIIH directs the ubiquitin/proteasome process.* EMBO J, 2011. **30**(3): p. 468-79.
263. Lin, H.K., et al., *Phosphorylation-dependent ubiquitylation and degradation of androgen receptor by Akt require Mdm2 E3 ligase.* EMBO J, 2002. **21**(15): p. 4037-48.
264. Astapova, O., C. Seger, and S.R. Hammes, *Ligand Binding Prolongs Androgen Receptor Protein Half-Life by Reducing its Degradation.* J Endocr Soc, 2021. **5**(5): p. bvab035.
265. Chen, S., et al., *Androgen receptor phosphorylation and stabilization in prostate cancer by cyclin-dependent kinase 1.* Proc Natl Acad Sci U S A, 2006. **103**(43): p. 15969-74.
266. Baron, S., et al., *Androgen receptor mediates non-genomic activation of phosphatidylinositol 3-OH kinase in androgen-sensitive epithelial cells.* J Biol Chem, 2004. **279**(15): p. 14579-86.
267. Foradori, C.D., M.J. Weiser, and R.J. Handa, *Non-genomic actions of androgens.* Front Neuroendocrinol, 2008. **29**(2): p. 169-81.
268. Gao, L., B. Han, and X. Dong, *The Androgen Receptor and Its Crosstalk With the Src Kinase During Castrate-Resistant Prostate Cancer Progression.* Front Oncol, 2022. **12**: p. 905398.
269. Cai, H., et al., *Invasive prostate carcinoma driven by c-Src and androgen receptor synergy.* Cancer Res, 2011. **71**(3): p. 862-72.
270. Lee, L.F., et al., *Interleukin-8 confers androgen-independent growth and migration of LNCaP: differential effects of tyrosine kinases Src and FAK.* Oncogene, 2004. **23**(12): p. 2197-205.
271. Migliaccio, A., et al., *Steroid receptor regulation of epidermal growth factor signaling through Src in breast and prostate cancer cells: steroid antagonist action.* Cancer Res, 2005. **65**(22): p. 10585-93.

272. Irwin, M.E., N. Bohin, and J.L. Boerner, *Src family kinases mediate epidermal growth factor receptor signaling from lipid rafts in breast cancer cells.* Cancer Biol Ther, 2011. **12**(8): p. 718-26.
273. Asim, M., et al., *Src kinase potentiates androgen receptor transactivation function and invasion of androgen-independent prostate cancer C4-2 cells.* Oncogene, 2008. **27**(25): p. 3596-604.
274. Guo, Z., et al., *Regulation of androgen receptor activity by tyrosine phosphorylation.* Cancer Cell, 2006. **10**(4): p. 309-19.
275. Kraus, S., et al., *Receptor for activated C kinase 1 (RACK1) and Src regulate the tyrosine phosphorylation and function of the androgen receptor.* Cancer Res, 2006. **66**(22): p. 11047-54.
276. Kaprara, A. and I.T. Huhtaniemi, *The hypothalamus-pituitary-gonad axis: Tales of mice and men.* Metabolism, 2018. **86**: p. 3-17.
277. Waterman, M.R. and D.S. Keeney, *Genes involved in androgen biosynthesis and the male phenotype.* Horm Res, 1992. **38**(5-6): p. 217-21.
278. Hou, J.W., D.C. Collins, and R.L. Schleicher, *Sources of cholesterol for testosterone biosynthesis in murine Leydig cells.* Endocrinology, 1990. **127**(5): p. 2047-55.
279. O'Shaughnessy, P.J. and L. Murphy, *Steroidogenic enzyme activity in the rat testis following Leydig cell destruction by ethylene-1,2-dimethanesulphonate and during subsequent Leydig cell regeneration.* J Endocrinol, 1991. **131**(3): p. 451-7.
280. Lambeth, J.D. and V.L. Stevens, *Cytochrome P-450scc: enzymology, and the regulation of intramitochondrial cholesterol delivery to the enzyme.* Endocr Res, 1984. **10**(3-4): p. 283-309.
281. Shi, L., et al., *Effects of phenolic compounds on 3beta-hydroxysteroid dehydrogenase activity in human and rat placenta: Screening, mode of action, and docking analysis.* J Steroid Biochem Mol Biol, 2023. **225**: p. 106202.
282. Miller, W.L., *Androgen biosynthesis from cholesterol to DHEA.* Mol Cell Endocrinol, 2002. **198**(1-2): p. 7-14.
283. Fluck, C.E., W.L. Miller, and R.J. Auchus, *The 17, 20-lyase activity of cytochrome p450c17 from human fetal testis favors the delta5 steroidogenic pathway.* J Clin Endocrinol Metab, 2003. **88**(8): p. 3762-6.
284. Lucas-Herald, A.K., et al., *Genomic and non-genomic effects of androgens in the cardiovascular system: clinical implications.* Clin Sci (Lond), 2017. **131**(13): p. 1405-1418.
285. Zhu, J.L., et al., *Sex hormone-binding globulin and polycystic ovary syndrome.* Clin Chim Acta, 2019. **499**: p. 142-148.
286. Czub, M.P., et al., *Testosterone meets albumin - the molecular mechanism of sex hormone transport by serum albumins.* Chem Sci, 2019. **10**(6): p. 1607-1618.
287. Li, H., et al., *Sex Hormone Binding Globulin Modifies Testosterone Action and Metabolism in Prostate Cancer Cells.* Int J Endocrinol, 2016. **2016**: p. 6437585.
288. ClevelandHeartLab. *Testosterone, Free and Total, Males (Adult), Immunoassay*. 2015 [cited 2024; Available from: https://www.clevelandheartlab.com/tests/testosterone-free-and-total-males-adult-immunoassay/.
289. Swerdloff, R.S., et al., *Dihydrotestosterone: Biochemistry, Physiology, and Clinical Implications of Elevated Blood Levels.* Endocr Rev, 2017. **38**(3): p. 220-254.

290. Wei, R., et al., *Steroid 5alpha-Reductase Type I Induces Cell Viability and Migration via Nuclear Factor-kappaB/Vascular Endothelial Growth Factor Signaling Pathway in Colorectal Cancer.* Front Oncol, 2020. **10**: p. 1501.
291. Azzouni, F., et al., *The 5 alpha-reductase isozyme family: a review of basic biology and their role in human diseases.* Adv Urol, 2012. **2012**: p. 530121.
292. Cantagrel, V., et al., *SRD5A3 is required for converting polyprenol to dolichol and is mutated in a congenital glycosylation disorder.* Cell, 2010. **142**(2): p. 203-17.
293. Bruchovsky, N. and J.D. Wilson, *The conversion of testosterone to 5-alpha-androstan-17-beta-ol-3-one by rat prostate in vivo and in vitro.* J Biol Chem, 1968. **243**(8): p. 2012-21.
294. Sharifi, N. and R.J. Auchus, *Steroid biosynthesis and prostate cancer.* Steroids, 2012. **77**(7): p. 719-26.
295. Ghotbaddini, M., V. Moultrie, and J.B. Powell, *Constitutive Aryl Hydrocarbon Receptor Signaling in Prostate Cancer Progression.* J Cancer Treatment Diagn, 2018. **2**(5): p. 11-16.
296. Ito, Y. and M.D. Sadar, *Enzalutamide and blocking androgen receptor in advanced prostate cancer: lessons learnt from the history of drug development of antiandrogens.* Res Rep Urol, 2018. **10**: p. 23-32.
297. Ziolkowska, E., et al., *The side effects of hormonal therapy at the patients with prostate cancer.* Contemp Oncol (Pozn), 2012. **16**(6): p. 491-7.
298. Sabbadin, C., et al., *Licorice: From Pseudohyperaldosteronism to Therapeutic Uses.* Front Endocrinol (Lausanne), 2019. **10**: p. 484.
299. Grant, P., *Spearmint herbal tea has significant anti-androgen effects in polycystic ovarian syndrome. A randomized controlled trial.* Phytother Res, 2010. **24**(2): p. 186-8.
300. Grant, P. and S. Ramasamy, *An update on plant derived anti-androgens.* Int J Endocrinol Metab, 2012. **10**(2): p. 497-502.
301. Skinner, M.K., *Encyclopedia of reproduction*. Second edition. ed. 2018, Amsterdam: Academic Press, an imprint of Elsevier.
302. Buchanan, G., et al., *Collocation of androgen receptor gene mutations in prostate cancer.* Clin Cancer Res, 2001. **7**(5): p. 1273-81.
303. Gottlieb, B., et al., *The androgen receptor gene mutations database: 2012 update.* Hum Mutat, 2012. **33**(5): p. 887-94.
304. Aurilio, G., et al., *Androgen Receptor Signaling Pathway in Prostate Cancer: From Genetics to Clinical Applications.* Cells, 2020. **9**(12).
305. Veldscholte, J., et al., *A mutation in the ligand binding domain of the androgen receptor of human LNCaP cells affects steroid binding characteristics and response to anti-androgens.* Biochem Biophys Res Commun, 1990. **173**(2): p. 534-40.
306. Wilding, G., M. Chen, and E.P. Gelmann, *Aberrant response in vitro of hormone-responsive prostate cancer cells to antiandrogens.* Prostate, 1989. **14**(2): p. 103-15.
307. Gregory, C.W., B. He, and E.M. Wilson, *The putative androgen receptor-A form results from in vitro proteolysis.* J Mol Endocrinol, 2001. **27**(3): p. 309-19.
308. Wadosky, K.M. and S. Koochekpour, *Androgen receptor splice variants and prostate cancer: From bench to bedside.* Oncotarget, 2017. **8**(11): p. 18550-18576.
309. Haile, S. and M.D. Sadar, *Androgen receptor and its splice variants in prostate cancer.* Cell Mol Life Sci, 2011. **68**(24): p. 3971-81.

310. Dehm, S.M., et al., *Splicing of a novel androgen receptor exon generates a constitutively active androgen receptor that mediates prostate cancer therapy resistance.* Cancer Res, 2008. **68**(13): p. 5469-77.
311. Chan, S.C., Y. Li, and S.M. Dehm, *Androgen receptor splice variants activate androgen receptor target genes and support aberrant prostate cancer cell growth independent of canonical androgen receptor nuclear localization signal.* J Biol Chem, 2012. **287**(23): p. 19736-49.
312. Cancer Genome Atlas Research, N., *The Molecular Taxonomy of Primary Prostate Cancer.* Cell, 2015. **163**(4): p. 1011-25.
313. Henzler, C., et al., *Truncation and constitutive activation of the androgen receptor by diverse genomic rearrangements in prostate cancer.* Nat Commun, 2016. **7**: p. 13668.
314. Kanayama, M., et al., *AR Splicing Variants and Resistance to AR Targeting Agents.* Cancers (Basel), 2021. **13**(11).
315. He, Y., et al., *Androgen receptor splice variants bind to constitutively open chromatin and promote abiraterone-resistant growth of prostate cancer.* Nucleic Acids Res, 2018. **46**(4): p. 1895-1911.
316. Khan, T., et al., *Choice of antibody is critical for specific and sensitive detection of androgen receptor splice variant-7 in circulating tumor cells.* Sci Rep, 2022. **12**(1): p. 16159.
317. Cao, S., Y. Zhan, and Y. Dong, *Emerging data on androgen receptor splice variants in prostate cancer.* Endocr Relat Cancer, 2016. **23**(12): p. T199-T210.
318. Chen, X., et al., *Overexpression of nuclear AR-V7 protein in primary prostate cancer is an independent negative prognostic marker in men with high-risk disease receiving adjuvant therapy.* Urol Oncol, 2018. **36**(4): p. 161 e19-161 e30.
319. Zhang, T., et al., *Androgen Receptor Splice Variant, AR-V7, as a Biomarker of Resistance to Androgen Axis-Targeted Therapies in Advanced Prostate Cancer.* Clin Genitourin Cancer, 2020. **18**(1): p. 1-10.
320. Wang, Z., et al., *The Prognostic Value of Androgen Receptor Splice Variant 7 in Castration-Resistant Prostate Cancer Treated With Novel Hormonal Therapy or Chemotherapy: A Systematic Review and Meta-analysis.* Front Oncol, 2020. **10**: p. 572590.
321. Sekhoacha, M., et al., *Prostate Cancer Review: Genetics, Diagnosis, Treatment Options, and Alternative Approaches.* Molecules, 2022. **27**(17).
322. Dunn, M.W. and M.W. Kazer, *Prostate cancer overview.* Semin Oncol Nurs, 2011. **27**(4): p. 241-50.
323. Taitt, H.E., *Global Trends and Prostate Cancer: A Review of Incidence, Detection, and Mortality as Influenced by Race, Ethnicity, and Geographic Location.* Am J Mens Health, 2018. **12**(6): p. 1807-1823.
324. Messina, C., et al., *BRCA Mutations in Prostate Cancer: Prognostic and Predictive Implications.* J Oncol, 2020. **2020**: p. 4986365.
325. Ewing, C.M., et al., *Germline mutations in HOXB13 and prostate-cancer risk.* N Engl J Med, 2012. **366**(2): p. 141-9.
326. Bluemn, E.G. and P.S. Nelson, *The androgen/androgen receptor axis in prostate cancer.* Curr Opin Oncol, 2012. **24**(3): p. 251-7.
327. Medicine, J.H. *Prostate Cancer: Age-Specific Screening Guidelines*. [cited 2024 11.1.]; Available from: https://www.hopkinsmedicine.org/health/conditions-and-diseases/prostate-cancer/prostate-cancer-age-specific-screening-guidelines.

328. Altwaijry, N., et al., *Regression of prostate tumors after intravenous administration of lactoferrin-bearing polypropylenimine dendriplexes encoding TNF-alpha, TRAIL, and interleukin-12.* Drug Deliv, 2018. **25**(1): p. 679-689.
329. David, M.K. and S.W. Leslie, *Prostate Specific Antigen,* in *StatPearls*. 2024: Treasure Island (FL).
330. Gurel, B., et al., *NKX3.1 as a marker of prostatic origin in metastatic tumors.* Am J Surg Pathol, 2010. **34**(8): p. 1097-105.
331. Wang, Z., et al., *Significance of the TMPRSS2:ERG gene fusion in prostate cancer.* Mol Med Rep, 2017. **16**(4): p. 5450-5458.
332. Meyer, A.R., et al., *Transperineal Prostate Biopsy Improves the Detection of Clinically Significant Prostate Cancer among Men on Active Surveillance.* J Urol, 2021. **205**(4): p. 1069-1074.
333. Chen, X., et al., *Non-invasive early detection of cancer four years before conventional diagnosis using a blood test.* Nat Commun, 2020. **11**(1): p. 3475.
334. Medicine, J.H. *Prostate Cancer Stages*. Health [cited 2024 3.2.]; Available from: https://www.hopkinsmedicine.org/health/conditions-and-diseases/prostate-cancer/prostate-cancer-stages.
335. Maatman, T.J., M.K. Gupta, and J.E. Montie, *Effectiveness of castration versus intravenous estrogen therapy in producing rapid endocrine control of metastatic cancer of the prostate.* J Urol, 1985. **133**(4): p. 620-1.
336. Lepor, H. and N.D. Shore, *LHRH Agonists for the Treatment of Prostate Cancer: 2012.* Rev Urol, 2012. **14**(1-2): p. 1-12.
337. Heidenreich, A., et al., *EAU guidelines on prostate cancer. Part II: Treatment of advanced, relapsing, and castration-resistant prostate cancer.* Eur Urol, 2014. **65**(2): p. 467-79.
338. Crawford, E.D. and A.H. Hou, *The role of LHRH antagonists in the treatment of prostate cancer.* Oncology (Williston Park), 2009. **23**(7): p. 626-30.
339. Seidenfeld, J., et al., *Single-therapy androgen suppression in men with advanced prostate cancer: a systematic review and meta-analysis.* Ann Intern Med, 2000. **132**(7): p. 566-77.
340. Sufrin, G. and D.S. Coffey, *Flutamide. Mechanism of action of a new nonsteroidal antiandrogen.* Invest Urol, 1976. **13**(6): p. 429-34.
341. Crawford, E.D., et al., *A controlled trial of leuprolide with and without flutamide in prostatic carcinoma.* N Engl J Med, 1989. **321**(7): p. 419-24.
342. Crownover, R.L., et al., *Flutamide-induced liver toxicity including fatal hepatic necrosis.* Int J Radiat Oncol Biol Phys, 1996. **34**(4): p. 911-5.
343. Osguthorpe, D.J. and A.T. Hagler, *Mechanism of androgen receptor antagonism by bicalutamide in the treatment of prostate cancer.* Biochemistry, 2011. **50**(19): p. 4105-13.
344. Chen, Y., N.J. Clegg, and H.I. Scher, *Anti-androgens and androgen-depleting therapies in prostate cancer: new agents for an established target.* Lancet Oncol, 2009. **10**(10): p. 981-91.
345. Nakai, Y., et al., *A Randomized Control Trial Comparing the Efficacy of Antiandrogen Monotherapy: Flutamide vs. Bicalutamide.* Horm Cancer, 2015. **6**(4): p. 161-7.
346. Rice, M.A., S.V. Malhotra, and T. Stoyanova, *Second-Generation Antiandrogens: From Discovery to Standard of Care in Castration Resistant Prostate Cancer.* Front Oncol, 2019. **9**: p. 801.
347. Scott, L.J., *Abiraterone Acetate: A Review in Metastatic Castration-Resistant Prostrate Cancer.* Drugs, 2017. **77**(14): p. 1565-1576.

348. Cookson, M.S., et al., *Castration-resistant prostate cancer: AUA Guideline.* J Urol, 2013. **190**(2): p. 429-38.
349. Zhu, Y., et al., *Inhibition of ABCB1 expression overcomes acquired docetaxel resistance in prostate cancer.* Mol Cancer Ther, 2013. **12**(9): p. 1829-36.
350. Abidi, A., *Cabazitaxel: A novel taxane for metastatic castration-resistant prostate cancer-current implications and future prospects.* J Pharmacol Pharmacother, 2013. **4**(4): p. 230-7.
351. Crawford, E.D., et al., *Treating Patients with Metastatic Castration Resistant Prostate Cancer: A Comprehensive Review of Available Therapies.* J Urol, 2015. **194**(6): p. 1537-47.
352. Wang, I., et al., *Prostate cancer immunotherapy: a review of recent advancements with novel treatment methods and efficacy.* Am J Clin Exp Urol, 2022. **10**(4): p. 210-233.
353. Cheever, M.A. and C.S. Higano, *PROVENGE (Sipuleucel-T) in prostate cancer: the first FDA-approved therapeutic cancer vaccine.* Clin Cancer Res, 2011. **17**(11): p. 3520-6.
354. Le, T.K., et al., *Castration-Resistant Prostate Cancer: From Uncovered Resistance Mechanisms to Current Treatments.* Cancers (Basel), 2023. **15**(20).
355. Feldman, B.J. and D. Feldman, *The development of androgen-independent prostate cancer.* Nat Rev Cancer, 2001. **1**(1): p. 34-45.
356. Hoang, D.T., et al., *Androgen receptor-dependent and -independent mechanisms driving prostate cancer progression: Opportunities for therapeutic targeting from multiple angles.* Oncotarget, 2017. **8**(2): p. 3724-3745.
357. Isaacs, J.T. and W.B. Isaacs, *Androgen receptor outwits prostate cancer drugs.* Nat Med, 2004. **10**(1): p. 26-7.
358. Kawata, H., et al., *Prolonged treatment with bicalutamide induces androgen receptor overexpression and androgen hypersensitivity.* Prostate, 2010. **70**(7): p. 745-54.
359. Quigley, D.A., et al., *Genomic Hallmarks and Structural Variation in Metastatic Prostate Cancer.* Cell, 2018. **175**(3): p. 889.
360. Saraon, P., K. Jarvi, and E.P. Diamandis, *Molecular alterations during progression of prostate cancer to androgen independence.* Clin Chem, 2011. **57**(10): p. 1366-75.
361. Linja, M.J., et al., *Amplification and overexpression of androgen receptor gene in hormone-refractory prostate cancer.* Cancer Res, 2001. **61**(9): p. 3550-5.
362. Hara, T., et al., *Novel mutations of androgen receptor: a possible mechanism of bicalutamide withdrawal syndrome.* Cancer Res, 2003. **63**(1): p. 149-53.
363. Sharp, A., et al., *Androgen receptor splice variant-7 expression emerges with castration resistance in prostate cancer.* J Clin Invest, 2019. **129**(1): p. 192-208.
364. Hu, R., et al., *Distinct transcriptional programs mediated by the ligand-dependent full-length androgen receptor and its splice variants in castration-resistant prostate cancer.* Cancer Res, 2012. **72**(14): p. 3457-62.
365. Parikh, M., et al., *Phase Ib trial of reformulated niclosamide with abiraterone/prednisone in men with castration-resistant prostate cancer.* Sci Rep, 2021. **11**(1): p. 6377.
366. Daniels, V.A., et al., *Therapeutic Approaches to Targeting Androgen Receptor Splice Variants.* Cells, 2024. **13**(1).
367. Hatano, K. and N. Nonomura, *Systemic Therapies for Metastatic Castration-Resistant Prostate Cancer: An Updated Review.* World J Mens Health, 2023. **41**(4): p. 769-784.

368. Tran, C., et al., *Inhibition of constitutive aryl hydrocarbon receptor (AhR) signaling attenuates androgen independent signaling and growth in (C4-2) prostate cancer cells.* Biochem Pharmacol, 2013. **85**(6): p. 753-62.
369. Ohtake, F., et al., *Intrinsic AhR function underlies cross-talk of dioxins with sex hormone signalings.* Biochem Biophys Res Commun, 2008. **370**(4): p. 541-6.
370. Kobayashi, A., et al., *CBP/p300 functions as a possible transcriptional coactivator of Ah receptor nuclear translocator (Arnt).* J Biochem, 1997. **122**(4): p. 703-10.
371. Ghotbaddini, M., et al., *Simultaneous inhibition of aryl hydrocarbon receptor (AhR) and Src abolishes androgen receptor signaling.* PLoS One, 2017. **12**(7): p. e0179844.
372. Thomas, C., et al., *Carbidopa enhances antitumoral activity of bicalutamide on the androgen receptor-axis in castration-resistant prostate tumors.* Prostate, 2012. **72**(8): p. 875-85.
373. Chen, Z., et al., *Carbidopa suppresses prostate cancer via aryl hydrocarbon receptor-mediated ubiquitination and degradation of androgen receptor.* Oncogenesis, 2020. **9**(5): p. 49.
374. Ohtake, F., Y. Fujii-Kuriyama, and S. Kato, *AhR acts as an E3 ubiquitin ligase to modulate steroid receptor functions.* Biochem Pharmacol, 2009. **77**(4): p. 474-84.
375. Ohoka, N., et al., *Development of Small Molecule Chimeras That Recruit AhR E3 Ligase to Target Proteins.* ACS Chem Biol, 2019. **14**(12): p. 2822-2832.
376. Endo, F., et al., *Effects of single non-ortho, mono-ortho, and di-ortho chlorinated biphenyls on cell functions and proliferation of the human prostatic carcinoma cell line, LNCaP.* Reprod Toxicol, 2003. **17**(2): p. 229-36.
377. Kizu, R., et al., *A role of aryl hydrocarbon receptor in the antiandrogenic effects of polycyclic aromatic hydrocarbons in LNCaP human prostate carcinoma cells.* Arch Toxicol, 2003. **77**(6): p. 335-43.
378. Sanada, N., et al., *An androgen-independent mechanism underlying the androgenic effects of 3-methylcholanthrene, a potent aryl hydrocarbon receptor agonist.* Toxicol Res (Camb), 2020. **9**(3): p. 271-282.
379. Gao, X., et al., *The antiandrogen flutamide is a novel aryl hydrocarbon receptor ligand that disrupts bile acid homeostasis in mice through induction of Abcc4.* Biochem Pharmacol, 2016. **119**: p. 93-104.
380. Chen, C.S., et al., *Cyproterone acetate acts as a disruptor of the aryl hydrocarbon receptor.* Sci Rep, 2021. **11**(1): p. 5457.
381. Sun, F., et al., *A novel prostate cancer therapeutic strategy using icaritin-activated arylhydrocarbon-receptor to co-target androgen receptor and its splice variants.* Carcinogenesis, 2015. **36**(7): p. 757-68.
382. ATCC. ***ATCC: The Global Bioresource Center - 22Rv1***. 2023 [cited 2023 05/10/2023]; Available from: https://www.atcc.org/products/crl-2505.
383. ATCC. *The Global Bioresource Center - LNCaP*. 2023 [cited 2023 05/10/2023]; Available from: https://www.atcc.org/products/crl-1740.
384. ATCC. ***ATCC: The Global Bioresource Center - C4-2***. 2023 [cited 2023 05/10/2023]; Available from: https://www.atcc.org/products/crl-3314.
385. ATCC. ***ATCC: The Global Bioresource Center - PC3***. 2023; Available from: https://www.atcc.org/products/crl-1435.
386. Bartonkova, I., A. Novotna, and Z. Dvorak, *Novel stably transfected human reporter cell line AIZ-AR as a tool for an assessment of human androgen receptor transcriptional activity.* PLoS One, 2015. **10**(3): p. e0121316.

387. Stockert, J.C., et al., *Tetrazolium salts and formazan products in Cell Biology: Viability assessment, fluorescence imaging, and labeling perspectives.* Acta Histochem, 2018. **120**(3): p. 159-167.
388. Feoktistova, M., P. Geserick, and M. Leverkus, *Crystal Violet Assay for Determining Viability of Cultured Cells.* Cold Spring Harb Protoc, 2016. **2016**(4): p. pdb prot087379.
389. Novotna, A., P. Pavek, and Z. Dvorak, *Novel stably transfected gene reporter human hepatoma cell line for assessment of aryl hydrocarbon receptor transcriptional activity: construction and characterization.* Environ Sci Technol, 2011. **45**(23): p. 10133-9.
390. Kciuk, M., et al., *Doxorubicin-An Agent with Multiple Mechanisms of Anticancer Activity.* Cells, 2023. **12**(4).
391. Lee, C.H., et al., *Transcript Levels of Androgen Receptor Variant 7 and Ubiquitin-Conjugating Enzyme 2C in Hormone Sensitive Prostate Cancer and Castration-Resistant Prostate Cancer.* Prostate, 2017. **77**(1): p. 60-71.
392. Tan, Z., et al., *Activation of mitogen-activated protein kinases (MAPKs) by aromatic hydrocarbons: role in the regulation of aryl hydrocarbon receptor (AHR) function.* Biochem Pharmacol, 2002. **64**(5-6): p. 771-80.
393. Dorababu, A., *Indole - a promising pharmacophore in recent antiviral drug discovery.* RSC Med Chem, 2020. **11**(12): p. 1335-1353.
394. Zgarbova, E. and R. Vrzal, *Skatole: A thin red line between its benefits and toxicity.* Biochimie, 2023. **208**: p. 1-12.
395. Suyama, Y. and C. Hirayama, *Serum indole and skatole in patients with various liver diseases.* Clin Chim Acta, 1988. **176**(2): p. 203-6.
396. Bray, T.M. and J.B. Kirkland, *The metabolic basis of 3-methylindole-induced pneumotoxicity.* Pharmacol Ther, 1990. **46**(1): p. 105-18.
397. Thornton-Manning, J.R., et al., *Metabolism and bioactivation of 3-methylindole by Clara cells, alveolar macrophages, and subcellular fractions from rabbit lungs.* Toxicol Appl Pharmacol, 1993. **122**(2): p. 182-90.
398. Ruangyuttikarn, W., M.L. Appleton, and G.S. Yost, *Metabolism of 3-methylindole in human tissues.* Drug Metab Dispos, 1991. **19**(5): p. 977-84.
399. Nichols, W.K., et al., *3-methylindole-induced toxicity to human bronchial epithelial cell lines.* Toxicol Sci, 2003. **71**(2): p. 229-36.
400. Pinney, V.R., *Non-lethal weapon systems*. 2000, Ecological Technologies Corporation (The Woodlands, TX): Texas (US).
401. Williams, A.B. and B. Schumacher, *p53 in the DNA-Damage-Repair Process.* Cold Spring Harb Perspect Med, 2016. **6**(5).
402. Tennoune, N., M. Andriamihaja, and F. Blachier, *Production of Indole and Indole-Related Compounds by the Intestinal Microbiota and Consequences for the Host: The Good, the Bad, and the Ugly.* Microorganisms, 2022. **10**(5).
403. Zannas, A.S., et al., *Gene-Stress-Epigenetic Regulation of FKBP5: Clinical and Translational Implications.* Neuropsychopharmacology, 2016. **41**(1): p. 261-74.

CURRICULUM VITAE

PERSONAL INFORMATION

Name: Eliška Zgarbová

Date of birth: 1. 9. 1994

Nationality: Czech

Email: Eliska.Zgarbova@seznam.cz

ORCID ID: 0000-0002-4536-281X

Current affiliation: Department of Cell Biology and Genetics
Faculty of Science
Palacký University in Olomouc
Šlechtitelů 27
783 71 Olomouc, Czech Republic

EDUCATION

2019 – present

Ph.D. study Molecular and Cell Biology
Department of Cell Biology and Genetics ◦ Palacký University

Thesis topic: "*The effect of indole derivatives on aryl hydrocarbon receptor activity in prostatic cell lines"*

2017 – 2019

Master's Degree Biotechnology and Genetic Engineering
Department of Biochemistry ◦ Palacký University

Thesis topic: "*Modulation of vitamin D receptor (VDR)-target genes expression by graphene oxide"*

2014 – 2017

Bachelor's Degree Biotechnology and Genetic Engineering
Department of Biochemistry ◦ Palacký University

Thesis topic: "*The effect of graphene oxide on transcription activity of vitamin D receptor (VDR)"*

RESEARCH INTERSHIPS

06/2016

Short-term Internship

AGEL Hospital, Prostějov, Czech Republic

Undergraduate Intern Laboratory Medicine Department

07/2023 – 12/2023

PhD Internship

Regenerative Medicine Institute, Cedars-Sinai Medical Center, Los Angeles, USA

Visiting Graduate Student Barrett Lab

CONFERENCES ATENDANCE

04/2022 **The Biomania Student Scientific Meeting**, Brno, Czech Republic

11/2022 **Interdisciplinary Postgraduate Conference**, Olomouc, Czech Republic

11/2023 **Symposium on Biomanufacturing**, Los Angeles, USA

05/2024 **XXIIIrd Interdisciplinary Meeting of Young Life Scientists**, Milovy, Czech Republic

HONORS & AWARDS

05/2023 **Dean's Award – Student Scientific Competition**
Overall winner of 2023

05/2023 **UP Endowment Fund for Talented Students**
One of 9 recipients of this prestigious fund to support international research projects of students of Palacký University

05/2024 **Dean's Award – Student Scientific Competition**
2nd place in Biology section, Ph.D. category

TEACHING EXPERIENCE

- Practical courses in Cell Biology
- Practical courses in Genetics
- Practical courses in Molecular Biology

PARTICIPATION IN RESEARCH PROJECTS

Internal Grant Agency of Palacký University:

IGA_PrF_2020_006	Novel use of indole drugs targeting AhR as an off-target
IGA_PrF_2021_005	Monocyclic monoterpenoids as allosteric modulators of AhR
IGA_PrF_2022_014	Indothiazinons as potent AhR agonists with anti-inflammatory effects
IGA_PrF_2023_008	Microbial Trp metabolites as structural scaffolds of selective and dual AhR and PXR agonists
IGA_PrF_2024_010	Modulation of the immune response by novel agonists and antagonists of AhR

LIST OF PUBLICATIONS

1. **Zgarbova, E.**, Vrzal, R. (2022): The Impact of Indoles Activating the Aryl Hydrocarbon Receptor on Androgen Receptor Activity in the 22Rv1 Prostate Cancer Cell Line. *Int. J. Mol. Sci.* 24, 502. [IF 5.6] DOI: 10.3390/ijms24010502.

2. Sladekova, L., **Zgarbova, E.**, Vrzal, R., Vanda, D., Soural, M., Jakubcova, K., Vazquez-Gomez, G., Vondracek, J. & Dvorak, Z. (2023): Switching on/off aryl hydrocarbon receptor and pregnane X receptor activities by chemically modified tryptamines. *Toxicol Lett.* [IF 3.5] DOI: 10.1016/j.toxlet.2023.09.012.

3. **Zgarbova, E.**, Vrzal R. (2023): Skatole: A thin red line between its benefits and toxicity. *Biochimie* 208: 1-12 [IF 3.9] DOI: 10.1016/j.biochi.2022.12.014.

CONFERENCE REPORTS

1. **Zgarbova, E.**, Vrzal, R. (2022): Suppression of androgen receptor activity via activation of aryl hydrocarbon receptor in prostate cancer cells. The Biomania Student Scientific Meeting; Apr 28-29; Brno; Czech Republic. Book of Abstracts; 1st edition 2022: Masaryk University Press, p 117. ISBN: 978-80-280-0040-0.

2. Patel, S., Wagner, M. S., Bay, O., **Zgarbova, E**., Valencia, C. W., Michelsen, K. S., Targan S. & Barrett, R. (2024): Development of a personalized human Paneth cell model using intestinal organoids. Crohn's & Colitis Congress®; Jan 25-27; Las Vegas; USA. *Gastroenterology* 166, Supplement Issue 3. DOI: 10.1053/j.gastro.2023.11.272

3. **Zgarbova, E.**, Valencia, C. W., Patel, S., Bay, O., Barrett, R. (2024): iPSC-derived intestinal organoids: A new personalized model to study IBD and intestinal fibrosis. XXIIIrd Interdisciplinary Meeting of Young Life Scientists. Czech Chemical Society Symposium Series 22 (1), p 50, ISBN: 2336-7210.

Publications connected with this thesis:

1. **Zgarbova, E.**, Vrzal, R. (2022): The Impact of Indoles Activating the Aryl Hydrocarbon Receptor on Androgen Receptor Activity in the 22Rv1 Prostate Cancer Cell Line. *Int. J. Mol. Sci.* 24, 502. [**IF 5.6**] DOI: 10.3390/ijms24010502.

2. **Zgarbova, E.**, Vrzal R. (2023): Skatole: A thin red line between its benefits and toxicity. *Biochimie* 208: 1-12 [**IF 3.9**] DOI: 10.1016/j.biochi.2022.12.014.

APPENDIX I.

Zgarbova, E., Vrzal, R. (2022): The Impact of Indoles Activating the Aryl Hydrocarbon Receptor on Androgen Receptor Activity in the 22Rv1 Prostate Cancer Cell Line. *Int. J. Mol. Sci.* 24, 502. [**IF 5.6**] DOI: 10.3390/ijms24010502.

International Journal of
Molecular Sciences

MDPI

Article

The Impact of Indoles Activating the Aryl Hydrocarbon Receptor on Androgen Receptor Activity in the 22Rv1 Prostate Cancer Cell Line

Eliška Zgarbová and Radim Vrzal *

Department of Cell Biology and Genetics, Faculty of Science, Palacky University Olomouc, Slechtitelu 27, 783 71 Olomouc, Czech Republic
* Correspondence: radim.vrzal@email.cz; Tel.: +420-585-634-904

Abstract: The activation of the aryl hydrocarbon receptor (AhR) by xenobiotic compounds was demonstrated to result in the degradation of the androgen receptor (AR). Since prostate cancer is often dependent on AR, it has become a significant therapeutic target. As a result of the emerging concept of bacterial mimicry, we tested whether compounds with indole scaffolds capable of AhR activation have the potential to restrict AR activity in prostate cancer cells. Altogether, 22 indolic compounds were tested, and all of them activated AhR. However, only eight decreased DHT-induced AR luciferase activity. All indoles, which met the AhR-activating and AR-suppressing criteria, decreased the expression of DHT-inducible AR target genes, specifically *KLK3* and *FKBP5* mRNAs. The reduced AR binding to the *KLK3* promoter was confirmed by a chromatin immunoprecipitation (ChIP) assay. In addition, some indoles significantly decreased AR protein and mRNA level. By using CRISPR/Cas9 AhR knockout technology, no relationship between AhR and AR, measured as target gene expression, was observed. In conclusion, some indoles that activate AhR possess AR-inhibiting activity, which seems to be related to the downregulation of AR expression rather than to AR degradation alone. Moreover, there does not seem to be a clear relationship that would connect AhR activation with AR activity suppression in 22Rv1 cells.

Keywords: prostate cancer; indoles; skatole; AR; AhR

Citation: Zgarbová, E.; Vrzal, R. The Impact of Indoles Activating the Aryl Hydrocarbon Receptor on Androgen Receptor Activity in the 22Rv1 Prostate Cancer Cell Line. *Int. J. Mol. Sci.* **2023**, *24*, 502. https://doi.org/10.3390/ijms24010502

Academic Editor: Yukio Naya

Received: 7 November 2022
Revised: 20 December 2022
Accepted: 22 December 2022
Published: 28 December 2022

1. Introduction

Prostate cancer is one of the most common types of cancer in men, and the risk of developing it increases with advanced age. More than 75% of patients with prostate cancer are men over the age of 65 [1]. According to Siegel's statistic (2022), it is estimated that about 268,490 new cases of prostate cancer will be reported in the United States in 2022 [2]. In most deaths associated with prostate cancer, there is a predominant type known as castration-resistant prostate cancer (CRPC) [3]. Typical CRPC cellular mechanisms include androgen receptor (AR) overexpression, intratumoral synthesis of androgens, and the expression of shortened AR variants. [4]. These AR variants arise from alternative splicing of cryptic exons, and their activity is mostly ligand-independent [5]. The most abundant variant is AR-v7, which was indicated as a possible biological marker of prostate cancer development [6] since its levels have been reported to be significantly lower in normal prostate tissue than in prostate cancer tissue, or CRPC [5]. Prostate cancer with this splicing variant shows only a minor therapeutic response to commonly used anti-androgenic drugs (e.g., enzalutamide; ENZ) [7].

AR belongs to the nuclear receptor superfamily. Upon androgen (ligand) binding, AR translocates to the nucleus and binds to specific responsive elements in DNA. The most vital androgens are testosterone (T), dihydrotestosterone (DHT), and dehydroepiandrosterone (DHEA) [8]. Testosterone is the main male sex hormone and is converted to DHT by 5α-reductase enzyme. This process occurs in several target tissues, e.g., in the prostate [8,9].

Because both hormones bind to the AR, they are the main AR ligands, with DHT being more potent to AR than T [9]. AR activation through DHT is also essential for normal prostate development and function [10]. Imbalanced androgen secretion is linked with the occurrence of several associated diseases or syndromes, e.g., congenital lipoid adrenal hyperplasia, pseudohermaphroditism, or even affecting the development of prostate cancer [8,10,11]. Androgens modulate a wide range of biological responses in the human body through AR and AR became a significant therapeutic target in prostate cancer treatment [8]. Nowadays, the most common group of therapeutic drugs (i.e., direct approach) used in prostate cancer treatment are AR antagonists (e.g., bicalutamide, nilutamide, or ENZ) [12].

More than a decade ago, a different prostate cancer therapeutic strategy was suggested, assuming suppression of AR function through activation of the aryl hydrocarbon receptor (AhR), i.e., an indirect approach. Similarl to AR, upon ligand binding, AhR translocates into the nucleus, where it binds to a specific xenobiotic-responsive element in DNA, with a consequent increase in the expression of the target genes [13,14]. AhR has been primarily associated with biotransformation, but its ability to affect the function of other receptor pathways has also been described [15,16]. This receptor binds a wide number of endo- or exogenous molecules, with polyaromatic hydrocarbons (PAHs) or dioxins, such as, 2,3,7,8-tetrachlondibenzo-p-dioxin (TCDD), being the most potent exogenous ligands. Some PAHs have also been studied for anti-estrogenic and anti-androgenic effects [17].

An in vivo connection between AhR and AR in relation to prostate cancer was suggested in the study by Fritz et al. 2007, who used three different genotypes of mice, namely $AhR^{+/+}$, $AhR^{+/-}$, and $AhR^{-/-}$, and studied the impact on prostate cancer development [18]. The obtained results suggested that the presence of AhR inhibits prostate carcinogenesis, and the model of prostate cancer development based on the genotype of the mice was as follows: $AhR^{+/+} < AhR^{+/-} < AhR^{-/-}$, where $AhR^{+/+}$ mice had the lowest incidence of prostate cancer development compared to $AhR^{-/-}$ mice (16% vs. 60%) [18].

Interestingly, only a limited number of studies have dealt with possible crosstalk between AhR and AR in human prostate cells. One such cross-talk can represent AhR-mediated AR degradation, since AhR has been demonstrated as a ligand-dependent E3 ubiquitin ligase that induces proteasomal degradation of AR in the androgen-sensitive prostate cancer cell line LNCaP [19]. However, it appears that the effect differs between cell lines since the castration-resistant type (C4-2 cell line), TCDD did not induce AR degradation through AhR activation [20]. The AhR and AR protein levels were significantly decreased after the treatment of LNCaP cells with another potent AhR agonist from the PAH group, 3-methylcholanthrene (3MC) [21]. The anti-androgenic effects of AhR ligands were also described for various AhR agonists, such as chrysene, benzo[k]fluoranthene, and benzoapyrene (B[a]P) but not for anthracene or pyrene. Moreover, listed AhR agonists with anti-androgenic effects also increased c-fos and c-jun mRNA levels [17].

The study of Arabnezhad et al. 2020 considered the effects of endogenously activated AhR on AR [22]. The prostate cell line LNCaP was treated with 6-formylindolo [3,2-b]carbazole (FICZ) in the presence or absence of the AR ligand testosterone. After treatment, mRNA (*AR*, *KLK2*, *TMPRSS2,* and *PSA*), PSA protein levels, and DHT levels were evaluated as the end points. The study confirmed that FICZ induced *CYP1A1* activity, which is a marker of AhR activation. In addition, a significant decrease in AR-target gene mRNA expression was observed with the combination of FICZ (50 nM) and testosterone (100 nM). PSA protein and DHT levels were reduced after treatment with FICZ + T. However, no decrease was observed in the absence of testosterone. The obtained results indicated that AhR plays an important role in AR signaling and that FICZ has anti-androgenic effects through the AhR/AR pathway [22]. Moreover, Morrow et al. 2004 study suggested that the stability of AR protein is strictly dependent on AhR ligand and that AhR/AR inhibitory crosstalk is more likely promoter specific [23]. Using a co-immunoprecipitation assay, it was demonstrated that AhR forms a complex with AR and that this process is fundamentally facilitated by DHT. Furthermore, the presence of DHT decreased 3MC-induced transcription of *CYP1A1* [21].

Interestingly, the concept of AhR-mediated degradation of AR was described for other compounds, namely Icaritin [24] and Carbidopa [25]. Icaritin is one of the major metabolites of the compound Icariin [26,27]. Both of these substances are naturally occurring polyphenols, which can be found in plants of the genus *Epimedium* [27]. Carbidopa is a decarboxylase inhibitor used to treat Parkinson's disease [28]. Both of these compounds have been shown to induce AhR activation with consequent degradation of AR [24,25]. However, while Icaritin induced this effect in LNCaP, C4-2 and 22Rv1 cells, Carbidopa was demonstrated to have such an effect in LNCaP cells only. Moreover, these compounds suppressed the tumor proliferation of LNCaP implanted cells in nude mice [24,25].

Therefore, available studies strongly indicate the presence of AhR/AR crosstalk in prostate cancer cells, as various AhR ligands were reported to inhibit prostate cancer development, probably through several different mechanisms [22]. Published data suggest that only strong and potent AhR ligands are capable of inducing AR degradation through AhR activation [19].

Recently, our research team observed that the group of mostly synthetic compounds with an indole scaffold has the ability to activate AhR in hepatocarcinoma cells (AZ-AhR, derived from the parental HepG2 cell line) [29] with efficacy comparable to TCDD (5 nM).

Therefore, the objective of this study was to determine whether these indoles have the ability to suppress AR function through AhR activation and thus slow the proliferation of cancer cells.

2. Results

2.1. The Effects of Indoles on AhR and AR Transcription Activity

Firstly, the new reporter cell line 22AhRv1 was constructed, characterized (Supplement S1), and subsequently used to monitor AhR transcription activity in a prostate-specific environment. The AIZ-AR reporter cell line [30] was used to monitor AR transcription activity in the absence (agonist mode) or presence (antagonist mode) of DHT.

In the 22AhRv1 reporter cell line, the ability of tested indoles to activate AhR was measured after 4 h and 24 h. Significant AhR activation was observed for 1MI, 2MI, 4MI, 5MI, 6MI, 7MI, 2,5DMI, 6MeO, 4MeO1MI, and 7MeO4MI after 4 h (Figure 1A). Interestingly, a positive control, TCDD, did not significantly activate AhR above the level of UT after 4 h, despite significant activation after 24 h (Supplementary S1 and Figure 1B). After 24 h, all indoles significantly and dose-dependently activated AhR with efficacy comparable to TCDD (Figure 1B). An exception to this rule was 3MI (skatole), which had no effect at the highest concentration.

In the AIZ-AR reporter cell line, the ability of the tested indoles to affect AR was measured after 24 h. DHT-inducible AR-dependent luciferase activity reached approximately 7-fold induction next to UT (Figure 2A). True AhR ligands, TCDD and FICZ, were tested as well. While TCDD had no effect, FICZ significantly induced AR-mediated luciferase activity. Furthermore, the anti-androgen ENZ significantly decreased this activity. This was probably due to the use of regular serum in the medium, which contains certain levels of androgens. Of all the compounds tested, only 7MeO markedly and significantly increased AR activity (approximately 2.5 times). Interestingly, a concentration-dependent decrease in luciferase activity was observed for 3MI (with an IC_{50} approx. 10 μM).

In antagonist mode, a positive control ENZ significantly inhibited DHT-inducible AR-dependent luciferase activity to the level of UT. Interestingly, TCDD decreased luciferase activity by approximately 30%, while FICZ increased it above DHT by approximately 20%. This finding suggests that the impact of AhR activation on AR activity may be strongly dependent on the nature of the AhR ligand. A significant concentration-dependent decrease in AR activation was observed for 3MI, 4MI, 1,3DMI, 2,3DMI, 2,3,7TMI, 4,6DMI, 5,6DMI, and 7MeO4MI (Figure 2B). A decrease in AR activity was most remarkable for 3MI (with IC_{50}~5 μM) and 4MI (IC_{50}~50 μM). Some compounds, such as 2,5DMI, 2,3,3TMI, 7MeO, or 5MeO2MI, were able to coactivate AR in combination with DHT (10 nM), but this was consistent with their activity observed in the agonist mode (Figure 2A). Compounds that

were able to significantly activate AhR and simultaneously inhibit DHT-activated AR were used for further experiments (Table 1).

Due to the decline in luciferase activity, we performed MTT and Crystal violet assays. After 24 h of incubation, most of the substances (concentration range 1–100 µM) have been described as nontoxic by both assays, since the decrease in cell viability was not less than 20% (Supplementary S2). However, an enormous decline was observed for 3MI and partially for 4MI by means of Crystal violet assay only (Supplementary S2B). We measured a decrease of 39% and 60% of untreated cells for 3MI and 4MI, respectively. A calculated inhibitory concentration for 3MI was estimated as IC_{50}~60 µM.

2.2. Effects of Selected Indoles on the Target Gene Expression

All tested indoles increased concentration-dependent *CYP1A1* mRNA expression, which is a marker of AhR activation [14]. The positive control, TCDD (10 nM), increased *CYP1A1* expression by 106-fold (Figure 3A). The weakest inducers of *CYP1A1* were 4,6DMI and 5,6DMI, while 4MI was the strongest. Another AhR target gene, *AhRR*, was induced by TCDD, and only 4MI, 1,3DMI, and 7MeO4MI showed weak induction (Figure 3B). Interestingly, 3 MI decreased *AhRR* mRNA levels.

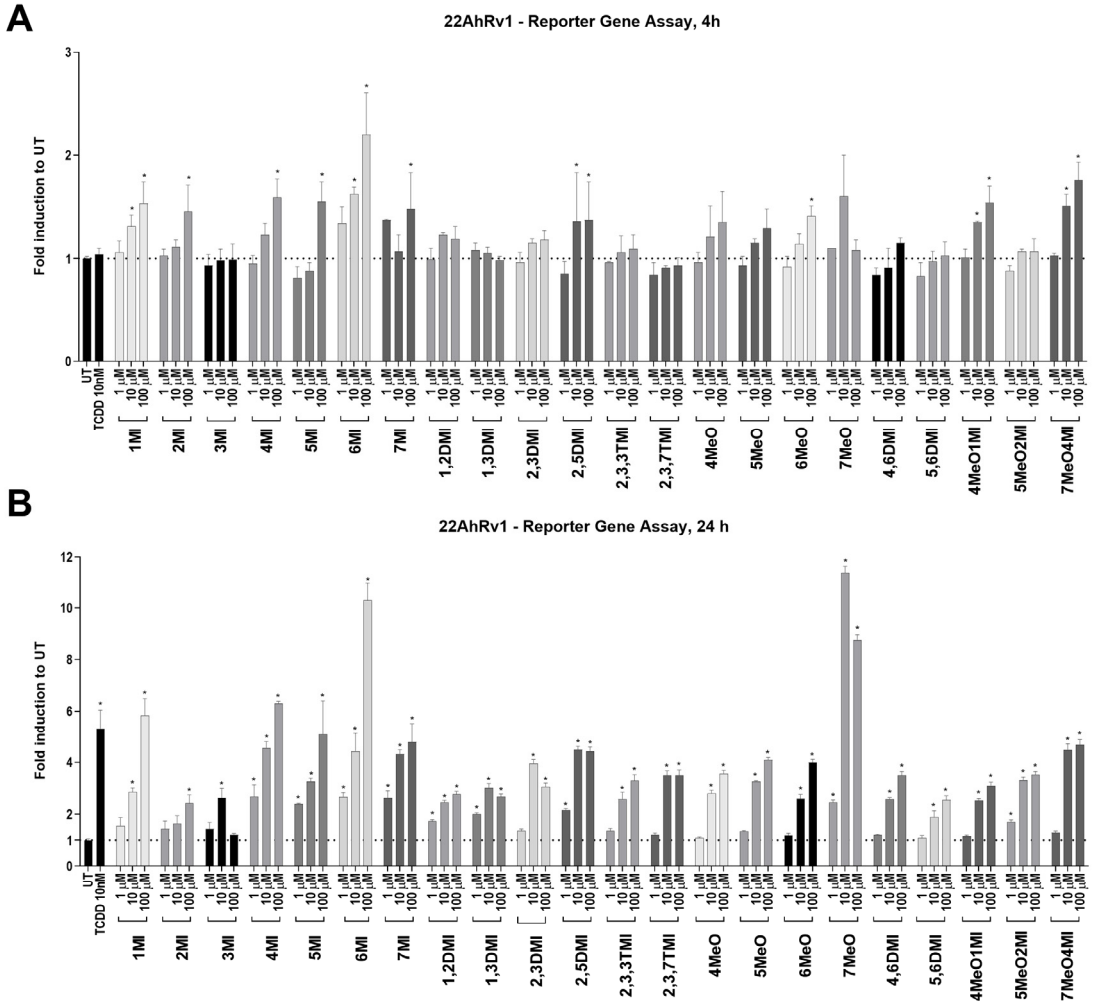

Figure 1. AhR transcription activity after indoles treatment. 22AhRv1 cells were incubated for 4 h (**A**) and 24 h (**B**) with indoles in the concentration range of 1 µM to 100 µM or controls (UT; TCDD 10 nM). The transcription activity of AhR was measured using RGA. The data obtained are averages of three to five experiments and are expressed as fold induction over untreated (UT; DMSO-treated) cells. * represents a significant difference ($p < 0.05$) between untreated (UT) and compound-treated cells.

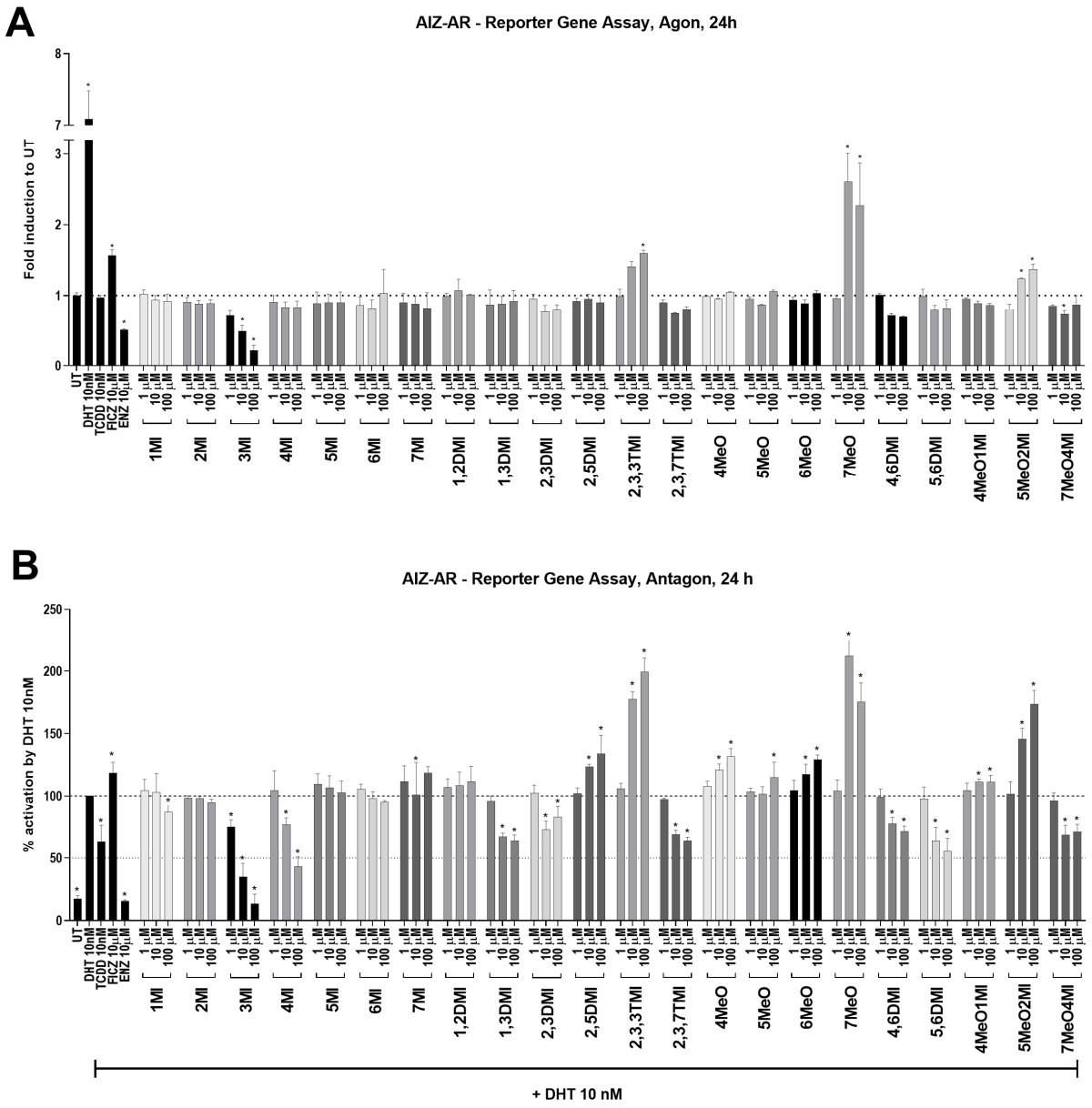

Figure 2. AR transcription activity after indoles treatment. AIZ-AR cells were incubated for 24 h with indoles and controls in the absence (**A**) or presence of 10 nM DHT (**B**). The transcription activity of AR was evaluated using RGA. In agonist mode (**A**), the data obtained are expressed as fold inductions to UT. In antagonist mode (**B**), the results are expressed as a percentage, when DHT 10 nM is set to 100%. * represents a significant difference ($p < 0.05$) between untreated (UT) and compound-treated cells.

Table 1. Compounds selected for further experiments based on RGA results.

Compound	AhR Activation (24 h)		AR Inactivation (24 h)
	10 µM	100 µM	100 µM
3MI	2.6 fold	1.2 fold	decrease to 13.5%
4MI	4.5 fold	6.3 fold	decrease to 43.1%
1,3DMI	3.0 fold	2.7 fold	decrease to 63.5%
2,3DMI	3.9 fold	3.1 fold	decrease to 82.8%
2,3,7TMI	3.5 fold	3.5 fold	decrease to 63.5%
4,6DMI	2.6 fold	3.5 fold	decrease to 70.9%
5,6DMI	1.9 fold	2.6 fold	decrease to 55.5%
7MeO4MI	4.5 fold	4.7 fold	decrease to 70.8%

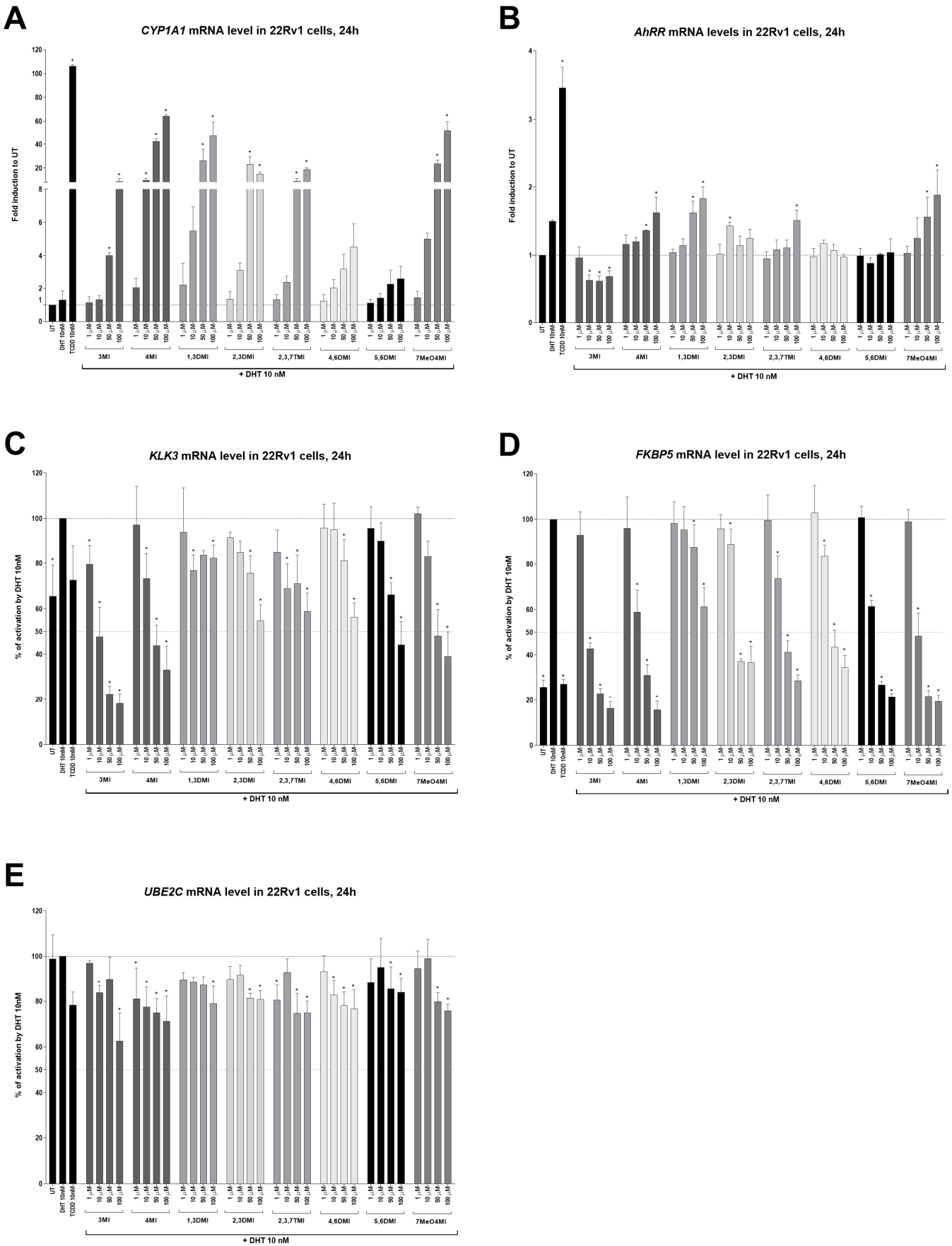

Figure 3. Effects of indoles on the expression of AhR- and AR-target genes. 22Rv1 cells were incubated with indoles (1 μM to 100 μM) in the presence of DHT 10 nM or controls (UT; DHT 10 nM;

TCDD 10 nM) for 24 h. The induction of AhR-target genes *CYP1A1* (**A**), *AhRR* (**B**) and AR-target genes *KLK3* (**C**), *FKPB5* (**D**), and *UBE2C* (**E**) were determined by RT-qPCR. The data obtained were normalized per the housekeeping gene *GAPDH* levels. The results are expressed as fold induction in untreated (UT; DMSO-treated) cells (for AhR-target genes) or as a percentage when DHT 10 nM is set to 100% (for AR-target genes). * represents a significant difference ($p < 0.05$) between untreated (UT) and compound-treated cells (**A**,**B**) or DHT and compound + DHT-treated cells (**C**–**E**).

All tested indoles significantly reduced the DHT-inducible expression of AR target genes, namely *KLK3* (Figure 3C) and *FKBP5* (Figure 3D). Induction by DHT was approx. 1.5-fold and 4-fold for *KLK3* and *FKBP5*, respectively. The expression of the *UBE2C* gene, which is regulated by AR-v7 only [31], was mildly decreased by all indoles (Figure 3E). The strongest decrease (up to 60% of control cells) was observed for 3MI.

2.3. Binding of AR to the KLK3 Promoter after Treatment with Selected Indoles

In order to demonstrate whether the impact of the tested indoles started at the transcription level, we performed the ChIP assay. 22Rv1 cells were incubated with tested indoles (10 μM) and controls in antagonist mode (with DHT, 10 nM) for 90 min. The positive control DHT (10 nM) enriched the *KLK3* promoter with AR by 2.8–4.9 fold (Figure 4A). The presence of anti-androgen ENZ resulted in a significant reduction compared to DHT. Well known AhR ligands, TCDD and FICZ, were able to decrease a DHT-stimulated AR enrichment. A mild decrease has been observed for all tested indoles. The obtained data suggest that the observed decrease in *KLK3* and *FKBP5* mRNAs started already at the level of binding of AR to DNA, thus affecting AR functionality.

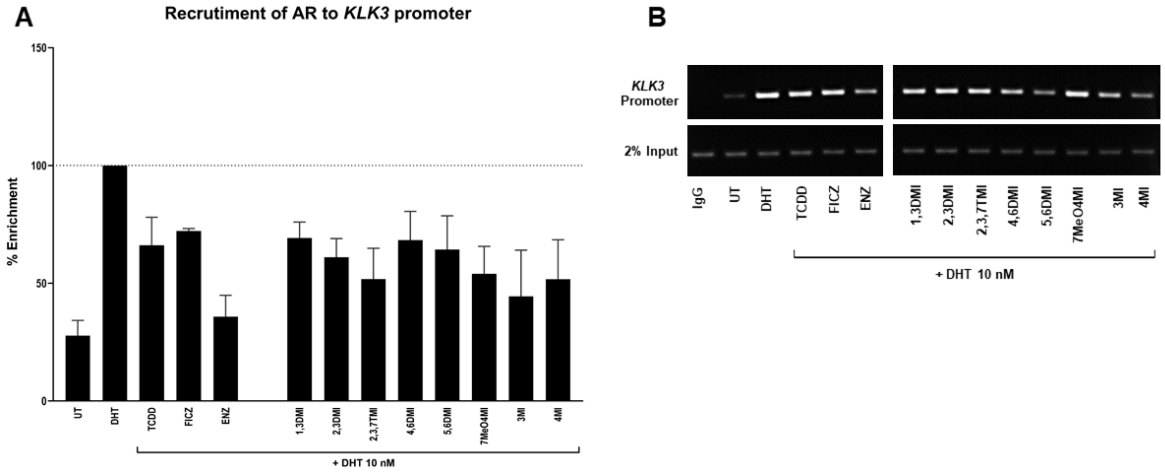

Figure 4. Chromatin immunoprecipitation. 22Rv1 cells were incubated with the tested compounds for 90 min (all indoles, FICZ, and ENZ at 10 μM; DHT and TCDD at 10 nM). Thereafter, the enrichment of the *KLK3* promoter with AR was evaluated. The results are expressed as a percentage of positive control. Enrichment of *KLK3* promoter by DHT was set to 100% (**A**). Representative DNA fragments were amplified using PCR and analyzed with agarose gel electrophoresis (**B**).

2.4. Effects of Selected Indoles on AR-fl and AR-v7 Protein Levels

In the context of the proposed hypothesis, we evaluated the AR protein level. A significant dose-dependent decrease was observed for both variants, AR-fl (110 kDa, Figure 5A,C) and AR-v7 (89 kDa, Figure 5B,C), exposed to 3MI, 4MI, 2,3,7TMI, and 7MeO4MI. Interestingly, 4MI in 1 μM increased the level of DHT-inducible AR-v7 protein by up to 200%. In order to verify the change in either degradation or transcription, we measured mRNA levels. And surprisingly, the mRNA levels of both AR variants decreased in a similar pattern, with the strongest effect shown by 3MI (IC_{50} approx. 10 μM), followed by 4MI,

2,3DMI, 2,3,7TMI, and 7MeO4MI (Figure 5D,E). Thus, the tested indoles probably induce downregulation in AR mRNA, which is further reflected in a decrease of AR proteins.

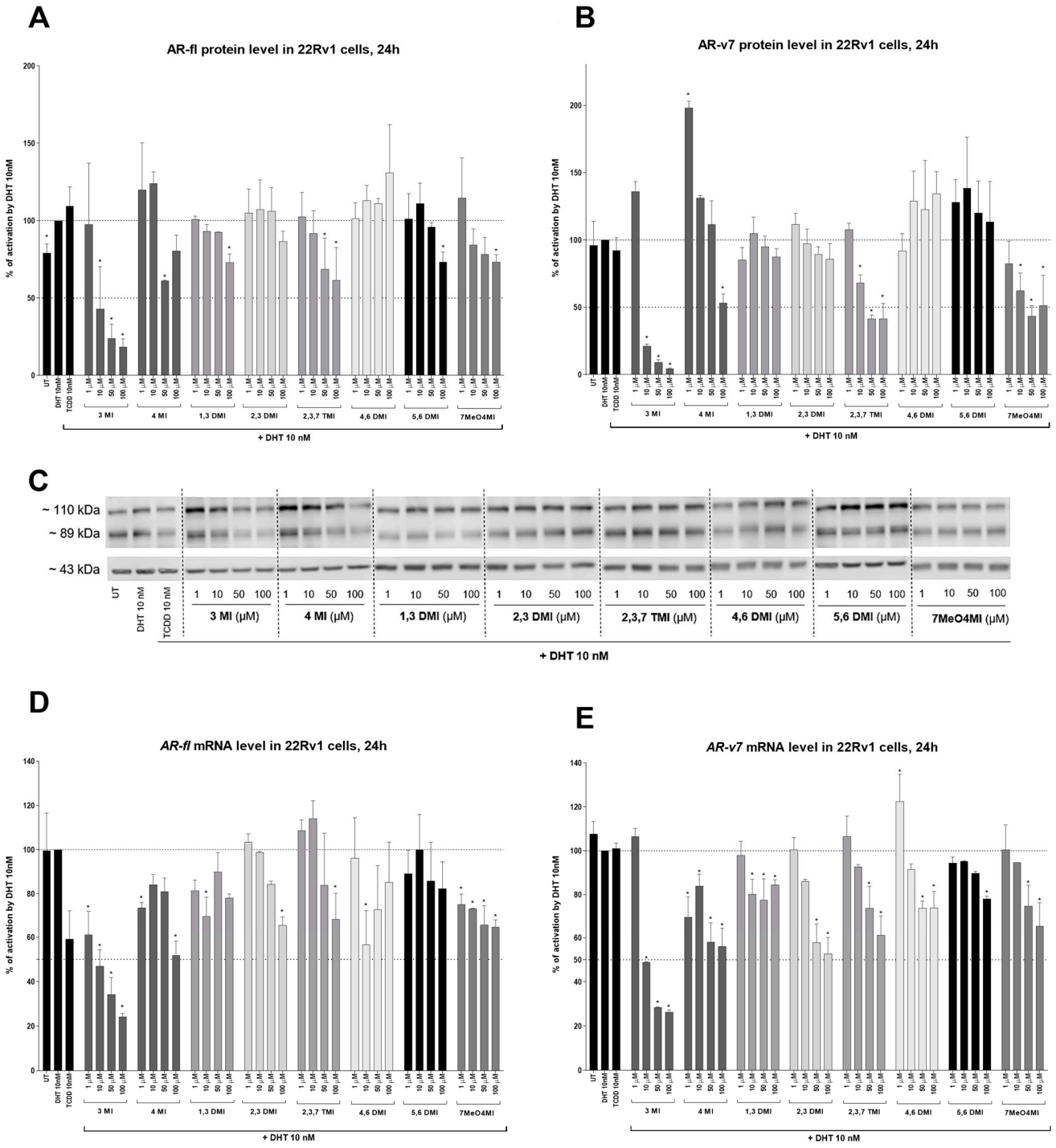

Figure 5. Effects of indoles on AR-fl and AR-v7 protein levels. 22Rv1 cells were incubated with indoles (1 μM to 100 μM) in the presence of 10 nM DHT or controls (UT; TCDD 10 nM; DHT 10 nM) for 24 h. The protein levels of AR-fl (110 kDa; **A**) and AR-v7 (89 kDa; **B**) were evaluated using semi-dry western blotting. The results obtained were normalized per β-actin (43 kDa). A representative blot is shown in (**C**). For comparison, *AR-fl* (**D**) and *AR-v7* (**E**) mRNA levels were also determined using RT-qPCR. The data obtained were normalized per the housekeeping gene *GAPDH*. The results are expressed in percentages, when DHT 10 nM is set to 100%. * represents a significant difference ($p < 0.05$) between DHT and compound + DHT-treated cells (**C**–**E**).

2.5. CRISPR/Cas9 AhR Knockout

Finally, we tried to evaluate the connection between AhR, AR, and the strongest AhR activator in 22Rv1 cells, 4 MI, by genetic knockout. For this purpose, 22Rv1 cells were transiently transfected with the CRISPR/Cas9 plasmid for AhR-KO. In all experiments, a decrease in *AhR* mRNA was successfully observed between WT and KO samples (Figure 6A). *CYP1A1* mRNA expression in AhR KO cells decreased slightly after treatment with TCDD or 4MI in combination with or without DHT (Figure 6B). However, the combined treatment of 4MI and DHT did not show any recurrent trend in *KLK3* mRNA level (Figure 6C) and had no impact on *FKBP5* mRNA level (Figure 6D) when comparing WT and AhR KO cells. The effect on *AR* mRNA levels is given in Supplementary S3.

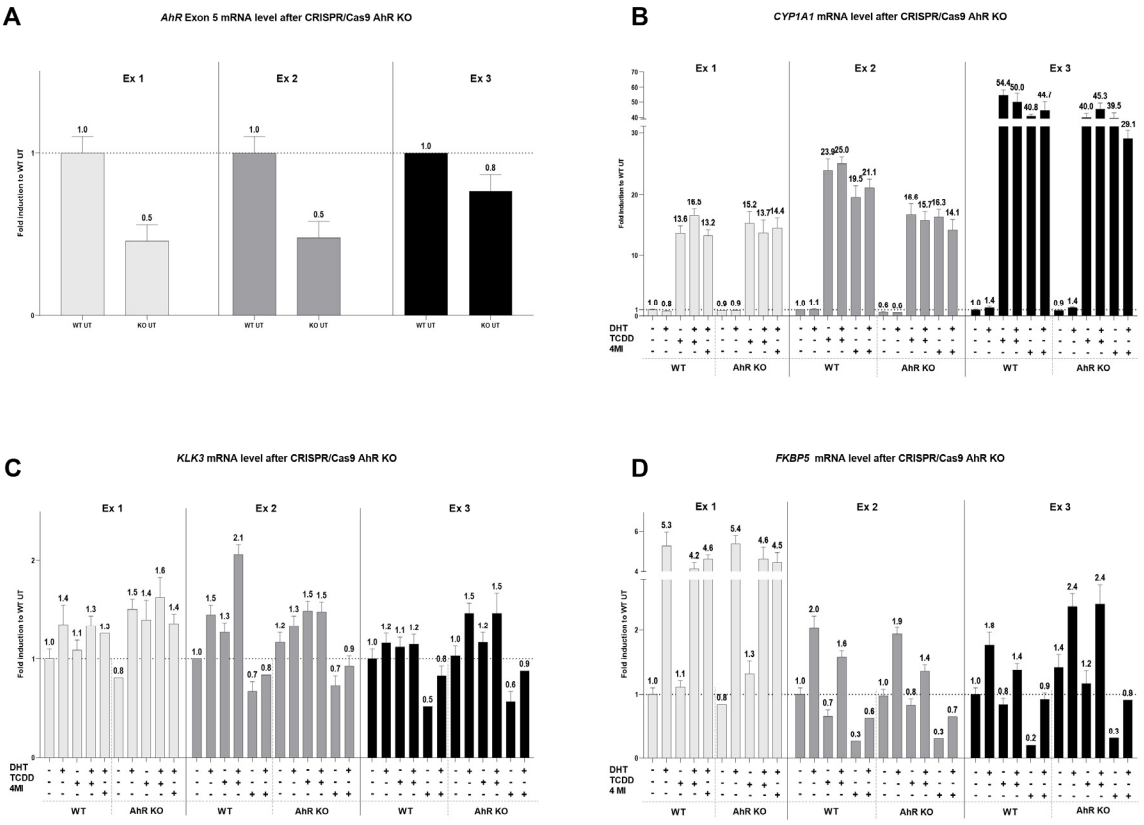

Figure 6. Expression of target genes after CRISPR/Cas9 AhR knockout. 22Rv1 cells were transiently transfected with the CRISPR/Cas9 AhR knockout plasmid or the Control CRISPR/Cas9 plasmid. After 48 h, transfected cells were treated with controls (UT; TCDD 10 nM with or without DHT 10 nM; DHT 10 nM) and 4MI 100 µM with or without DHT 10 nM. The induction of *AhR* (**A**), *CYP1A1* (**B**), *KLK3* (**C**), and *FKBP5* (**D**) was determined by RT-qPCR. The data obtained were normalized per the housekeeping gene *GAPDH*. The results are expressed as fold induction in wild-type UT. In total, three independent experiments were analyzed.

3. Discussion

The main goal of this study was to demonstrate if AhR activation by certain indoles can result in the degradation or at least suppression of AR activity in prostate cancer cells. This assumption was based on the observations that strong AhR ligands degraded AR in the LNCaP prostate cell line [15,19] and that two other compounds, namely Icaritin [24] and Carbidopa [25], which could activate AhR, suppressed prostate cancer via AhR-mediated degradation of AR. Effects of these compounds and indoles from our study on AhR and AR pathways are summarized in Table 2. The tested indoles were selected on the basis of a recent report by our research group, in which methyl- and methoxyindoles were identified as AhR agonists [29]. In the human hepatocarcinoma AZ-AhR cell line, all indoles activated

AhR to some extent, and the strongest ones were reported to be 4 MI, 5 MI, 6 MI, 2,5 DMI, and 7MeO [29]. Similarly, all tested indoles activated AhR in the 22Rv1 prostate cell line after 24 h with efficacy comparable to TCDD, which drastically less activated AhR (5-fold, 10 nM) than AZ-AhR (1000-fold, 5 nM). A partial explanation of such a huge difference lies in the significantly lower amount of AhR protein in the prostate (22Rv1) than in AZ-AhR cells (personal observation).

Table 2. Comparison of the effects of different compounds on AhR and AR receptors (↑ increase, ↓ decrease, - no effect; * only for certain compounds).

		AhR	AR
Tested Compound	**Model**		
Icaritin	**22Rv1**	↑ *CYP1A1* mRNA[24]; ↑ AhR protein level[24]	↓ protein levels[24]; ↓ *UBE2C, KLK3* mRNA[24]; ↓ recruitment to AR-target genes promoters[24]
	LNCaP	↑ *CYP1A1* mRNA[24]; ↑ AhR protein level[24]	↓ protein levels[24]; ↓ *UBE2C, KLK3* mRNA[24]; ↓ recruitment to AR-target genes promoters[24]
	C4-2		↓ protein levels[24]; ↓ *UBE2C, KLK3* mRNA[24]
TCDD	**22Rv1**	↑ *CYP1A1* mRNA	
	LNCaP	↑ *CYP1A1, CYP1B1* mRNA[20]; ↓ AhR protein level[20]	↓ AR protein level[20]; ↑ *KLK3* mRNA[20]; ↑ AR phosphorylation[20]
	C4-2	↑ *CYP1A1, CYP1B1* mRNA[20]; ↓ AhR protein level[20]	-AR protein level[20]
Carbidopa	**LNCaP**	↑ *CYP1A1* mRNA[25]; ↑ AhR protein level[25]	↓ AR protein level[25]; ↓ *PSA* mRNA[25]
3 MI *	**22Rv1 (this study)**	↑ AhR activity (RGA); ↑ *CYP1A1* mRNA	↓ DHT-induced AR activity (RGA); ↓ AR-target genes mRNA; ↓ AR recruitment to *KLK3* promoter * ↓ AR protein level (dose-dependently)
4 MI *			
1,3 DMI			
2,3 DMI			
2,3,7 TMI *			
4,6 DMI			
5,6 DMI			
7MeO4MI *			

Despite the fact that all indoles activated AhR comparably to TCDD (Figure 1), only some of them were able to suppress AR activity (Figure 2) and consequently AR-target gene expression (Figure 3). Interestingly, typical high affinity AhR ligands, TCDD and FICZ, had a opposite impact on the DHT-inducible AR-mediated luciferase activity (Figure 2), despite concentration-dependent induction of AhR-mediated luciferase activity (Supplementary S1). Furthermore, selected indoles that suppressed AR activity inhibited DHT-inducible AR binding to the *KLK3* promoter to some extent, suggesting an impact on the initial transcription event. Additionally, these indoles suppressed AR mRNA levels, which were consequently reflected in AR protein levels. This suggests a different type of mechanism from that initially expected. Additionally, despite very strong AhR activation next to TCDD, most of the indoles have not been demonstrated to be true AhR ligands so far, and thus, the lack of AR degradation effect may stand beyond this fact. This is consistent with the original observation by Ohtake et al., 2007 [19], who found that only full agonists such as TCDD, BaP, and 3MC could degrade AR but weaker ligands (e.g., indirubin–indole scaffold, β-naphthoflavone) could not.

Further, next to the nature of a ligand/agonist of AhR, probably a specific environment plays a role since the study by Ohtake et al., 2007 [19] used LNCaP cells treated for 3 h in medium with 0.2% charcoal-stripped serum, while we used 22Rv1 cells in medium with 10% regular serum and added 10 nM DHT to mimic basal androgen secretion in the human

body. Another difference between these two cell lines lies in the presence of AR variants, where LNCaP has one (AR-fl), while 22Rv1 has two (AR-fl, AR-v7) [5]. Furthermore, AR-v7 displays nuclear localization even in the absence of androgen and acts as a transcription factor [5].

Additionally, it seems that different types of prostate cancer cells have shown different sensitivity to affecting the AR pathways through AhR activation. The AR degradation process through AhR activation was not identified in all types of prostate cancer cells. In the androgen-sensitive LNCaP cell line, which was isolated from the left supraclavicular lymph [32], the mechanism of AR degradation through AhR activation by a strong ligand has been observed multiple times [20,22]. LNCaP cells are classified as AR and AhR-positive [21]. However, the same AhR ligand (TCDD) did not induce AR degradation in the castration-resistant C4-2 cell line [20], which was derived from the parental LNCaP [33]. This may be due to the fact that different types of prostate cancer are diverse in AhR and AR receptor content, and subcellular localization, and that AhR presence may affect AR phosphorylation status [34]. This is probably also reflected in our data, since ChIP results demonstrated a decrease in AR binding to the *KLK3* promoter after 90 min (Figure 4), while AR protein levels (Figure 5) were almost unaffected by most of the tested indoles after 24 h with the 10 µM concentrations used in ChIP. Thus, our results suggest a mix of potential post-translational modification of AR or affected interaction with other transcription partners. This consequently leads to a decrease in AR binding to the *KLK3* promoter and a decrease in the mRNA levels of AR-target genes.

Probably the most interesting finding is the impact of 3MI (skatole) on AR activity and cell viability. Skatole is naturally a product of the intestinal microbiota and can be found in wide range of concentrations in the serum at least of patients with hepatic encephalopathy [35]. Unfortunately, it is not known what the average concentration of skatole in the serum of healthy individuals is. Therefore, our results may suggest a hypothesis that men with detectable skatole concentration in the serum are less likely to develop/have AR-dependent prostate cancer. The proposition of this hypothesis is based on the observation of a decline in all AR-mediated parameters we studied, as well as on the strongest decline in the Crystal violet assay, which is a reflection of the proliferative capacity of the cells.

Furthermore, we observed a visible morphological change in 22Rv1 cells at the end of skatole treatment (personal observation). Thus, it is likely that skatole triggers some sort of apoptotic event and apparently has more molecular targets inside the cells. Our assumption is based on the observation of different skatole action in relation to other indoles as it reduced rather than induced *AhRR* mRNA (Figure 3B) and consistently induced concentration-dependently *AhR* mRNA (personal observation). The expression of *AhRR* and *AhR* is regulated by NF-kB [36], and the combination of genotoxic action, demonstrated for skatole in bronchial cells [37] (that is, activation of p53), and activation of NF-kB could explain these differences. However, this must be revealed in future research as a possible relationship (if any) between skatole blood level and prostate cancer incidence in men.

We believe that skatole deserves further investigation in the future in relation to prostate cancer.

The hypothesis of AR degradation through AhR activation by selected indolic compounds was tested. All 22 tested indoles displayed promising AhR-activating potential in the newly developed 22AhRv1 reporter cell line. However, only 8 of them were able to supress DHT-induced AR activation, namely 3MI, 4MI, 1,3DMI, 2,3DMI, 2,3,7TMI, 4,6DMI, 5,6DMI, and 7MeO4MI. At the mRNA level, 8 selected indoles increased *CYP1A1* expression and significantly reduced DHT-inducible *KLK3* and *FKBP5* expression. Moreover, following ChIP analysis revealed reduced DHT-inducible binding of AR to the *KLK3* promoter by selected indoles. The effect of the strongest AhR activator in this study, 4MI, was further monitored using transient transfection with the CRISPR/Cas9 AhR KO plasmid. However, after AhR KO, no change in AR-targets was observed. To conclude, some tested indoles showed the ability to suppress DHT-induced AR activation; however, this phe-

nomenon does not seem to be associated with AhR activation. Therefore, the hypothesis of AR degradation via AhR activation for selected indoles has not been confirmed.

4. Materials and Methods

4.1. Cell Lines

Human prostate carcinoma epithelial cell lines 22Rv1 (ECACC No. 105092802) and AIZ-AR [30] were cultured in Rosewell Park Memorial Institute (RPMI) 1640 medium supplemented with 10% fetal bovine serum (FBS), 1% non-essential amino acids, and 2 mM L-glutamine (Sigma-Aldrich, Missouri, USA). At the beginning of the experiments, GENERI BIOTECH s.r.o. (Hradec Králové, Czech Republic) performed the authentication of the 22Rv1 cell line. Cells were maintained in a humidified incubator at 37 °C and 5% CO_2. Cell lines were regularly tested for the presence of mycoplasma using the MycoAlert™ Mycoplasma Detection Kit (Lonza, Basilej, Switzerland).

4.2. Compounds and Reagents

The tested indoles were selected based on previous research [29] in our laboratory and are listed in Table 3. The table contains key structures of tested indoles is given in Supplementary S4. The chemicals used are listed in Supplementary S5.

Table 3. List of used indolic compounds and abbreviations.

Compound	Abbreviation	Purity
1-methylindole	1MI	≥97%
2-methylindole	2MI	98%
3-methylindole	3MI	98%
4-methylindole	4MI	98%
5-methylindole	5MI	99%
6-methylindole	6MI	97%
7-methylindole	7MI	97%
1,2-methylindole	1,2DMI	99%
1,3-methylindole	1,3DMI	95%
2,3-methylindole	2,3DMI	≥97%
2,5-methylindole	2,5DMI	97%
2,3,3-trimethylindolenine	2,3,3TMI	98%
2,3,7-trimethylindole	2,3,7TMI	≥97%
4-methoxyindole	4MeO	99%
5-methoxyindole	5MeO	99%
6-methoxyindole	6MeO	98%
7-methoxyindole	7MeO	≥97%
4,6-dimethoxyindole	4,6DMI	≥98%
5,6-dimethoxyindole	5,6DMI	99%
4-methoxy-1-methylindole	4MeO1MI	98%
5-methoxy-2-methylindole	5MeO2MI	99%
7-methoxy-4-methylindole	7MeO4MI	95%

4.3. Reporter Gene Assay (RGA)

Initially, a cellular system was established to monitor AhR transcription activity in the 22Rv1 cell line (Supplementary S1). AIZ-AR reporter cell line [30] was used for evaluation of AR transcription activity. Cells were seeded in 96-well plates at a density of 2×10^4 cells per well in a volume of 200 µL and stabilized overnight. 22AhRv1 cells were incubated with tested indoles for 4 h and 24 h. AIZ-AR cells were treated with indoles for 24 h in agonist and antagonist mode (in the presence of DHT 10 nM). DMSO (untreated; 0.1%; v/v) was used as the vehicle/negative control, TCDD (10 nM) was used as the positive control in 22AhRv1 and DHT (10 nM) was used as the AIZ-AR positive control. Furthermore, anti-androgen ENZ (10 µM) was used as AR suppression control in AIZ-AR cells, and the effects of TCDD (10 nM) and FICZ (10 µM) in the presence or absence of DHT (10 nM) were

also evaluated. After treatments, cells were lysed with 1x Reporter Lysis Buffer (Promega, Wisconsin, USA) and luciferase activity was measured with the Infinite M200.

4.4. Quantitative Reverse Transcriptase PCR (RT-qPCR)

Only indoles capable of activating AhR and simultaneously suppressing AR activity were selected for PCR analysis. Cells were seeded in 6-well plates at a density of 1.5×10^6 cells per well in a volume of 1.5 mL and stabilized overnight. Cells were treated with 8 selected indoles in 4 concentrations (1, 10, 50, and 100 μM) in antagonist conditions (with DHT at 10 nM). After 24 h of treatment, cells were washed with PBS, and total mRNA was isolated using TRI Reagent® (Molecular Research Centre, Ohio, USA), according to protocol. Quality was monitored in the A260/A280 ratio. cDNA was synthesized from 1000 ng of total RNA using M-MuLV Reverse Transctiptase (New England BioLabs, Massachusetts, USA) at 42 °C for 60 min in the presence of Random Primer 6 (100 pmol/μL; New England BioLabs). Subsequently, enzyme activity was inactivated when incubated at 65 °C for 10 min in Dry Bath Incubator (Major Science, California, USA). The mRNA expression was evaluated with KiCqStart® Probe Assays (Sigma-Aldrich) or with SYBR® Green (Roche Diagnostics, Prague, Czech Republic) according to the manufacturer's recommendations. The expression of genes related to the AhR pathway (*AhR, AhRR, CYP1A1*) and AR-target genes (*AR-fl, AR-v7, FKBP5, KLK3, UBE2C*) was monitored. The list of used probes and primers is given in Table 4. qRT-PCR was performed on the Light Cycler 480 II apparatus (Roche Diagnostic), and the reaction settings for KiCqStart® Probe Assays analysis are shown in Table 5. The reaction by SYBR® Green analysis was performed according to the manufacturer´s recommendations. Sample measurements, including the non-template control (NTC), were performed in triplicate, and gene expression was normalized to the housekeeping gene *GAPDH*. The data obtained were evaluated by the delta-delta method.

Table 4. Sequences of used primers and probes.

Target Gene	Sequence
AhR exon 5	f: 5′ TGAATTTCAGCGTCAGCTACA 3′ r: 5′ AACAGACTACTGTCTGGGGGA 3′
AhRR	f: 5′GAGATGAAAATGAGGAGCGC 3′ r: 5′TTTTACTTTTGCATCCGCGG 3′ p: 5′[6FAM]AAACCCAGAGCAGACACCGCAGCCA[OQA] 3′
AR-fl	f: 5′TGTGTCAAAAGCGAAATGGG 3′ r: 5′TTCATCTCCACAGATCAGGC 3′ p: 5′[6FAM]TGCGTTTGGAGACTGCCAGGGACCA[OQA] 3′
AR-v7	f: 5′GAAATGTTAGAAGCAGGGATGACT 3′ r: 5′GGTCATTTTGAGATGCTTGCAA 3′
CYP1A1	f: 5′GGAAGTGTATCGGTGAGACC 3′ r: 5′CATAGATGGGGGTCATGTCC 3′ p: 5′[6FAM]GCAACGGGTGGAATTCAGCGTGCCA[OQA] 3′
FKBP5	f: 5′TCCAAGACTCAGATGATGCC 3′ r: 5′GGCACCCTGTAGTTATTTGC 3′ p: 5′[6FAM]AAGTGTGTGTGGGGAGGGGAAGGGT[OQA] 3′
GAPDH	f: 5′GAAGGAAATGAATGGGCAGC 3′ r: 5′TCTAGGAAAAGCATCACCCG 3′ p: 5′[6FAM]ACTAACCCTGCGCTCCTGCCTCGAT[OQA] 3′
KLK3	f: 5′ACTGCATCAGGAACAAAAGC 3′ r: 5′GGAGGCTCATATCGTAGAGC 3′ p: 5′[6FAM]TGGGTCGGCACAGCCTGTTTCATCC[OQA] 3′
UBE2C	f: 5′CCACAGTGAAGTTCCTCACG 3′ r: 5′GTTGGGTTCTCCTAGAAGGC 3′ p: 5′[6FAM]ACCCCAACGTGGACACCCAGGGTAA[OQA] 3′

Table 5. RT-qPCR reaction setting for Taq-Man.

Detection Format Reaction Volume	Mono Color Hydrolysis Probe/UPL Probe 10 µL		
Program	**Temperature**	**Time**	**Number of Cycles**
Pre-incubation	95 °C	20 s	1
Amplification	95 °C 58 °C	5 s 30 s	45
Cooling	40 °C	30 s	1

4.5. Western Blot

Cells were seeded in 6-well plates at a density of 1.5×10^6 cells per well in a 1.5 mL volume and stabilized. The treatment was similar to that for RT-qPCR. Total protein extracts were isolated for each sample after 24 h of treatment. Cells were washed with 1× PBS, scraped into 1 mL of PBS (cold) and centrifuged (4000 rpm/1500 rcf, 3 min, 4 °C). Pellet was re-suspended in 80 µL protein lysis buffer (pH 7.5; 50 mM HEPES, 5 mM EDTA, 150 mM NaCl, 1% Triton X-100 with anti-protease and anti-phosphatase cocktail) and centrifuged at 13 000 rpm (14,500 rcf), 15 min, 4 °C. The supernatant was collected, and the protein concentration in each sample was determined by 1x Bradford reagent (Sigma Aldrich). Protein samples were separated by sodium dodecyl sulfate-polyacrylamide gel electrophoresis (SDS-PAGE; 10% running gel, 4% stacking gel) in the BioRad Miniprotean system (California, USA), according to the manufacturer's recommendations. SDS-PAGE was followed by semi-dry protein transfer onto a polyvinylidene difluoride (PVDF) membrane. The membranes were stained with Ponceau S Rouge solution (0.1% *w/v* in 5% acetic acid), washed with 1xTBS/Tween, and incubated with 5% non-fat dried milk for 1 h at room temperature (RT). Membranes were incubated overnight with appropriate antibody diluted in 5% solution of bovine serum albumin (BSA) in 1xTBS/Tween at 4 °C. After incubation, the membranes were washed with 1xTBS/Tween and incubated with secondary horseradish peroxidase-conjugated antibody diluted in 5% non-fat dried milk for 1 h at RT. List of used antibodies and their concentrations is given in Table 6. Membranes were analyzed using WesternSure® PREMIUM Chemiluminiscent Substrate (Li-Cor, Nebraska USA) and the C-DiGit Chemiluminiscence Western Blot Scanner (Li-Cor). Obtained results were processed by Image Studio 5.0 for C-DiGit Scanner software. Protein expression was normalized per β-actin (43 kDa).

Table 6. List of used antibodies.

Antibody	Type	Manufacturer	Dilution
Primary antibody			
β-actin	mouse monoclonal	Santa cruz Biotechnology	1: 2000
AR	mouse monoclonal	Santa cruz Biotechnology	1: 500
Secondary antibody			
Anti-mouse	IgG, HRP-linked	Santa cruz Biotechnology	1: 2000
Anti-rabbit	IgG, HRP-linked	Santa cruz Biotechnology	1: 2000

4.6. Chromatin Immunoprecipitation (ChIP)

22Rv1 cells were seeded in a 60-mm plate at a density of 4×10^6 cells per plate in a 4 mL volume and stabilized overnight. The following day, cells were incubated with selected indoles in antagonist mode (only 10 µM concentration with DHT 10 nM) and controls (DMSO in a ratio of 1:1000; DHT 10 nM). Furthermore, the effect of some other compounds (TCDD 10 nM; FICZ 10 µM; ENZ 10 µM) in combination with DHT 10 nM was evaluated. Cells were incubated with the tested compounds for 90 min at 37 °C. Subsequently, ChIP was performed according to the manufacturer's recommendations in the manual for the

Simple ChIP Plus Enzymatic Chromatin IP Kit (Cell Signaling Technology, Danvers, MA, USA) as previously described, with minor modifications [29]. Briefly, an aliquot of 15 µg of digested chromatin was resuspended in ChIP buffer in total volume of 500 µL for each sample and incubated overnight with ChIP validated antibody (4 µL of anti-AR antibody; Cell Signalling Technology). Also, a control sample with normal rabbit IgG was prepared (1 µL of IgG antibody). The following day, 25 µL of Protein G magnetic beads were added to each sample and incubated with rotation for 45 min at 4 °C. The beads were separated in the Magnetic Separation Rack, and subsequently several washing steps (using low- and high-salt buffer, according to the manufacturer) were performed. Then, 150 µL of ChIP elution buffer was added to each sample. The elution was achieved with incubation at 65 °C for 30 min with shaking (1200 rpm/100 rcf). Magnetic beads were separated, and eluted chromatin was transferred into a clear tube. After that, 6 µL of NaCl (5 M) and 2 µL of proteinase K were added to each sample and incubated at 65 °C for 15 min with shaking (1200 rpm/100 rcf). Thus, 750 µL of DNA binding buffer were added to each sample, which was briefly vortexed and centrifuged. Samples were transferred to spin columns and washed with 600 µL of DNA wash buffer. Chromatin was eluted from columns by adding 45 µL of DNA elution buffer and collected in new tubes. The result analysis was performed using RT-qPCR in Light Cycler 480. For each well, the reaction mix contained 2 µL of eluted ChIP sample, 5 µL SYBR Green (Roche), 2 µL of PCR grade H_2O (Roche) and 1 µL of *KLK3* Promoter Primers (SimpleChIP, Cell Signaling). The setting of this reaction is given in Table 7. For the purpose of agarose gel analysis, the next PCR run was performed with elongation for 30 cycles only. The product of such a reaction was analyzed using agarose electrophoresis (4% gel, 65 V, 1.5 h). Samples were dyed with GelRed® nucleic acid stain (Biotium, California, USA). The result was visualized with the Syngene G:BOX gel documentation system (Cambridge, UK).

Table 7. ChIP RT-qPCR reaction setting.

Detection Format **Reaction Volume**		**SYBR Green I/HRM Dye** **10 µL**	
Program	**Temperature**	**Time**	**Number of Cycles**
Pre-incubation	95 °C	10 min	1
Amplification	95 °C 60 °C	15 s 1 min	40
Melting curve	95 °C 65 °C 97 °C	5 s 1 min -	1
Cooling	40 °C	10 s	1

4.7. CRISPR/Cas9 AhR Knock-Out

To verify the relationship between AhR and AR, 22Rv1 cells were transiently transfected with an AhR CRISPR/Cas9 KO plasmid according to the manufacturer's protocol (Santa cruz Biotechnology, Texas, USA), with minor modifications. Briefly, 22Rv1 cells were seeded in a 6-well plate (2×10^5 cells and 3 mL of medium per well) and stabilized for 24 h in a humidified incubator (80% confluence). Subsequently, cells were transfected with the CRISPR/Cas9 AhR KO plasmid or with the control CRISPR/Cas9 plasmid, as a negative control. Solution A, 1 µg of plasmid DNA in Plasmid Transfection Medium in a total volume of 150 µL, and solution B, 5 µL of UltraCruz® Transfection Reagent in Plasmid Transfection Medium in a total volume of 150 µL, were prepared for each well and let stand for 5 min at RT. Subsequently, solution A was added to solution B, vortexed, and incubated for 20 min at RT.

Plates with stabilized cells were transferred to the flow box, and the growth medium was replaced by a fresh one. To each well, 300 µL of transfection solution A + B was added dropwise. The plate was gently mixed by swirling, and cells were incubated with

transfection reagents for 48 h. After incubation, the transfection process was visually confirmed by fluorescence microscopy by detection of green fluorescence protein (GFP). Subsequently, transiently transfected cells were exposed to the tested compounds (UT, DHT 10 nM, TCDD 10 nM with or without DHT 10 nM, 4 MI 100 μM with or without DHT 10 nM) for 24 h. Total mRNA was isolated, and the expression of genes (*AhR*, *CYP1A1*, *AR-fl*, *KLK3*, and *FKBP5*) was evaluated as described earlier (Section 4.4). For evaluating *AhR* mRNA levels, specific primers were designed for exon 5, which is the target DNA sequence for the CRISPR/Cas9 AhR KO plasmid.

4.8. Statistical Analysis

The obtained data were processed using GraphPad Prism Version 9.4.1 (GraphPad Software, San Diego, CA, USA). Significant values in all experiments were determined by two-way ANOVA (symbol * in the charts). Western blot results were analysed using Image Studio 5.0 for C-DiGit Scanner software (Li-cor, Nebraska, USA).

Supplementary Materials: The supporting information can be downloaded at: https://www.mdpi.com/article/10.3390/ijms24010502/s1. See Ref. [38].

Author Contributions: Conceptualization, R.V.; methodology, R.V.; software, R.V., E.Z.; validation, R.V., E.Z.; formal analysis, R.V., E.Z.; investigation, R.V., E.Z.; writing—original draft preparation, E.Z.; writing—review and editing, R.V., E.Z.; supervision, R.V.; project administration, R.V. All authors have read and agreed to the published version of the manuscript.

Funding: This research was funded by the student grant from Palacký University in Olomouc [PrF-2022-009].

Institutional Review Board Statement: Not applicable.

Informed Consent Statement: Not applicable.

Data Availability Statement: The data presented in this study are available online in this article.

Acknowledgments: The structures were obtained from the free chemical structure database ChemSpider. The references were created using reference management software EndNote.

Conflicts of Interest: The authors declare no conflict of interest.

References

1. Dunn, M.W.; Kazer, M.W. Prostate cancer overview. *Semin. Oncol. Nurs.* **2011**, *27*, 241–250. [CrossRef] [PubMed]
2. Siegel, R.L.; Miller, K.D.; Fuchs, H.E.; Jemal, A. Cancer statistics, 2022. *CA Cancer J. Clin.* **2022**, *72*, 7–33. [CrossRef] [PubMed]
3. Siegel, R.; Naishadham, D.; Jemal, A. Cancer statistics, 2013. *CA Cancer J. Clin.* **2013**, *63*, 11–30. [CrossRef]
4. Montgomery, R.B.; Mostaghel, E.A.; Vessella, R.; Hess, D.L.; Kalhorn, T.F.; Higano, C.S.; True, L.D.; Nelson, P.S. Maintenance of Intratumoral Androgens in Metastatic Prostate Cancer: A Mechanism for Castration-Resistant Tumor Growth. *Cancer Res.* **2008**, *68*, 4447–4454. [CrossRef] [PubMed]
5. Hu, R.; Dunn, T.A.; Wei, S.; Isharwal, S.; Veltri, R.W.; Humphreys, E.; Han, M.; Partin, A.W.; Vessella, R.L.; Isaacs, W.B.; et al. Ligand-independent androgen receptor variants derived from splicing of cryptic exons signify hormone-refractory prostate cancer. *Cancer Res.* **2009**, *69*, 16–22. [CrossRef]
6. Zhang, T.; Karsh, L.I.; Nissenblatt, M.J.; Canfield, S.E. Androgen Receptor Splice Variant, AR-V7, as a Biomarker of Resistance to Androgen Axis-Targeted Therapies in Advanced Prostate Cancer. *Clin. Genitourin. Cancer* **2020**, *18*, 1–10. [CrossRef]
7. Antonarakis, E.S.; Lu, C.; Wang, H.; Luber, B.; Nakazawa, M.; Roeser, J.C.; Chen, Y.; Mohammad, T.A.; Chen, Y.; Fedor, H.L.; et al. AR-V7 and resistance to enzalutamide and abiraterone in prostate cancer. *N. Engl. J. Med.* **2014**, *371*, 1028–1038. [CrossRef]
8. Kenji, A. *Androgens and Androgen Receptor: Mechanisms, Functions and Clinical Applications*, 1st ed.; Springer: Boston, MA, USA, 2002; ISBN 978-1-4615-1161-8.
9. Bruchovsky, N.; Wilson, J.D. The conversion of testosterone to 5-alpha-androstan-17-beta-ol-3-one by rat prostate in vivo and in vitro. *J. Biol. Chem.* **1968**, *243*, 2012–2021. [CrossRef]
10. Sharifi, N.; Auchus, R.J. Steroid biosynthesis and prostate cancer. *Steroids* **2012**, *77*, 719–726. [CrossRef]
11. Ghotbaddini, M.; Moultrie, V.; Powell, J.B. Constitutive Aryl Hydrocarbon Receptor Signaling in Prostate Cancer Progression. *J. Cancer Treat. Diagn* **2018**, *2*, 11–16. [CrossRef]

12. Schellhammer, P.F.; Sharifi, R.; Block, N.L.; Soloway, M.S.; Venner, P.M.; Patterson, A.L.; Sarosdy, M.F.; Vogelzang, N.J.; Chen, Y.; Kolvenbag, G.J. A controlled trial of bicalutamide versus flutamide, each in combination with luteinizing hormone-releasing hormone analogue therapy, in patients with advanced prostate carcinoma. Analysis of time to progression. CASODEX Combination Study Group. *Cancer* **1996**, *78*, 2164–2169. [CrossRef]
13. Poellinger, L. Mechanistic aspects–the dioxin (aryl hydrocarbon) receptor. *Food Addit. Contam.* **2000**, *17*, 261–266. [CrossRef] [PubMed]
14. Mimura, J.; Fujii-Kuriyama, Y. Functional role of AhR in the expression of toxic effects by TCDD. *Biochim. Biophys. Acta* **2003**, *1619*, 263–268. [CrossRef] [PubMed]
15. Ohtake, F.; Baba, A.; Fujii-Kuriyama, Y.; Kato, S. Intrinsic AhR function underlies cross-talk of dioxins with sex hormone signalings. *Biochem. Biophys. Res. Commun.* **2008**, *370*, 541–546. [CrossRef] [PubMed]
16. De Anna, J.S.; Darraz, L.A.; Painefilu, J.C.; Carcamo, J.G.; Moura-Alves, P.; Venturino, A.; Luquet, C.M. The insecticide chlorpyrifos modifies the expression of genes involved in the PXR and AhR pathways in the rainbow trout, Oncorhynchus mykiss. *Pestic. Biochem. Physiol.* **2021**, *178*, 104920. [CrossRef] [PubMed]
17. Kizu, R.; Okamura, K.; Toriba, A.; Kakishima, H.; Mizokami, A.; Burnstein, K.L.; Hayakawa, K. A role of aryl hydrocarbon receptor in the antiandrogenic effects of polycyclic aromatic hydrocarbons in LNCaP human prostate carcinoma cells. *Arch. Toxicol.* **2003**, *77*, 335–343. [CrossRef]
18. Fritz, W.A.; Lin, T.M.; Cardiff, R.D.; Peterson, R.E. The aryl hydrocarbon receptor inhibits prostate carcinogenesis in TRAMP mice. *Carcinogenesis* **2007**, *28*, 497–505. [CrossRef] [PubMed]
19. Ohtake, F.; Baba, A.; Takada, I.; Okada, M.; Iwasaki, K.; Miki, H.; Takahashi, S.; Kouzmenko, A.; Nohara, K.; Chiba, T.; et al. Dioxin receptor is a ligand-dependent E3 ubiquitin ligase. *Nature* **2007**, *446*, 562–566. [CrossRef]
20. Ghotbaddini, M.; Powell, J.B. The AhR Ligand, TCDD, Regulates Androgen Receptor Activity Differently in Androgen-Sensitive versus Castration-Resistant Human Prostate Cancer Cells. *Int. J. Environ. Res. Public Health* **2015**, *12*, 7506–7518. [CrossRef]
21. Sanada, N.; Gotoh, Y.; Shimazawa, R.; Klinge, C.M.; Kizu, R. Repression of activated aryl hydrocarbon receptor-induced transcriptional activation by 5alpha-dihydrotestosterone in human prostate cancer LNCaP and human breast cancer T47D cells. *J. Pharmacol. Sci.* **2009**, *109*, 380–387. [CrossRef]
22. Arabnezhad, M.R.; Montazeri-Najafabady, N.; Chatrabnous, N.; Ghafarian Bahreman, A.; Mohammadi-Bardbori, A. Anti-androgenic effect of 6-formylindolo[3,2-b]carbazole (FICZ) in LNCaP cells is mediated by the aryl hydrocarbon-androgen receptors cross-talk. *Steroids* **2020**, *153*, 108508. [CrossRef] [PubMed]
23. Morrow, D.; Qin, C.; Smith, R., 3rd; Safe, S. Aryl hydrocarbon receptor-mediated inhibition of LNCaP prostate cancer cell growth and hormone-induced transactivation. *J. Steroid Biochem. Mol. Biol.* **2004**, *88*, 27–36. [CrossRef] [PubMed]
24. Sun, F.; Indran, I.R.; Zhang, Z.W.; Tan, M.H.; Li, Y.; Lim, Z.L.; Hua, R.; Yang, C.; Soon, F.F.; Li, J.; et al. A novel prostate cancer therapeutic strategy using icaritin-activated arylhydrocarbon-receptor to co-target androgen receptor and its splice variants. *Carcinogenesis* **2015**, *36*, 757–768. [CrossRef] [PubMed]
25. Chen, Z.; Cai, A.; Zheng, H.; Huang, H.; Sun, R.; Cui, X.; Ye, W.; Yao, Q.; Chen, R.; Kou, L. Carbidopa suppresses prostate cancer via aryl hydrocarbon receptor-mediated ubiquitination and degradation of androgen receptor. *Oncogenesis* **2020**, *9*, 49. [CrossRef] [PubMed]
26. He, C.; Wang, Z.; Shi, J. Chapter Seven—Pharmacological effects of icariin. In *Advances in Pharmacology*; Du, G., Ed.; Academic Press: Cambridge, MA, USA, 2020; Volume 87, pp. 179–203. ISBN 0128201851.
27. Szabo, R.; Racz, C.P.; Dulf, F.V. Bioavailability Improvement Strategies for Icariin and Its Derivates: A Review. *Int. J. Mol. Sci.* **2022**, *23*, 7519. [CrossRef]
28. Seeberger, L.C.; Hauser, R.A. Levodopa/carbidopa/entacapone in Parkinson's disease. *Expert Rev. Neurother.* **2009**, *9*, 929–940. [CrossRef] [PubMed]
29. Stepankova, M.; Bartonkova, I.; Jiskrova, E.; Vrzal, R.; Mani, S.; Kortagere, S.; Dvorak, Z. Methylindoles and Methoxyindoles are Agonists and Antagonists of Human Aryl Hydrocarbon Receptor. *Mol. Pharmacol.* **2018**, *93*, 631–644. [CrossRef]
30. Bartonkova, I.; Novotna, A.; Dvorak, Z. Novel stably transfected human reporter cell line AIZ-AR as a tool for an assessment of human androgen receptor transcriptional activity. *PLoS One* **2015**, *10*, e0121316. [CrossRef] [PubMed]
31. Lee, C.H.; Ku, J.Y.; Ha, J.M.; Bae, S.S.; Lee, J.Z.; Kim, C.S.; Ha, H.K. Transcript Levels of Androgen Receptor Variant 7 and Ubiquitin-Conjugating Enzyme 2C in Hormone Sensitive Prostate Cancer and Castration-Resistant Prostate Cancer. *Prostate* **2017**, *77*, 60–71. [CrossRef]
32. ATCC The Global Bioresource Center—LNCaP. Available online: https://www.atcc.org/products/crl-1740 (accessed on 20 June 2022).
33. Wu, H.C.; Hsieh, J.T.; Gleave, M.E.; Brown, N.M.; Pathak, S.; Chung, L.W. Derivation of androgen-independent human LNCaP prostatic cancer cell sublines: Role of bone stromal cells. *Int. J. Cancer* **1994**, *57*, 406–412. [CrossRef]
34. Tran, C.; Richmond, O.; Aaron, L.; Powell, J.B. Inhibition of constitutive aryl hydrocarbon receptor (AhR) signaling attenuates androgen independent signaling and growth in (C4-2) prostate cancer cells. *Biochem. Pharmacol.* **2013**, *85*, 753–762. [CrossRef] [PubMed]
35. Suyama, Y.; Hirayama, C. Serum indole and skatole in patients with various liver diseases. *Clin. Chim. Acta* **1988**, *176*, 203–206. [CrossRef] [PubMed]
36. Larigot, L.; Juricek, L.; Dairou, J.; Coumoul, X. AhR signaling pathways and regulatory functions. *Biochim. Open* **2018**, *7*, 1–9. [CrossRef] [PubMed]

37. Nichols, W.K.; Mehta, R.; Skordos, K.; Macé, K.; Pfeifer, A.M.; Carr, B.A.; Minko, T.; Burchiel, S.W.; Yost, G.S. 3-methylindole-induced toxicity to human bronchial epithelial cell lines. *Toxicol. Sci.* **2003**, *71*, 229–236. [CrossRef]
38. Novotna, A.; Pavek, P.; Dvorak, Z. Novel stably transfected gene reporter human hepatoma cell line for assessment of aryl hydrocarbon receptor transcriptional activity: Construction and characterization. *Environ Sci. Technol.* **2011**, *45*, 10133–10139. [CrossRef]

APPENDIX II.

Zgarbova, E., Vrzal R. (2023): Skatole: A thin red line between its benefits and toxicity. *Biochimie* 208: 1-12 [IF 3.9] DOI: 10.1016/j.biochi.2022.12.014.

Biochimie 208 (2023) 1–12

Contents lists available at ScienceDirect

Biochimie

journal homepage: www.elsevier.com/locate/biochi

Skatole: A thin red line between its benefits and toxicity

Eliška Zgarbová, Radim Vrzal*

Department of Cell Biology and Genetics, Faculty of Science, Palacky University, Slechtitelu 27, 783 71, Olomouc, Czech Republic

ARTICLE INFO

Article history:
Received 19 August 2022
Received in revised form
21 December 2022
Accepted 22 December 2022
Available online 28 December 2022

Handling Editor: J.L. Mergny

Keywords:
Skatole
AhR
Intestine
Dysbiosis
Mutagen

ABSTRACT

Skatole (3-methylindole) is a heterocyclic compound naturally found in the feces of vertebrates and is produced by certain flowers. Skatole has been used in specific products of the perfume industry or as a flavor additive in ice cream. Additionally, skatole is formed by tryptophan pyrolysis of tobacco and has been demonstrated to be a mutagen. Skatole-induced pulmonotoxicity was reliably described in ruminants and rodents, but no studies have been conducted in humans. Initially, we provide basic knowledge and a historical overview of skatole. Then, skatole bacterial formation in the intestine is described, and the importance of the microbiome during this process is evaluated. Increased skatole concentrations could serve as a marker for intestinal disease development. Therefore, the human molecular targets of skatole that may have significant effects on various processes in the human body are described. Ultimately, we suggest a link between skatole intestinal formation in humans and skatole-induced pulmonotoxicity, which should be explored further in the future.

Contents

1. Introduction

Skatole or 3-methylindole (3MI) is an organoheterocyclic compound that can be found naturally in some vegetables, such as orange blossoms, jasmine [1] or beetroot [2], but the highest levels of

* Corresponding author.
E-mail address: radim.vrzal@email.cz (R. Vrzal).

https://doi.org/10.1016/j.biochi.2022.12.014

Abbreviations

3MEIN	3-methyleneindolenine
3MI	3-methylindole; skatole
ABT	1-aminobenzotriazole
AhR	aryl-hydrocarbon receptor
AN	androstenone
ARNT	AhR nuclear translocator
BW	body weight
Caco-2	human colorectal adenocarcinoma cell line
CYP	cytochrome P450 enzymes
GSH	glutathione
HE	hepatic encephalopathy
HepG2	human hepatocyte carcinoma cell line
HepaRG	human hepatoma cell line
HT-29	human colon adenocarcinoma cell line, primary tumor
IAA	indole acetic acid
IAD	indoleacetate decarboxylase enzyme
IBD	inflammatory bowel disease
IC50	inhibitory concentration 50%
IEC	intestinal epithelial cell
IPY	indole pyruvic acid
LD50	lethal dose 50
LS180	human colon adenocarcinoma cell line, Dukes type B
MAPKs	mitogen-activated protein kinases
NHBE	normal human bronchial epithelial cells
PXR	pregnane X receptor
RXR	retinoid X receptor
TCDD	2,3,7,8-tetrachlordibenzo-p-dioxin
Trp	L-tryptophan

skatole are derived from the metabolism of the essential amino acid L-tryptophan (Trp) by intestinal bacteria in the mammalian digestive tract. In particular, in the human body, skatole is detected mainly in feces [3,4] and more recently in human saliva [5].

Pure skatole was originally named and described by Ludwig Brieger as a white crystalline substance with 'an extremely unpleasant (fecal) and fascinating odor' [3]. Therefore, it is surprising that this unpleasant odor turns into a floral scent at lower concentrations (less than 1%; approx. 60 mM stock solution in ethanol). Thus, skatole is also present in essential oils and is widely used as a fragrance in perfumes [6,7] or even as a flavor enhancer in ice cream [8].

Skatole is a volatile compound that is soluble in hot water, alcohol, benzene, chloroform, and ether. According to the Human Metabolome Database, the solubility of skatole in water is 0.498 mg/ml (approx. 3.8 mM). The melting point is 95 °C, and the boiling point is 266 °C [4]. The molecular weight of skatole is 131.1745 g/mol. Under laboratory conditions, pure skatole is a white crystalline compound but tends to darken upon exposure to air [1,9].

Today, an increasing number of researchers are focused on understanding the intestinal microbiome in human health, although the complexity of the gut microbial structure represents a significant challenge. The results obtained show a direct correlation between the appropriate gut microbiome composition and the health of the individual [10]. Among the many compounds identified in the stool of humans and other animal species, skatole belongs to the group of compounds, the presence of which appears to be connected with dysbiosis of the gut microbiota [3,10,11].

Therefore, the purpose of this minireview is to evaluate and connect the basic knowledge about skatole from various scientific fields, such as microbiology, ecology, molecular biology, and medicine, and suggest possible directions for skatole research. In general, this review provides an interdisciplinary overview of skatole natural occurrence, biological synthesis, and known molecular targets in humans or adequate human *in vitro* cellular models. Individually published discoveries suggest novel insight into the patho-/physiological effects of this prodigious compound.

2. Historical overview

The first mention of this compound appeared in 1877 in a study published by Ludwig Brieger '*On volatile components of human excrement*' [3], which focused on the analysis of the intestine content. In those days, it was already clear that this type of analysis would be very difficult, and not much has changed since then. As raw experimental material, L. Brieger used fresh human feces from healthy donors. Excrements were mixed with acetic acid solution and distilled multiple times, and the resulting small-volume solution was evaporated. After evaporation, a new indole-like substance, namely, skatole, was detected [3]. The name of this compound is derived from the Greek word 'skato', which means feces or dung. According to Dunstan (1889), skatole was later isolated from the products of putrefaction of albumen, flesh, or various forms of animal proteins [12]. In the laboratory, skatole can be synthesized by indigo reduction (described by von Baeyer and O. R. Jackson in 1880) or using the method based on warming the phenylhydrazine of propionaldehyde with zinc chloride (known as Fischer indole synthesis; described by Emile Fischer in 1886) [13].

3. Skatole all around us

Vertebrate excrements are one of the largest sources of skatole in nature. Therefore, the occurrence of skatole, as an odor, is associated with different parts of industry. High skatole values were detected in swine manure [14,15], air samples near livestock farms [16,17], and wastewater and air near wastewater treatment plants [18,19]. However, given that the smell of skatole is altered based on its concentration, we encounter skatole more often than we realize.

3.1. Skatole – the scent of blossoms

At lower concentrations, the smell of indolic compounds is described as floral and pleasant. Due to its odor intensifying properties, skatole is widely used in the perfume industry as a fixative [6,7]. *Nuit de Chine* (Chinese Nights) is among the most well-known perfumes containing skatole. This perfume exhibits a combined scent of sandalwood, peach, rose, and skatole. Its 1% solution in ethanol (approx. 60 mM stock solution) is commonly available in specialized stores for perfumery purposes [6].

Naturally occurring sources of skatole in addition to feces include beetroot, *Nectandra* wood, orange blossom, and jasmine [1,2]. Using a combination of gas chromatography and mass spectrometry methods, it was found that skatole is one of the most significant components that form the typical aroma of Laoshan green tea. Among other components, compounds, such as dimethyl sulfide, indole, furaneol, (Z)-jasmone and vanillin, have been identified as important carriers of Laoshan green tea odor [20]. Skatole is partly responsible for specific odors during flowering in some *Araceae* species, particularly in *Arum dioscoridis*, *Arum*

italicum and *Sauromatum guttatum* [21].

The presence of skatole in such sources confirms its role as an attractant for a wide number of insects. Field tests have shown that the smell of skatole is highly intriguing for Tasmanian grass grub beetles (*Aphodius tasmaniae*), Sexton beetles (*Necrophorus orbicollis, Necrophorus americanis),* or beetles of the genus *Geotrupes* [2]. In addition, skatole seems to attract gravid mosquitoes (*Culex quinquefasciatus*) in both laboratory tests and in the field [22] as the rate of oviposition responses shows concentration dependence on skatole [23]. Therefore, the role of skatole as a mosquito attractant may contribute to the spread of insect-borne diseases, such as West Nile virus, Japanese or Venezuela equine encephalitis virus [24].

3.2. Skatole – the stinky molecule

The improper treatment of animal wastes can cause serious environment pollution, as well as spread of pathogenic bacteria. Over the years, many compounds (skatole, indole or dimethyl trisulfide) have been considered possible foul agents in wastewater and have been identified as the main elements of unpleasant odors [19,25]. Skatole is one of the most offensive, odor-active compounds in wastes and for that reason it was analyzed. Maximum concentration of skatole in wastewater was reported up to 700 μg/l (5.3 μM) [18] and odor threshold concentrations (OTCs) in water were determined to be 1 μg/l (approx. 7.6 nM) [25]. Moreover, the presence of skatole was also detected in the air near the wastewater treatment plants with OTC of 0.327 ng/l (approx. 2.5 pM) [18]. This odor nuisance represents a major challenge in wastewater industry and different approaches (e.g. chemical scrubbing, biofiltration) have been tested to remove fecal odors (indication of compounds such indole or skatole), including microbiota-driven skatole degradation (see section 4.1.).

The properties of skatole have been studied in many different scientific fields. One such field is the taste quality of boar meat, which was reported to be affected by the presence of skatole. Several sensory tests revealed that consumers preferred boar meat patties with lower skatole content [26]. Consumption of pork is often associated with the term *boar taint*, which is an unpleasant smell or taste that occurs during cooking and consumption of pork meat from uncastrated pigs. The reason for this repulsive taint seems to be the excessive accumulation of skatole and androstenone (AN) in the adipose tissue of pigs [27,28]. In a study by *Bañón* et al., it was determined that the average AN content in the backfat was 0.576 ± 0.179 μg/g and that the average skatole content was 0.053 ± 0.026 μg/g [29]. Another study by *Aldal* et al. determined a mean skatole level of 0.14 μg/g fat and 0.36 μg/g fat for AN in slaughtered Noroc boars pigs [30]. Interestingly, a study performed by *Bonneau* et al. reported a mean AN concentration up to 1.27 μg/g for heavier pigs in six different European countries [31]. Interestingly, this was not found for skatole. Thus, with the exception of the last mention study by *Bonneau* et al., the abovementioned AN and skatole levels are probably not problematic since backfat concentrations of 1 μg/g and 0.2 μg/g are frequently reported as consumer acceptance thresholds for AN and skatole, respectively [32].

Interestingly, skatole accumulation in subcutaneous adipose tissue was reported after high-fat high-chicken protein (45 and 40% calorie, respectively) diet in rats as well [11]. This finding, together form pigs, suggest a speculation about skatole accumulation in human adipose tissue as well, despite not proven experimentally. This would probably represent a toxicological risk as skatole might be released from adipose tissue similarly to some hydrophobic environmental pollutants after weight loss diets and consequently, via blood stream, reach certain susceptible tissues, such as pulmonary system (see section 4.3).

Despite the occurrence of skatole throughout nature, an unexpected observation was reported in 1968. Specifically, skatole was found in cigarette smoke as a result of Trp pyrolysis in burning tobacco. Skatole levels in cigarette smoke range from 0.4 to 1.4 μg per cigarette and can reach up to 16 μg [33].

An intentional use of skatole as a putrid molecule was emphasized in 2000, when skatole was registered under patent number US 6386113 B1 as a malodorant substance in nonlethal weapon systems in the USA [34]. This should be kept in mind if pulmonotoxicity will occur in exposed people.

Thus, skatole is a compound that we may encounter daily from the environment without realizing it. In addition to these nonhuman sources, the greatest natural source of skatole is potentially the microbiota present in the human gastrointestinal tract.

4. Skatole inside of us

Human feces contain enormous amounts of volatile organic compounds. Their concentration may reveal sensitive information about the patient's health condition. Therefore, these compounds represent a very important group of useful biomarkers in the human body that can be assessed without the use of invasive medical techniques. However, the potential usage of such information for clinical treatment is complicated by the fact that the concentrations of some fecal substances vary considerably in healthy and unhealthy individuals [35,36], and the findings of such studies are occasionally contradictory. Moreover, significant variation was observed in different populations of healthy subjects. When evaluating fecal concentrations, many factors must be considered (such as dietary habits, age, gender or lifestyle).

The potential use of skatole as a biomarker of gastrointestinal diseases has also been studied. In 1925, the presence of indole and skatole in human urine samples was reported to indicate chronic kidney disease (CDK) and intestinal dysbiosis [37]. Currently, the 3-methylindole kit (Eureka Lab Division, Chiaravalle, AN, Italy) can be used to determine the levels of these compounds in urine, and the results are evaluated by high-performance liquid chromatography (HPLC). Greater than 20 ng/l skatole (approx. 152 pM) in urine indicate dysbiosis [38,39]. Furthermore, skatole was recognized as a possible agent involved in emphysema or schizophrenia [40]. This connection was suggested after monitoring of the presence of skatole derivatives in the urine of 23 experimental male subjects with chronic schizophrenia. In this study, significantly increased levels of 6-hydroxyskatole appeared in the urine of schizophrenic patients compared with healthy controls [41]. Thus, skatole (or its metabolites) could be used as a biomarker for the detection of various pathological conditions in the human body. However, before using this compound (or its metabolites) as a biomarker, its physiological level and role in the intestine must be determined.

The appearance of skatole in the intestine is dependent on many factors. In addition to Trp-containing proteins, the intake of fibers and polyphenols is also important given that their fermentation in the colon contributes to a decrease in the bacterial populations associated with protein metabolism and the production of deleterious metabolites, including skatole [42,43]. Moreover, the increase in skatole levels is generally accompanied by the production of other protein-derived metabolites, including *p*-cresol, indole, NH_3, H_2S or polyamines, many of which have potentially deleterious effects at local and systemic levels. In addition, the presence of skatole is further dependent on the occurrence of certain microorganisms. Their optimal ratio widely affects the health of the host [10,44]. Changes in the composition of the gut microbiome lead to the modulation of Trp and its metabolite concentrations in the intestine as well in plasma [45]. Qualitative or quantitative changes in Trp metabolites either in feces or plasma might serve as

biomarkers for specific diseases in individuals with deteriorating health conditions. Moreover, Trp deficiency can cause an outbreak of diseases, such as fibromyalgia or chronic fatigue syndrome [46].

The importance of the intestinal microbiome for human life begins as early as birth. It is well known that the newborn microbiota is established at delivery. A mutual relationship exists between the development of the immune system and its modulation by the gut microbiota [47]. In the human intestine, Trp can be metabolized either by the host (endogenously) or by the microbiota (occasionally referred to as pseudoendogenously). Endogenous metabolism occurs after the entry of Trp by the neutral amino acid transporter SLC6A19 (sodium-dependent neutral amino acid transporter B(0)AT1) into enterocytes and enterochromaffin cells, where it enters the kynurenine and serotonin pathways, respectively (Fig. 1). In the first pathway, 95% of the Trp is degraded to kynurenine, kynurenic acid, picolinic acid, quinolinic acid and nicotinamide adenine dinucleotide (NAD). In the second pathway, namely, the serotonin pathway, generally 1–2% of ingested Trp is converted to serotonin and melatonin [48].

The remaining Trp is metabolized by the gut microbiota (i.e., pseudoendogenously) to indole derivatives, such as tryptamine, indole pyruvic acid or skatole (Fig. 1). Intestinal production and absorption of skatole are mainly localized in the distal colon [48,49]. The chemical structure of Trp indicates that the following reactions occur on the pyrrole ring structure at position 3 [40]. It has been observed that the main pathway of skatole production is a two-part process [50]. Synthesis is initiated by Trp deamination mediated by the tryptophanase enzyme (TnaA; EC: 4.1.99.1) of *Escherichia coli* (strain K12) [51]. The product of such a reaction is indole-3-pyruvic acid (IPY), which is decarboxylated to indole-3-aldehyde by enzyme indole-3-pyruvate decarboxylase (EC: 4.1.1.74) from the bacterium *Enterobacter cloacae* [52,53]. Indole-3-aldehyde undergoes a dehydrogenation process and is converted to indole-3-acetic acid (IAA), a known plant growth regulator [54] and the main precursor of skatole in the intestine [40,48]. This reaction has been observed with *Lactobacillus reuteri*, *L. murius,* and *L. acidophilus*, but only in a murine model [55,56]. The following stage is IAA decarboxylation by the indoleacetate decarboxylase enzyme (IAD; EC: 4.1.1.115), resulting in the formation of the skatole molecule itself [57]. All of these reactions are mediated by intestinal bacteria and are sensitive to antibiotics [58].

Despite IAA is a precursor for skatole, it is not easy to predict skatole concentration just on the presence of more often detected IAA. Since IAA is metabolized not only to skatole but to 2-hydroxyindole-3-acetic acid as well, it can be expected that IAA will be present in much higher amount than skatole in the intestine. A possible approximation of the amount of IAA vs. skatole can be derived from publication [59], where the ratio of IAA/skatole was roughly two-fold for humans on *defined* diet. However, in case of samples from humans on an *ad libitum* diet, the ratio was approx. 0.27-fold. Therefore, it is difficult to extrapolate what skatole concentration might be even if IAA concentration is known. Moreover, it is important to notice that skatole was detected in only 6 human samples while IAA was detected in all 29 samples [59].

Unlike the relatively simple endogenous metabolism of Trp, bacterial metabolism of Trp is more complex due to the large number of intestinal bacteria that differentially metabolize Trp and significant variability of microbiota among individuals.

Despite the fact that scientists around the world are constantly studying the metabolic processes of all gut microbes, the interconnectedness of these pathways has not yet been fully revealed.

Several factors affect the levels of Trp metabolites in the human intestine: a) the availability of Trp, which is determined either by diet but also by the health of the host; b) the low oxidation–reduction potential in the intestine; and c) the presence of intermediate metabolites of Trp metabolism that may serve as precursors for the production of secondary metabolites (e.g., IAA, tryptamine, melatonin) [40,60]. In addition, other significant

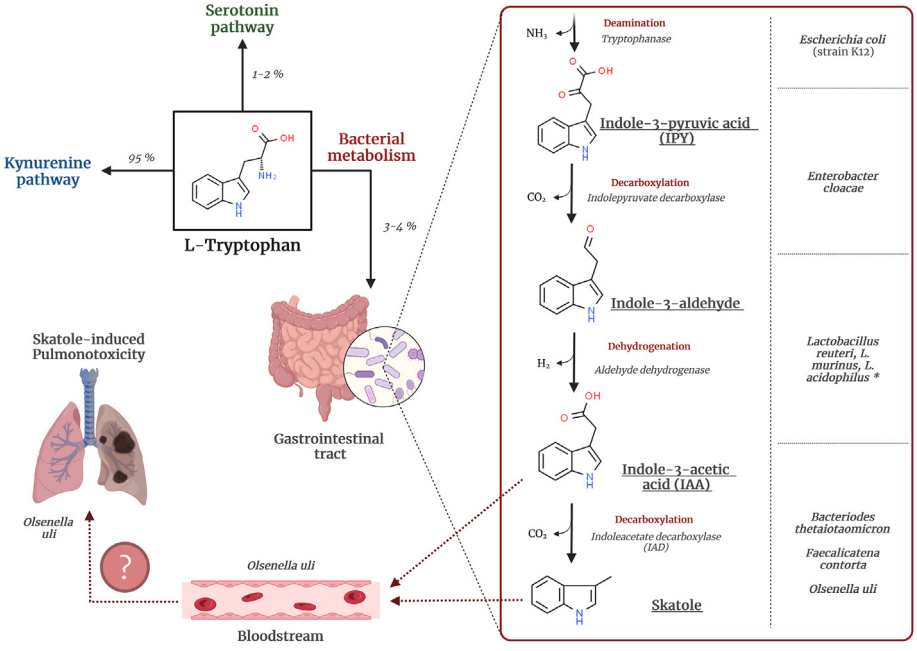

Fig. 1. Trp metabolism and skatole formation. Trp undergoes a distinct fate when metabolized in the host or by the microbiota. There are three possible pathways that describe Trp metabolism in the human body. The first two pathways are endogenous metabolic pathways (kynurenine and serotonin), and the third pathways represents a pseudoendogenous pathway of Trp metabolism mediated by the gut microbiota. This scheme was created based on information from Refs. [48,49,53]. The symbol * indicates *Lactobacillus* capable of indole-3-aldehyde conversion to IAA. However, this reaction has only been observed in a murine model [55,56]. *Olsenella uli* is a skatole-forming bacteria, but it was also found in the blood of patients with GI diseases [57,117]. Moreover, this bacterium is associated with the development of pneumonia [87]. Many studies describe skatole as a possible pulmonotoxic agent, and this bacterium could represent a link between skatole formation in GI and its observed pulmonotoxicity.

factors must be considered, such as fecal transit time or Trp absorption rates [40].

To clarify the relationship between the concentration of some Trp metabolites and a particular health condition, exact *in situ* concentrations must be determined. However, Trp metabolites excreted in the feces are a poor indicator of *in situ* concentrations given that a large amount can be metabolized by the host or excreted via urine [61]. This notion also applies to skatole given that the concentration is usually low and varies greatly compared to other Trp metabolites produced by intestinal bacteria. A recent study found skatole in only 38% of human fecal samples [59,61]. Another limiting factor is the concentration of IAA, as it is a precursor of skatole [40,48]. In healthy individuals, the concentration of skatole in feces fluctuates around approximately 5 μg/g of feces [40,62]. However, in patients with disturbed intestinal digestion, fecal skatole levels reached up to 100 μg/g of fresh stool [62]. Taking into account the average density of feces 1.07 g/mL (range 1.06–1.09) and average water content 75% (range 63–86%) [63], than there is an average molar concentration of skatole in healthy and dysbiotic patients approx.. 54 and 1080 μM, respectively. Although intestinal disturbance was not closely defined at that time (1908), a study comparing healthy volunteers and ulcerative colitis patients 100 years later (2007) found that skatole is present in human feces in approximately 75% and 22%, respectively [35]. Therefore, the terminology 'gut dysbiosis' apparently has broad meaning and should not be used uniformly. Furthermore, although asymptomatic patients provided information on their diets during stool collection, this information was not provided for patients with ulcerative colitis [35,64]. Moreover, higher skatole levels (more than 100 μg/g) have been reported in the stool of patients with colorectal cancer [65].

Dietary habits appear to be important as skatole concentration increases in the case of high meat consumption in humans [66,67]. This may be because meat (or animal proteins in general) contains more Trp than other common dietary components (Table 1) [68,69]. In addition, the amount of skatole in the digestive tract is also affected by the type of meat consumed.

Two groups of men (18–30 years; 20 volunteers in each group), one consisting of chicken eaters and the second consisting of pork eaters, were analyzed. Volunteers were divided into these groups based on a dietary questionnaire that evaluated long-term dietary habits. Groups were identified as follows: chicken eaters preferred chicken meat as the main meat dish, whereas pork eaters preferred pork. In the group that preferred chicken meat, skatole levels in the feces reached up to 100 μg/g, whereas only approximately 20 μg/g skatole was detected in the group consuming pork [67]. Additionally, the composition of the gut microbiome differed slightly (see further information in Section 4.1).

Interestingly, while there seems to be a relationship between type of meat that is consumed (particularly chicken) and skatole level in feces, it was not defined a quantitative relationship that would define skatole amount in the feces as a function of consumed meat amount. However, since colorectal cancer patients have higher skatole levels in feces [65], it is worth of mention, that some studies connect, particularly red meat consumption with a cancer incidence. As an example, red meat consumption was found to be significantly associated with colorectal, colon, rectal, lung or hepatocellular carcinoma in recent study [70].

In general, the amount or source of Trp is important for skatole production, but the essential component potentially lies in the intestinal microbial community. Specifically, two-step skatole synthesis is mediated by different bacterial strains (see more below in 'Skatole forming microbiota'), the simultaneous presence of which is crucially related to the final skatole concentration.

Although one would expect skatole to be found in the intestine, a surprising discovery in 1968 confirmed the presence of skatole in human saliva. A total volume of 15 ml of saliva was mixed with 30 ml of ether solution and incubated for 5 days. Thin layer chromatography was subsequently performed. The results showed the presence of 4 main ether-extractable components: phenol, cresol, indole, and skatole [5]. Recently, the increased presence of skatole in human saliva was associated with the appearance of bad breath, which was assessed using modern approaches, such as a Halimeter® [71]. Unfortunately, the concentration of skatole was not determined. Neither the web page dedicated to saliva and its components (https://salivametabolome.ca/concentrations?page=20, visited on 19.12.2022) has no information about skatole concentration in saliva.

Regrettably, only a limited number of publications exist that deal with the occurrence of skatole in the human circulatory system. Suyama and Hirayama measured serum levels of indole and skatole in patients with various liver diseases and healthy patients [72]. Venous blood samples were collected early in the morning from 20 healthy subjects, 55 patients with various liver diseases (chronic hepatitis, alcoholic fatty liver, liver cirrhosis, or hepatocellular carcinoma) and 34 patients with hepatic encephalopathy (HE). According to the results, serum skatole was not detected in healthy individuals or patients suffering from liver diseases other than HE. However, in all patients with HE, skatole was detected with mean values of 41 nmol/l (range from 0 to 442 nmol/l) [72]. This research suggests that skatole may also be detected in blood serum. The concentrations of skatole vary significantly from one individual to another due to a number of factors – different ages, lifestyles, or genetic predispositions. The fact that its levels differ between healthy and sick individuals may indicate a possible use as a biomarker for specific disease. Nevertheless, no additional articles are available that confirm the connection between serum skatole levels and various diseases to date (March 2022).

4.1. Skatole-forming microbiota

The large number of bacteria present in the human gut are capable of transforming aromatic amino acids, some of which subsequently decarboxylate to form aromatic substances, such as skatole, cresol, or toluene. Although many of these bacteria generate indole or IAA, only a few are capable of skatole production. In 1925, a species of the genus *Clostridium*, namely, *C. scatologenes*, was identified among 53 bacterial cultures as a producer of skatole using the dimethylaniline test [37]. All other tested samples were negative. Furthermore, *C. scatologenes* was shown to be the only known bacterial strain capable of producing skatole directly from Trp [58]. A second species of *Clostridium*, *C. nauseum,* was isolated

Table 1
The percentage of Trp content in proteins in selected types of nutrition components [67].

Type of food	Amount of Trp [%]	Type of food	Amount of Trp [%]
Lysozyme (egg yolk)	16.2	**Soybean (flour)**	8.32
Soy protein	14.0	**Lima bean (flour)**	3.32
Casein (mammal milk)	13.6	**Oat (flour)**	2.56
Minced beef	13.6	**Rice (flour)**	0.98

from topsoil [73]. Furthermore, bacterial strains assigned to the genera *Lactobacillus* [74], *Pseudomonas* [75], and *Olsenella scatoligenes* [76] also produce skatole, which is typically formed as an intermediate product in the formation of catechol from decarboxylation of IAA [74,75]. These bacterial strains were isolated from bovine rumen fluid, soil, and pig feces. Skatole-degrading activity was also reported for several pure isolated bacteria, such as *Pseudomonas putida* [77], *Pseudomonas aeruginosa* [78], *Burkholderia* strain [79], *Acinetobacter toweneri* and *Acinetobacter guillouiae* [80]. Moreover, the soil bacterium *Cupriavidus* sp. strain KK10 is also capable of skatole degradation (100 mg/l in 24 h) [81]. An *in vitro* study of *Lactobacillus brevis* demonstrated its strong ability to remove skatole from the medium [82]. Skatole-degrading activity was also reported for bacteria isolated from activated sludge, e.g., *Rhodococcus* [83].

IAA decarboxylation leading to skatole formation is catalyzed by the indoleacetate decarboxylase enzyme (IAD), which may serve as a marker for the identification of skatole-producing bacteria. IAD sequences were identified in two bacteria of human origin, namely, *Olsenella uli* and *Faecalicatena contorta* [57]. The relevance of these bacteria to human health is based on their findings in the human gingival crevice [84] and gangrenous appendicitis [85]. Additionally, both bacteria were found in the human oral system, which implies skatole contributes to halitosis, a noticeable unpleasant breath odor [86]. In a case study, *Olsenella uli* was reported to be involved in the development of pneumonia (see further in Chapter 4.3) [87] (Fig. 1). Furthermore, *Bacterioides thetaiotaomicron* was reported to be a skatole-producing bacterium that occurs in the human colon [88].

The high amount of animal waste due to meat production and consumption probably contributes to the spread of insect-borne diseases [22–24] as a result of intriguing skatole properties. Therefore, the degradation of skatole seems to be crucial. Interestingly, activated sludge containing various genera of bacteria (e.g., *Zoogloea, Arthrobacter*, and *Rhodococcus*) was able to degrade 250 mg/l skatole (approx. 1.9 mM) within 48 h completely [89]. This process may help suppress the spread of pathogenic bacteria-mediated infections [90].

On the other hand, the presence of skatole in feces is inevitable since both the genera *Clostridium* and *Lactobacillus* are the main populations in the animal and human gastrointestinal tract [91]. It was observed that approx. 190–250 μM skatole has a bacteriostatic effect on Gram-negative bacterial strains *Escherichia*, *Salmonella,* and *Shigella* [92]. Furthermore, skatole completely inhibits *L. acidophilus* growth at concentrations greater than 3 mM [92,93].

In general, it is known that dietary habits have a huge effect on the intestinal microbiome composition. Skatole production is particularly associated with higher meat consumption, and it is well known that protein quality and quantity differ in various types of meat. This feature may affect (but not exclusively) the composition of intestinal bacteria and subsequently also the formation of their metabolites, including skatole [94]. Shi et al. reported that a more diverse intestinal microbiome was detected in a test group of individuals who consumed chicken compared with those who eat pork [67]. The first group had a higher abundance of *Prevotella 2*, *Prevotella 9*, *Megamonas*, *Dialister* and *Faecalibacterium*, whereas the second group exhibited an increased abundance of *Bacteriodes*, *Roseburia*, *Ruminococcus 2*, *Dialister,* and *Faecalibacterium*. Additionally, the study revealed a positive correlation between *Prevotella 2* and *Prevotella 9* abundance and skatole fecal levels [67].

Thus, it is clear that skatole may affect intestinal bacteria and consequently the host. The finding that increased microbiota diversity simultaneously occurred with a high production of skatole in chicken eaters compared with pork eaters raises the question “Does skatole formation result in a healthy gut or dysbiosis?” Although this question may be difficult to answer with current scientific knowledge, the impact of high skatole concentrations on signaling in intestinal cells can give us an idea of whether skatole is involved in intestinal inflammatory conditions. Therefore, we further describe specific signaling pathways that may participate in this phenomenon.

4.2. Gastrointestinal tract

There are only a few identified molecular targets associated with the patho/physiological action of skatole in humans. As a result of the presence of *aromatic* structures, one of the obvious molecular targets skatole interacts with is the aryl hydrocarbon receptor (AhR).

AhR is a ligand-activated transcription factor that plays a crucial role in many physiological functions, such as regulation of the cell cycle, immune response, biotransformation of xenobiotics [53,95] and tumor promotion [96]. In the absence of ligand, AhR resides in the cytosol together with cochaperone proteins. After ligand binding, AhR translocates to the nucleus, where it forms a heterodimer with the AhR nuclear translocator (ARNT). Together, this complex binds to specific dioxin/xenobiotic-responsive elements in DNA. This process results in the expression of the appropriate target genes. The spectrum of AhR ligands is wide, and polycyclic aromatic hydrocarbons (PAHs), dioxins, and various tryptophan metabolites (e.g., indole-3-acrylate, indole-3-acetamide, indole) are noted among typical ligands with *aromatic/planar* structures [97]. Naturally, skatole is not an exception.

Skatole is an activator of AhR and a weak inducer of AhR target genes, particularly cytochromes P450 (CYP) 1A1/1A2 and CYP1B1, in human liver cell lines and primary cultures of human hepatocytes [64,98,99] (Fig. 2, step 1). AhR dependence was demonstrated by analyzing the time course of AhR-dependent luciferase activity and *CYP1A1* mRNA using siRNA for AhR or a specific AhR antagonist (CH223191) in HepG2-C3 cells [98]. In general, the induction of CYP1A1/1A2/1B1 was much weaker than for the positive control, 2,3,7,8-tetrachlordibenzo-p-dioxin (TCDD) [95,98]. At that time, it was not confirmed whether skatole is a true ligand of AhR.

This question was answered in a recent study, in which skatole was tested together with other intestinal microbial metabolites of Trp. However, the ability to displace radiolabeled TCDD from mouse AhR was demonstrated with an IC_{50} of greater than 100 μM. Despite this finding, 200 μM skatole initiated nuclear translocation and induced AhR:ARNT complex formation and AhR enrichment on the *CYP1A1* promoter in human LS180 cells [53]. Furthermore, the induction of *CYP1A1* mRNA in intestinal HT-29 cells was abolished in the AhR-knockout HT-29 counterpart [53]. Consistent observations were also made by other authors [64,100,101].

The use of another intestinal cell line, Caco-2, which is often used as an *in vitro* model of a ‘normal’ intestinal phenotype after spontaneous differentiation, demonstrated that incubation with skatole (1000 μM) for 24 h resulted in CYP1A1 protein induction. This induction was reversed with the AhR antagonist CH22319 [102]. Moreover, skatole activated mitogen-activated protein kinases (MAPKs), namely, p38, ERK and JNK (Fig. 2, step 4), and significantly increased apoptosis after 48 and 72 h of incubation (Fig. 2, step 3). The decline in cellular viability was partially reversed by the AhR antagonist and promoted by the p38 inhibitor. This finding suggests that although AhR activation by skatole promotes apoptosis (Fig. 2, step 2), p38 activation has a suppressive effect on cell viability (Fig. 2, step 5). Given that increased intestinal epithelial cell (IEC) apoptosis has been observed among patients with inflammatory bowel disease (IBD) (e.g., ulcerative colitis, Crohn's disease) [103], these data suggest that skatole may contribute to the initiation and/or progression of intestinal

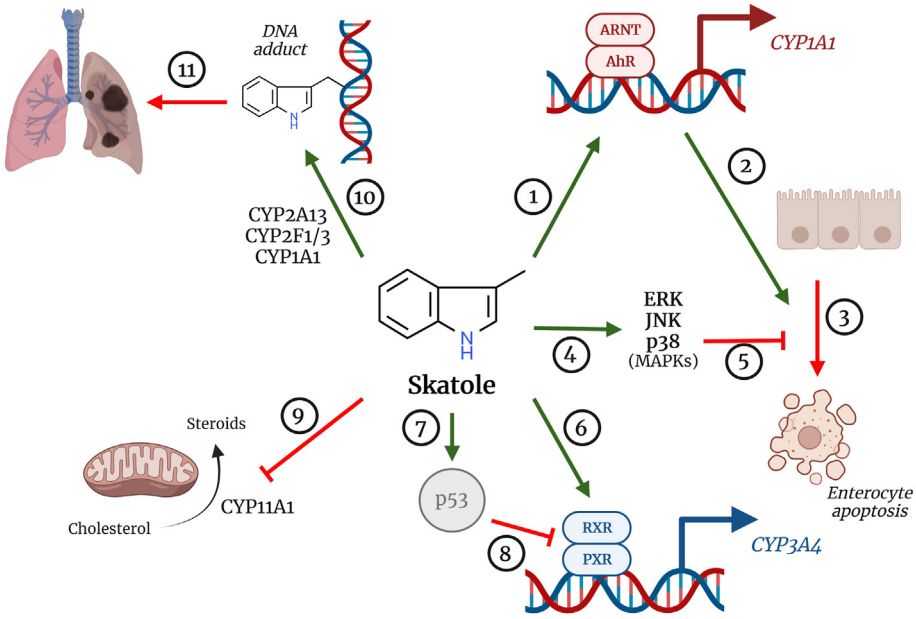

Fig. 2. Molecular targets of skatole. Skatole activates AhR as demonstrated by the induction of *CYP1A* mRNA expression (1). Skatole significantly increase enterocytes apoptosis (3), which is associated with AhR (2). Furthermore, skatole activates specific MAPKs (4). Only p38 activation appears to be important for enterocyte apoptosis. Skatole activates PXR and induces *CYP3A4* mRNA expression (6). Moreover, skatole activates p53 (7), which inhibits the binding of PXR to the CYP3A4 promoter (8). In mitochondria, skatole inhibits the CYP11A1 enzyme. This results in suppressed cholesterol conversion to steroid hormones (9). In lung tissue, CYP2A13, CYP2F1/3 and CYP1A1 are the main factors involved in skatole-induced pulmonotoxicity. These lung enzymes catalyze the dehydrogenation of 3MI to its reactive intermediate 3MEIN, which forms DNA adducts (10). This process may result in lung damage or even cancer development (11). This figure was created based on information from the references provided in the text.

diseases. However, this finding is in contrast to the observations that some AhR ligands with indole scaffolds (e.g., 6-formylindolo [3,2-b] carbazole, FICZ; 2-(1H-indole-3-carbonyl)-thiazole-4-carboxylic acid methyl ester, ITE) improve experimentally induced conditions mimicking the IBD state [104,105]. However, AhR activation by ligands, such as TCDD [106] or kynurenine [107], has been reported to suppress the apoptotic response in both murine and human cells.

Thus, the causal relationship between skatole and IBD remains to be confirmed, but it is astonishing that inevitable skatole should be involved in the initiation or progression of IBD. However, in these *in vitro* cellular models, skatole metabolism is typically not considered (host or microbiota driven), extreme skatole concentrations are used (for which the justification is missing), and *in vitro* cellular models lack intestinal motility. Therefore, the exact mechanism of action and possible causal relationships between intestinal cell apoptosis and skatole concentration require further investigation.

Another molecular target that is involved in intestinal barrier integrity and functions similarly to AhR as a ligand-activated transcription factor is pregnane X receptor (PXR) [108]. Skatole was shown to activate PXR (Fig. 2, step 6) in the reporter gene assay with an EC_{50} of approx. 50 μM and approximately 47% efficacy (in relation to the ligand rifampicin) [109]. However, skatole only mildly and insignificantly induced PXR-driven gene expression, as measured by *CYP3A4* or *MDR1* mRNA expression in LS180 cells [109]. This finding is in contrast to another study, in which skatole decreased the basal expression of *CYP3A4*, *CYP2B6,* and *CYP2A6* in differentiated HepaRG cells but not in primary human hepatocytes [110,111]. Moreover, skatole also had stimulatory effects on CYP2A6 protein expression in porcine hepatocytes [112]. The importance of such finding is emphasized by a study from 2021 that revealed that primary porcine hepatocytes show a similar pattern as primary human hepatocytes and are comparable [113].

The abovementioned downregulation of CYP basal expression directly correlates with the decrease in *PXR* mRNA expression in HepaRG cells. Interestingly, similar to TCDD, 100 μM skatole suppressed rifampicin-induced *CYP3A4* expression in HepaRG cells (by approximately 20%) as well as in human hepatocytes (by approximately 60%) [111]. This finding highlights the functional crosstalk between AhR and PXR signaling.

A possible explanation for the relatively high PXR activation but relatively low induction of PXR-driven genes may be that skatole activates p53, which inhibits the binding of PXR to the CYP3A4 promoter in HepG2 cells [114] (Fig. 2, steps 7 and 8).

Interestingly, skatole also affects mitochondria. Skatole inhibited the enzyme CYP11A1 with an IC_{50} of approximately 1.45 mM [115] (Fig. 2, step 9). Given that this enzyme is responsible for the synthesis of various steroid hormones, this finding suggests a link between skatole and the development of IBD [115]. This idea is supported by the disruption of steroidogenesis and decreased glucocorticoid production that are involved in the development of IBD [116].

4.3. Pulmonary system

As mentioned earlier, *Olsenella uli* is a Gram-positive bacterium that can produce skatole from IAA [57]. It is also a common bacterium in the oral cavity or gastrointestinal tract [57,86]. However, its involvement in the development of pulmonary pneumonia is currently being assessed. In the Yufen et al. case study, a 70-year-old man, formerly a heavy smoker, was diagnosed with pneumonia from the pulmonary abscess. The patient's sputum sample was analyzed, and the results confirmed the presence of *Olsenella uli*. After 10 days of specific treatment, the patient showed a significant improvement in the pulmonary lesion and was discharged [87]. This case suggests a possible link between the presence of *Olsenella uli* in the lungs and pneumonia. Additionally, this bacterium was detected in the blood of patients suffering from diseases associated with the gastrointestinal tract (cholangiocarcinoma, choledochal

cyst) [117].

Although it is logical to investigate the role of skatole in intestinal patho-/physiology due to its possibly high local concentrations, the case reveals another organ where skatole was found to be toxic. This organ is the lungs, and skatole pulmonotoxicity was demonstrated in various species (such as cattle or rodents) but not in boars or pigs [118]. In particular, ruminants are highly susceptible given that a skatole dose of 20–40 mg/kg body weight (BW) is usually fatal within 72 h after intravenous infusion or intraruminal administration, e.g., for goats, cattle, and sheep [119,120]. In sheep, signs of respiratory distress manifested with of 200 mg/kg BW of skatole [120,121], and the time period of manifestation was similar for goats and cattle [121]. Interestingly, in cattle, skatole reaches a maximum plasma concentration (18.5 μg/ml ~141 μM for 0.2 g/kg BW) within 3–9 h and then declines to often low to undetectable levels within 24–48 h [119,120]. This finding suggests rapid metabolism and/or excretion. However, these studies are outdated, and more recent studies do not exist.

In contrast, rodents and rabbits are less sensitive to skatole-induced lung damage. The intraperitoneal LD_{50} of skatole for mice was 578 mg/kg BW, and the fatal dose for rabbits was greater than 900 mg/kg [122]. In accordance, the oral LD_{50} for skatole was 3450 mg/kg for rat [123]. Therefore, the route of exposure is significant for skatole pulmonotoxicity.

Given that acute pulmonary edema and emphysema were observed in cattle after intraruminal doses of skatole, it is clear that skatole is absorbed into the bloodstream and selectively disturbs the lungs of the affected animal [40,119]. A similar observation found significantly more residual radioactivity in the lungs 4 h after dosing compared to other tissues after intratracheal infusion of radiolabeled skatole in rabbits [124]. Thus, skatole seems to be rapidly absorbed from the lung tissue and simultaneously rapidly metabolized before being excreted in the urine in non-human species. Therefore, there is a question of whether skatole is absorbed in sufficient amounts into human lungs despite minimal detectable skatole levels in human blood as a product of intestinal Trp metabolism. To date, this route is only hypothetical for humans, but data from other species indicate the presence of this route.

Unrelated to the GI tract, a significant impact of skatole on the human pulmonary system is attributed to tobacco pyrolysis of Trp during burning [33]. Several *in vitro* studies helped to understand the toxic action of skatole on airway cells, which involves cytochrome P450 enzymes. Namely, human CYP2A13 and 2F1/3 [125], goat CYP4B2 [126] and rabbit CYP4B1 [127] are the main factors of skatole-induced pulmonary toxicity (Fig. 2, steps 10, 11).

Rabbit Clara cells are susceptible to skatole-induced toxicity in comparison to type II alveolar epithelial cells and alveolar macrophages [128]. The IC_{50} for skatole-induced cytotoxicity was approximately 750 μM within 4 h in Clara cells, and the toxicity was inhibited with 1-aminobenzotriazole (ABT), a nonspecific and irreversible inhibitor of cytochrome P450. Interestingly, both isolated rabbit Clara cells and alveolar macrophages bioactivate skatole to the same metabolites despite the use of different oxidative pathways [129]. The reactive intermediate was identified as 3-methyleneindolenine (3MEIN), which is detoxified by glutathione (GSH) [129,130].

In normal human bronchial epithelial cells (BEAS-2B) transfected with different CYP enzymes, those expressing CYP2F1 and CYP3A4 were most susceptible to skatole-induced cytotoxicity (34% and 45% of control, respectively) as measured by leakage of lactate dehydrogenase (LDH) after incubation with 1 mM skatole for 48 h [131]. Cells susceptible to skatole-mediated toxicity were conclusively protected with ABT. Interestingly, depletion of GSH with diethylmaleate (DEM) decreased the onset and increased the extent of cell death (i.e., cytotoxicity) induced by skatole [131]. Furthermore, a low concentration of skatole (10 μM) induced apoptosis as measured by DNA fragmentation, and the presence of ABT reversed this effect. Given that CYP3A4 is naturally absent in lung tissue/cells, it is clear that CYP2F1 is an important protein that may bioactivate 3MI to 3MEIN, which induces apoptosis and DNA fragmentation at relatively low (5–10 μM) concentrations [131].

Extrahepatic CYP1B1 and the main liver and intestinal P450s CYP2A6, CYP2C19, CYP2D6, CYP2B6 and CYP2E1 do not form 3MEIN from 3MI [132] despite their ability to form other metabolites, such as 3-methyloxindole or indole-3-carbinol [133]. It appears that CYPs present predominantly in the lungs, such as CYP2F1, CYP1A1, CYP2A13 and CYP4B1, catalyze the dehydrogenation of 3MI to 3MEIN [134]. This intermediate is highly mutagenic [125] and generates levels of mutagenicity similar to or greater than typical cigarette smoke mutagens, such as benzo[a]pyrene (B[a]P) and 4-(methylnitrosamino)-1-(3-pyridyl)-1-butanone (NNK) [134]. Furthermore, the formation of DNA adducts (Fig. 2, step 10) was observed after the incubation of rat liver, goat lung, and human liver microsomes with skatole [135]. Although liver microsomes contain abundant levels of CYP3A4 and CYP1A2 and are involved in 3MI metabolism to 3MEIN [131,132], their involvement in skatole-induced pulmonotoxicity is likely negligible due to the high GSH content in the liver and/or the high level of other CYPs that detoxify 3MI to less reactive metabolites. Furthermore, using genetically engineered mice, it was shown that although CYP2F2 (ortholog of human CYP2F1) plays a significant role in the metabolism of 3MI in the lungs, both CYP2F2 and CYP2A5 (ortholog of human CYP2A13) are significant players in skatole-mediated toxicity in the olfactory mucosa [136].

Based on the ability of 3MEIN to form DNA adducts, skatole can be classified as a human pro-carcinogen that contributes to the promotion of lung cancer (Fig. 2, step 11). The *in vitro* study confirmed that low concentrations of skatole (0.1–10 μM) induced markers of carcinogenesis, including DNA damage, p53 phosphorylation, and nuclear localization in human bronchial epithelial cells (NHBEs) [125]. Maximum DNA damage (measured by comet assay) was observed after 4 h of treatment with 5 μM skatole and decreased to untreated levels within 24 h. Moreover, DNA damage was mainly caused by single-strand breaks [125].

5. Concluding remarks and further perspectives

(1) Skatole toxicity potentially reflects the biotransformation potential of a given tissue that results in the formation of 3MEIN, which is most likely responsible for DNA modification, pulmonotoxicity, and possibly intestinal apoptosis. Furthermore, both important CYPs, namely, CYP1A1 and CYP2F1, are induced by the same 3MI concentrations that damaged DNA in primary NHBE cells [134]. The involvement of AhR in the induction of CYP1A1 was confirmed by the use of the AhR antagonist α-naphthoflavone. In contrast, CYP2F1 induction does not appear to require AhR [134]. This finding suggests that a positive feedback loop (through AhR activation) may contribute to an increased risk of (not only) skatole-induced carcinogenesis in chronic smokers.

(2) Skatole is a product of bacterial metabolism in the intestine. To date, it is difficult to determine whether the presence of skatole is physiological and what concentrations indicate dysbiosis. With the exception of smoking, we cannot avoid skatole exposure, as it comes from the combination of diet and microbiome composition. Thus, we conclude that optimal intestinal (and possibly blood) concentrations contribute to healthy living. This notion is further supported by an increased presence of skatole in the feces of healthy subjects compared with patients with ulcerative colitis or

Crohn's disease [36]. On the other hand, there are studies that indicate that higher levels of skatole are associated with the occurrence of various intestinal diseases. Due to complex human and microbiota interactions and some studies suggesting the toxicity of skatole, particularly for high doses, we believe that skatole should be maintained at a low but detectable intestinal level.

(3) Given that the role of skatole in intestinal patho-/physiology has been insufficiently investigated, a couple of important questions must be addressed: a) Does consumption of plant-based proteins (meal) build up the level of skatole similar as animal meat (e.g., chicken, pork)?; b) Is a high intestinal skatole concentration the cause or the result of specific intestinal bowel diseases? c) Can absorption of low doses of intestinal microbiota-produced skatole into the bloodstream result in the induction of pulmonary damage and eventually lung cancer after 3-5 decades of human life? These questions are still very difficult to answer, as no studies to date addressing skatole benefits or negative consequences to the human body have been reported.

(4) Skatole exhibits great potential for use as a biomedical marker for the development of various GI diseases. Unfortunately, determining the concentration of skatole in feces may not be an ideal solution, as the content in excreted feces may not completely correspond to the physiological conditions in the gut (due to external influences such as oxidation in the air, etc.). Thus, more suitable samples for skatole detection, e.g., urine-based analyses [38], should be examined. One of the best samples would be human blood, where skatole levels were already measured in 1988 in healthy individuals and patients with HE [72]. A direct correlation was observed between HE patients and increased skatole levels. Despite the fact that the intestinal microbiome shows high variability among individuals and is widely affected by lifestyle habits (dietary tryptophan content, smoking, alcohol consumption, drug abuse or genetic predispositions), skatole blood levels under precisely defined conditions might serve as a suitable marker for patient diagnosis.

(5) According to available interdisciplinary studies, we suggest a connection between bacterial skatole synthesis in the intestine and skatole-induced pulmonotoxicity. For a long time, the link between these two phenomena was missing given that each process had been described separately. The process of skatole synthesis has been described in detail, but pulmonotoxicity was successfully described only in ruminants and rodents after intravenous infusion [119,120]. The link between these two processes could be the skatole-forming bacterium *Olsenella uli*. It is possible that skatole is transported from the site of synthesis (intestine) through blood to the lungs, where it is converted into its reactive intermediate and mutagen 3MEIN and induces pulmonotoxicity [129,130]. Given that *Olsenella uli* was found in the blood of patients with GIT-associated diseases [117], it may represent a crucial link between skatole metabolism in the intestine and its subsequent pulmonotoxicity. Due to the limited data from human studies, future research should focus on the confirmation or rejection of this gut-lung axis.

(6) In light of demonstrated skatole-induced pulmonotoxicity in animals, it is important to determine whether the use of skatole as a patented malodorant [34] is safe for humans. Therefore, a great deal of research will be required before it is possible to completely understand the impact of this stinky molecule on human patho-/physiology.

Ethics approval and consent to participate

Not applicable.

Availability of data and material

Not applicable.

Funding

This work was supported by the student grant from Palacký University in Olomouc [PrF-2022-009] and by the Czech Health Research Council [grant number NV19-05-00220].

Author contributions

Eliška Zgarbová; Writing – original draft; Writing – review & editing.

Radim Vrzal: Writing – original draft; Writing – review & editing; Supervision.

Declaration of competing interest

Not applicable.

Acknowledgments

The figures were created with BioRender.com. The structures were obtained from the free chemical structure database ChemSpider. The references were created using reference management software EndNote.

References

[1] G. Fenaroli, N. Bellanca, T.E. Furia, Fenaroli's Handbook of Flavor Ingredients, CRC press, Cleveland (Ohio), 1975, p. 551.
[2] G. Osborne, D. Penman, R. Chapman, Attraction of aphodius-tasmaniae hope to skatole, Aust. J. Agric. Res. 26 (1975) 839–841.
[3] L. Brieger, Ueber die fliichtigen Bertandtheile der menechlichen Excremente [On the volatile components of human excrement], Ber. Dtsch. Chem. Ges. 10 (1877) 1027–1032.
[4] H.M. Database, Showing Metabocard for 3-Methylindole, 2021.
[5] Y. Mishiro, K. Kirimura, T. Koyama, Chromatographic separation of ether-extractable components of aerobically incubated human whole saliva, J. Dent. Res. 48 (1969).
[6] PellWall, Skatole 1%, 2021.
[7] S. Arctander, Perfume and Flavor Chemicals (Aroma Chemicals), Allured Publishing Corporation, Illinois, 1969.
[8] CompoundInterest, The Chemistry of Ice Cream - Components, structure and flavour, 2015.
[9] G.G. Hawley, The Condensed Chemical Dictionary, Van Nostrand Reinhold Co, New York, 1975, p. 957.
[10] J.I. Gordon, Honor thy gut symbionts redux, Science 336 (2012) 1251–1253.
[11] J. Shi, D. Zhao, S. Song, M. Zhang, G. Zamaratskaia, X. Xu, G. Zhou, C. Li, High-meat-protein high-fat diet induced dysbiosis of gut microbiota and tryptophan metabolism in wistar rats, J. Agric. Food Chem. 68 (2020) 6333–6346.
[12] W.R. Dunstan, On the occurrence of skatole in the vegetable kingdom, Proc. Roy. Soc. Lond. 46 (1889) 211–215.
[13] J.R. Partington, A History of Chemistry, Macmillan and Company Limited, St Martin's Street London WC, 1964, p. 1007.
[14] A.A. Szogi, J.H. Loughrin, M.B. Vanotti, Improved water quality and reduction of odorous compounds in anaerobic lagoon columns receiving pre-treated pig wastewater, Environ. Technol. 39 (2018) 2613–2621.
[15] T.R. Whitehead, N.P. Price, H.L. Drake, M.A. Cotta, Catabolic pathway for the production of skatole and indoleacetic acid by the acetogen Clostridium drakei, Clostridium scatologenes, and swine manure, Appl. Environ. Microbiol. 74 (2008) 1950–1953.
[16] M.H. Lee, K.H. Kim, B.H. Jeon, S.H. Jo, Y.H. Kim, B.W. Kim, S.B. Cho, O.H. Hwang, S.S. Bhattacharya, Effect of slurry treatment approaches on the reduction of major odorant emissions at a hog barn facility in South Korea, Environ. Technol. 38 (2017) 506–516.
[17] S. Trabue, B. Kerr, B. Bearson, C. Ziemer, Swine odor analyzed by odor panels and chemical techniques, J. Environ. Qual. 40 (2011) 1510–1520.
[18] Y. Zhou, S.A. Hallis, T. Vitko, I.H. Suffet, Identification, quantification and

treatment of fecal odors released into the air at two wastewater treatment plants, J. Environ. Manag. 180 (2016) 257–263.
[19] Z. Yan, Y. Zhang, J. Yu, H. Yuan, M. Yang, Identification of odorous compounds in reclaimed water using FPA combined with sensory GC-MS, J. Environ. Sci. (China) 23 (2011) 1600–1604.
[20] J. Zhu, Y. Niu, Z. Xiao, Characterization of the key aroma compounds in Laoshan green teas by application of odour activity value (OAV), gas chromatography-mass spectrometry-olfactometry (GC-MS-O) and comprehensive two-dimensional gas chromatography mass spectrometry (GC × GC-qMS), Food Chem. 339 (2021), 128136.
[21] B.N. Smith, B.J. Meeuse, Production of volatile amines and skatole at anthesis in some arum lily species, Plant Physiol. 41 (1966) 343–347.
[22] J.W. Beehler, J.G. Millar, M.S. Mulla, Field evaluation of synthetic compounds mediating oviposition inCulex mosquitoes (Diptera: Culicidae), J. Chem. Ecol. 20 (1994) 281–291.
[23] L. Mboera, W. Takken, K. Mdira, G. Chuwa, J. Pickett, Oviposition and behavioral responses of Culex quinquefasciatus to skatole and synthetic oviposition pheromone in Tanzania, J. Chem. Ecol. 26 (2000) 1193–1203.
[24] D. Hughes, J. Pelletier, C. Luetje, W. Leal, Odorant receptor from the southern house mosquito narrowly tuned to the oviposition attractant skatole, J. Chem. Ecol. 36 (2010) 797–800.
[25] L. Malleret, A. Bruchet, M.C. Hennion, Picogram determination of "earthly-musty" odorous compounds in water using modified closed loop stripping analysis and large volume injection GC/MS, Anal. Chem. 73 (2001) 1485–1490.
[26] M. Aluwe, M. Aaslyng, G. Backus, M. Bonneau, P. Chevillon, J. Haugen, L. Meier-Dinkel, D. Morlein, M. Oliver, H. Snoek, F. Tuyttens, M. Font-i-Furnols, Consumer acceptance of minced meat patties from boars in four European countries, Meat Sci. 137 (2018) 235–243.
[27] R. Patterson, 5ALPHA-ANDROST-16-ENE-3-1 - compound responsible for taint in boar fat, J. Sci. Food Agric. 19 (1968) 31(. -+).
[28] J. Haugen, C. Brunius, G. Zamaratskaia, Review of analytical methods to measure boar taint compounds in porcine adipose tissue: the need for harmonised methods, Meat Sci. 90 (2012) 9–19.
[29] S. Bañón, E. Costa, M.D. Gil, M.D. Garrido, A comparative study of boar taint in cooked and dry-cured meat, Meat Sci. 63 (2003) 381–388.
[30] I. Aldal, O. Andresen, A. Egeli, J. Haugen, A. Grodum, O. Fjetland, J. Eikaas, Levels of androstenone and skatole and the occurrence of boar taint in fat from young boars, Livest. Prod. Sci. 95 (2005) 121–129.
[31] M. Bonneau, P. Walstra, C. Claudi-Magnussen, A.J. Kempster, E. Tornberg, K. Fischer, A. Diestre, F. Siret, P. Chevillon, R. Claus, G. Dijksterhuis, P. Punter, K.R. Matthews, H. Agerhem, M.P. Béague, M.A. Oliver, M. Gispert, U. Weiler, G. von Seth, H. Leask, M. Font I Furnols, D.B. Homer, G.L. Cook, An international study on the importance of androstenone and skatole for boar taint: IV. Simulation studies on consumer dissatisfaction with entire male pork and the effect of sorting carcasses on the slaughter line, main conclusions and recommendations, Meat Sci. 54 (2000) 285–295.
[32] L. Lundstrom, A. Mira-Agudelo, P. Artal, Peripheral optical errors and their change with accommodation differ between emmetropic and myopic eyes, J. Vis. 9 (2009) 17 11–11.
[33] E.L. Wynder, D. Hoffmann, Experimental tobacco carcinogenesis, Science 162 (1968) 862–871.
[34] V.R. Pinney, Non-lethal Weapon Systems, The Woodlands, TX), Ecological Technologies Corporation, Texas (US), 2000.
[35] C. Garner, S. Smith, B. Costello, P. White, R. Spencer, C. Probert, N. Ratcliffe, Volatile organic compounds from feces and their potential for diagnosis of gastrointestinal disease, Faseb. J. 21 (2007) 1675–1688.
[36] V. De Preter, K. Machiels, M. Joossens, I. Arijs, C. Matthys, S. Vermeire, P. Rutgeerts, K. Verbeke, Faecal metabolite profiling identifies medium-chain fatty acids as discriminating compounds in IBD, Gut 64 (2015) 447–458.
[37] C.R. Fellers, R.W. Clough, Indol and skatol determination in bacterial cultures, J. Bacteriol. 10 (1925) 105–133.
[38] L. Prospero, G. Riezzo, M. Linsalata, A. Orlando, B. D'Attoma, M. Di Masi, M. Martulli, F. Russo, Somatization in patients with predominant diarrhoea irritable bowel syndrome: the role of the intestinal barrier function and integrity, BMC Gastroenterol. 21 (2021) 235.
[39] M. Simeoni, M.L. Citraro, A. Cerantonio, F. Deodato, M. Provenzano, P. Cianfrone, M. Capria, S. Corrado, E. Libri, A. Comi, A. Pujia, L. Abenavoli, M. Andreucci, M. Cocchi, T. Montalcini, G. Fuiano, An open-label, randomized, placebo-controlled study on the effectiveness of a novel probiotics administration protocol (ProbiotiCKD) in patients with mild renal insufficiency (stage 3a of CKD), Eur. J. Nutr. 58 (2019) 2145–2156.
[40] M.T. Yokoyama, J.R. Carlson, Microbial metabolites of tryptophan in the intestinal tract with special reference to skatole, Am. J. Clin. Nutr. 32 (1979) 173–178.
[41] A. Nakao, M. Ball, The appearance of a skatole derivative in the urine of schizophrenics, J. Nerv. Ment. Dis. 130 (1960) 417–419.
[42] R. Ose, K. Hirano, S. Maeno, J. Nakagawa, S. Salminen, T. Tochio, A. Endo, The ability of human intestinal anaerobes to metabolize different oligosaccharides: novel means for microbiota modulation? Anaerobe 51 (2018) 110–119.
[43] X. Wang, G.R. Gibson, A. Costabile, M. Sailer, S. Theis, R.A. Rastall, Prebiotic supplementation of in vitro fecal fermentations inhibits proteolysis by gut bacteria, and host diet shapes gut bacterial metabolism and response to intervention, Appl. Environ. Microbiol. (2019) 85.
[44] A.N. Thorburn, L. Macia, C.R. Mackay, Diet, metabolites, and "western-lifestyle" inflammatory diseases, Immunity 40 (2014) 833–842.
[45] G. Clarke, R.M. Stilling, P.J. Kennedy, C. Stanton, J.F. Cryan, T.G. Dinan, Minireview: gut microbiota: the neglected endocrine organ, Mol. Endocrinol. 28 (2014) 1221–1238.
[46] A. Blankfield, A brief historic overview of clinical disorders associated with tryptophan: the relevance to chronic fatigue syndrome (CFS) and fibromyalgia (FM), Int. J. Tryptophan Res. 5 (2012) 27–32.
[47] J.K. Nicholson, I.D. Wilson, Opinion: understanding 'global' systems biology: metabonomics and the continuum of metabolism, Nat. Rev. Drug Discov. 2 (2003) 668–676.
[48] J. Gao, K. Xu, H. Liu, G. Liu, M. Bai, C. Peng, T. Li, Y. Yin, Impact of the gut microbiota on intestinal immunity mediated by tryptophan metabolism, Front. Cell. Infect. Microbiol. 8 (2018) 13.
[49] J.C. Peters, Tryptophan nutrition and metabolism: an overview, Adv. Exp. Med. Biol. 294 (1991) 345–358.
[50] M. Yokoyama, J. Carlson, Dissimilation of tryptophan and related indolic compounds by ruminal microorganisms in-vitro, Appl. Microbiol. 27 (1974) 540–548.
[51] UniProt, Tryptophanase - tnaA Gene & Protein, 2021.
[52] J. Koga, T. Adachi, H. Hidaka, Purification and characterization of INDOLE-PYRUVATE decarboxylase - a novel enzyme for INDOLE-3-ACETIC-ACID biosynthesis in enterobacter-cloacae, J. Biol. Chem. 267 (1992) 15823–15828.
[53] B. Vyhlídalová, K. Krasulová, P. Pečinková, A. Marcalíková, R. Vrzal, L. Zemánková, J. Vančo, Z. Trávníček, J. Vondráček, M. Karasová, S. Mani, Z. Dvořák, Gut microbial catabolites of tryptophan are ligands and agonists of the aryl hydrocarbon receptor: a detailed characterization, Int. J. Mol. Sci. 21 (2020).
[54] R.D. Schultz, D. Norman, Effects of plant growth regulators (auxins and auxin esters) on the survival of free cells of the ehrlich ascites carcinoma, Nature 199 (1963) 260–262.
[55] N. Wilck, M.G. Matus, S.M. Kearney, S.W. Olesen, K. Forslund, H. Bartolomaeus, S. Haase, A. Mähler, A. Balogh, L. Markó, O. Vvedenskaya, F.H. Kleiner, D. Tsvetkov, L. Klug, P.I. Costea, S. Sunagawa, L. Maier, N. Rakova, V. Schatz, P. Neubert, C. Frätzer, A. Krannich, M. Gollasch, D.A. Grohme, B.F. Côrte-Real, R.G. Gerlach, M. Basic, A. Typas, C. Wu, J.M. Titze, J. Jantsch, M. Boschmann, R. Dechend, M. Kleinewietfeld, S. Kempa, P. Bork, R.A. Linker, E.J. Alm, D.N. Müller, Salt-responsive gut commensal modulates Th17 axis and disease, Nature 551 (2017) 585–589.
[56] L. Cervantes-Barragan, J.N. Chai, M.D. Tianero, B. Di Luccia, P.P. Ahern, J. Merriman, V.S. Cortez, M.G. Caparon, M.S. Donia, S. Gilfillan, M. Cella, J.I. Gordon, C.S. Hsieh, M. Colonna, Lactobaccillus reuteri induces gut intraepitelial CD4+ Cd8aa+ T cells, Science 357 (2017) 806–810.
[57] D. Liu, Y. Wei, X. Liu, Y. Zhou, L. Jiang, J. Yin, F. Wang, Y. Hu, A.N. Nanjaraj Urs, Y. Liu, E.L. Ang, S. Zhao, H. Zhao, Y. Zhang, Indoleacetate decarboxylase is a glycyl radical enzyme catalysing the formation of malodorant skatole, Nat. Commun. 9 (2018).
[58] M.T. Jensen, R.P. Cox, B.B. Jensen, 3-Methylindole (skatole) and indole production by mixed populations of pig fecal bacteria, Appl. Environ. Microbiol. 61 (1995) 3180–3184.
[59] F. Dong, F. Hao, I.A. Murray, P.B. Smith, I. Koo, A.M. Tindall, P.M. Kris-Etherton, K. Gowda, S.G. Amin, A.D. Patterson, G.H. Perdew, Intestinal microbiota-derived tryptophan metabolites are predictive of Ah receptor activity, Gut Microb. 12 (2020) 1–24.
[60] T. Pavlova, V. Vidova, J. Bienertova-Vasku, P. Janku, M. Almasi, J. Klanova, Z. Spacil, Urinary intermediates of tryptophan as indicators of the gut microbial metabolism, Anal. Chim. Acta 987 (2017) 72–80.
[61] A. Mori, Y. Yasaka, K. Masamoto, M. Hiramatsu, GAS-CHROMATOGRAPHY of 5-HYDROXY-3-METHYLINDOLE in human urine, Clin. Chim. Acta 84 (1978) 63–68.
[62] C.A. Herter, The occurrence of skatol in the human intestine, J. Biol. Chem. 4 (1908) 9.
[63] R. Penn, B.J. Ward, L. Strande, M. Maurer, Review of synthetic human faeces and faecal sludge for sanitation and wastewater research, Water Res. 132 (2018) 222–240.
[64] M. Stepankova, I. Bartonkova, E. Jiskrova, R. Vrzal, S. Mani, S. Kortagere, Z. Dvorak, Methylindoles and methoxyindoles are agonists and antagonists of human aryl hydrocarbon receptor, Mol. Pharmacol. 93 (2018) 631–644.
[65] D.A. Karlin, A.J. Mastromarino, R.D. Jones, J.R. Stroehlein, O. Lorentz, Fecal skatole and indole and breath methane and hydrogen in patients with large bowel polyps or cancer, J. Cancer Res. Clin. Oncol. 109 (1985) 135–141.
[66] N.J.W. Novello, W. Wolf, C.P. Sherwin, A quantitative determination of intestinal putrefaction, Am. J. Med. Sci. 170 (1925) 888–894.
[67] J. Shi, D. Zhao, F. Zhao, C. Wang, G. Zamaratskaia, C. Li, Chicken-eaters and pork-eaters have different gut microbiota and tryptophan metabolites, Sci. Rep. 11 (2021), 11934.
[68] M. Friedman, Analysis, nutrition, and health benefits of tryptophan, Int. J. Tryptophan Res. 11 (2018).
[69] H.M. Roager, T.R. Licht, Microbial tryptophan catabolites in health and disease, Nat. Commun. 9 (2018) 3294.
[70] M.S. Farvid, E. Sidahmed, N.D. Spence, K. Mante Angua, B.A. Rosner, J.B. Barnett, Consumption of red meat and processed meat and cancer incidence: a systematic review and meta-analysis of prospective studies, Eur. J. Epidemiol. 36 (2021) 937–951.

[71] D. Codipilly, I. Kleinberg, Generation of indole/skatole during malodor formation in the salivary sediment model system and initial examination of the oral bacteria involved, J. Breath Res. 2 (2008).
[72] Y. Suyama, C. Hirayama, Serum indole and skatole in patients with various liver diseases, Clin. Chim. Acta 176 (1988) 203–206.
[73] R.S. Spray, Three new species of the genus Clostridium, J. Bacteriol. 55 (1948) 839–842.
[74] M. Yokoyama, J. Carlson, L. Holdeman, Isolation and characteristics of a skatole-producing lactobacillus SP from bovine rumen, Appl. Environ. Microbiol. 34 (1977) 837–842.
[75] M.H. Proctor, Bacterial dissimilation of indoleacetic acid: a new route of breakdown of the indole nucleus, Nature 181 (1958) 1345.
[76] X. Li, R. Jensen, O. Hojberg, N. Canibe, B. Jensen, Olsenella scatoligenes sp nov., a 3-methylindole- (skatole) and 4-methylphenol- (p-cresol) producing bacterium isolated from pig faeces, Int. J. Syst. Evol. Microbiol. 65 (2015) 1227–1233.
[77] P. Li, L. Tong, K. Liu, Y.X. Wang, BIODEGRADATION OF 3-METHYLINDOLE BY Pseudomonas putida LPC24 UNDER OXYGEN LIMITED CONDITIONS, Fresenius Environ. Bull. 19 (2010) 238–242.
[78] B. Yin, J.D. Gu, Aerobic degradation of 3-methylindole by Pseudomonas aeruginosa Gs isolated from mangrove sediment, Hum. Ecol. Risk Assess. 12 (2006) 248–258.
[79] Q. Ma, H. Qu, N. Meng, S. Li, J. Wang, S. Liu, Y. Qu, Y. Sun, Biodegradation of skatole by Burkholderia sp. Ido3 and its successful bioaugmentation in activated sludge systems, Environ. Res. 182 (2020), 109123.
[80] T.A. Tesso, A. Zheng, H. Cai, G. Liu, Isolation and characterization of two Acinetobacter species able to degrade 3-methylindole, PLoS One 14 (2019), e0211275.
[81] K. Fukuoka, Y. Ozeki, R.A. Kanaly, Aerobic biotransformation of 3-methylindole to ring cleavage products by Cupriavidus sp. strain KK10, Biodegradation 26 (2015) 359–373.
[82] X. Meng, Z.F. He, H.J. Li, X. Zhao, Removal of 3-methylindole by lactic acid bacteria in vitro, Exp. Ther. Med. 6 (2013) 983–988.
[83] Q. Ma, N. Meng, J.C. Su, Y.J. Li, J.Z. Gu, Y.D. Wang, J.W. Wang, Y.Y. Qu, Z.L. Zhao, Y.Q. Sun, Unraveling the skatole biodegradation process in an enrichment consortium using integrated omics and culture-dependent strategies, J. Environ. Sci., 127 (2023) 688-699.
[84] I. Olsen, J. Johnson, L. Moore, W. Moore, LACTOBACILLUS-ULI SP-NOV and lactobacillus-rimae SP-NOV from the human gingival crevice and emended descriptions of lactobacillus-minutus and streptococcus-parvulus, Int. J. Syst. Bacteriol. 41 (1991) 261–266.
[85] M. Sakamoto, T. Iino, M. Ohkuma, Faecalimonas umbilicata gen. nov., sp nov., isolated from human faeces, and reclassification of Eubacterium contortum, Eubacterium fissicatena and Clostridium oroticum as Faecalicatena contorta gen. nov., comb. nov., Faecalicatena fissicatena comb. nov and Faecalicatena orotica comb. nov, Int. J. Syst. Evol. Microbiol. 67 (2017) 1219–1227.
[86] J. Tonzetich, Production and origin of oral malodor - review of mechanisms and methods of analysis, J. Periodontol. 48 (1977) 13–20.
[87] Y. Yufen, L. Hong, L. Shuai, L. Shushui, J. Nan, L. Yanfei, L. Quing, H. Chuanhua, The Olsenella uli induced pneumonia: a case report, Ann. Clin. Microbiol. Antimicrob. 21 (2022) 1–6.
[88] E.A. Smith, G.T. Macfarlane, Enumeration of human colonic bacteria producing phenolic and indolic compounds: effects of pH, carbohydrate availability and retention time on dissimilatory aromatic amino acid metabolism, J. Appl. Bacteriol. 81 (1996) 288–302.
[89] Q. Ma, S. Liu, S. Li, J. Hu, M. Tang, Y. Sun, Removal of Malodorant Skatole by Two Enriched Microbial Consortia: Performance, Dynamic, Function Prediction and Bacteria Isolation, Science of the Total Environment, 2020, p. 725.
[90] S. Sakar, K. Yetilmezsoy, E. Kocak, Anaerobic digestion technology in poultry and livestock waste treatment - a literature review, Waste Manag. Res. 27 (2009) 3–18.
[91] E. Thursby, N. Juge, Introduction to the human gut microbiota, Biochem. J. 474 (2017) 1823–1836.
[92] R.P. Tittsler, L.A. Sandholzer, E.T. Callahan, The bacteriostatic action of skatole on gram-negative enteric bacilli, J. Infect. Dis. 57 (1935) 57–60.
[93] S. Dreizen, T. Spies, Further studies on the association between the products of protein putrefaction and dental caries activity, J. Dent. Res. 27 (1948) 305–315.
[94] L. Madsen, L.S. Myrmel, E. Fjære, B. Liaset, K. Kristiansen, Links between dietary protein sources, the gut microbiota, and obesity, Front. Physiol. 8 (2017) 1047.
[95] F.P. Guengerich, Cytochrome p450 and chemical toxicology, Chem. Res. Toxicol. 21 (2008) 70–83.
[96] M. Ghotbaddini, V. Moultrie, J.B. Powell, Constitutive aryl hydrocarbon receptor signaling in prostate cancer progression, J. Cancer Treatment Diagn. 2 (2018) 11–16.
[97] M.S. Denison, S.R. Nagy, Activation of the aryl hydrocarbon receptor by structurally diverse exogenous and endogenous chemicals, Annu. Rev. Pharmacol. Toxicol. 43 (2003) 309–334.
[98] M.K. Rasmussen, P. Balaguer, B. Ekstrand, M. Daujat-Chavanieu, S. Gerbal-Chaloin, Skatole (3-methylindole) is a partial aryl hydrocarbon receptor agonist and induces CYP1A1/2 and CYP1B1 expression in primary human hepatocytes, PLoS One 11 (2016), e0154629.
[99] B. Vyhlídalová, K. Poulíková, I. Bartoňková, K. Krasulová, J. Vančo, Z. Trávníček, S. Mani, Z. Dvořák, Mono-methylindoles induce CYP1A genes and inhibit CYP1A1 enzyme activity in human hepatocytes and HepaRG cells, Toxicol. Lett. 313 (2019) 66–76.
[100] T.D. Hubbard, I.A. Murray, G.H. Perdew, Indole and tryptophan metabolism: endogenous and dietary routes to ah receptor activation, Drug Metab. Dispos. 43 (2015) 1522–1535.
[101] T. Hubbard, I. Murray, W. Bisson, T. Lahoti, K. Gowda, S. Amin, A. Patterson, G. Perdew, Adaptation of the human aryl hydrocarbon receptor to sense microbiota-derived indoles, Sci. Rep. 5 (2015).
[102] K. Kurata, H. Kawahara, K. Nishimura, M. Jisaka, K. Yokota, H. Shimizu, Skatole regulates intestinal epithelial cellular functions through activating aryl hydrocarbon receptors and p38, Biochem. Biophys. Res. Commun. 510 (2019) 649–655.
[103] J. Blander, Death in the intestinal epithelium-basic biology and implications for inflammatory bowel disease, FEBS J. 283 (2016) 2720–2730.
[104] T. Ji, C. Xu, L. Sun, M. Yu, K. Peng, Y. Qiu, W. Xiao, H. Yang, Aryl hydrocarbon receptor activation down-regulates IL-7 and reduces inflammation in a mouse model of DSS-induced colitis, Dig. Dis. Sci. 60 (2015) 1958–1966.
[105] J.A. Goettel, R. Gandhi, J.E. Kenison, A. Yeste, G. Murugaiyan, S. Sambanthamoorthy, A.E. Griffith, B. Patel, D.S. Shouval, H.L. Weiner, S.B. Snapper, F.J. Quintana, AHR activation is protective against colitis driven by T cells in humanized mice, Cell Rep. 17 (2016) 1318–1329.
[106] Y. Huang, J. He, H. Liang, K. Hu, S. Jiang, L. Yang, S. Mei, X. Zhu, J. Yu, A. Kijlstra, P. Yang, S. Hou, Aryl hydrocarbon receptor regulates apoptosis and inflammation in a murine model of experimental autoimmune uveitis, Front. Immunol. 9 (2018).
[107] K. Bekki, H. Vogel, W. Li, T. Ito, C. Sweeney, T. Haarmann-Stemmann, F. Matsumura, C.F. Vogel, The aryl hydrocarbon receptor (AhR) mediates resistance to apoptosis induced in breast cancer cells, Pestic. Biochem. Physiol. 120 (2015) 5–13.
[108] A. Garg, A. Zhao, S.L. Erickson, S. Mukherjee, A.J. Lau, L. Alston, T.K. Chang, S. Mani, S.A. Hirota, Pregnane X receptor activation attenuates inflammation-associated intestinal epithelial barrier dysfunction by inhibiting cytokine-induced myosin light-chain kinase expression and c-jun N-terminal kinase 1/2 activation, J. Pharmacol. Exp. Therapeut. 359 (2016) 91–101.
[109] B. Vyhlídalová, I. Bartoňková, E. Jiskrová, H. Li, S. Mani, Z. Dvořák, Differential activation of human pregnane X receptor PXR by isomeric mono-methylated indoles in intestinal and hepatic in vitro models, Toxicol. Lett. 324 (2020) 104–110.
[110] J. Staudinger, Y. Liu, A. Madan, S. Habeebu, C.D. Klaassen, Coordinate regulation of xenobiotic and bile acid homeostasis by pregnane X receptor, Drug Metab. Dispos. 29 (2001) 1467–1472.
[111] M.K. Rasmussen, M. Daujat-Chavanieu, S. Gerbal-Chaloin, Activation of the aryl hydrocarbon receptor decreases rifampicin-induced CYP3A4 expression in primary human hepatocytes and HepaRG, Toxicol. Lett. 277 (2017) 1–8.
[112] G. Chen, R.A. Cue, K. Lundstrom, J.D. Wood, O. Doran, Regulation of CYP2A6 protein expression by skatole, indole, and testicular steroids in primary cultured pig hepatocytes, Drug Metab. Dispos. 36 (2008) 56–60.
[113] S. Gerbal-Chaloin, P. Briolotti, M. Daujat-Chavanieu, M.K. Rasmussen, Primary hepatocytes isolated from human and porcine donors display similar patterns of cytochrome p450 expression following exposure to prototypical activators of AhR, CAR and PXR, Curr. Res. Toxicol. 2 (2021) 149–158.
[114] A. Elias, J. Wu, T. Chen, Tumor suppressor protein p53 negatively regulates human pregnane X receptor activity, Mol. Pharmacol. 83 (2013) 1229–1236.
[115] A. Mosa, A. Gerber, J. Neunzig, R. Bernhardt, Products of gut-microbial tryptophan metabolism inhibit the steroid hormone-synthesizing cytochrome P450 11A1, Endocrine 53 (2016) 610–614.
[116] G. Bouguen, L. Dubuquoy, P. Desreumaux, T. Brunner, B. Bertin, Intestinal steroidogenesis, Steroids 103 (2015) 64–71.
[117] S.K. Lau, P.C. Woo, A.M. Fung, K.M. Chan, G.K. Woo, K.Y. Yuen, Anaerobic, non-sporulating, Gram-positive bacilli bacteraemia characterized by 16S rRNA gene sequencing, J. Med. Microbiol. 53 (2004) 1247–1253.
[118] T.M. Bray, J.B. Kirkland, The metabolic basis of 3-methylindole-induced pneumotoxicity, Pharmacol. Ther. 46 (1990) 105–118.
[119] J. Carlson, E. Dickinson, M. Yokoyama, B. Bradley, PULMONARY-EDEMA and emphysema in cattle after intraruminal and intravenous administration of 3-METHYLINDOLE, Am. J. Vet. Res. 36 (1975) 1341–1347.
[120] B.J. Bradley, J.R. Carlson, E.O. Dickinson, 3-methylindole-induced pulmonary edema and emphysema in sheep, Am. J. Vet. Res. 39 (1978) 1355–1358.
[121] J.D. Popp, T.A. McAllister, J.P. Kastelic, W. Majak, M. Ayroud, M.A. VanderKop, D. Karren, G.S. Yost, K.J. Cheng, Effect of melengestrol acetate on development of 3-methylindole-induced pulmonary edema and emphysema in sheep, Can. J. Vet. Res. 62 (1998) 268–274.
[122] G.S. Yost, Mechanisms of 3-methylindole pneumotoxicity, Chem. Res. Toxicol. 2 (1989) 273–279.
[123] ThermoFisher, 3-methylindole, in: Fisher-scientific, 2010.
[124] T.M. Bray, J.R. Carlson, Tissue and subcellular distribution and excretion of 3-[14C]methylindole in rabbits after intratracheal infusion, Can. J. Physiol. Pharmacol. 58 (1980) 1399–1405.
[125] J.M. Weems, N.S. Cutler, C. Moore, W.K. Nichols, D. Martin, E. Makin, J.G. Lamb, G.S. Yost, 3-Methylindole is mutagenic and a possible pulmonary carcinogen, Toxicol. Sci. 112 (2009) 59–67.
[126] B.A. Carr, S. Ramakanth, G.A. Dannan, G.S. Yost, Characterization of pulmonary CYP4B2, specific catalyst of methyl oxidation of 3-methylindole, Mol. Pharmacol. 63 (2003) 1137–1147.
[127] J. Thornton-Manning, M.L. Appleton, F.J. Gonzalez, G.S. Yost, Metabolism of

3-methylindole by vaccinia-expressed P450 enzymes: correlation of 3-methyleneindolenine formation and protein-binding, J. Pharmacol. Exp. Therapeut. 276 (1996) 21–29.
[128] W.K. Nichols, D.N. Larson, G.S. Yost, Bioactivation of 3-methylindole by isolated rabbit lung cells, Toxicol. Appl. Pharmacol. 105 (1990) 264–270.
[129] J.R. Thornton-Manning, W.K. Nichols, B.W. Manning, G.L. Skiles, G.S. Yost, Metabolism and bioactivation of 3-methylindole by Clara cells, alveolar macrophages, and subcellular fractions from rabbit lungs, Toxicol. Appl. Pharmacol. 122 (1993) 182–190.
[130] W. Ruangyuttikarn, M.L. Appleton, G.S. Yost, Metabolism of 3-methylindole in human tissues, Drug Metab. Dispos. 19 (1991) 977–984.
[131] W.K. Nichols, R. Mehta, K. Skordos, K. Macé, A.M. Pfeifer, B.A. Carr, T. Minko, S.W. Burchiel, G.S. Yost, 3-methylindole-induced toxicity to human bronchial epithelial cell lines, Toxicol. Sci. 71 (2003) 229–236.
[132] D.L. Lanza, G.S. Yost, Selective dehydrogenation/oxygenation of 3-methylindole by cytochrome p450 enzymes, Drug Metab. Dispos. 29 (2001) 950–953.
[133] M. Ociepa-Zawal, B. Rubiś, M. Laciński, W.H. Trzeciak, The effect of indole-3-carbinol on the expression of CYP1A1, CYP1B1 and AhR genes and proliferation of MCF-7 cells, Acta Biochim. Pol. 54 (2007) 113–117.
[134] J.M. Weems, J.G. Lamb, J. D'Agostino, X. Ding, G.S. Yost, Potent mutagenicity of 3-methylindole requires pulmonary cytochrome P450-mediated bioactivation: a comparison to the prototype cigarette smoke mutagens B(a)P and NNK, Chem. Res. Toxicol. 23 (2010) 1682–1690.
[135] K.A. Regal, G.M. Laws, C. Yuan, G.S. Yost, G.L. Skiles, Detection and characterization of DNA adducts of 3-methylindole, Chem. Res. Toxicol. 14 (2001) 1014–1024.
[136] X. Zhou, J. D'Agostino, L. Li, C. Moore, G. Yost, X. Ding, Respective roles of CYP2A5 and CYP2F2 in the bioactivation of 3-methylindole in mouse olfactory mucosa and lung: studies using cyp2a5-null and cyp2f2-null mouse models, Drug Metabol. Dispos. 40 (2012) 642–647.

Palacký University in Olomouc

Faculty of Science

Department of Cell Biology and Genetics

The Effects of Indole Derivatives on Aryl hydrocarbon Receptor Activity in Prostatic Cancer Cell Lines

SUMMARY OF DISSERTATION THESIS

Author:	**Mgr. Eliška Zgarbová**
Study program:	P0511D030006 Biology
Branch of study:	Molecular and Cell Biology
Form of study:	Full-time
Supervisor:	**doc. Ing. Radim Vrzal, Ph.D.**
Submitted:	2024

The submitted dissertation thesis is based on my own research carried out from September 2019 to May 2024 within the framework of the Ph.D. study program P0511D030006 Biology, branch of study Molecular and Cell Biology, at the Department of Cell Biology and Genetics, Faculty of Science, Palacký University in Olomouc.

Ph.D. candidate: **Mgr. Eliška Zgarbová**
Department of Cell Biology and Genetics
Faculty of Science, Palacký University in Olomouc
Šlechtitelů 27, 783 71 Olomouc, Czech Republic

Supervisor: **doc. Ing. Radim Vrzal, Ph.D.**
Department of Cell Biology and Genetics
Faculty of Science, Palacký University in Olomouc
Šlechtitelů 27, 783 71 Olomouc, Czech Republic

Reviewers:

The summary of the dissertation thesis was sent for distribution on …….. .

The oral defense will take place at the Faculty of Science, Palacký University in Olomouc …… in front of the committee for the Ph.D. study program P0511D030006 Biology, branch of study Molecular and Cell Biology.

This dissertation thesis is available in the Library of the Biological Departments of the Faculty of Science at Palacký University Olomouc, Šlechtitelů 11, 783 71 Olomouc, Czech Republic, and also at the Department of Cell Biology and Genetics, Šlechtitelů 27, 783 71 Olomouc, Czech Republic.

TABLE OF CONTENTS

1 INTRODUCTION

Prostate cancer is a prevalent cancer in men, with over 1.4 million new cases detected every year, affecting one in six men in their lifetime. The development of this disease is a result of uncontrolled cellular growth of prostate, which is a small gland situated below the bladder and around the urethra. Male sex hormones androgens regulate the growth of prostate epithelial cells by influencing the signalling pathway of androgen receptor (AR), a member of the nuclear receptor (NRs) superfamily. The AR is a ligand-activated transcription factor that induce the expression of AR-target genes, such as *KLK3* or *FKBP5*, upon ligand binding. The AR signalling pathway is responsible for the normal development and maintenance of the male reproductive system, along with prostate epithelial cell proliferation and apoptosis. However, uncontrolled overstimulation of AR signalling is considered a significant factor in prostate cancer progression by regulating an oncogenic gene signature that promotes uncontrolled cell growth.

The treatment of prostate cancer depends on the stage of disease progression. Local approaches include surgical removal of the prostate gland (prostatectomy), targeted cryotherapy or radiation therapy. Once the disease progresses into the nearby tissues, advanced therapy methods are required, which are often referred to as androgen deprivation therapy (ADT). The suppression of circulating androgens or the blockage of AR signalling pathway are an effective approach of inhibition of the prostate cancer progression. Advanced methods include hormone therapy, chemotherapy or immunotherapy. Hormone therapy is mediated through administration of antiandrogens, such as Bicalutamide or Enzalutamide, which inhibits the binding of androgens to AR. Chemotherapy is based on usage of anticancer medication to kill or inhibit the growth of cancer cells. Docetaxel is a typical chemotherapeutic drug used in prostate cancer treatment.

Initially, ADT shows successful results as it slows down or even stops the growth of androgen-dependent prostate cancer. However, this type of cancer often develops into a castration-resistant type (CRPC) during the ADT. CRPC is characterized by the ability of the cancer cells to continue growing and progressing even in the absence of androgens. The risks of ADT include not only the development of currently untreatable CRPC but also a wide range of severe side effects associated with the administration of these drugs, such as cardiovascular diseases, osteoporosis, hepatic dysfunction, renal failure, neurotoxicity fatigue, or even death with the most severe cases. For this reason, constant investigation of novel therapies in prostate cancer aims to overcome extreme side effects.

A novel approach for treating prostate cancer involves suppressing the AR signalling pathway through the activation of aryl hydrocarbon receptor (AhR). AhR is a ligand-activated transcription factor that plays a crucial role in maintaining homeostasis and various patho-/physiology processes such as inflammation, biotransformation of xenobiotics, and cancer progression. Although AhR is not a member of NRs, it shares similarities in structure and signalling mechanisms.

The predominant canonical genomic pathway of AhR is activated by endogenous or exogenous ligands, which translocate AhR into the nucleus. AhR then forms a heterodimer with its dimerization partner, AhR nuclear translocators (ARNT). The AhR/ARNT complex binds to specific responsive elements in the promoter, which induces the expression of AhR-target genes. AhR can also regulate various processes through non-canonical genomic pathways or in a non-genomic manner. A non-canonical genomic pathway includes the interaction of AhR with other receptors and proteins, such as Kruppel-like factor 6 (KLF6), or members of the NF-κB protein family. In a non-genomic pathway, AhR acts as a ligand-dependent E3 ubiquitin ligase, inducing proteasomal degradation of other receptors, such as estrogen receptor (ER) or AR.

Studies have demonstrated that AhR-mediated proteasomal degradation of AR occurs for various AhR ligands and activators, such as icaritin or Carbidopa. However, original research data has indicated that AR degradation only occurs for potent AhR ligands (dioxin, 3-methylcholanthrene). Consequently, several studies have shown a close association between AhR and AR in prostate cancer cells. Different AhR ligands have been reported to suppress prostate cancer development through various mechanisms, indicating that AhR/AR interactions could represent a potential target for prostate cancer treatment.

AhR ligands and activators include a variety of molecules of both endogenous and exogenous origin. Among them, many of these compounds carries an indole ring in their structure. Therefore, the aim of this study was to determine whether selected substances with an indole structure are capable of induction of the previously mentioned mechanism, meaning AR suppression through simultaneous AhR activation. To achieve this, 22 indolic compounds of endogenous and exogenous origin were selected. Our research team has previously reported that some of these indoles were capable of AhR activation in human hepatoma carcinoma cells. However, the effect of these substances on prostate cancer cells has not yet been tested.

The theoretical section of this thesis provides an overview of the current state of the art in this field. The first few chapters thoroughly describe both receptors, covering topics such as their structure, signalling mechanisms, respective ligands, and biological functions.

The subsequent chapter focuses on prostate cancer and its current therapies. Finally, the last chapter of the theoretical section summarizes the information and establishes a connection between the interaction of AhR and AR in the context of prostate cancer.

The experimental part of this study was divided into three main experimental phases. In **Phase I**, the aim was to identify indolic compounds that activate AhR and suppress AR simultaneously using Reporter gene assay (RGA). Only indoles that met both requirements were selected for further experiments. **Phase II** assessed how these particular indoles affected the expression of AhR- and AR-target genes, and respective protein levels. **Phase III** involved further in-depth functional experiments, where the effects of selected indoles were investigated by chromatin immunoprecipitation (ChIP) to analyse the recruitment of the *KLK3* promoter or by using flow cytometry for cell cycle analysis. To assess the effects of indoles in an AhR-free environment, stable AhR CRISPR/Cas9 knockout of 22Rv1 cells was constructed.

2 AIMS OF THIS STUDY

The main goal of this study is to evaluate the effects of selected indole derivatives on the activity of aryl hydrocarbon receptor (AhR) in prostatic cancer cell lines and identify the predicted connection between AhR activation and suppression of the androgen receptor (AR) signalling pathway. The aims of this thesis were divided into the following subtasks:

1. To assemble a comprehensive literature review on the topic of AhR/AR crosstalk, providing a detailed description of both receptors and their connection to prostate cancer
2. Analyse the potential cytotoxic effects of selected indoles in prostate cancer cell lines
3. To screen the effects of selected indoles on AhR and AR transcription activity using the Reporter gene assay
4. To monitor the AhR- and AR-target gene's expression at both mRNA and protein levels
5. To clarify the mechanisms of action by analysing the effects of selected indolic compounds through Chromatin immunoprecipitation or Flow cytometry method
6. To develop a novel AhR-knockout prostate-specific model
7. Attempt to formulate a general conclusion about the relationship between the structure of indolic compounds and AhR-mediated impact on prostate cancer cells based on the findings of this study

3 THEORETICAL BACKGROUND

3.1 Aryl Hydrocarbon Receptor

Although not classified as a member of the nuclear receptors (NRs) superfamily, the aryl hydrocarbon receptor (AhR) shares several similarities with NRs, including structure or signalling mechanisms, and is considered more of a xenoreceptor. AhR is also a ligand-activated transcription factor essential for regulating host physiology. Developing and regulating a broad range of pathophysiological conditions, including cancer, inflammation, or immune disorders, are also closely affiliated with this receptor. The existence of AhR was confirmed in 1976 by Poland and Glover using specific radiolabelled potent inducer 2,3,7,8-tetrachlorodibenzo-*p*-dioxin (TCDD) [1]. However, based on *in vivo* experiments, the existence of AhR was already predicted in the 1960s [2]. A study conducted in 1993 by Dolwick *et al*. compared human AhR with its murine homologue using cDNA analysis. Additionally, this study showed that the expression of human AhR on mRNA level occurs highly in the placenta, lungs, pancreas, and liver. This experimental evidence proved the expression of human AhR for the first time [3, 4].

Over the years, it was demonstrated that AhR is widely distributed in various vertebrate tissues. Additionally, the occurrence of homologous AhR genes has also been demonstrated in invertebrates. The *Spineless* gene in *Drosophila melanogaster* is an example of such AhR homolog. It encodes a specific transcription factor that plays a role in specifying the identity of distal antennal segments. AhR-like genes and their encoded proteins act through different pathways in invertebrates' systems than vertebrates [2, 5].

In the human genome, AhR is encoded by the *AhR* gene, which consists of 11 exons [6]. This gene is localized on the short p arm of chromosome 7 (p21-15) [7, 8]. Due to its wide distribution in organism and the capability of influencing many metabolic pathways, AhR recently became a promising therapeutic target for various diseases, e.g., atopic dermatitis, inflammatory bowel disease, or multiple sclerosis [9]. Several synthetic and environmental substances, including elements found in food, components originating from the microbiota, and endogenous tryptophan (Trp) metabolites, can trigger or influence AhR signalling pathways [10].

3.1.1 AhR Structure

AhR belongs to the basic-helix-loop-helix/Per-Arnt-Sim (bHLH/PAS) family [11]. Members of this family are divided into two main classes based on their function. Class I includes proteins directly involved in regulating the response to changes in the surrounding environment [2, 12]. Proteins classified as class II members are heterodimerization partners for class I proteins. The proper function of regulating target gene expression can only be accomplished if the dimer of two bHLH-PAS proteins is formed [13]. AhR is classified as a class I protein, while its dimerization partner, AhR nuclear translocator (ARNT), is classified as a class II protein. AhR shares a similar structure with ARNT but also with AhR repressor (AhRR) [14, 15]. Besides DBD, AhR, ARNT, and AhRR contain the PAS-A domain responsible for dimerization. Despite having a PAS-B domain, ARNT is incapable of binding ligands. AhRR lacks the PAS-B region completely [14]. The function of individual domains is well understood today. However, the isolation and crystallization of pure human AhR have not yet been achieved [16, 17].

3.1.2 AhR Signalling

AhR activation triggers downstream signalling pathways that result in various physiological responses. Therefore, the regulation of AhR signalling is critical for maintaining proper cellular function and homeostasis.

In its inactive form, AhR is localized in the cytoplasm as a complex with two heat shock protein 90 chaperons (Hsp90), co-chaperone p23, and the immunophilin-like X-associated protein 2 (XAP2; also known as AhR-interacting protein, AIP) [18]. It was previously demonstrated that Hsp90 can bind to both domains, bHLH and PAS, to maintain the conformation susceptible to ligand binding [19, 20]. Studies indicate that the protein tyrosine kinase c-Src is also a member of this protein aggregate [20, 21]. The entire complex is responsible for maintaining the appropriate folding and stability of unliganded AhR. This conformation helps to recognize ligands correctly. Additionally, it prevents unwanted nuclear translocation in the absence of ligands [18, 22]. Once the ligand is bound to the LBD, Hsp90, and XAP2 are released from the multiprotein complex, leading to the conformational changes of AhR. Triggered changes expose NLS, which can be recognized by members of the importin superfamily (IMPα, IMPβ1), enabling a nuclear import. [23, 24]. Subsequently, the whole complex is transported into the nucleus through the nuclear pore complexes.

On the nuclear interface, IMPβ1 binds to the RanGTP, and subsequently, NLS dissociates [25]. Thus, AhR nuclear translocation is completed.

For a long time, AhR common canonical genomic signalling pathway was believed to be the primary mechanism through which AhR agonists elicit their biological and toxicological impacts. However, additional AhR signalling pathways have been identified over time, proving that AhR can exert its influence through various non-canonical and non-genomic mechanisms.

3.1.3 Ligands and Activators of AhR

The spectrum of AhR ligands is composed of various components with different structures. These components include endogenous compounds, like Trp microbial metabolites or eicosanoids, and exogenous compounds, such as PAHs, synthetic compounds, or drugs [26]. Generally, endogenous ligands of AhR are reported to have a range of low to moderate affinity [27]. Because of its ability to bind many structurally diverse chemicals, AhR is commonly referred to as a "*promiscuous receptor*" [28]. However, it is essential to differentiate between AhR ligands (agonists or antagonists) and activators [29].

3.1.4 The Role of AhR in Human Patho-/Physiology

Upon its discovery, AhR was believed to be a xenoreceptor that responded to toxic chemicals, posing a risk to human health. At that time, it was not considered a potential therapeutic target [29]. However, several studies revealed that AhR plays a crucial role in various physiological functions, such as chemical and microbial defence, cell differentiation, angiogenesis, or immune response [4, 30].

One of the first areas investigated regarding AhR's involvement in human metabolism was the biotransformation of xenobiotics. AhR signalling mediates the activation of respective biotransformation proteins, such as cytochrome P450 enzymes, UDP-glucuronosyltransferases, and ATP-binding cassette transporters [14, 31].

In addition, AhR activation was also connected to gut or skin inflammation, skin barrier function, and wound healing [32]. Nowadays, some skin diseases, like plaque psoriasis [33] or atopic dermatitis [34], are already treated through targeted AhR therapy [35].

In conclusion, AhR was previously associated only with toxicity, but recent research has revealed its potential as an important therapeutic target. While some treatment methods are still in the proposal stage, others have already entered clinical studies. Regardless, the significance of AhR in human patho-/physiology cannot be denied.

3.2 Androgen Receptor

Androgen receptor (AR) activity is closely related to the group of steroid hormones, androgens. Together, AR and androgens play an irreplaceable role in the development of male phenotype during prenatal development and later in the maintenance of the proper function of male reproductive organs [36]. Additionally, it has a vital role in affecting the nervous system [37]. AR is widely distributed in tissues of the male's urogenital tract, like the testis or prostate. On the other hand, numerous other tissues, such as the kidney, liver, brain, mammary gland, or salivary glands, showed low AR expression [38]. AR, a 110 kDa protein consisting of approximately 919 amino acids, is encoded by the *AR* gene localized on the human X chromosome between q13 and centromere [39, 40]. This gene is about 90 kb in size, consisting of 8 exons divided by 0.7-2.6 kb introns [40, 41]. Moreover, the existence of several AR splicing variants was reported due to the presence of cryptic exons (further in *Chapter 3.3.4*) [42]. The outcomes of several studies, including transcriptome analysis or next-generation sequencing, have validated the importance of AR activity in the progression of prostate cancer [43].

3.2.1 AR Structure

AR is a member of NRs and can also be found under the abbreviation NR3C4 (nuclear receptor subfamily 3, group C, member 4) [44]. Therefore, it is also a ligand-activated transcription factor and shares the same structural division described in previous chapter. Briefly, AR is composed of four domains. NH_2 terminal transactivation domain (NTD) is encoded by exon 1, DBD by exons 2–3, HR by exon 4, and exons 5–6 encode LBD [41].

3.2.2 AR Signalling

AR, like other NRs, is initially located in the cytoplasm in the absence of ligands, forming a complex with heat shock proteins (Hsp90, Hsp70, Hsp56, Hsp27), cytoskeletal proteins (e.g., filamin-A), and other chaperones [45-47].

In genomic signalling pathway, AR undergoes conformational changes upon ligand biniding, enabling it to interact with co-regulators [48]. Hsp27 plays a crucial role in the activation of receptors. Subsequently, AR dimerize forms a homodimer with itself [49]. The tissue-specific binding of AR/AR to ARE in the promoter of target genes is followed by the recruitment of co-regulators and histone acetyltransferase enzymes (HATs), which subsequently trigger transcription [50, 51]. Approximately, the existence of 170 different AR

coregulators was reported [50]. One of the well-known AR-target gene is *KLK3*, which encodes the prostate specific antigen (PSA) protein [52]. Another known AR-regulated gene is *FKBP5*, which encodes a small protein immunophilin. This protein regulates the distribution of steroid hormones between the cytosol and nucleus [53].

After the ligand dissociates, NES coordinates the export of AR from the nucleus to the cytoplasm. There, AR returns to the initial inactive conformation and awaits the rebinding of a ligand [47, 54]. Alternatively, AR degradation can be achieved by targeting it for the ubiquitin-proteasome system, which leads to a decrease in AR protein level. The recognition of AR by E3 ubiquitin ligase requires phosphorylation of specific residues [55, 56].

Additionally, previous studies have demonstrated that AR can interact with other signalling pathways beyond its well-known genomic pathways. This type of interaction is known as a non-genomic pathway, where the cellular response time is rapid, within minutes. Unlike genomic signalling, these pathways do not appear to involve transcription or translation from AR-target genes, suggesting a direct interaction and stimulation of other signalling cascades [57, 58].

3.2.3 Androgens and Antiandrogens

Androgens, main agonists of the AR, play a crucial role in male phenotype development and modulate various biological responses in the human body, such as fertility. Testosterone (T), dihydrotestosterone (DHT), and dehydroepiandrosterone (DHEA) are the most essential androgens. These male sex steroid hormones are synthesised within Leydig cells in the testicles, or the adrenal gland [59]. The process of androgen synthesis and secretion is initially regulated through the hypothalamic-pituitary-gonadal axis (HPG) [60]. Androgens, like other steroid hormones such as estrogens, glucocorticoids, or mineralocorticoids, are also derived from cholesterol [61].

Antiandrogens inhibit the activity of androgens by competing with them for AR binding sites [36]. They are often used in clinical applications, particularly for prostate cancer treatment. Antiandrogens can be divided into four groups: steroidal (Cyproterone acetate), first-generation nonsteroidal (Flutamide, Bicalutamide), second-generation nonsteroidal antiandrogens (Enzalutamide, Apalutamide), and N-terminal domain antagonists (Ralaniten) [62]. However, treatment with synthetic antiandrogens may cause undesirable side effects [63].

3.3 AhR/AR Crosstalk in the Context of Prostate Cancer

The crosstalk between AhR and AR is a topic that has been discussed extensively, but its mechanisms are yet to be fully comprehended. Both of these receptors have been found to interact with other NRs, which suggests that a potential mechanism for AhR and AR interaction is through direct contact with these receptors [64, 65].

Ohtake *et al*. investigated the connection between AhR and sex hormone signalling. Findings suggest that upon AhR activation by strong and potent ligands or through the expression of a constitutively active AhR, the AR protein levels were significantly reduced. In contrast, mRNA levels remained unchanged [66].

AhR and AR may also interact through shared coactivator proteins such as SRC1 and p300 [65, 67]. Another possible AhR/AR crosstalk mechanism involves the phosphorylation of AR by Src kinase. As described previously in *Chapters 3.2.2.3* and *3.3.2.2*, the crosstalk between AhR and AR with Src kinase has been reported multiple times. AhR may play a crucial role in controlling AR signalling in CRPC through Src as an intermediary signal. The simultaneous inhibition of AhR and Src kinase decreased AR signalling in CRPC cells [68]. Thus, research suggest that AhR/Src kinase crosstalk could result in maintaining the AR signalling in CRPC [65].

A recent study investigated the connection between AhR activation and AR suppression, reducing prostate cancer progression in DU145 and LNCaP cell lines. This study revealed that AhR activation by Carbidopa induced proteasomal degradation of AR. Furthermore, treatment with Carbidopa in a murine cancer model increased AhR protein level, decreased AR protein level, and suppressed prostate cancer progression [69].

Several PAHs and dioxins were connected to antiandrogenic properties. In LNCaP cells, these AhR ligands decreased cell proliferation, reduced PSA levels, and inhibited the 5α-reductase enzyme [70, 71]. AR degradation in LNCaP cells induced by 3MC, another AhR ligand, is suggested to occur due to direct interaction between AhR and AR proteins [72].

In summary, recent research indicates that AhR ligands can precisely regulate the degradation of proteins and gene expression through the E3 ubiquitin ligase activity of AhR. This mechanism of action may make AhR a promising target for prostate cancer therapy, as it could potentially avoid the harsh side effects associated with commonly used antiandrogenic drugs and chemotherapeutics.

3.4 Suggested Hypothesis

Based on the available literature and published research, it is evident that substances containing an indole aromatic ring are significant AhR ligands and activators. Therefore, this study aimed to investigate whether selected indole compounds can induce the same effect, i.e., AR proteasomal degradation through the activation of AhR. The tested substances were selected based on the previous experiments of our research group when it was found that some of the 22 tested indoles demonstrated the ability to activate AhR in the human hepatoma carcinoma cell line [73]. Four different prostate cancer cell lines were used as a model of different conditions: 22Rv1, human prostate carcinoma epithelial cell line derived from a xenograft with AhR, AR-fl, and AR-v7 [74]; LNCaP androgen-sensitive prostate cancer cell line from the biopsy of the left supraclavicular lymph node with AhR and AR-fl [75]; its clone C4-2 [76], and PC-3 cell line from bone metastasis containing only AhR and no AR variant [77].

4 MATERIALS

4.1 Biological Materials

Humane prostate carcinoma epithelial cell lines PC-3 (ATCC No. CRL-1435), 22Rv1 (ATCC No. CRL-2505), and AIZ-AR [78] were cultured in Rosewell Park Memorial Institute (RPMI) 1640 medium. RPMI medium was supplemented with 10% fetal bovine serum (FBS), 1% non-essential amino acids (NEAA), and 2 mM L-glutamine (L-Gln). Human prostate carcinoma cell line LNCaP (ATCC No. CRL-1740) and C4-2 (ATCC No. CRL-3314) were cultured in Dulbecco's modified Eagle's Medium (DMEM) supplemented with 10% FBS, 1% NEAA, and 2 mM L-Gln. Cells were maintained in a humidified incubator at 37°C and 5% CO_2. All cell lines were regularly tested for the presence of mycoplasma using MycoAlert™ Mycoplasma Detection Kit (Lonza).

Before the beginning of this project, 22Rv1, PC-3, and LNCaP cell lines were subjected to authentication by genotyping. This was performed by GENERI BIOTECH s. r. o.

4.2 Tested compounds

Compounds of interest were selected based on the previous study by our research group. In this preceding research, the effect of the same indoles on AhR activity was monitored in the intestinal LS180 cell line [73]. Tested indoles are given in **Figure 1**.

Compound	Abbreviation	Structure	Compound	Abbreviation	Structure
1-methylindole	1MI		2,3,3-trimethylindolenine	2,3,3TMI	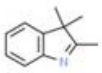
2-methylindole	2MI	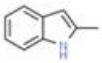	2,3,7-trimethylindole	2,3,7TMI	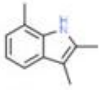
3-methylindole	3MI		4-methoxyindole	4MeO	
4-methylindole	4MI		5-methoxyindole	5MeO	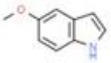
5-methylindole	5MI		6-methoxyindole	6MeO	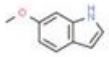
6-methylindole	6MI		7-methoxyindole	7MeO	
7-methylindole	7MI		4,6-dimethoxyindole	4,6DMI	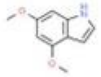
1,2-dimethylindole	1,2DMI	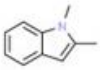	5,6-dimethoxyindole	5,6DMI	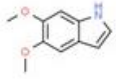
1,3-dimethylindole	1,3DMI		4-methoxy-1-methylindole	4MeO1MI	
2,3-dimethylindole	2,3DMI	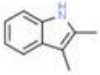	5-methoxy-2-methylindole	5MeO2MI	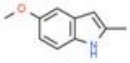
2,5-dimethylindole	2,5DMI	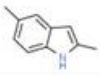	7-methoxy-4-methylindole	7MeO4MI	

Figure 1: Tested indoles. A total of 22 indolic compounds were tested and divided into four groups: monomethylindole, di- and tri-methylindoles, monomethoxyindoles, and methoxyindole. The name, abbreviation, and chemical structure of each compound are displayed in this figure.

5 METHODS

5.1 Cytotoxicity and Proliferation Assays

Cells, either 22Rv1, PC-3, or C4-2, were seeded in 96-well plates at a density of 2.5 x 10^4 cells per well in a total volume of 200 µl. The cells were then left to stabilize overnight. The medium was then replaced with a fresh one containing compounds of interest with increasing concentrations (0.1-100 µM) or control compounds such as DMSO (untreated/UT; 0.1%; v/v), doxorubicin (20 µM), or Triton X-100 (2%) for 24 h. Results were analysed using MTT Assays and Crystal Violet Assay.

5.2 Stable Transfection of 22Rv1 and PC-3 Cells

Initially, a new model was needed to conduct further experiments on AhR transcription activity in a prostate-specific environment. To achieve this, two stably transfected cell lines containing luciferase reporter gene were constructed. For this purpose, pGL4.27 [luc2P/minP/Hygro] plasmid originally designed by Novotna *et al.* in 2011 was utilized [79].

The cells were seeded in RPMI medium at a density of 5 x 10^4 cells per well of a 12-well plate, and then immediately transfected with pGL4.27-DRE reporter plasmid (concentration of 200 ng per well) using FuGENE® Transfection Kit, following the manufacturer's protocol. The cells were then incubated with the transfection medium for 48 h. After this, the transfection medium was replaced with selection medium containing Hygromycin B (HygB). Finally, after the selection process, polyclonal and subsequently monoclonal populations were isolated.

Subsequently, isolated monoclonal populations were subjected to further characterisation, such as dose-dependent analysis with model AhR ligands (TCDD, BaP, FICZ), analysis of maintenance of luciferase activity after TCDD treatment, time-dependent cryopreservation analysis, and analysis of AhR antagonists' treatment.

5.3 Reporter Gene Assay

For monitoring AhR transcription activity in prostate-specific environment, newly developed cell lines 22AhRv1 and PAhRC3 were used (detailed in *Chapter 5.2*). Stably transfected cell line AIZ-AR [78] derived from the parental 22Rv1 cell line was used as a cellular model for monitoring AR activity.

Cells were treated with selected indoles at concentrations of 1, 10, and 100 µM. Treatment was terminated by aspiration of the medium. Adherent cells were lysed with 25 µl of 1x Reporter Lysis Buffer and kept at -80°C for at least 1 h. The samples were then thawed

at room temperature (RT). A total sample volume of 6 µl was mixed with 30 µl of luciferase substrate. The emitted light was measured with the TECAN Infinite M200. The intensity of the luminescence is directly proportional to the activity of the monitored receptor.

5.4 Quantitative Reverse Transcriptase PCR (RT-qPCR)

Only indoles that met both primary criteria at the RGA level, meaning AhR activation and simultaneous AR suppression, were chosen to proceed to the second experimental phase. The impact of 8 selected indoles on the mRNA expression of AhR- and AR-target genes was evaluated using RT-qPCR.

22Rv1 or PC-3 cells were seeded in a 6-well plate at a density of 1.5 x 10^6 cells per well in of 1.5 ml RPMI medium. After overnight stabilization, the cells were treated with selected indoles and control compounds for 24 h.

After the incubation, total RNA was isolated, reverse transcription was performed and samples were analysed using RT-qPCR. AhR- and AR-target genes expressions were determined using either TaqMan® or SYBR® Green reagent systems.

5.5 Western blot

In the **Phase II** experiments, Western blot analysis was the second technique used to investigate the possibility of 8 previously selected indoles affecting the levels of proteins of interest.

To carry out the experiment, prostate cancer cells were seeded into a 6-well plate at a density of 1.5 x 10^6 cells per well in 1.5 ml of RPMI or DMEM medium, stabilized overnight, and subsequently treated with tested indoles and control compounds for 24 h.

After the incubation, total protein extracts were isolated from each sample and Western blot analysis was performed, following chemiluminescence detection of proteins of interest.

5.6 Chromatin Immunoprecipitation

Phase III experiments began with an investigation of recruitment to the *KLK3* promoter after treatment with 8 previously selected indoles. 22Rv1 cells were seeded in a 60-mm Petri dish at a density of 4 x 10^6 cells per well in 4 ml of RPMI medium and stabilized overnight. Afterward, cells were treated with 8 selected indoles (10 µM) or control compounds. The results of all tested conditions were evaluated in the presence of DHT (10 nM). Cells were incubated with tested compounds for 90 min at 37°C. Subsequently, Chromatin immunoprecipitation

(ChIP) was performed with SimpleChIP® Plus Enzymatic Chromatin IP Kit according to the manufacturer's recommendations with minor modifications.

5.7 CRISPR/Cas9 AhR Knock-out System

In the next step of **Phase III** experiments, the relationship between AhR and AR was investigated. To achieve this, a transient and stable CRISPR/Cas9 AhR knock-out systems were developed using the 22Rv1 cell line. The AhR CRISPR/Cas9 KO plasmid system (Santa Cruz Biotechnology) was used according to manufacturer's protocol, with minor modifications. Prior to transfection, the appropriate ratios of plasmid DNA and UltraCruz® Transfection Reagent were determined. Specific *AhR exon 5* primers were designed for RT-qPCR analysis of AhR KO samples, as this sequence corresponds with one of the target DNA sequences for the used CRISPR/Cas9 AhR KO plasmid.

5.8 Cell Cycle Analysis

Fluorescent-activated Cell Sorting (FACS) was used to analyse the impact of one selected indole, 3MI, on the cell cycle in different prostatic cell lines.

22Rv1, PC-3, LNCaP, and C4-2 cells were seeded in a 60-mm Petri dish at a density of 4 x 10^6 cells per well in 4 ml of appropriate media. Following overnight stabilization, cells were treated with 3MI (100 μM) and control compounds – DMSO (untreated; 0.1%; v/v) or doxorubicin 20 μM for 24 h. Subsequently, cells were harvested and analysed by FACS Verse Machine.

5.9 Statistical Analysis

The data obtained from the experiments were analysed using GraphPad Prism Version 9.4.1. The figure legends specify the number of independent repeats and technical replicates for each experiment. If applicable, the obtained values were subjected to two-way analysis of variance (ANOVA) followed by Dunnett's test or Student's t-test. Results with $p < 0.05$ were considered significant. The IC_{25} and IC_{50} values were calculated using the nonlinear regression with the least-squares fitting method.

6 SUMMARY OF THE RESULTS

6.1 Cytotoxicity and Proliferation Assays after Treatment with Indoles

Before beginning the experiments, the viability and cell proliferation effects of 22 tested indoles were evaluated. To determine whether the selected indolic compounds have any cytotoxic effects against 22Rv1, PC-3, and C4-2 cells, the MTT assay was performed. The proliferation analysis was carried out using the crystal violet assay.

According to the obtained results, all tested indoles were determined as nontoxic in 22Rv1, PC-3, and C4-2 cell lines, as the decrease in cell viability did not exceed 20 %. Only 3MI (100 μM) displayed a decrease of approximately 23 % in the C4-2 cell line. This decrease was considered non-significant by statistical analysis.

However, the Crystal violet assay showed that cell proliferation significantly decreased in the 22Rv1 cell line for 3MI and partially for 4MI. Compared to the untreated (UT) cells, cell proliferation decreased by approximately 60 % for 3MI (100 μM) and 40 % for 4MI (100 μM). In C4-2 cells, 3MI (100 μM) also decreased cell proliferation by approximately 20 %. On the other hand, the decrease in cell proliferation was not observed in the PC-3 cell line for any of the tested indolic compounds.

6.2 Development of Novel Prostate-specific AhR Reporter Cell Lines

Initially, a cellular system was established to monitor AhR transcriptional activity in the 22Rv1 and PC-3 cell lines. To achieve this, stably transfected 22AhRv1 and PAhRC3 cell lines with the luciferase reporter gene were constructed. The parental 22Rv1 and PC-3 cells were transfected with the plasmid pGL4.27 [luc2P/minP/Hygro] designed by Novotna *et al*. 2011 [79]. Monoclones were isolated for each cell line and incubated with the model AhR ligand TCCD (10 nM) for 24 h. Results were analysed using RGA. Two novel prostate-specific AhR reporter cell lines, titled as 22AhRv1 (parental cell line 22Rv1), PAhRC3 (parental cell line PC-3), were successfully developed and characterized.

6.3 The Effects of Indoles on AhR and AR Transcription Activity

Prostate-specific monitoring of AhR transcription activity was performed using novel 22AhRv1 and PAhRC3 cell lines. The AIZ-AR reporter cell line [78] was used to monitor AR transcription activity in the presence or absence of DHT.

In the 22AhRv1 reporter cell line, all tested indoles, except 3MI, displayed the ability to significantly activate AhR after 24 h. In the PAhRC3 reporter cell line, only some tested indoles displayed the ability to activate AhR. Interestingly, 3MI exhibited the highest dose-dependent increase in AhR transcription activity with efficacy highest than TCDD (10 nM).

In the AIZ-AR reporter cell line, the ability of tested indoles to influence AR transcription activity was determined after 24 h. These experiments were carried out in agonist (in the absence of DHT) and antagonist mode (with the presence of DHT). In the antagonist mode, the ability of tested indoles to suppress the AR transcription activity induced by DHT was evaluated. These results are expressed in percentage, where the induction of AR transcription activity by ligand DHT (10 nM) represents 100 %. The positive control, antiandrogen ENZ (10 μM), decreased DHT-inducible AR-dependent luciferase activity to the level of UT. A significant dose-dependent suppression of AR activity was observed with 3MI, 4MI, 1,3DMI, 2,3DMI, 2,3,7TMI, 4,6DMI, 5,6DMI, and 7MeO4MI. The most significant decrease in DHT-induced AR activity was observed with 3MI and 4MI.

Only the compounds that met both criteria, significant induction of AhR transcription activity and simultaneous suppression of DHT-activated AR, were selected for further experiments in **Phase II**. Out of 22 tested indoles, only 8 satisfied both criteria.

6.4 The Effects of Indoles on the Expression of Target Genes

The first series of experiments in experimental **Phase II** were to determine the effect of indoles in the presence of absence of DHT (10 nM) on the expression of AhR- and AR-target genes in 22Rv1 and PC-3 cell lines. Based on previous experiments, 8 indoles out of 22 were selected, namely 3MI, 4MI, 1,3DMI, 2,3DMI, 2,3,7TMI, 4,6DMI, 5,6DMI, and 7MeO4MI.

In 22Rv1 cell line, all 8 tested indoles showed a dose-dependent increase in the expression of *CYP1A1* mRNA. All selected indoles significantly reduced the DHT-induced expression of AR-target genes in 22Rv1 cell line.

6.5 The Effects of Indoles on Protein Levels

The second series of experiments in the **Phase II** were to determine the effect of indoles in the presence of absence DHT (10 nM) on the levels of target proteins. To begin with, the basal levels of AhR protein were evaluated in untreated prostate cancer cell lines other cell types using Western blot analysis. Evaluation of AR protein levels was performed in the context

of the proposed hypothesis. Both variants, AR-fl and AR-v7 exhibited a significant dose-dependent decrease when exposed to 3MI, 4MI, 2,3,7TMI, and 7MeO4MI. To determine whether the change in degradation or transcription is responsible, mRNA levels were measured.

Surprisingly, the mRNA level of both AR variants decreased in a similar pattern, with the strongest effect shown by 3MI, followed by 4MI, 2,3DMI, 2,3,7TMI, and 7MeO4MI. Therefore, the tested indoles are likely to induce downregulation in *AR* mRNA, which is further reflected in a decrease of AR proteins.

6.6 The Effects of Indoles on the Enrichment of the *KLK3* Promoter

Phase III experiments began by investigating changes in the recruitment to the *KLK3* promoter, one of the AR-target genes, after the treatment with 8 previously selected indoles. A ChIP assay was conducted to assess the impact of the tested indoles on the transcription of the *KLK3* gene.

All tested indoles showed a decrease in the enrichment of the *KLK3* promoter by approximately 30-50 %, which was determined as significant by statistical analysis. These data suggest that the previously observed decrease in *KLK3* and *FKBP5* mRNA levels began already during AR binding to the response element in DNA, thereby affecting AR functionality.

6.7 CRISPR/Cas9 AhR Knock-out Model

At the second part of the **Phase III** experiments, a novel CRISPR/Cas9 AhR Knock-out model was developed by transient and stable transfection to further investigate the suggested interaction between AhR and AR signalling pathways.

A transiently transfected 22Rv1 AhR KO model was successfully developed, as a decrease in *AhR* (exon 5) mRNA levels was observed between WT and AhR KO samples in all conducted experiments. Therefore, 22Rv1 cells with transient AhR KO were incubated with only 1 indole (4MI 100 μM), which displayed the most potent effects in previous experiments with the 22Rv1 cell line. After the treatment with TCDD (10 nM) or 4 MI (100 μM) in the presence or absence of DHT (10 nM), *CYP1A1* mRNA levels in transient AhR KO cells decreased slightly.

The construction of a stably transfected AhR-KO model was visually confirmed by Western blot analysis. Subsequently, newly developed stable AhR KO cells were used to evaluate changes in the expression of AhR- and AR-target genes. TCDD-elicited DHT inducible *KLK3* mRNA decrease was observed in 22Rv1 WT, but not in 22Rv1 AhR KO cells. The very same

effect was observed for 10 μM, but not for 100 μM 4MI at *KLK3* and *FKBP5* mRNA. These results indicate the reversal of the process and the existence of the connection between AhR and AR signalling. However, since 100 μM 4MI elicited the suppression of DHT-induced *KLK3* and *FKBP5* mRNAs in AhR KO cells. This might suggest either non-genomic action of AhR or 4MI off-target, which affects AR signalling.

In the presence of DHT (10 nM), the expression of the *UBE2C* gene did not change upon incubation with 4MI (10 or 100 μM) in 22Rv1 AhR KO cells, while *UBE2C* levels decreased to less than 80 % upon the incubation with 4MI in 22Rv1 WT cells.

6.8 The Effects of 3MI on Cell Cycle Analysis

During the final phase of the **Phase III** experiments, the FACS Verse Machine was used to analyse the cell cycle. This analysis was conducted due to the observation that different prostatic cell lines exhibited varying effects on cell viability and proliferation after incubation with selected indoles during experiments. Out of all the examined indoles, 3MI (skatole) displayed the most interesting results, which varied notably between individual cell lines. Therefore, only this compound (3MI 100 μM) was used to determine its effect on changes in the cell cycle of 22Rv1, PC-3, LNCaP, and C4-2 cell lines. Individual phases of the cell cycle were analysed (G1, G2, S), as well as the induction of apoptosis.

The results obtained from the study indicate that incubation with 3MI caused apoptosis in 93 % of the 22Rv1 cells. However, in the PC-3 cell line, only about 10 % of the cells underwent apoptosis. In the case of LNCaP cells, apoptosis was observed in 62 % of the cells, and in C4-2 cells, the percentage was 70 %.

7 CONCLUSION

The presented dissertation thesis tested the hypothesis of AR-signalling pathway suppression through the AhR activation with selected indolic compounds. This study evaluated the hypothesis of AhR-mediated proteasomal degradation of AR upon the activation of AhR by selected indolic compounds. The newly developed 22AhRv1 and PAhRC3 reporter cell line were used to test all 22 indoles, and all of them showed promising AhR-activating potential. However, only 8 of 22 tested compounds were able to simultaneously suppress DHT-induced AR activation. These 8 indoles (3MI, 4MI, 1,3DMI, 2,3DMI, 2,3,7TMI, 4,6DMI, 5,6DMI, and 7MeO4MI) were selected for further experiments. At the mRNA level, the 8 selected indoles increased *CYP1A1* expression and significantly reduced DHT-inducible *KLK3* and *FKBP5* expression (AR-target genes). The ChIP analysis also revealed that selected indoles reduced DHT-inducible binding of AR to the *KLK3* promoter. The study further monitored the effect of the strongest AhR activator in 22Rv1, 4MI, using transient and stable transfection with the CRISPR/Cas9 AhR KO plasmid. However, only significant change in the expression of AR-target genes was observed with *FKBP5*, which is also regulated by other signalling pathways (such as GR) and not only by AR-signalling [80].

The main findings of this study are:

1. All tested indoles displayed the ability to activate AhR in prostate-specific environment
2. Eight selected indoles were capable of simultaneous suppression of DHT-induced AR signalling
3. The decrease was observed already on the *AR* mRNA level, thus it not likely mediated by AhR-induced proteasomal degradation of AR
4. Selected indolic compounds inhibit AR signalling pathway already at the point of AR-target genes expression initiation
5. Results suggest a potential relationship between the structure of tested indoles and suppression of AR activity; however, further experiments are required to confirm this claim

8 REFERENCES

1. Poland, A., E. Glover, and A.S. Kende, *Stereospecific, high affinity binding of 2,3,7,8-tetrachlorodibenzo-p-dioxin by hepatic cytosol. Evidence that the binding species is receptor for induction of aryl hydrocarbon hydroxylase.* J Biol Chem, 1976. **251**(16): p. 4936-46.
2. Skálová, L., *Ah Receptor*, in *Metabolismus léčiv a jiných xenobiotik*. 2018, Charles University, Karolinum. p. 170.
3. Dolwick, K.M., et al., *Cloning and expression of a human Ah receptor cDNA.* Mol Pharmacol, 1993. **44**(5): p. 911-7.
4. Bock, K.W., *From TCDD-mediated toxicity to searches of physiologic AHR functions.* Biochem Pharmacol, 2018. **155**: p. 419-424.
5. Hahn, M.E., *Aryl hydrocarbon receptors: diversity and evolution.* Chem Biol Interact, 2002. **141**(1-2): p. 131-60.
6. Bennett, P., D.B. Ramsden, and A.C. Williams, *Complete structural characterisation of the human aryl hydrocarbon receptor gene.* Clin Mol Pathol, 1996. **49**(1): p. M12-6.
7. Le Beau, M.M., et al., *Chromosomal localization of the human AHR locus encoding the structural gene for the Ah receptor to 7p21-->p15.* Cytogenet Cell Genet, 1994. **66**(3): p. 172-6.
8. Micka, J., et al., *Human Ah receptor (AHR) gene: localization to 7p15 and suggestive correlation of polymorphism with CYP1A1 inducibility.* Pharmacogenetics, 1997. **7**(2): p. 95-101.
9. Cannon, A.S., P.S. Nagarkatti, and M. Nagarkatti, *Targeting AhR as a Novel Therapeutic Modality against Inflammatory Diseases.* Int J Mol Sci, 2021. **23**(1).
10. Gargaro, M., et al., *The Landscape of AhR Regulators and Coregulators to Fine-Tune AhR Functions.* Int J Mol Sci, 2021. **22**(2).
11. Gu, Y.Z., J.B. Hogenesch, and C.A. Bradfield, *The PAS superfamily: sensors of environmental and developmental signals.* Annu Rev Pharmacol Toxicol, 2000. **40**: p. 519-61.
12. Fribourgh, J.L. and C.L. Partch, *Assembly and function of bHLH-PAS complexes.* Proc Natl Acad Sci U S A, 2017. **114**(21): p. 5330-5332.
13. Wu, D. and F. Rastinejad, *Structural characterization of mammalian bHLH-PAS transcription factors.* Curr Opin Struct Biol, 2017. **43**: p. 1-9.
14. Larigot, L., et al., *AhR signaling pathways and regulatory functions.* Biochim Open, 2018. **7**: p. 1-9.
15. Mimura, J., et al., *Identification of a novel mechanism of regulation of Ah (dioxin) receptor function.* Genes Dev, 1999. **13**(1): p. 20-5.
16. Schulte, K.W., et al., *Structural Basis for Aryl Hydrocarbon Receptor-Mediated Gene Activation.* Structure, 2017. **25**(7): p. 1025-1033 e3.
17. Sakurai, S., T. Shimizu, and U. Ohto, *The crystal structure of the AhRR-ARNT heterodimer reveals the structural basis of the repression of AhR-mediated transcription.* J Biol Chem, 2017. **292**(43): p. 17609-17616.
18. Petrulis, J.R. and G.H. Perdew, *The role of chaperone proteins in the aryl hydrocarbon receptor core complex.* Chem Biol Interact, 2002. **141**(1-2): p. 25-40.
19. Fukunaga, B.N., et al., *Identification of functional domains of the aryl hydrocarbon receptor.* J Biol Chem, 1995. **270**(49): p. 29270-8.
20. Antonsson, C., et al., *Distinct roles of the molecular chaperone hsp90 in modulating dioxin receptor function via the basic helix-loop-helix and PAS domains.* Mol Cell Biol, 1995. **15**(2): p. 756-65.
21. Enan, E. and F. Matsumura, *Identification of c-Src as the integral component of the cytosolic Ah receptor complex, transducing the signal of 2,3,7,8-tetrachlorodibenzo-p-dioxin (TCDD) through the protein phosphorylation pathway.* Biochem Pharmacol, 1996. **52**(10): p. 1599-612.
22. Pongratz, I., G.G. Mason, and L. Poellinger, *Dual roles of the 90-kDa heat shock protein hsp90 in modulating functional activities of the dioxin receptor. Evidence that the dioxin receptor functionally belongs to a subclass of nuclear receptors which require hsp90 both for ligand*

binding activity and repression of intrinsic DNA binding activity. J Biol Chem, 1992. **267**(19): p. 13728-34.
23. Petrulis, J.R., et al., *The hsp90 Co-chaperone XAP2 alters importin beta recognition of the bipartite nuclear localization signal of the Ah receptor and represses transcriptional activity.* J Biol Chem, 2003. **278**(4): p. 2677-85.
24. Ikuta, T., Y. Kobayashi, and K. Kawajiri, *Phosphorylation of nuclear localization signal inhibits the ligand-dependent nuclear import of aryl hydrocarbon receptor.* Biochem Biophys Res Commun, 2004. **317**(2): p. 545-50.
25. Kosyna, F.K. and R. Depping, *Controlling the Gatekeeper: Therapeutic Targeting of Nuclear Transport.* Cells, 2018. **7**(11).
26. Lin, L., Y. Dai, and Y. Xia, *An overview of aryl hydrocarbon receptor ligands in the Last two decades (2002-2022): A medicinal chemistry perspective.* Eur J Med Chem, 2022. **244**: p. 114845.
27. Henry, E.C., S.L. Welle, and T.A. Gasiewicz, *TCDD and a putative endogenous AhR ligand, ITE, elicit the same immediate changes in gene expression in mouse lung fibroblasts.* Toxicol Sci, 2010. **114**(1): p. 90-100.
28. Soshilov, A.A. and M.S. Denison, *Ligand promiscuity of aryl hydrocarbon receptor agonists and antagonists revealed by site-directed mutagenesis.* Mol Cell Biol, 2014. **34**(9): p. 1707-19.
29. Sladekova, L., S. Mani, and Z. Dvorak, *Ligands and agonists of the aryl hydrocarbon receptor AhR: Facts and myths.* Biochem Pharmacol, 2023. **213**: p. 115626.
30. Ichihara, S., et al., *A role for the aryl hydrocarbon receptor in regulation of ischemia-induced angiogenesis.* Arterioscler Thromb Vasc Biol, 2007. **27**(6): p. 1297-304.
31. Wang, X., B.T. Hawkins, and D.S. Miller, *Aryl hydrocarbon receptor-mediated up-regulation of ATP-driven xenobiotic efflux transporters at the blood-brain barrier.* FASEB J, 2011. **25**(2): p. 644-52.
32. Fernandez-Gallego, N., F. Sanchez-Madrid, and D. Cibrian, *Role of AHR Ligands in Skin Homeostasis and Cutaneous Inflammation.* Cells, 2021. **10**(11).
33. Stein Gold, L., et al., *A phase 2b, randomized clinical trial of tapinarof cream for the treatment of plaque psoriasis: Secondary efficacy and patient-reported outcomes.* J Am Acad Dermatol, 2021. **84**(3): p. 624-631.
34. Paller, A.S., et al., *Efficacy and patient-reported outcomes from a phase 2b, randomized clinical trial of tapinarof cream for the treatment of adolescents and adults with atopic dermatitis.* J Am Acad Dermatol, 2021. **84**(3): p. 632-638.
35. Smith, S.H., et al., *Tapinarof Is a Natural AhR Agonist that Resolves Skin Inflammation in Mice and Humans.* J Invest Dermatol, 2017. **137**(10): p. 2110-2119.
36. Tan, M.H., et al., *Androgen receptor: structure, role in prostate cancer and drug discovery.* Acta Pharmacol Sin, 2015. **36**(1): p. 3-23.
37. Sheridan, P.J., *Androgen receptors in the brain: what are we measuring?* Endocr Rev, 1983. **4**(2): p. 171-8.
38. Ruizeveld de Winter, J.A., et al., *Androgen receptor expression in human tissues: an immunohistochemical study.* J Histochem Cytochem, 1991. **39**(7): p. 927-36.
39. Lubahn, D.B., et al., *Cloning of human androgen receptor complementary DNA and localization to the X chromosome.* Science, 1988. **240**(4850): p. 327-30.
40. Gelmann, E.P., *Molecular biology of the androgen receptor.* J Clin Oncol, 2002. **20**(13): p. 3001-15.
41. Kenji, A. and a.t.o. authors, *Androgens and androgen receptor: Mechanisms, functions and clinical applications*. 1st ed. 2002: Springer, Boston, MA.
42. Hu, R., et al., *Ligand-independent androgen receptor variants derived from splicing of cryptic exons signify hormone-refractory prostate cancer.* Cancer Res, 2009. **69**(1): p. 16-22.
43. Baca, S.C., et al., *Punctuated evolution of prostate cancer genomes.* Cell, 2013. **153**(3): p. 666-77.
44. Lu, N.Z., et al., *International Union of Pharmacology. LXV. The pharmacology and classification of the nuclear receptor superfamily: glucocorticoid, mineralocorticoid, progesterone, and androgen receptors.* Pharmacol Rev, 2006. **58**(4): p. 782-97.

45. Veldscholte, J., et al., *Hormone-induced dissociation of the androgen receptor-heat-shock protein complex: use of a new monoclonal antibody to distinguish transformed from nontransformed receptors.* Biochemistry, 1992. **31**(32): p. 7422-30.
46. Loy, C.J., K.S. Sim, and E.L. Yong, *Filamin-A fragment localizes to the nucleus to regulate androgen receptor and coactivator functions.* Proc Natl Acad Sci U S A, 2003. **100**(8): p. 4562-7.
47. Bennett, N.C., et al., *Molecular cell biology of androgen receptor signalling.* Int J Biochem Cell Biol, 2010. **42**(6): p. 813-27.
48. Cutress, M.L., et al., *Structural basis for the nuclear import of the human androgen receptor.* J Cell Sci, 2008. **121**(Pt 7): p. 957-68.
49. Nadal, M., et al., *Structure of the homodimeric androgen receptor ligand-binding domain.* Nat Commun, 2017. **8**: p. 14388.
50. Heinlein, C.A. and C. Chang, *Androgen receptor (AR) coregulators: an overview.* Endocr Rev, 2002. **23**(2): p. 175-200.
51. Powell, S.M., et al., *Mechanisms of androgen receptor signalling via steroid receptor coactivator-1 in prostate.* Endocr Relat Cancer, 2004. **11**(1): p. 117-30.
52. Penney, K.L., et al., *Association of KLK3 (PSA) genetic variants with prostate cancer risk and PSA levels.* Carcinogenesis, 2011. **32**(6): p. 853-9.
53. Davies, T.H., Y.M. Ning, and E.R. Sanchez, *A new first step in activation of steroid receptors: hormone-induced switching of FKBP51 and FKBP52 immunophilins.* J Biol Chem, 2002. **277**(7): p. 4597-600.
54. He, B., et al., *Dependence of selective gene activation on the androgen receptor NH2- and COOH-terminal interaction.* J Biol Chem, 2002. **277**(28): p. 25631-9.
55. Gaughan, L., et al., *Regulation of androgen receptor and histone deacetylase 1 by Mdm2-mediated ubiquitylation.* Nucleic Acids Res, 2005. **33**(1): p. 13-26.
56. Lee, D.K. and C. Chang, *Endocrine mechanisms of disease: Expression and degradation of androgen receptor: mechanism and clinical implication.* J Clin Endocrinol Metab, 2003. **88**(9): p. 4043-54.
57. Baron, S., et al., *Androgen receptor mediates non-genomic activation of phosphatidylinositol 3-OH kinase in androgen-sensitive epithelial cells.* J Biol Chem, 2004. **279**(15): p. 14579-86.
58. Foradori, C.D., M.J. Weiser, and R.J. Handa, *Non-genomic actions of androgens.* Front Neuroendocrinol, 2008. **29**(2): p. 169-81.
59. Andersson, S., R.W. Bishop, and D.W. Russell, *Expression cloning and regulation of steroid 5 alpha-reductase, an enzyme essential for male sexual differentiation.* J Biol Chem, 1989. **264**(27): p. 16249-55.
60. Kaprara, A. and I.T. Huhtaniemi, *The hypothalamus-pituitary-gonad axis: Tales of mice and men.* Metabolism, 2018. **86**: p. 3-17.
61. Waterman, M.R. and D.S. Keeney, *Genes involved in androgen biosynthesis and the male phenotype.* Horm Res, 1992. **38**(5-6): p. 217-21.
62. Ito, Y. and M.D. Sadar, *Enzalutamide and blocking androgen receptor in advanced prostate cancer: lessons learnt from the history of drug development of antiandrogens.* Res Rep Urol, 2018. **10**: p. 23-32.
63. Ziolkowska, E., et al., *The side effects of hormonal therapy at the patients with prostate cancer.* Contemp Oncol (Pozn), 2012. **16**(6): p. 491-7.
64. Tran, C., et al., *Inhibition of constitutive aryl hydrocarbon receptor (AhR) signaling attenuates androgen independent signaling and growth in (C4-2) prostate cancer cells.* Biochem Pharmacol, 2013. **85**(6): p. 753-62.
65. Ghotbaddini, M., V. Moultrie, and J.B. Powell, *Constitutive Aryl Hydrocarbon Receptor Signaling in Prostate Cancer Progression.* J Cancer Treatment Diagn, 2018. **2**(5): p. 11-16.
66. Ohtake, F., et al., *Intrinsic AhR function underlies cross-talk of dioxins with sex hormone signalings.* Biochem Biophys Res Commun, 2008. **370**(4): p. 541-6.
67. Kobayashi, A., et al., *CBP/p300 functions as a possible transcriptional coactivator of Ah receptor nuclear translocator (Arnt).* J Biochem, 1997. **122**(4): p. 703-10.
68. Ghotbaddini, M., et al., *Simultaneous inhibition of aryl hydrocarbon receptor (AhR) and Src abolishes androgen receptor signaling.* PLoS One, 2017. **12**(7): p. e0179844.

69. Chen, Z., et al., *Carbidopa suppresses prostate cancer via aryl hydrocarbon receptor-mediated ubiquitination and degradation of androgen receptor*. Oncogenesis, 2020. **9**(5): p. 49.
70. Endo, F., et al., *Effects of single non-ortho, mono-ortho, and di-ortho chlorinated biphenyls on cell functions and proliferation of the human prostatic carcinoma cell line, LNCaP*. Reprod Toxicol, 2003. **17**(2): p. 229-36.
71. Kizu, R., et al., *A role of aryl hydrocarbon receptor in the antiandrogenic effects of polycyclic aromatic hydrocarbons in LNCaP human prostate carcinoma cells.* Arch Toxicol, 2003. **77**(6): p. 335-43.
72. Ohtake, F., et al., *Dioxin receptor is a ligand-dependent E3 ubiquitin ligase.* Nature, 2007. **446**(7135): p. 562-6.
73. Stepankova, M., et al., *Methylindoles and Methoxyindoles are Agonists and Antagonists of Human Aryl Hydrocarbon Receptor.* Mol Pharmacol, 2018. **93**(6): p. 631-644.
74. ATCC. ***ATCC: The Global Bioresource Center - 22Rv1***. 2023 [cited 2023 05/10/2023]; Available from: https://www.atcc.org/products/crl-2505.
75. ATCC. *The Global Bioresource Center - LNCaP*. 2023 [cited 2023 05/10/2023]; Available from: https://www.atcc.org/products/crl-1740.
76. ATCC. ***ATCC: The Global Bioresource Center - C4-2***. 2023 [cited 2023 05/10/2023]; Available from: https://www.atcc.org/products/crl-3314.
77. ATCC. ***ATCC: The Global Bioresource Center - PC3***. 2023; Available from: https://www.atcc.org/products/crl-1435.
78. Bartonkova, I., A. Novotna, and Z. Dvorak, *Novel stably transfected human reporter cell line AIZ-AR as a tool for an assessment of human androgen receptor transcriptional activity.* PLoS One, 2015. **10**(3): p. e0121316.
79. Novotna, A., P. Pavek, and Z. Dvorak, *Novel stably transfected gene reporter human hepatoma cell line for assessment of aryl hydrocarbon receptor transcriptional activity: construction and characterization.* Environ Sci Technol, 2011. **45**(23): p. 10133-9.
80. Zannas, A.S., et al., *Gene-Stress-Epigenetic Regulation of FKBP5: Clinical and Translational Implications.* Neuropsychopharmacology, 2016. **41**(1): p. 261-74.

9 LIST OF AUTHOR'S PUBLICATIONS

LIST OF PUBLICATIONS

1. **Zgarbova, E.**, Vrzal, R. (2022): The Impact of Indoles Activating the Aryl Hydrocarbon Receptor on Androgen Receptor Activity in the 22Rv1 Prostate Cancer Cell Line. *Int. J. Mol. Sci.* 24, 502. [IF 5.6] DOI: 10.3390/ijms24010502.

2. Sladekova, L., **Zgarbova, E.**, Vrzal, R., Vanda, D., Soural, M., Jakubcova, K., Vazquez-Gomez, G., Vondracek, J. & Dvorak, Z. (2023): Switching on/off aryl hydrocarbon receptor and pregnane X receptor activities by chemically modified tryptamines. *Toxicol Lett.* [IF 3.5] DOI: 10.1016/j.toxlet.2023.09.012.

3. **Zgarbova, E.**, Vrzal R. (2023): Skatole: A thin red line between its benefits and toxicity. *Biochimie* 208: 1-12 [IF 3.9] DOI: 10.1016/j.biochi.2022.12.014.

CONFERENCE REPORTS

1. **Zgarbova, E.**, Vrzal, R. (2022): Suppression of androgen receptor activity via activation of aryl hydrocarbon receptor in prostate cancer cells. The Biomania Student Scientific Meeting; Apr 28-29; Brno; Czech Republic. Book of Abstracts; 1st edition 2022: Masaryk University Press, p 117. ISBN: 978-80-280-0040-0.

2. Patel, S., Wagner, M. S., Bay, O., **Zgarbova, E**., Valencia, C. W., Michelsen, K. S., Targan S. & Barrett, R. (2024): Development of a personalized human Paneth cell model using intestinal organoids. Crohn's & Colitis Congress®; Jan 25-27; Las Vegas; USA. *Gastroenterology* 166, Supplement Issue 3. DOI: 10.1053/j.gastro.2023.11.272

3. **Zgarbova, E.**, Valencia, C. W., Patel, S., Bay, O., Barrett, R. (2024): iPSC-derived intestinal organoids: A new personalized model to study IBD and intestinal fibrosis. XXIIIrd Interdisciplinary Meeting of Young Life Scientists. Czech Chemical Society Symposium Series 22 (1), p 50, ISBN: 2336-7210.

10 SOUHRN (Summary in Czech)

Jméno a příjmení autora	Mgr. Eliška Zgarbová
Název práce	Vliv indolových derivátů na aktivitu aryl uhlovodíkového receptoru v prostatických liniích
Typ práce	Disertační
Pracoviště	Katedra buněčné biologie a genetiky
Vedoucí práce	doc. Ing. Radim Vrzal, Ph.D.
Rok obhajoby práce	2024

Abstrakt

Karcinom prostaty se řadí mezi převládající typy onkologického onemocnění u mužů. Rozvoj tohoto typu rakoviny je velmi úzce spojen se signální dráhou androgenního receptoru (AR) a z toho důvodu se také tento receptor stal velice významným terapeutickým cílem. Nedávné studie ukázaly, že aktivace aryl uhlovodíkového receptoru (AhR) silnými ligandy může vyvolat proteasomální degradaci AR. Cílem této studie bylo analyzovat, zda vybrané indolové sloučeniny mohou vyvolat degradaci AR jako důsledek aktivace AhR a tím také narušit signální dráhu AR. Na základě předchozího výzkumu byly vybrány kandidátní sloučeniny obsahujících ve své struktuře indolový skelet, u nichž byla prokázána schopnost aktivace AhR. Z celkového počtu 22 testovaných indolů bylo zjištěno, že 8 z nich bylo schopno indukovat transkripční aktivitu AhR a současně také potlačovat DHT-indukovanou transkripční aktivitu AR, snižovat expresi AR-cílových genů, konkrétně *KLK3* a *FKBP5* na úrovni mRNA i proteinu. Pomocí chromatinové precipitace (ChIP) byla potvrzena snížená vazba AR do promotoru genu *KLK3* po inkubaci s vybranými indoly. Pro studium vztahu mezi AhR a AR byla také vytvořena AhR knock-out buněčná linie (CRISPR/Cas9 systém). Získané výsledky naznačují, že suprese AR pozorovaná na úrovni proteinu nebyla důsledkem proteasomální degradace AR, protože inhibice byla detekovaná už na úrovni transkripce (mRNA). Nicméně vybrané indolové sloučeniny vykazovaly silný potenciál potlačení signální dráhy AR. Tento mechanismus však bude odlišný, než bylo původně předpokládáno.

Klíčová slova	indolové deriváty, AhR, AR
Počet stran	139
Počet příloh	2
Jazyk	Anglický